

CRANFIELD UNIVERSITY

Toby Balaam, Paul Causon, Debora Cevasco,
Philip Dirisu, Mareike Leimeister, Mark Richmond

Human-Free Offshore Lifting Solutions

Cranfield University
University of Oxford
REMS CDT
DONG
G+

REMS - Group Project

Academic Year: 2016 - 2017

Supervisor: Prof. Feargal Brennan
April 2017

ABSTRACT

With single elements weighing up to hundreds of tonnes and lifted up to heights of 100 meters, offshore wind turbines can pose risks to personnel, equipment, and environment during installation. Guidelines and standards for health and safety in lifting operations are existing. Despite this, having people directly under the load for guiding and securing is still common practice in offshore wind turbine installations. Statistics for the reasons, areas, and consequences for incidents during lifting operations in offshore wind turbine installation processes, resulting from incident reports provided by G+, substantiate the importance of safer and improved handling in offshore lifting operations. This is used as motivation for this report, which presents an alternative guideline for human-free offshore lifting solutions. Different concepts for human-free offshore lifting operations in the categories of guidance and control, connections, and assembly are proposed and developed in detail. The final ideas range from holistic guiding systems linked with control instruments, to automatic bolting and hydraulic sea fastening, on through to novel assembly concepts and a program for optimising the pre-assembly and installation methods. Those recommended concepts are finally ranked by applying a multi-criteria decision analysis, using experts' opinions for the importance of defined criteria, obtained by conducting a survey. Thus, a combined guidance and control system consisting of Boom Lock and taglines turned out to be the most worthwhile solution, followed by a combined visual and mechanical guiding system, and automated bolt installation and fastening method.

Keywords:

health & safety, offshore wind energy, multi-criteria decision method, lifting operations, floating wind turbines, automation, bolted connections, sea fastening, guidance and control, assembly, cranes, dropped objects

ACKNOWLEDGEMENTS

This group project lasted for more than five months and was conducted by six research students: Toby Balaam, Paul Causon, Debora Cevasco, Philip Dirisu, Mareike Leimeister, and Mark Richmond. However, it required a lot more resource and the group received much support from various sides. For all this help, the group wants to thank everyone who was involved and contributed anyhow to the successful completion of this project.

In particular, thanks are extended to the figures who helped define the scope of this report: our supervisor and overseer of the group project, Prof Feargal Brennan; Kate Harvey, Bir Virk, and Andrew Sykes from G+, for whom we hope this helps bring a safer culture to the industry; as well as David Delamore, Peter Geddes, and Joe O'Toole from DONG energy, who provided us with insights into the industry and aided us throughout. It was great to work together with the industry and learn from the experiences of company workers. Thanks are also extended to all of the individuals who filled in the survey for the multi-criteria decision analysis.

Furthermore, the group wants to thank Cranfield University's staff, especially Dr Ali Mehmanparast and Dr Athanasios Kolios for their support in specialist topics, as well as Antony Charnley, Dr Supriyo Ganguly, Flemming Nielsen, Nisar Shah, Graham Hartwell, and Derek Brown for their help with the organisation and realisation of the experimental tests at the welding centre of Cranfield University.

For the technical support, the group wants to thank especially the Cranfield University IT service and the printing service at the Radcliffe Science Library at Oxford University. Many thanks to Sally Dring, from Cranfield University, for her constant support in any organisational matters.

Final thanks go to the REMS Centre for Doctoral Training for the financial support within this group project.

TABLE OF CONTENTS

ABSTRACT.....	i
ACKNOWLEDGEMENTS	iii
LIST OF FIGURES	viii
LIST OF TABLES.....	xiv
LIST OF EQUATIONS	xv
LIST OF ABBREVIATIONS.....	xvi
NOMENCLATURE	xviii
1 INTRODUCTION	1
1.1 Lifting Procedure	1
1.1.1 Relevance of Lifting Procedure to the Wind Energy Sector	2
1.1.2 Lifting Elements in the Wind Energy Industry	4
1.1.3 The Elements of a Lifting Procedure.....	6
1.2 Relevance of Human-Free Lifting Solutions	10
1.2.1 Statistics and Incident Reports	12
1.2.2 Reasons for Incidents.....	14
1.2.3 Areas of Risk.....	15
1.2.4 Actual Consequences	16
1.3 Guideline for Human-Free Offshore Lifting Operations.....	17
1.3.1 Motivation.....	17
1.3.2 Approach.....	18
1.3.3 Report Overview.....	19
2 SUMMARY OF EXISTING GUIDELINES.....	20
2.1 Guidelines for Lifting Operations	20
2.1.1 Regulatory Requirements and Codes of Practice for Lifting Operations	20
2.1.2 Offshore and Marine Energy Regulations for Lifting Operations	21
2.2 Existing Human-Free Lifting Operation Systems	22
2.2.1 Support in Lifting Operations	22
2.2.2 Guiding Systems	23
2.2.3 Support in Connecting.....	24
2.2.4 Assembly Solutions	25
3 CONCEPTS FOR HUMAN-FREE OFFSHORE LIFTING OPERATIONS.....	29
3.1 Concepts for Guidance and Control	29
3.1.1 Introduction	29
3.1.1.1 Global and Fine Hoisting	29
3.1.1.2 Current Practices.....	30
3.1.2 Initial Proposed Solutions	31
3.1.2.1 Mechanical Guidance	31
3.1.2.2 Visual Guidance	35
3.1.2.3 Sensorial Guidance	38
3.1.2.4 Automated Guidance.....	39
3.1.2.5 Fine Tuning Control	40
3.1.3 Selection of Most Promising Solutions.....	44
3.1.4 Development of Solutions in Detail.....	45
3.1.4.1 Global Hoisting	45
3.1.4.2 Fine Hoisting	48
3.1.5 Conclusion and Recommendations	71

3.1.5.1 Mechanical Guiding Elements for Increased Tolerance Margin	71
3.1.5.2 Holistic Solution for Guidance and Control.....	74
3.1.5.3 Realisation and Application in Practice	74
3.2 Concepts for Connections and Seafastening.....	76
3.2.1 Introduction	76
3.2.2 Initial Ideas	78
3.2.2.1 Friction Connection.....	78
3.2.2.2 ConXtech Connection.....	80
3.2.2.3 Single, Large Thread	81
3.2.2.4 Hydraulic Seafastening	82
3.2.2.5 Internal Jack Seafastening.....	83
3.2.2.6 Bolting Robot Arm	84
3.2.2.7 External Climbing Bolt Robot.....	86
3.2.3 Selection of Most Promising Solutions.....	86
3.2.4 Development of Solutions in Detail.....	87
3.2.4.1 Automated Bolting System.....	87
3.2.4.2 Hydraulic Seafastening	92
3.3 Concepts for Assembly	93
3.3.1 Introduction	93
3.3.2 Initial Proposed Solutions	97
3.3.2.1 Onshore Pre-Assembly Solutions: Bottom-Fixed Wind Turbines	97
3.3.2.2 Onshore Pre-Assembly Solutions: Floating Wind Turbines.....	103
3.3.2.3 Offshore Assembly Solutions.....	104
3.3.3 Selection of Most Promising Solutions.....	105
3.3.4 Development of Solutions in Detail.....	105
3.3.4.1 Optimising Current Pre-Assembly Practice	105
3.3.4.2 Novel Assembly Concepts	121
4 MULTI-CRITERIA DECISION ANALYSIS	135
4.1 Decision Context: Aims, Stakeholders and Key Players	135
4.2 Criteria	136
4.3 Survey.....	139
4.4 Evaluation of Criteria Satisfaction.....	140
4.5 Methods	141
4.5.1 Weighted Sum and Weighted Product Methods	142
4.5.1.1 Weighted Sum Method	142
4.5.1.2 Weighted Product Method	142
4.5.2 Analytical Hierarchy Process	143
4.5.3 PROMETHEE	143
4.5.4 ELECTRE.....	144
4.6 TOPSIS.....	145
4.6.1 TOPSIS Method	145
4.7 Methodology	147
4.7.1 Weights Used and Evaluation of Survey Data	147
4.8 Results and Discussion	151
4.8.1 First Stage TOPSIS Analysis.....	151
4.8.2 Second Stage TOPSIS Analysis.....	152
4.9 Conclusions	153
5 CONCLUSIONS.....	155

5.1 Summary of Report	155
5.2 Drawbacks of Human-Free Operations	156
5.3 Benefits of Human-Free Operations	156
5.4 Recommendations	157
5.5 Outlook and Future Work	158
REFERENCES	159
APPENDICES.....	A-1
Appendix A Project Management and Planning	A-1
A.1 Project Management Plan.....	A-1
A.1.1 Time Schedule	A-1
A.1.2 Work Packages and Distribution	A-3
A.2 Project Risk Assessment	A-7
A.2.1 Problem Area: Data	A-7
A.2.2 Problem Area: Human.....	A-8
A.2.3 Problem Area: Ideas	A-10
A.2.4 Problem Area: Communication	A-10
A.3 Communication Plan.....	A-12
A.3.1 Communication with the Industry	A-12
A.3.2 Group Meetings	A-13
A.4 Resources	A-14
A.4.1 Personnel.....	A-14
A.4.2 Technological.....	A-15
A.4.3 Financial	A-15
Appendix B Experimental Results	B-17
B.1 Graphs of Each Case.....	B-17
B.2 Tables of Raw Data	B-20
Appendix C Mechanical Guidance	C-24
C.1 3D-Printed Initial Design	C-24
C.1.1 Top Element	C-24
C.1.2 Bottom Element	C-26
C.1.3 Assembly	C-28
C.2 3D-Printed Revised Design.....	C-29
C.2.1 Top Element	C-29
C.2.2 Bottom Element	C-32
C.2.3 Assembly.....	C-35
C.3 Simplified Design for Experimental Tests.....	C-36
C.3.1 Top Assembly	C-36
C.3.2 Socket Section.....	C-38
C.3.3 Bottom Assembly.....	C-40
C.3.4 Test Setup	C-42
C.4 Full-Scale Design	C-43
C.4.1 Calculating Loads (DNV GL, 2016a)	C-44
C.4.2 CAD Drawing of Full-Scale Design	C-48
C.4.3 FEA Analysis	C-50
C.5 Mechanical Guiding Systems in Comparison	C-55
Appendix D Program Code for the Optimisation of the Assembly.....	D-56
D.1 Simple_GUI.m	D-56
D.2 fittingBE.m	D-81

D.3 timeBE.m.....	D-88
D.4 fittingROT.m	D-90
D.5 timeROT.m	D-97
D.6 fittingSP.m	D-98
D.7 timeSP.m.....	D-103
Appendix E MCDA Appendix	E-104
E.1 Detailed Survey Responses.....	E-104
E.1.1 Response Histograms.....	E-104
E.1.2 Criteria Weight Values	E-108
E.2 TOPSIS Code	E-108

LIST OF FIGURES

Figure 1-1 Technology progression of the offshore wind turbine installations (W. Musial et al., 2006)	3
Figure 1-2 Lifting of blade into hub (London Array, 2013).....	4
Figure 1-3 Lifting of tower onto transition piece (London Array, 2013).....	4
Figure 1-4 Lifting sequence of turbine components	5
Figure 1-5 Wind energy components lifting sequence for conventional installation method.....	6
Figure 1-6 Lifting procedure preparation cycle	7
Figure 1-7 Six key focus areas during the planning stages of a good lifting procedure.....	8
Figure 1-8 Installed capacity of offshore wind turbines within Europe (EWEA, 2016)	10
Figure 1-9 (Fred. Olsen Windcarrier, 2016a).....	11
Figure 1-10 (Fred. Olsen Windcarrier, 2016a).....	11
Figure 1-11 Total incidents and dropped objects per number of hours worked.....	13
Figure 1-12 Reason for incidents at project sites	14
Figure 1-13 Area of incidents at project sites	16
Figure 1-14 Actual consequences of incidents at project sites	17
Figure 1-15 Project Schedule.....	18
Figure 2-1 The Boom Lock (High Wind, 2014)	22
Figure 2-2 Tagline master winch (AH-Industries, 2016).....	23
Figure 2-3 Blade Dragon (Liftra, 2014).....	23
Figure 2-4 Guide cones (Forewind, 2013)	24
Figure 2-5 Guide pins (MacFarlane, 2016).....	24
Figure 2-6 Robot guided bolt tensioning tool (Müller et al., 2014).....	25
Figure 2-7 ITH Autostretch (ITH Bolting Technology, 2016)	25
Figure 2-8 Bolt robot, adapted by the author from (Johst, Jagd, Bovin, & Marinitsch, 2013).....	25
Figure 2-9 Climbing robots, left (Lombardo, 2013) and right (Webster, 2013)	25
Figure 2-10 Installation vessel for fully-assembled wind turbines (Vuyk Engineering Rotterdam b.v., 2017)	26
Figure 2-11 Tow out of Principle Power's WindFloat (Bush, 2015)	26
Figure 2-12 Tow out of Fukushima Hamakaze 5MW Hitachi wind turbine (Trabish, 2016)	26
Figure 2-13 WindFlip (Jensen, 2010)	27
Figure 2-14 Hinged self-erecting tower (Dehlsen & Mikhail, 2005)	27
Figure 2-15 Telescoping self-erecting tower (Gee & FL, 2011)	27

Figure 3-1 People guiding manually the load (Fred. Olsen Windcarrier, 2016b)	31
Figure 3-2 Current use of guide pins (SCHEUERLE Fahrzeugfabrik, 2012)	32
Figure 3-3 Patent for an aligning tool, adapted by the author from (Jensen, 2013).....	32
Figure 3-4 Patent for an aligning arrangement, adapted by the author from (Moeller et al., 2016)	33
Figure 3-5 Patent for an alignment tool with a resiliently deformable part, adapted by the author from (Øllgaard, 2014b).....	33
Figure 3-6 Patent for an apparatus for mounting wind turbine blades, adapted by the author from (Bitsch & Baun, 2012).....	33
Figure 3-7 Patent for a tower assembly system, adapted by the author from (Moestrup & Westergaard, 2014).....	33
Figure 3-8 Patent for an aligning device, adapted by the author from (Øllgaard, 2014a)	34
Figure 3-9 Patent for an alignment system, adapted by the author from (Spence & Russell, 2013)	34
Figure 3-10 Guide cones for human-free met mast installation (Forewind, 2013).....	35
Figure 3-11 High Wind 'Boom Lock' (Nielsen, 2016)	41
Figure 3-12 Tagline master with the Blade Yoke by AH Industries, showing the remote control set-up (AH-Industries, 2016).....	42
Figure 3-13 Liftra products. Left - Blade Dragon, Right - Self-hoisting crane (Liftra, 2016)	42
Figure 3-14 Image displayed in the cabin, which shows the position of the target and the correct vertical position as an overlaid circle (Wilson, 2012)	43
Figure 3-15 Boom Lock system; red arrows indicates restricted movement, green arrows indicate allowable movement. (High Wind, 2014).....	47
Figure 3-16 Tower and Nacelle installation of an offshore wind turbine.....	49
Figure 3-17 Left) Marked 'Ideal Position' representing the bottom fixed tower/transition piece. Right) Measurement of the centre-point, marked as a cross beneath the intersection.	50
Figure 3-18 Left) Set-up of the cameras and crane system. Top right) typical view of 360 camera feed and monitor. Bottom right) Monitor feed of cameras 1, 2, 3 & 4.	51
Figure 3-19 Experiment A - Representation of cases of camera configurations	52
Figure 3-20 A) Measurement of Error – Blue indicates drawn ideal section on ground with the centre point marked. Black indicates the landed section. Red indicates the measured error. B) Example of this in practice	54
Figure 3-21 Average test results across the six tests for accuracy and time.....	56
Figure 3-22 Comparison of time taken (blue) and accuracy (orange) for both banksmen.....	56
Figure 3-23 Measurement of rotational error - Blue indicates the drawn ideal section, black indicates the landed section and red measurements of error.	57
Figure 3-24 Experiment B - Representation of cases of camera configurations	58
Figure 3-25 Average test results for rotational alignment	60
Figure 3-26 Box and Whisker Plot of Crane precision test. The cross indicates the mean.	61

Figure 3-27 Initial design including mechanical guiding elements	63
Figure 3-28 3D-print of the initial design.....	64
Figure 3-29 Revised design including mechanical guiding elements	66
Figure 3-30 3D-print of the revised design	67
Figure 3-31 Manufactured simplified design.....	68
Figure 3-32 Individual times for the tests with mechanical and visual guidance (C1).....	69
Figure 3-33 All test results in comparison	70
Figure 3-34 Tolerance margins in comparison	73
Figure 3-35 View of bolts inside tower section during installation (Fred. Olsen Windcarrier, 2015)	76
Figure 3-36 Bolt loads and torque values (alfadoc, 2013)	77
Figure 3-37 Friction connection (Heistermann et al., 2009)	78
Figure 3-38 ConXtech connection drawing (Olson & Steel co, 2017)	80
Figure 3-39 Various hydraulic seafastening options mentioned in (Hoeksema, 2014)	83
Figure 3-40 Hydraulic internal seafastening design proposed in (Hoeksema, 2014)	84
Figure 3-41 Rotor hub, bearing bolt tightening robot (Müller et al., 2014).....	85
Figure 3-42 Automated bolted seafastening, concept illustration. CAD by M. Richmond.....	88
Figure 3-43 Mechanical manipulation robot discussed in (Duan et al., 2013)	89
Figure 3-44 Fastener feed system discussed in (Sydenham & Brown, 2015).....	91
Figure 3-45 Offshore wind turbine current used and proposed installation methods. Adapted from (Ahn, Shin, Kim, Kharoufi, & Kim, 2016)	94
Figure 3-46 Offshore wind farm installation vessels (Ahn et al., 2016)	96
Figure 3-47 Example of onshore pre-assembly site (harbour) for offshore wind farm installation (Asgarpour, 2016).....	98
Figure 3-48 Jack-up vessels and barge comparison (during lifting and installation phases of BE pre-assembly) (Fred. Olsen Windcarrier, 2013; Uraz, 2011)	98
Figure 3-49 BE configuration offshore transportation examples (Fred. Olsen Windcarrier, 2013; Uraz, 2011).....	100
Figure 3-50 ROT configuration offshore installation examples (C-power, 2017; offshoreWIND.biz, 2015)	100
Figure 3-51 Possible BE configuration optimization: Left) tower and third-blade pre-assembly transportation solutions; Right) pre-assemblies two-lifts installation and BE transportation mode detail. Adapted from (Anders Soe-Jensen, 2010).....	101
Figure 3-52 Conceptual designs for fully pre-assembled turbines transportation and installation on pre-installed bottom-fixed foundation (Ulstein Offshore Wind Team, 2017; Vuyk Engineering Rotterdam b.v., 2017)	102
Figure 3-53 Left) BAM's Group gravity based design for EDF's Blyth demonstration project (4C Offshore, 2017b; BAM Nuttal, 2016; theconstructionindex, 2017). Right) Gravity based (middle	

right) and bucket (extreme right) foundations feasibility designs (4C Offshore, 2017b; P. Zhang, Han, Ding, & Zhang, 2015)	103
Figure 3-54: Floating wind turbines stability classes.....	104
Figure 3-55: Floating wind turbine transportation possibilities. Top-left) Tri-floater top-right) spar , bottom) TLP (Amate, Sánchez, & González, 2016; Principle Power, 2011)	104
Figure 3-56: JUVs working together on the tower-nacelle and the rotor pre-assembly installations at the Global Tech I wind farm (offshoreWIND.biz, 2014)	106
Figure 3-57: EOSIM installation-simulating program example (Petcu, 2009).....	107
Figure 3-58: Flowchart of the program for the installation phase simulation	108
Figure 3-59: Program complete user-interface (e.g. after the three blocks use)	110
Figure 3-60: Turbine characteristics (left) and jack-up units (right) schematics. CAD adapted by M. Richmond	112
Figure 3-61: Time variables input section.....	113
Figure 3-62: Possible solution to be adopted when the entire tower transportation is not possible (error); split (left) and adjustment of the tower base/support structure dimensions (right). From Thanet Wind Farm case study.	114
Figure 3-63: Blade "cage", transportation gathering structure examples (Fred. Olsen Windcarrier, 2017; Lawson, 2012)	115
Figure 3-64: Schematic example of a SP transportation solutions. CAD adapted by M. Richmond	116
Figure 3-65: Schematic examples of BE transportation solutions; transverse-1T (left) and longitudinal-2T (right). CAD adapted by M. Richmond	117
Figure 3-66: Schematic examples of BE transportation solutions; mode1-2T (left) and mode2-1T (right). CAD adapted by M. Richmond	118
Figure 3-67: Vestas V90-3.0MW characteristic (Vestas Wind Systems A/S, 2017)	119
Figure 3-68: JUV, port and farm characteristics (MPI Offshore, 2011b; Vattenfall, 2005, 2014) ..	120
Figure 3-54 Trends in offshore wind foundations (European Wind Energy Association, 2013)	122
Figure 3-55 Cost of offshore wind turbine structures with respect to the water depth (W. Musial et al., 2006)	123
Figure 3-56 Wind turbine novel assembly concepts	124
Figure 3-57 Partially self-erecting wind turbine tower (Dehlsen & Mikhail, 2005).....	125
Figure 3-58 Fully self-erecting tower and method for raising the tower (Gee & FL, 2011)	126
Figure 3-59 Partially self-erecting wind turbine using hydraulic pulling device (Hau, 2008)	128
Figure 3-60 Partially self-erecting wind turbine using tower as track (Hau, 2008).....	128
Figure 3-61 Partially pre-assembly using crane (Hau, 2008).....	128
Figure 3-62 Fully pre-assembly using special vessel (single lift) (Vuyk Engineering Rotterdam b.v., 2017)	129
Figure 3-63 Tri-floater vertical transportation concept (Principle Power, 2011).....	131

Figure 3-64 Other concepts of floating wind turbines (European Wind Energy Association, 2013)	132
Figure 3-65 WindFlip, horizontal transportation concept with a fully self-erecting wind turbine (Barker, 2012).....	133
Figure 4-1 Criteria to be considered.....	137
Figure 4-2 Illustration of the idea of 'Closeness'.....	147
Figure 4-3 Averaged responses to the section 'R+D & Manufacture'.....	148
Figure 4-4 Averaged responses to the section 'Operational'	148
Figure 4-5 Standard deviation of responses.....	149
Figure 4-6 Maturity of technology.....	150
Figure 4-7 Limitations	150
Figure 4-8 Environmental impact	150
Figure 4-9 Reduction of risk	150
Figure A-1 Gantt chart for group project.....	A-2
Figure A-2 Work packages, responsibilities, and time schedule	A-3
Figure A-3 Involved people and working groups	A-4
Figure A-4 Risk Matrix	A-7
Figure A-5 Risks in the problem area data	A-8
Figure A-6 Risks in the problem area human	A-9
Figure A-7 Risks in the problem area ideas.....	A-10
Figure A-8 Risks in the problem area communication	A-11
Figure A-9 Plan for the communication with the industry.....	A-12
Figure A-10 Plan for group meetings and internal communications.....	A-13
Figure B-1 Graphs of time and error for five no. tests undertaken for each case.....	B-20
Figure C-1 Top element of the 3D-printed initial design	C-24
Figure C-2 Bottom element of the 3D-printed initial design	C-26
Figure C-3 Assembly of the 3D-printed initial design.....	C-28
Figure C-4 Top element of the 3D-printed revised design	C-29
Figure C-5 Bottom element of the 3D-printed revised design	C-32
Figure C-6 Assembly of the 3D-printed revised design	C-35
Figure C-7 Fixation of bottom element to floor	C-42
Figure C-8 Setup of mechanical and visual guiding systems.....	C-42

Figure C-9 Nacelle to tower connection. Right (Fred. Olsen Windcarrier, 2015)..... C-43

Figure C-10 Drag forces on a rectangular section (DNV, 2014b, sec. 5.4.2) C-47

Figure C-11 Table 4-3 from (DNV, 2013), material properties to be used for S355 steel..... C-50

Figure C-12 ABAQUS Model Loads. Load case 30 and 41 C-51

Figure C-13 Load case 41 in two views. Von misses stresses across the **20 mm** thick section.
Black indicates positions where stresses are below yield C-53

Figure C-14 Recommended weights for lifting (Health and Safety Executive, 2012) C-53

Figure E-1 Response histograms.....E-107

LIST OF TABLES

Table 1-1 Total incidents and dropped objects from 2014 to Q3 of 2016.....	12
Table 1-2 Total incidents and dropped objects from 2014 to Q3 of 2016.....	13
Table 3-1 MCDA results for guidance and control	45
Table 3-2 Experiment A - Description of cases of camera configurations.....	53
Table 3-3 Experiment B - Description of cases of camera configurations.....	59
Table 3-4 North Sea Wind farm installation requirements and characteristics. Adapted from (4C Offshore, 2017c),(C-power, 2017) and (Uraz, 2011)	95
Table 3-5: MCDA results for assembly	105
Table 3-6: Results table for Thanet case study	120
Table 3-5 Current floating wind turbine manufacturers and concepts (European Wind Energy Association, 2013)	130
Table 4-1 Description of criteria	137
Table 4-2 First stage TOPSIS results for 'Guidance and Control'	152
Table 4-3 First stage TOPSIS results for 'Connections and Seafastening'	152
Table 4-4 First stage TOPSIS results for 'Assembly Methods'.....	152
Table 4-5 Final ranking of all proposed ideas.....	153
Table A-1 Contribution of each group member to report, indicated by means of page numbers..	A-6
Table C-1 Input data from the 8MW reference wind turbine (Desmond et al., 2016). * indicates dimensions which were approximated based on realistic proportions	C-44
Table C-2 Loadcases to be analysed	C-52
Table C-3 Material properties of a lay-up FRP. Values edited from ("Technical Design Guide for FRP Composite Products And Parts," 2017) Imperial-metric. Poisson's ratio from (Hussain, Reddy, & Reddy, 2008)	C-54
Table C-4 Results of the tolerance margin computations	C-55
Table E-1 Criteria weighting	E-108

LIST OF EQUATIONS

(3-1)	57
(3-2)	58
(4-1)	142
(4-2)	142
(4-3)	145
(4-4)	145
(4-5)	146
(4-6)	146
(4-7)	146
(C-1)	C-44
(C-2)	C-45
(C-3)	C-45
(C-4)	C-45
(C-5)	C-46
(C-6)	C-46
(C-7)	C-46
(C-8)	C-47
(C-9)	C-47
(C-10)	C-47
(C-11)	C-47
(C-12)	C-48
(C-13)	C-48

LIST OF ABBREVIATIONS

1/2T	One/Two Tower-Elements Transportation and Installation Method
3D	Three Dimensional
ABS	Automated Bolting System
AHP	Analytical Hierarchy Process
BE	Bunny-Ear Pre-Assembly Method
BM	Banksman
BS	British Standard
CCTV	Closed-Circuit Television
CHT	Circular Hough Transforms
CI	Consistency Index
CoG	Centre of Gravity
DAF	Dynamic Application Factor
DHL	Dynamic Hook Load
DM	Decision Maker
DNV	Det Norske Veritas
DNV-GL	Det Norske Veritas - Germanischer Lloyd
DP	Dynamic Positioning
DPV	Dynamically Positioning Vessel
DVR	Digital Video Recorder
E	Exposure
ELECTRE	Elimination and Choice Expressing Reality
FEA	Finite Element Analysis
FMEA	Failure Modes and Effect Analysis
Fraunhofer IWES	Fraunhofer Institute for Wind Energy and Energy System Technology
FRP	Fibre-Reinforced Polymer
GL	Germanischer Lloyd
GUI	Graphical User Interface
HAWT	Horizontal Axis Wind Turbine
I	Impact
IMCA	International Marine Contractors Association
JUB	Jack-Up Barge
JUV	Jack-Up Vessel
LOLER	Lifting Operations and Lifting Equipment Regulations
MCDA	Multi-Criteria Decision Analysis

MCDM	Multi-Criteria Decision Method
MDW	Module Design Weight
ML	Mareike Leimeister
MR	Mark Richmond
NIS	Negative Ideal Solution
O	Occurrence
OWT	Offshore Wind Turbine
PIS	Positive Ideal Solution
PLC	Programmable Logic Control
PoC	Point of Contact
PPE	Personal Protective Equipment
PROMETHEE	Preference Ranking Organisation Method for Enrichment Evaluations
PUWER	Provision and Use of Work Equipment Regulations
REMS	Renewable Energy Marine Structures
REMS-CDT	Renewable Energy Marine Structures – Centre for Doctoral Training
RI	Random Index
ROT	Rotor Pre-Assembly Method
RP	Recommended Practice
RW	Rigging Weight
SE	Service Specification
SHL	Static Hook Load
SP	Single Pieces Assembly Method
ST	Standard
TB	Toby Balaam
TIU	Turbine and Installation Unit
TOPSIS	Technique for Order of Preference by Similarity to Ideal Solution
TP	Transition Piece
TVL	Television Lines
VR	Virtual Reality
WPM	Weighted Product Method
WSM	Weighted Sum Method
WTG	Wind Turbine Generator

NOMENCLATURE

C	Shape Coefficient
F_w	Wind Force
q	Basic Wind Pressure
S	Projected Area
$U_{T,z}$	Characteristic Wind Speed
W	Hook Load
$W_{\text{Report,Factored}}$	Reported Weight
W_{rigging}	Rigging Weight
$W_{u,d}$	Upper Bound Design Weight
α	Angle Between Wind Direction and Axis of Member
κ	Reduction Factor
λ_{weight}	Factor of Weight Inaccuracy
ρ_a	Mass Density of Air

1 INTRODUCTION

1.1 Lifting Procedure

UK renewable wind energy consumption has been growing dramatically in the last decade. The main drivers that have influenced the shift to wind energy have been the need to cut down the use of fossil fuels, which are not environmental-friendly, and the increasing climate change due to huge carbon dioxide (CO₂) emissions (Vis & Ursavas, 2016). The falling price of oil in the world led investment in the oil and gas sector to a halt since the cost of production of a barrel is far higher than the current prevailing market price for crude oil, resulting in a low return on investment. All of this is paving ways for a cleaner way of generating energy by wind. Despite the huge cost, offshore wind energy farms are most preferred to onshore wind energy farms due to the availability of stronger winds offshore and less noise pollution. Also, offshore farms are more cost effective in the long run because of the huge power generation potentials due to stronger, more consistent wind. The availability of wind energy with consistent speed contributes to less components deteriorations unlike the onshore wind farms that is characterized by seasonal variation in operations, and this will aid the mechanical components to deteriorate faster when not in operation (W. Musial, Butterfield, & Ram, 2006).

A recent EU wind power project for the year 2020 is pegged at 40,000 MW with annual CO₂ savings of 102 million tons, annual investment of £10.4 billion and cumulative investment of £65.9 billion within 2011 to 2020 (Cairney, 2015). This really calls for mass investment in the wind energy industry and the only way to harness this opportunity is to find a way of reducing the cost of wind turbine projects from start to commissioning. The current cost of construction of per kWh of an offshore wind turbine is between £128,000 and £140,000 in the UK. In a bid to fast track this process the British Department of Energy and Climate Change has proposed that they are targeting to reduce the cost to £100,000 per kWh by the year 2020 (Cairney, 2015). Other major challenges with the offshore wind turbine installation beside costs are the safety issues associated with its construction and installation activities. The mass and weights of the various components are on the increase because of moving installation into deep waters due to its seemingly visible

benefits but posed with safety challenges to both equipment and personnel. Lifting operations have been a major concern with offshore installation in recent years because of the water depth and the height of installation. Optimizing the lifting operation will be an aid to achieving the targeted cost reduction proposed by the UK government for the year 2020. Most wind turbine companies have suffered various degrees of financial losses and compensation payments in the last years because of lost workdays cases and fatalities recorded at their sites.

Hence this report will be focusing on various lifting concepts that could be developed further for “human-free lifting” in the wind energy sector, thus reducing the fatalities and lost work days.

1.1.1 Relevance of Lifting Procedure to the Wind Energy Sector

The installation of wind turbine substructures and main structures are becoming more and more challenging as a result of government interest in the prospect of deep offshore because of the huge amount and consistent availability of wind energy here (Bøe & Nestegård, 2010). Lifting operations offshore are usually affected by factors like wind speeds and high tidal movements of the sea, hence the installation process in the North Sea is limited to only certain times in the year as a result of this (Vis & Ursavas, 2016). Lifting operations are an important aspect of any installation in the offshore wind energy industry and going with the recent quest by the EU to produce 20% of their energy consumption from the renewable wind industry by the year 2020 (RenewableUK, 2015). This means that lots of offshore installation projects will be faced with a high risk of lifting operations in the severe and most wanted coastal environments coupled with the high cost of installation equipment rentals. Some of this equipment, like barges, vessels and cranes, become underutilised after being mobilized to the offshore location because of inclement weather, thus increasing project construction cost. Figure 1-1 depicts the outcome of current shifting to deep waters; installation cost becomes bigger and lifting operations become more complex with this shifting. Lifting operation accidents are more severe than any other accidents because of the huge equipment masses and people involved (McMorran, 1998). Bøe & Nestegård (2010) worked out quick and simplified formulas for determining the dynamic loading conditions and the limiting sea state conditions for lifting operations and came out with two main criteria in

determining the performance of offshore lifting operations under the inclement weather conditions. Li, Gao & Moan (2016) also worked on the shielding effect during the lifting of a monopile to analyse the wave forces on the monopiles caused by the presence of the vessels and the effects of the wave spreading. Some of the major causes of incidents and fatalities in the offshore operations are mostly classified into the lifting and hoisting categories. Safe and efficient lifting procedures are required in the wind energy industry not basically for work planning, but to be a guard to the designer, when sizing equipment of energy systems, and a guard to invest when taking a decision on investment cost in further improvement. To further enhance safety in lifting operations in the offshore wind energy industry, different simulation methods are being deployed to simulate real life parameters like crane sizes, vessel heights, size, length and spatial constraint at the work area. Zhang & Hammad (2012) carried out a research on motion path planning of safe use of cranes during lifting using planning and replanning algorithms.

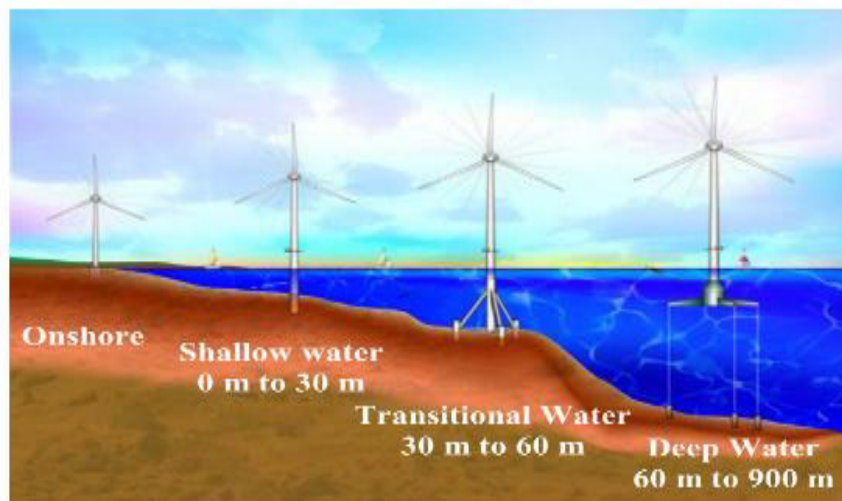


Figure 1-1 Technology progression of the offshore wind turbine installations (W. Musial et al., 2006)

Despite all the good models and algorithms for lift planning and execution, there remains the fact that without people (riggers banksmen, and tag line holders) the lifting will not be possible to execute as a human will be physically responsible for clamping the lift points to the cranes, directing the crane operators, guarding the load in place, and finally removing the talons as can be seen in Figure 1-2 and Figure 1-3.

The adequacy of a well-planned, written and managed lifting procedure can never be over emphasized as the lifting procedure will provide step by step sequence of carrying out both routine and non-routine lifting operation in the wind energy industry.



Figure 1-2 Lifting of blade into hub (London Array, 2013)



Figure 1-3 Lifting of tower onto transition piece (London Array, 2013)

1.1.2 Lifting Elements in the Wind Energy Industry

Despite the several regulations, guidelines and standards currently being used in the industry today, there has been a considerable focus on some key elements to enhanced good lifting operations (Lawrie, 2010). In the year 2005, the Oil and Gas producer's safety committee agreed on some other guidelines recommended practice for its operators and contractors to help them reduce the number of associated incidents to lifting and hoisting.

The kind of lifting equipment deployed for lifting in the onshore and offshore wind energy industry differs significantly and mostly depends on the weight, sizes of components, height of installation (height of lifting), weather conditions at the installation location, and metocean details of water

bodies. The onshore lifting equipment are mostly stand alone and driven on wheels to the installation location while for the offshore installation location they are carried or pre-installed on barges or floating vessels. The size capacity of this equipment is also dependent on design loads with factors of safety, height of installations, sea conditions included etc. Currently, research is being undertaken to design humans out of the lifting areas to compliment the lapses in the current lifting procedures. some of the lifting elements of a wind turbine are listed in Figure 1-5 and the conventional installation sequence is shown in Figure 1-4.

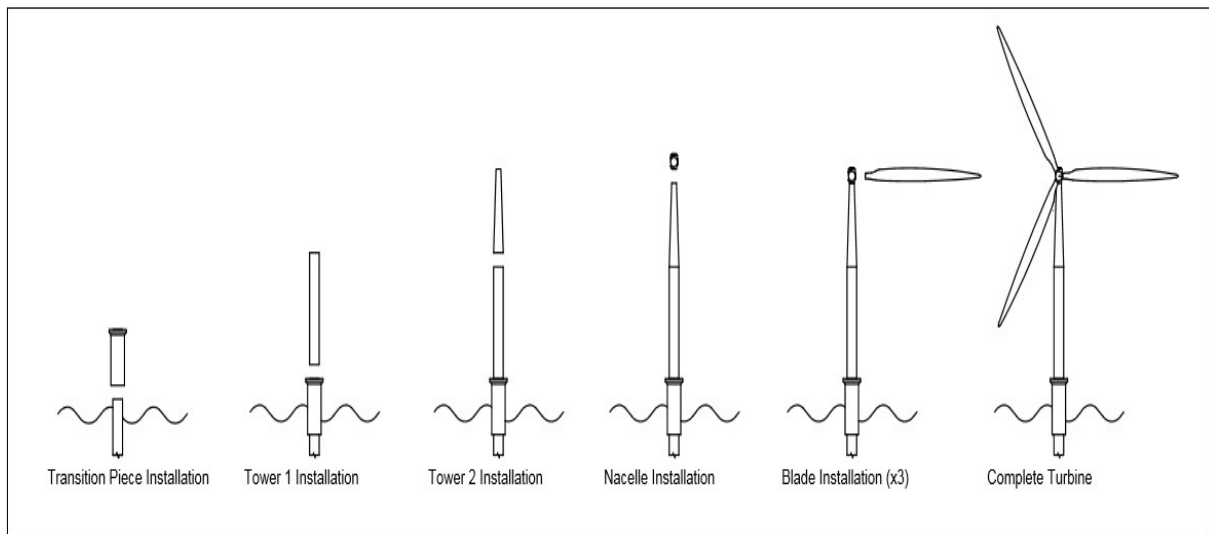


Figure 1-4 Lifting sequence of turbine components

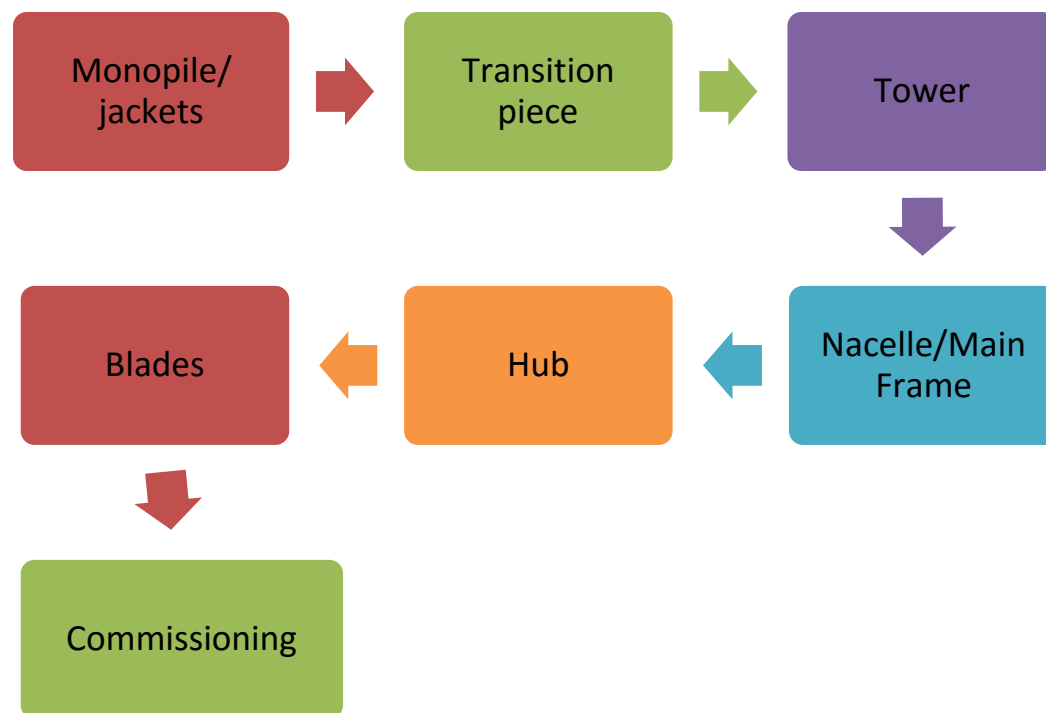


Figure 1-5 Wind energy components lifting sequence for conventional installation method

1.1.3 The Elements of a Lifting Procedure

Guidelines and standards are existing as presented in Section 2.1 to regulate lifting operations and lifting equipment conformance. One of this guideline is the Lifting Operation and Lifting Equipment Regulations (LOLER) of 1998 (renewableUK, 2013) . Other guidelines available in industry are the Det Norske Veritas (DNV) rules for the planning and execution of marine operations (2000), and GL Noble Denton guidelines for marine lifting and lowering operations.

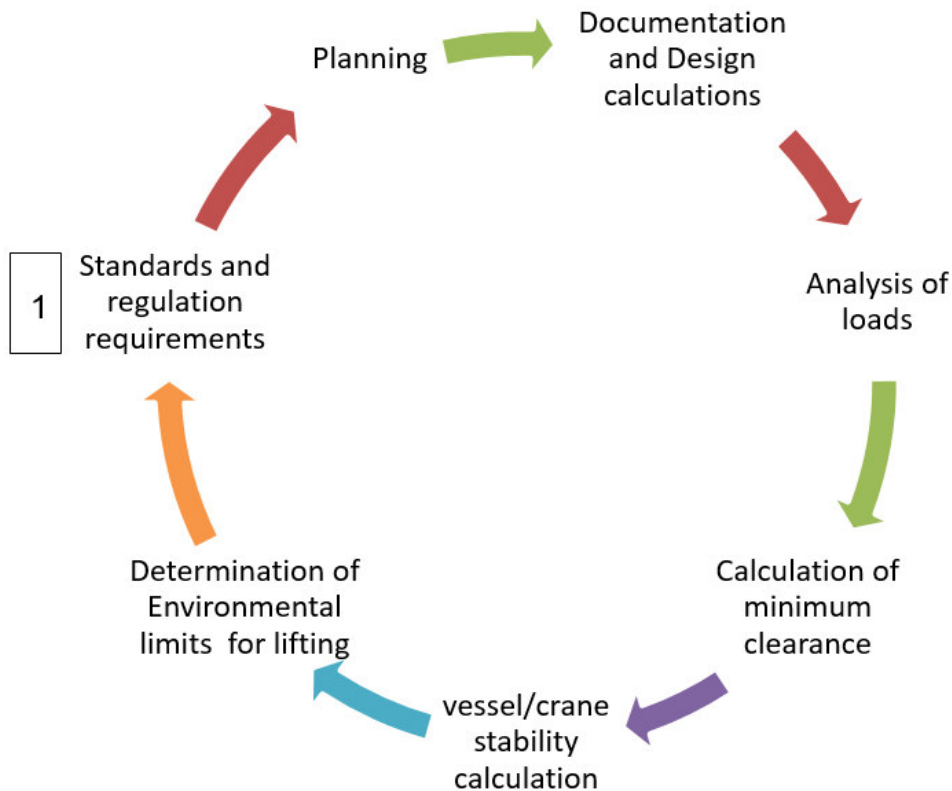


Figure 1-6 Lifting procedure preparation cycle

The first stage in the preparation of a lifting procedure is for the company to determine the statutory requirements of the country for this operation, to know the mandatory expectations to meet while planning for this activity, as shown in stage 1 of Figure 1-6. Non-compliance could amount to legal cases and fine payment since health and safety issues are keenly looked upon by the government. Most of this statutory regulation defines some of the key elements (Figure 1-7) to address in the planning operation stages.



Figure 1-7 Six key focus areas during the planning stages of a good lifting procedure

The planning stages for lifting operation, as shown above, includes roles and responsibilities definitions of key personnel involved in the lifting operation planning, execution and management. Definition of competency requirements for key personnel needed at each level of the operations, trainings and certification required of them. Another aspect of the planning stage is the definition of lifting and hoisting hardware's requirements, definition and colour coding strategy and lastly outlining a robust health and safety strategy to mitigate any foreseen safety and health risk associated with the lifting operation (Lawrie, 2010).

The third stage of the lifting procedure preparation is the documentation and design calculation stage which involves the verification of objective evidence from stage 2. The review of crane inspection reports showing load curve capacity and lifting capacity, lifting and hoisting hardware's certifications verifications, and finally lifting arrangement design calculation in cases where more than two cranes are needed based on the design.

The fourth stage, which is analysis of loads, involves detailed design and definition of module design weight (MDW), rigging weight (RW), module centre of gravity (CoG) determination, calculation of static hook load (SHL) and comparison with the results from stage 3. Dynamic hook load (DHL) and dynamic application factor (DAF) will be determined and compared with result from stage 3 (DNV, 2014a) as well.

In stage five, the lift characteristics, the limiting weather conditions and the consequence frequency shall be used to calculate the minimum load clearance.

In stage six, the load and stability calculations will be carried out using the various lifting conditions. For dynamically positioned barges a failure mode and effect analysis (FMEA) is always required. All conditions of the weather at elevated heights will be taken into consideration during the calculation and determination of stability of vessels and cranes anchored to the vessel deck.

In stage 7, critical assessment of lifting limits for different loads at different environmental conditions will be carried out using the prevailing wind speed at the location. In some other instance the limits specified by the crane manufacturer, aerodynamic attributes of the object to be lifted and facility owners specified limits should not be taken for granted (renewableUK, 2013).

A comprehensive lifting procedure or manual will contain details of all outlined above in a chronological order, this is a live document and should be updated daily once any of the existing parameters has changed, and the procedure cycle as outlined in Figure 1-6 should be repeated to ascertain the desired safety of equipment and personnel. Improper planning of the lifting process because of overconfidence even when prevailing condition changes are some of the reasons why accidents happens during lifting operations.

1.2 Relevance of Human-Free Lifting Solutions

Offshore wind energy has seen considerable investment in the last decade, driven by a growing awareness of the effects of climate change and a need to diversify energy production (Szulecki, Fischer, Gullberg, & Sartor, 2016; Voormolen, Junginger, & van Sark, 2016). By the end of 2006 the cumulative installed capacity of European offshore windfarms was approximately 1 GW, yet by the end of 2016 the total installed capacity had grown to 12.631 GW (EWEA, 2016). The offshore wind energy industry is set to show continued expansion and it has been estimated that the installed capacity across Europe would reach 24.6 GW by 2020 (EWEA, 2016).

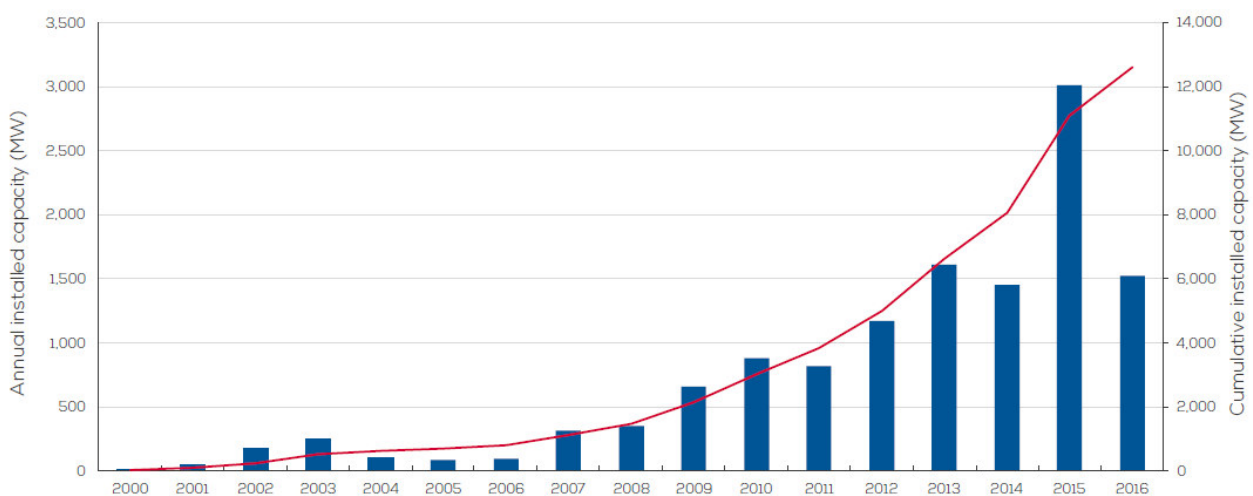


Figure 1-8 Installed capacity of offshore wind turbines within Europe (EWEA, 2016)

The installation of new turbines and continued maintenance of existing turbines will see the need for frequent onshore and offshore lifting operations. These may range from lifting large wind farm components, such as the tower or nacelle, or smaller loads such as tools, bolts, bags and personnel.

Whilst current guidelines attempt to preclude personnel from standing or walking below suspended loads this is not always possible. As illustrated by Figure 1-9 and Figure 1-10, personnel are frequently under lifts to guide loads in to position and secure them once in place.



Figure 1-9 (Fred. Olsen Windcarrier, 2016a)



Figure 1-10 (Fred. Olsen Windcarrier, 2016a)

1.2.1 Statistics and Incident Reports

To better understand the incidents that had occurred during lifting operations at offshore wind turbine sites, and to identify areas of risk, we made a request to G+ for the full data on incidents reported from across the wind industry. We received data from 2014, 2015 and from first to the third quarter (Q1 - Q3) of 2016. The fourth quarter of 2016 was not available at the time.

For the purposes of this study only incidents that had occurred at the site of the turbine were considered. Thus, reports related to activities in other locations, such as on vessels, at the quayside or in workshops, were removed. Table 1-1 below shows the total number of incidents reported each year and, of those, the number of incidents that involved dropped objects.

Table 1-1 Total incidents and dropped objects from 2014 to Q3 of 2016

	2014	2015	2016
Total incidents	66	58	50
Dropped objects	19	21	18

The number of working hours and operations differed from year to year. As such, we divided the total number of incidents and the total number of dropped objects by the number of hours worked for each year. This allowed comparisons to be made on the same scale. The number of hours worked for 2014 (23 710 000) and 2015 (21 220 000) were obtained from the published 2015 G+ incident data report (G9, 2015). As the 2016 incident data report had not been published we requested the number of hours worked in 2016 (15 460 000) directly from G+. Below, Figure 1-11 compares the total number of incidents and dropped objects per number of hours worked each year.

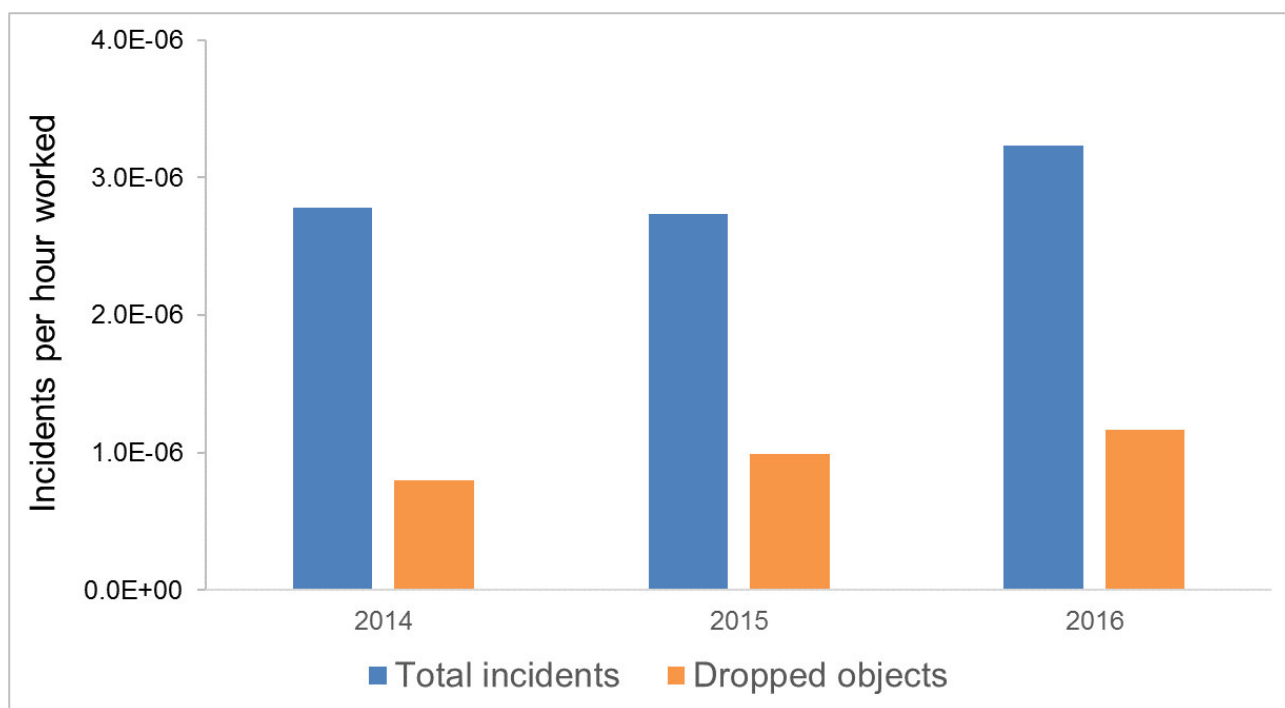


Figure 1-11 Total incidents and dropped objects per number of hours worked

From the data, we can see that 2016 saw the highest number of incidents and dropped objects per hour. Although the increase is relatively small, it does indicate that the safety of lifts offshore has not improved.

Sites were categorised within the data as either project sites, in which turbines were under construction, or operation sites, where turbines were operational. For each year, the number of incidents, including dropped objects, were far higher at operation sights than at project sites (Table 1-2).

Table 1-2 Total incidents and dropped objects from 2014 to Q3 of 2016

Operation site	2014	2015	2016
Total incidents	57	53	45
Dropped objects	40	19	16
Project site			
Total incidents	9	5	5
Dropped objects	7	1	2

However, the breakdown of hours worked between project and operation sites were unavailable so the data could not be normalised. It is possible that the increased incidents at operation sites were a result of greater working hours spent performing maintenance on existing turbines.

1.2.2 Reasons for Incidents

In reviewing the data, where possible, the underlying reasons for the occurrence of incidents were identified. These fell in to seven categories: existing procedures, incorrect personal protective equipment, human error, equipment failure, sea state, untrained personnel performing task, and unknown.

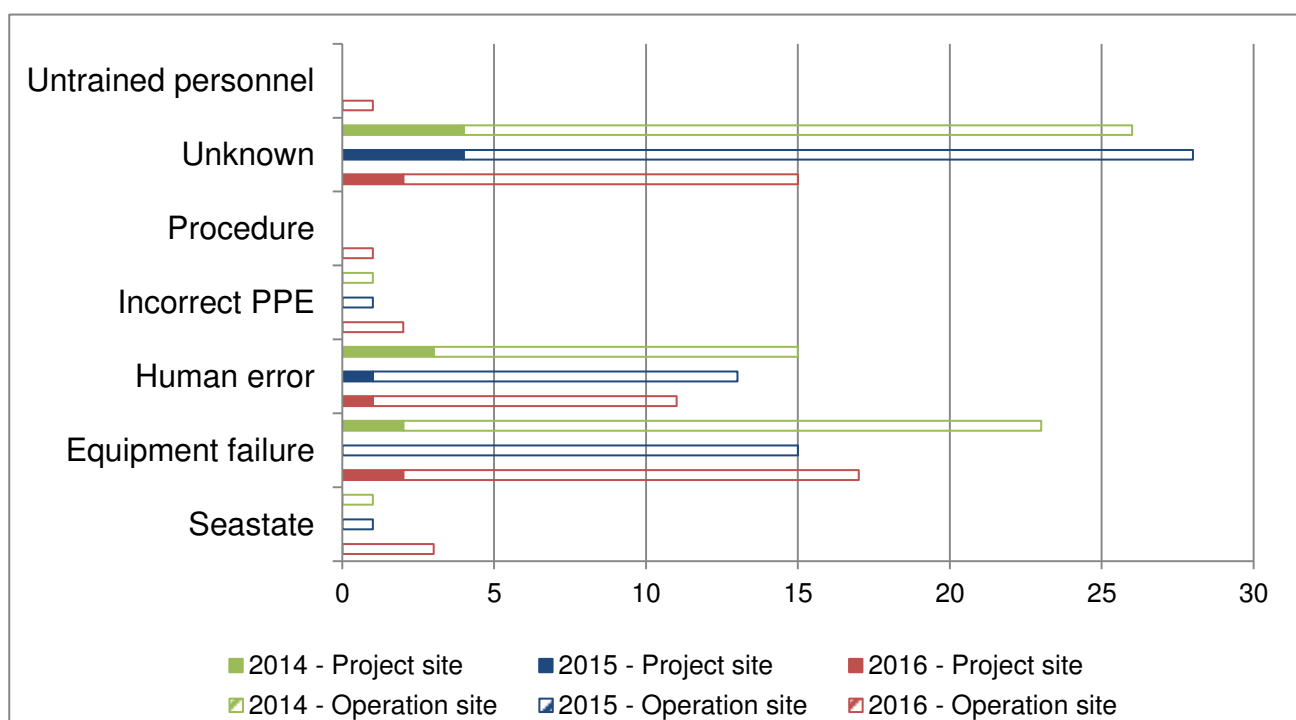


Figure 1-12 Reason for incidents at project sites

At both project and operation sites (Figure 1-12) human error and equipment failure appeared to be the most common causes of incidents. Indeed, at project sites, except for incidents with unknown underlying causes, either human error or equipment failure was responsible.

In comparison, other causes of incidents were few. At operation sites, adverse weather conditions were determined to be the cause of one incident in 2014 and 2015, and 3 in 2016. In addition, non-compliance with personal protective equipment (PPE) requirements was the reason for one report

in 2014 and 2015, and 2 in 2016. Personnel performing tasks without the proper training was the reason behind one report in 2016.

It is interesting that the reason for one report in 2016 was identified (by the personnel who reported it) as the procedures in place, which allowed personnel to be positioned beneath the bomb-bay doors of the nacelle.

Unfortunately, for most incidents at both project and operation sites the cause could not be determined as not enough detail was provided in the reports. This may well be because at the time of the incident the reason it had occurred was not clear to those on site. In some cases, incident investigations were pending however, the outcome of those investigations, if completed, were not included within the incident reports.

1.2.3 Areas of Risk

The data included the area in which incidents occurred. These were compared to identify high-risk zones. It should be noted that the number of hours spent working in each area were not available. Therefore, we cannot be sure that most incidents were simply occurring in areas where most of the work was being performed.

In each year, the transition piece and nacelle were the locations of the highest number of incidents at both project and operation sites (Figure 1-13).

Additionally, at project sites the turbine tower was a location of a relatively high number of incidents in 2014. However, far fewer incidents were reported to have occurred at project sites than at operation sites.

At operation sites, there was a high occurrence of incidents on turbine towers, particularly in 2014 where 18 incidents were reported. This was equal to the transition piece and the nacelle for the same year. In subsequent years, a higher number of incidents were reported on transition pieces and nacelles than turbine towers.

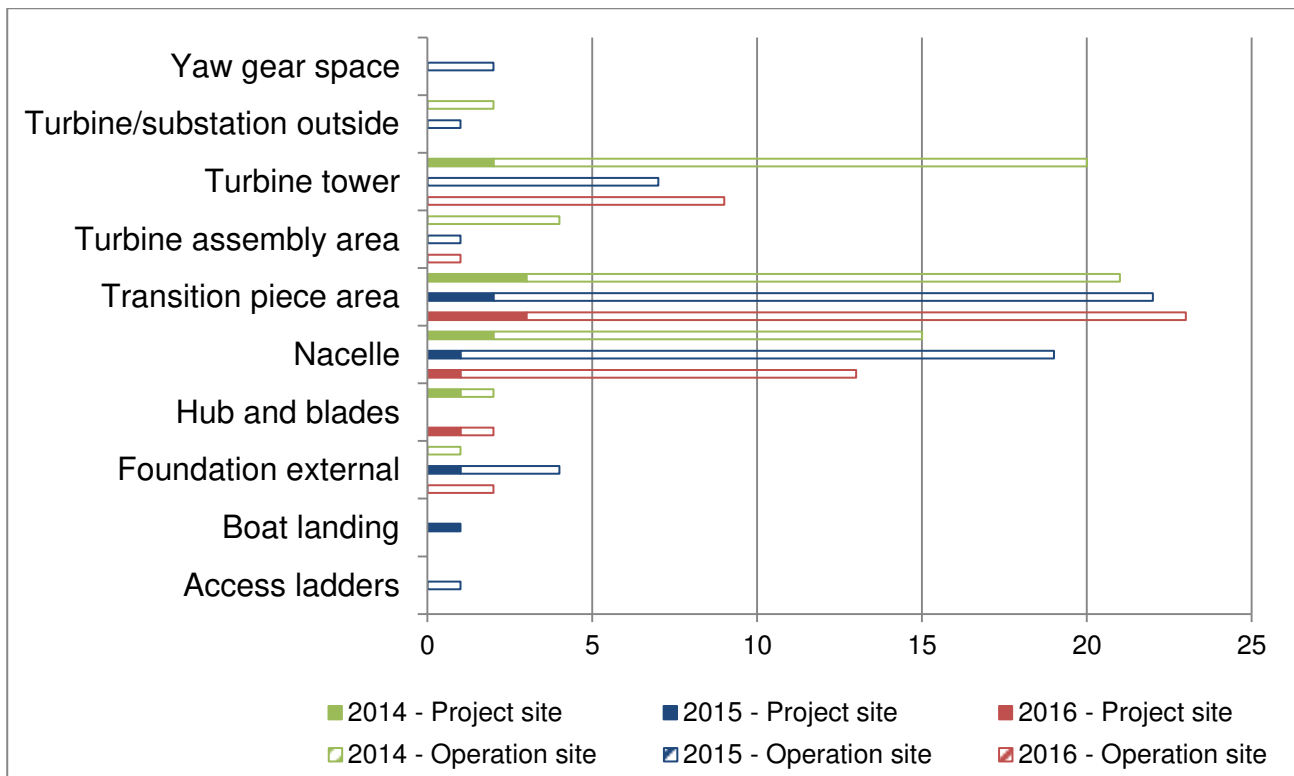


Figure 1-13 Area of incidents at project sites

1.2.4 Actual Consequences

Actual consequences of incidents were specified in the data from G+. No medical evacuations (Medivac) occurred between 2014 and Q3 of 2016.

For both project sites and operation sites, near hits were the most common consequence in 2014 and 2015. At project sites in 2016 reported hazards were equal to near hits, with 2 occurrences. Identified hazards were comparatively common in 2014, with 3 occurrences. In 2014, medical treatment was required following 1 incident and in 2016, 1 incident resulted in a restricted work day. Near hits and identified hazards were also the most common consequences in each year at operation sites. Although near hits were far greater in 2014, whilst hazards were relatively low. In addition, there was 1 restricted work day in 2014 and in 2015. There was also 1 lost work day in 2014 and in 2015. In 2014, there was 1 incident that required first aid, and in 2015 2 incidents required further medical treatment after personnel had returned home.

Many incidents were identified as high potential incidents in the data. These are incidents that had a high potential for severe consequences, such as serious injury, mortality, or structural damage. In 2014, 10 incidents at operation sites and 1 at a project site were highlighted as being high potential incidents. In 2015, the highest number of high potential incidents at operations sites were reported, with 25, and there was 1 at a project site. In 2016, there were 17 high potential incidents reported at operations sites, however all 5 incidents that occurred at project sites were identified as high potential incidents.

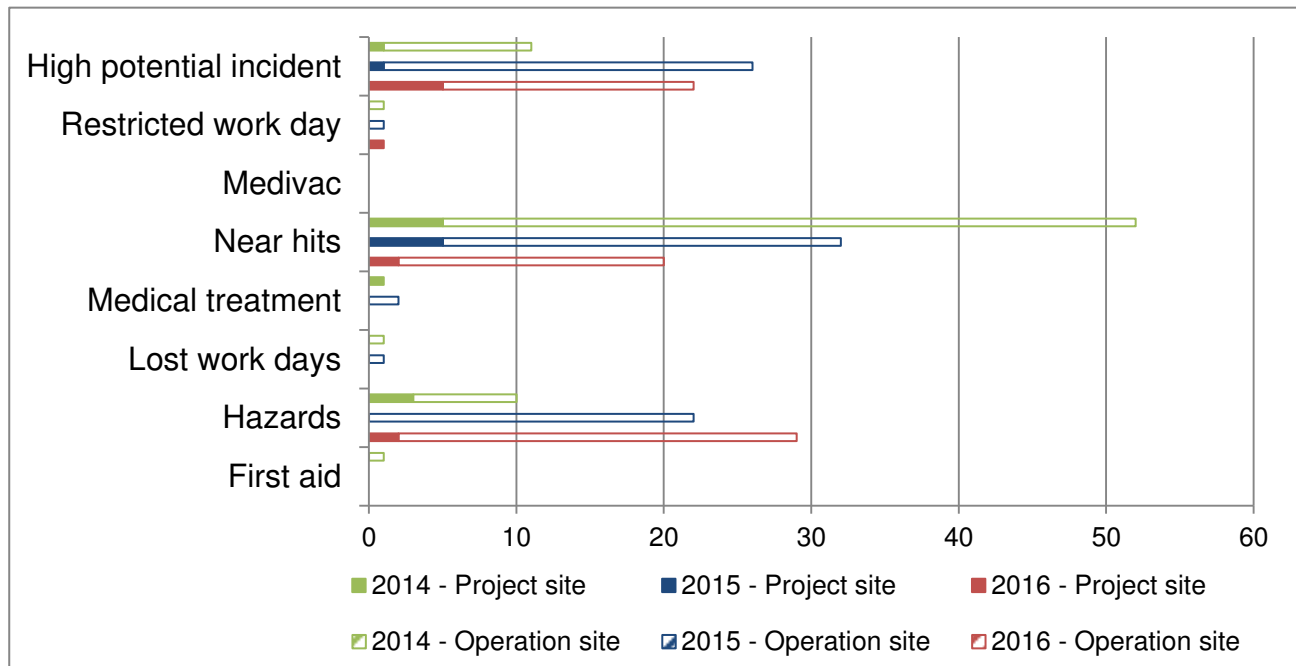


Figure 1-14 Actual consequences of incidents at project sites

1.3 Guideline for Human-Free Offshore Lifting Operations

1.3.1 Motivation

There will always be a degree of risk in lifting operations. Such risks may be reduced through careful planning and procedures and guidelines have been brought in place to ensure personnel follow safe practices. However, it is highly unlikely that failures or errors can be prevented or avoided 100 percent of the time.

In reviewing the incident data available, the most common incidents included dropped objects, such as tools, chains and bolts. Equipment failure or human error were frequent causes of dropped

objects. If such objects were to hit personnel, it could result in serious injury or loss of life. Thus, removing personnel from areas where falling objects could land would greatly reduce the risks to personnel.

The motivation for this project was to conduct research in to methods and technologies that could reduce the need for personnel in the vicinity of lifting operations and assess their feasibility.

1.3.2 Approach

A clear project management plan, presented in Appendix A, was prepared which included a breakdown according to a schedule (Figure 1-15)

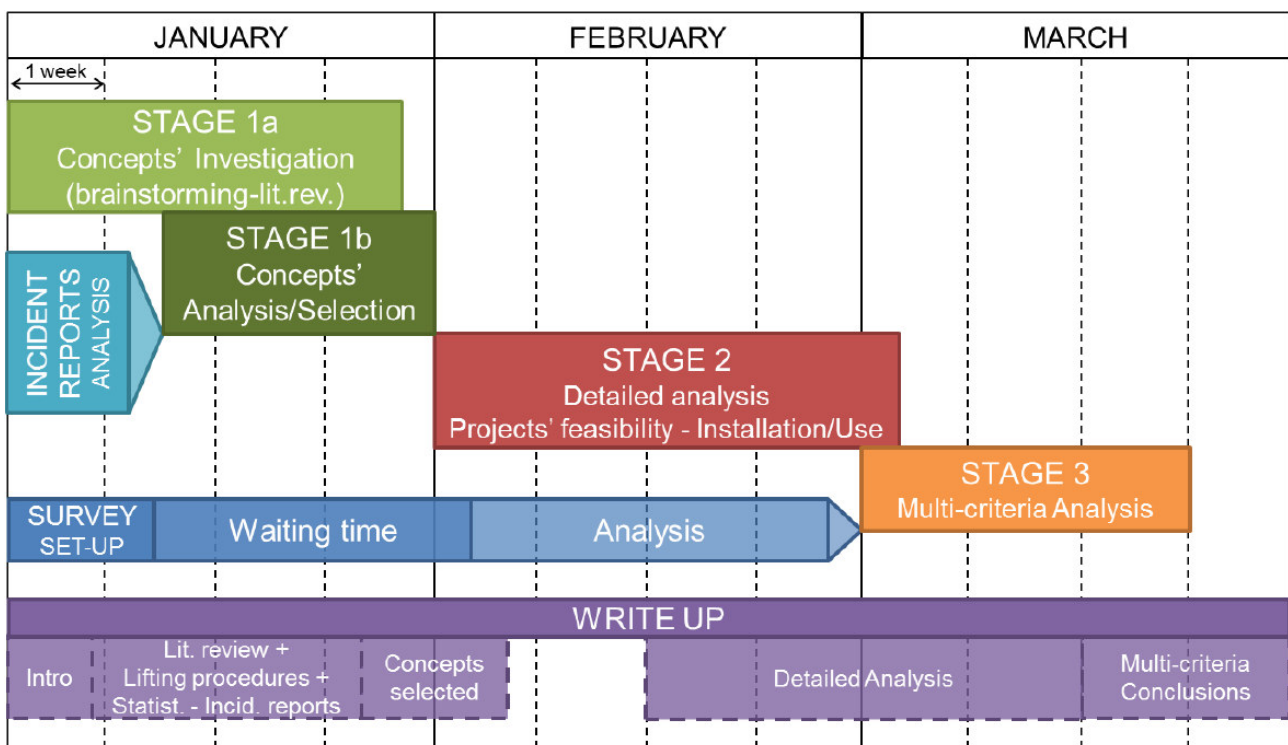


Figure 1-15 Project Schedule

Having identified some of the reasons for the occurrence of incidents, the areas of risk and the actual consequences of those incidents, the first stage was the concept investigation. This involved a literature review and websearch for existing technologies for reducing the human element in areas of high-risk during lifting operations. These included tools currently in use in industry, as well as new and conceptual designs. Some innovative solutions were also developed within group.

Technologies were separated into three areas, guiding and control, connections, and assembly. These were assessed by team members, in terms of their feasibility, and were either eliminated from further consideration or taken forward to the next stage.

The second stage was a detailed analysis of selected concepts. Technologies were assessed according to a set of criteria, which included feasibility, maturity of technology, cost and reduction of risk. In addition, some possible solutions were trialled.

During the third stage, a survey was circulated to collect opinions from those in industry and academia within field of offshore wind energy, in regard to the importance of certain criteria when considering the viability of new technology and techniques. The data was kept anonymous and was used as part of a multi-criteria decision analysis. The results of this analysis were to inform the refinement of options and to rank final recommendations.

1.3.3 Report Overview

This report details our findings for solutions for lifting operations on offshore wind turbines. In Section 2 current guidelines for existing offshore lifting operations are discussed, and existing human-free lifting operation systems are presented.

Section 2 is separated into the three concept areas, 'Concepts for Guiding and Control', 'Concepts for Connections and Seafastening' and 'Concepts for Assembly'. In each of these sections a detailed analysis of new and existing concepts are provided, along with the results from any experiments or trials.

In Section 4 the positive and negative aspects of human-free lifting solutions are addressed, and the multi-criteria decision analysis, including results, are discussed.

Section 5 summarises the findings of the study and outlines our recommendations and potential outlook for human-free lifting in the offshore wind energy industry.

2 SUMMARY OF EXISTING GUIDELINES

Offshore lifting operations are performed quite often, already with a long history in the oil & gas industry and more recently in the offshore wind industry. Thus, a literature review is conducted to provide an overview of guidelines for lifting operations (Section 2.1), as well as existing human-free lifting operation systems (Section 2.2).

2.1 Guidelines for Lifting Operations

The guidelines for lifting operations can be divided into more general standards (Section 2.1.1) and special regulations for offshore lifting operations (Section 2.1.2). The following sections are not presenting a complete list of existing guidelines and regulations, but should rather give an overview and refer to some main guidelines for further detailed information.

2.1.1 Regulatory Requirements and Codes of Practice for Lifting Operations

There are various standards, guidelines, and regulations existing for lifting operations. The most essential ones, which are also often used as basis for further guidelines, are presented in the following.

The Lifting Operations and Lifting Equipment Regulations (LOLER) 1998 (Statutory Instruments, 1998) “applies to lifting equipment and builds on the requirements of the Provision and Use of Work Equipment Regulations (PUWER)” (Health and Safety Executive, 2014, p. 1). Those regulations cover topics such as lifting equipment installation, examination, as well as the planning of the lifting operation, and special equipment for lifting personnel. Phrases like “shall ensure” and “as to reduce to as low as is reasonable practicable the risk”, both (Statutory Instruments, 1998, p. 4), are helpful formulations with respect to health and safety in lifting operations, but do not give any recommendations for the practical realisation.

Some more details about the planning, control, and management of the lifting operation, as well as about the equipment and load integrity are mentioned in (International Association of Oil & Gas Producers, 2006) and (British Standards, 2006). The latter standard gives, in addition, further recommendations regarding cranes. Besides this general part of the British Standard “Code of

Practice for the Safe Use of Cranes” BS 7121, other parts focus on more specific topics, such as part 11 which covers offshore cranes (British Standards, 1998).

2.1.2 Offshore and Marine Energy Regulations for Lifting Operations

While the guidelines, mentioned above in Section 2.1.1, only cover lifting operations in general, with the exception of a few specific additions, some regulations are explicitly for offshore lifting operations.

The International Marine Contractors Association (IMCA) aims “to improve performance in the marine contracting industry” (IMCA Holdings Ltd & IMCA Trading Ltd, 2017) and provides guidelines for lifting operations, as well as documents about crane specifications. However, those publications are only available for IMCA members.

Concerning health and safety topics such restrictions should not apply, but many other guidelines are publicly available. The G9 Offshore Wind Health & Safety Association (now G+) for example focuses on improving offshore operations with respect to health and safety. In their good practice guideline for work at height (G9 Offshore Wind Health & Safety Association, 2014) they cover issues such as risk assessment, dropped objects, and transfer of personnel, as well as specific topics related to the offshore wind industry.

Another quite specific guideline is given in (renewableUK, 2013) which only looks at offshore renewable energy operations using jack-ups, but also covers the lifting operation, including load calculation and analysis.

The well-known companies Germanischer Lloyd (GL), Noble Denton, and Det Norske Veritas (DNV), finally merged to DNV GL, have provided many rules, standards (ST), and recommended practices (RP) for classification, service specifications (SE), marine services, and renewables certifications (DNV GL, 2016b). Many of those documents are now collected in one standard DNVGL-ST-N001 (DNV GL, 2016a), which covers various topics about marine operations and marine warranty in great detail.

2.2 Existing Human-Free Lifting Operation Systems

Although the human is currently directly involved in offshore lifting processes, and thus exposed to the risk of being under the load, there are several existing concepts, some already used in industry, which reduce the risks in offshore lifting operations and could make a valuable contribution to human-free offshore lifting solutions. In the following, some selected systems are presented, grouped into four categories: supports in the lifting operation itself, guiding systems, support at the stage of connecting, and assembly solutions.

2.2.1 Support in Lifting Operations

A main problem in offshore lifting operations is the large motion of the lifted component. This could be due to the element being freely hanging on some ropes, connected to the hook of the crane, but also amplified by wind loads and sudden gusts, which occur regularly in the offshore environment.

A great amount of the motion of the load can be reduced by the Boom Lock, presented in Figure 2-1. This system locks the hook of the crane and thus reduces the degrees of freedom for the motions of the lifted element. This way the load can be controlled even at high wind speeds. (High Wind, 2014)

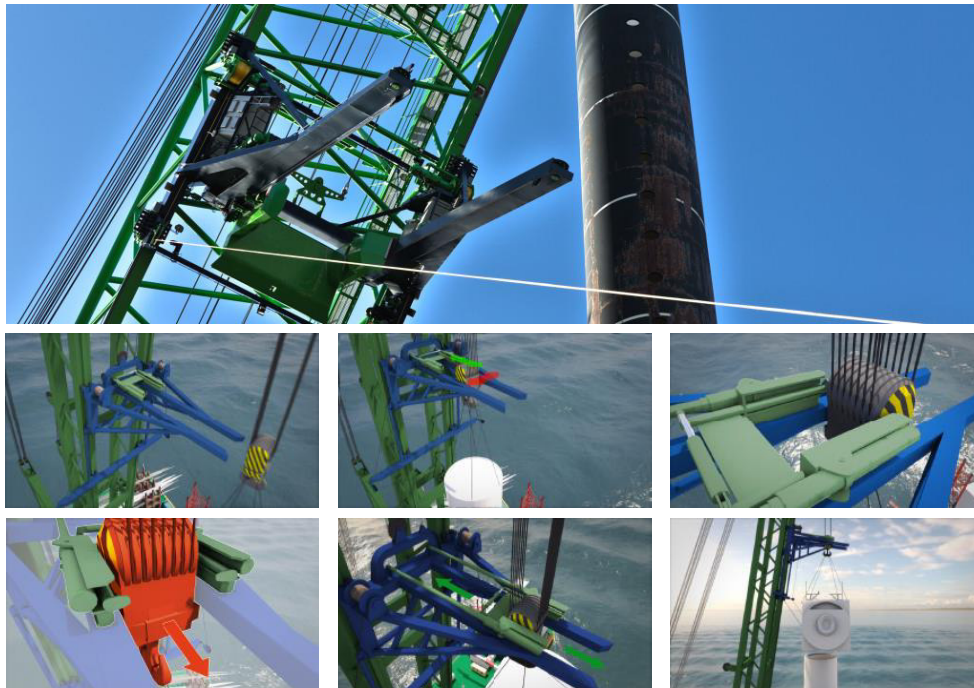


Figure 2-1The Boom Lock (High Wind, 2014)

Another issue in the lifting process is the correct orientation of the load. Especially for installation of the blades, which are typically mounted to the hub in horizontal direction, special lifting tools are needed. AH-Industries (2016) offers several products for lifting and handling blades, towers, and nacelles. One example is the tagline master winch, presented in Figure 2-2, which can be used for safe and accurate lifting of blades, rotors, or nacelles. A similar tool, however more advanced, is the Blade Dragon, shown in Figure 2-3. With this remote controlled equipment, blades can be lifted and installed at any angle (Liftra, 2014). Lacking some experience with this enhanced tool, currently the horizontal installation method with the common used blade yokes is currently still mostly preferred, especially onshore.

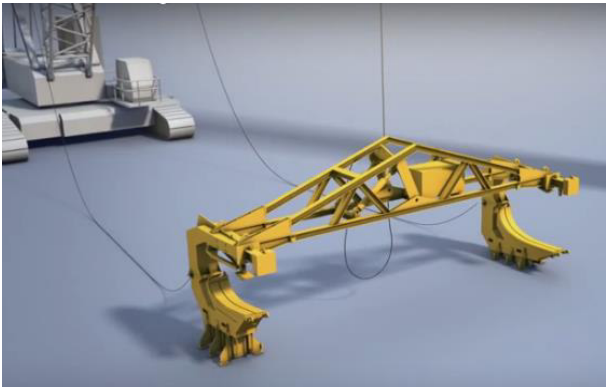


Figure 2-2 Tagline master winch (AH-Industries, 2016)



Figure 2-3 Blade Dragon (Liftra, 2014)

2.2.2 Guiding Systems

In the final stage of the lifting process, accurate placement of the load is required. In order to get both elements centralised and fitting with respect to the connection parts, special guiding systems are used.

One example of a guiding system are guide cones. Those were used at the installation of two meteorology masts on Dogger Bank. During this operation, the met mast sections were installed without having people under the load. This was feasible with the help of taglines and plastic guide

cones, tied around the flanges, as shown in Figure 2-4. Without significantly increasing the total costs, the lifting operation could be sped up and made safer. (Forewind, 2013)

Other common guiding elements are guide pins, which are especially used for the installation of wind turbine blades. The blades typically come with already installed bolts. Two, diametrically opposed, are replaced by guide pins, which are longer than the bolts and thus sticking out, allowing correct positioning of the blade bolts with respect to the bolt holes at the hub. Such a guide pin can be seen in Figure 2-5.



Figure 2-4 Guide cones (Forewind, 2013)



Figure 2-5 Guide pins (MacFarlane, 2016)

2.2.3 Support in Connecting

Having positioned the lifted element correctly onto the counterpart, the next step in the installation process would then be the connection of both elements. It is not uncommon to have more than 120 bolts at each flange connection. Mostly, the bolts are already assembled on the lifted element, which at least saves the labour of manually placing the bolts in the holes. Still, every single bolt needs to be tightened accurately.

For assembly on the ground, robots are already used. Müller et al., (2014) introduce a robot guided bolt tensioning tool, presented in Figure 2-6, which enables automated tensioning of bolts for connecting rotor blade bearings to the hub. A similar robot is designed by ITH Bolting Technology (2016). This ITH Autostretch bolting robot arm identifies the bolts with a camera, tensions them with auto-bolt-tensioning-cylinders, and automatically controls the hydraulic pumps.

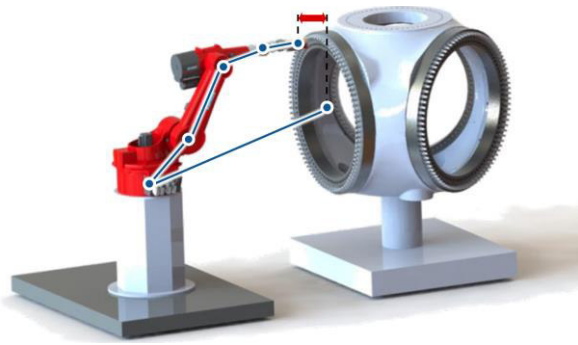


Figure 2-6 Robot guided bolt tensioning tool (Müller et al., 2014)

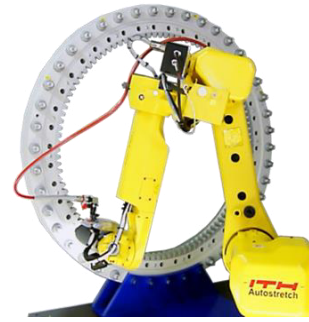


Figure 2-7 ITH Autostretch (ITH Bolting Technology, 2016)

For connections offshore at the installation site, such a robot has to be at the flange connection of the two wind turbine elements. A bolt robot for those uses, which includes a robot control system, is proposed in the patent by (Johst, Jagd, Bovin, & Marinitsch, 2013) and presented in Figure 2-8.

However, the remaining question is still, how the robot itself will be place at the high elevated flange connections. Maybe climbing robots (Figure 2-9), currently used for wind turbine inspection, could be a helpful basis for further ideas of having a climbing bolt robot.

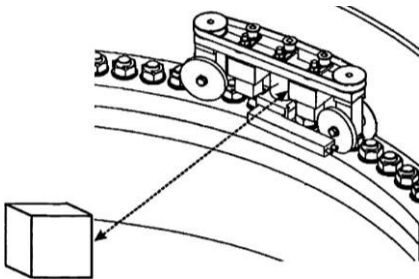


Figure 2-8 Bolt robot, adapted by the author from (Johst, Jagd, Bovin, & Marinitsch, 2013)



Figure 2-9 Climbing robots, left (Lombardo, 2013) and right (Webster, 2013)

2.2.4 Assembly Solutions

A completely different human-free offshore lifting solution would be reduction or exclusion of any lifting operation during installation. This, however, requires transport of fully pre-assembled wind turbines. Vuyk Engineering Rotterdam b.v. (2017) presents a specially designed wind turbine

installation vessel, shown in Figure 2-10, which uses a heavy lift crane with motion compensation for installing fully pre-assembled wind turbines. The vessel itself can carry several wind turbines and remains floating during the installation process.



Figure 2-10 Installation vessel for fully-assembled wind turbines (Vuyk Engineering Rotterdam b.v., 2017)

Another option is to use floating wind turbine designs. Tri-floater- or semi-submersible-type floating wind turbines can be fully assembled at the quayside and then tugged vertically to the installation site. Thus, no offshore lift is needed anymore. This installation method has already been used, for example for the WindFloat (Figure 2-11) or the Fukushima Hamakaze (Figure 2-12).



Figure 2-11 Tow out of Principle Power's WindFloat (Bush, 2015)



Figure 2-12 Tow out of Fukushima Hamakaze 5MW Hitachi wind turbine (Trabish, 2016)

Also for transporting a spar-type floating wind turbine, a human-free installation solution exists: the WindFlip, presented in Figure 2-13. This specialised barge transports the fully pre-assembled spar-

type wind turbine horizontally. Buoyancy control facilities at the WindFlip allow self-tilting of the entire system.

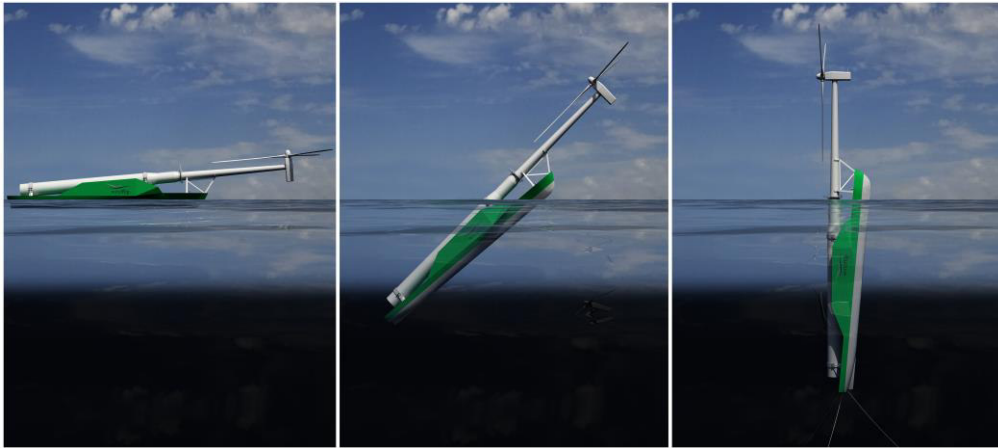
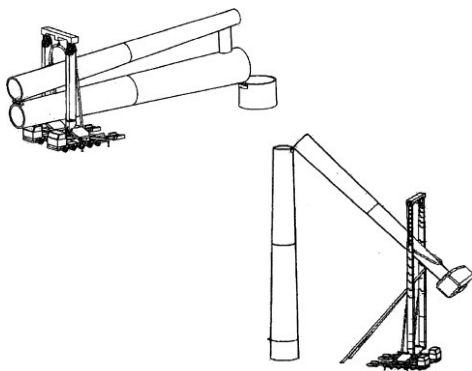
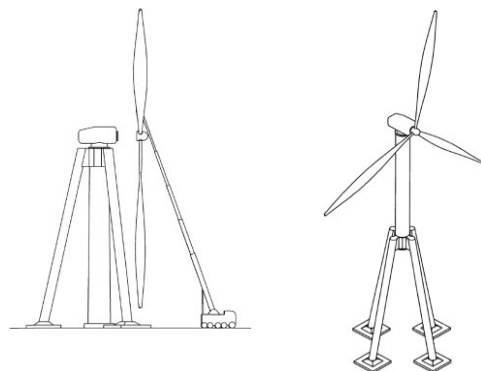


Figure 2-13 WindFlip (Jensen, 2010)

Besides these already used offshore human-free assembly and installation solutions, there are some more ideas for self-erecting wind turbines, which only exist as patents for onshore installation. Dehlsen & Mikhail (2005) present a self-erecting wind turbine, which consists of hinged tower elements. The tower is then raised by using a telescopic crane, schematically shown in Figure 2-14. Conversely, no crane for erecting the tower is needed in the proposal by (Gee & FL, 2011). In this solution, presented in Figure 2-15, the tower is erected with the aid of a telescoping pylon on three legs, using a hydraulic pulling device.



**Figure 2-14 Hinged self-erecting tower
(Dehlsen & Mikhail, 2005)**



**Figure 2-15 Telescoping self-erecting tower
(Gee & FL, 2011)**

3 CONCEPTS FOR HUMAN-FREE OFFSHORE LIFTING OPERATIONS

To come up with solutions for human-free offshore lifting concepts, the further work was split up into three categories: guidance and control (Section 3.1), connections (Section 3.2), and assembly (Section 3.3). Each section is structured in a similar way. First, the category itself is introduced and the main objectives explained. Afterwards, the initial proposed human-free offshore lifting solutions are presented, based on the detailed literature review, carried out at the beginning of this group project work. Finally, the selected most promising ideas and their detailed development are presented. Each section then closes with a short summary.

3.1 Concepts for Guidance and Control

The first concepts for human-free offshore lifting operations, which will be presented, can be categorised into guidance and control of the offshore lifting process.

3.1.1 Introduction

Wind turbine installation includes lifting of single parts, such as the tower, nacelle, or blades, from the vessel onto the already installed parts of the offshore wind turbine. Independent of how many lifts are performed and which element is lifted it has to be ensured that the lifted part is finally placed correctly, so that both elements can be connected to each other. Around 120 or even more bolts are used at each flange connection, which shows how relevant accurate alignment of the bolt holes of both sections is. For this reason, guidance and control are the main supports during lifting operations. However, guidance and control not only ensure correct positioning, but also are used to avoid clashes, react to sudden gusts, and reduce large motions of the load.

3.1.1.1 Global and Fine Hoisting

In order to break down the lifting process, two stages are defined in the following: global hoisting and fine hoisting.

3.1.1.1.1 Global Hoisting

Global hoisting describes mainly the lift from the stationary position of the element on the vessel close to the aimed position. Close in this context means that the load should be brought above (for vertical connection) or next to (for connection in horizontal direction or at an angle) the already installed counterpart. No precise alignment is yet needed at this stage. However, it is more important to keep the unwanted movement of the lifted part as low as possible, as global hoisting covers the longest lifting distance. Furthermore, wind loads affect the motion of the lifted element, and thus strong gusts have to be taken into account during global hoisting. Finally, it has to be ensured that throughout the lift, the load does not collide with other elements, such as structures on the vessel, the vessel itself, the crane, or the already installed wind turbine segment.

3.1.1.1.2 Fine Hoisting

In the stage called fine hoisting, the load should be brought close to the counterpart, positioned correctly, and connected for installation. Thus, in this stage, accurate positioning plays an important role. Due to the fact that one is dealing with circular connections at any level of the wind turbine, centring of the load with respect to the installed part is one step of the fine hoisting procedure. Another step is the correct rotational orientation. However, not only the bolt holes have to be aligned, but also the two elements have to be in the correct global orientation to each other. The latter one refers for example to the ladder inside the tower, which is already pre-installed at one location, the nacelle, which has to face in the right direction, or the blades, which are not even symmetric elements.

3.1.1.2 Current Practices

In order to lift single wind turbine components into the correct position, certain guiding and control devices, such as taglines or guide pins, are already used. However, the human is still involved in this lifting procedure. Either people are holding the taglines and thus are standing in the area where the part is being lifted, or they are directly within the already installed wind turbine part in order to give commands to the crane operator. This is because the operator may not be able to see the connection at certain heights, or to manually push and guide the lifted part into its final correct position (Figure 3-1).



Figure 3-1 People guiding manually the load (Fred. Olsen Windcarrier, 2016b)

3.1.2 Initial Proposed Solutions

3.1.2.1 Mechanical Guidance

Mechanical guidance systems are currently, together with fine tuning control devices, the most common supports used in offshore lifting operations. Mechanical tools can be classified according to their guiding orientation into two groups: guide pins or similar tools for rotational alignment of the bolt holes, and funnels or cones for centralisation. In the following, some examples of already used or proposed mechanical guidance systems, which could support human-free lifting operations, are presented.

3.1.2.1.1 Guide Pins

For aligning the bolt holes of the two sections that are to be connected, some bolts can be replaced by 'guide pins', which are slightly longer than the bolts and have a conical end. An example of such a guide pin is presented in Figure 3-2, which again highlights the involvement of people directly under the load.



Figure 3-2 Current use of guide pins (SCHEUERLE Fahrzeugfabrik, 2012)

This basic idea of guide pins is modified in several patents. M. J. S. Jensen (2013) proposes an aligning tool, similar to such a guide pin, which is screwed onto the bolts (Figure 3-3, with aligning tools coloured in red). In (Moeller, Nielsen, & Svinth, 2016) an arrangement of two guide pins of different lengths, presented in Figure 3-4, is used to align two parts of a wind turbine, so that the longer one (coloured in red) matches the first, and afterwards the shorter one (coloured in yellow) gives the final total alignment of the elements. Finally, Øllgaard (2014b) suggests an adapted guide pin with a resiliently deformable part, shown in Figure 3-5.

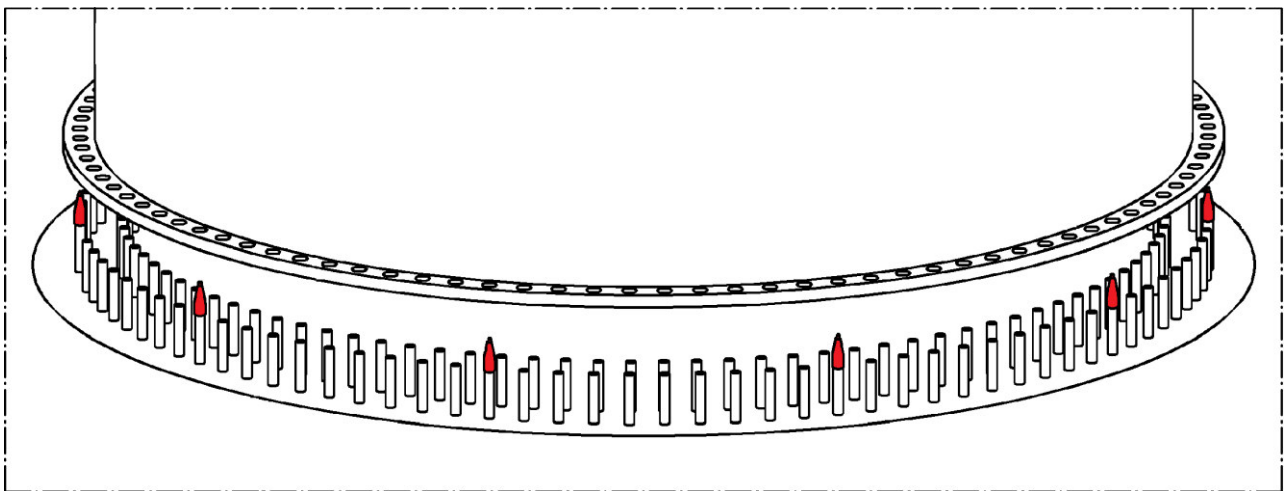


Figure 3-3 Patent for an aligning tool, adapted by the author from (Jensen, 2013)

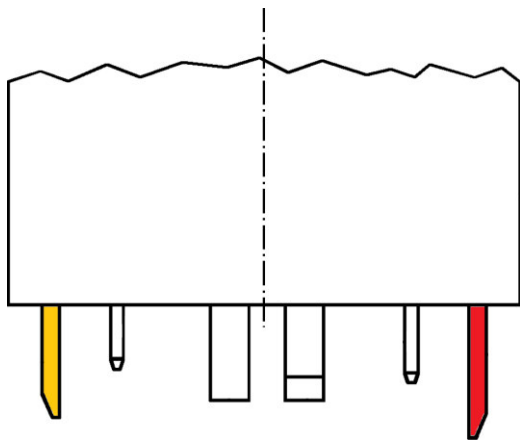


Figure 3-4 Patent for an aligning arrangement, adapted by the author from (Moeller et al., 2016)

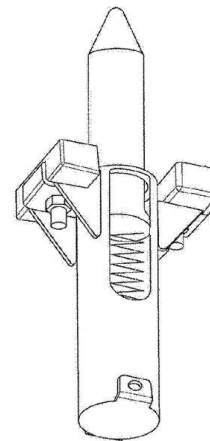


Figure 3-5 Patent for an alignment tool with a resiliently deformable part, adapted by the author from (Øllgaard, 2014b)

Besides using these typical guide pins, other concepts, such as the method by (Bitsch & Baun, 2012), presented in Figure 3-6, which is composed of a special shaped guide rod (coloured in red) on one tower element, fitting into a socket section (coloured in yellow), which is attached to the counterpart, exist. A composed solution for centring and rotational positioning is proposed by Moestrup & Westergaard (2014). Figure 3-7 shows in red the guide pin for aligning the bolt holes, and in yellow the guidance device for easier positioning of the lifted upper tower segment.

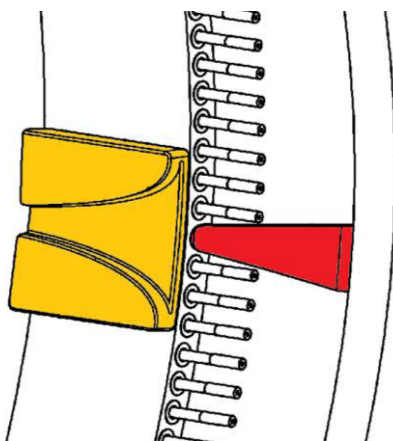


Figure 3-6 Patent for an apparatus for mounting wind turbine blades, adapted by the author from (Bitsch & Baun, 2012)

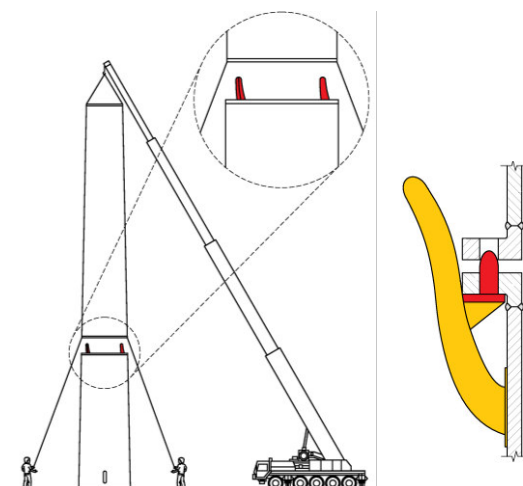


Figure 3-7 Patent for a tower assembly system, adapted by the author from (Moestrup & Westergaard, 2014)

3.1.2.1.2 Funnels and Cones

The latter example, presented in Figure 3-7 in the previous Section 3.1.2.1.1 directly leads over to the next type of mechanical guiding systems: funnels and cones, which allow centring of two elements. A similar design, although without any rotational guiding elements, is presented by Øllgaard (2014a) and shown in Figure 3-8. Another concept for aligning two elements with respect to their central axes is proposed by Spence & Russell (2013) and visualised in Figure 3-9.

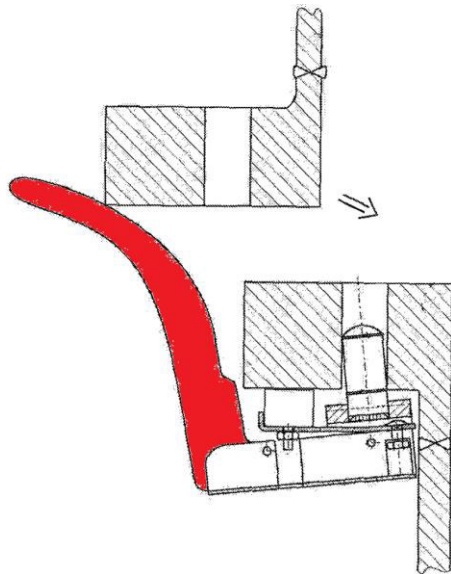


Figure 3-8 Patent for an aligning device, adapted by the author from (Øllgaard, 2014a)

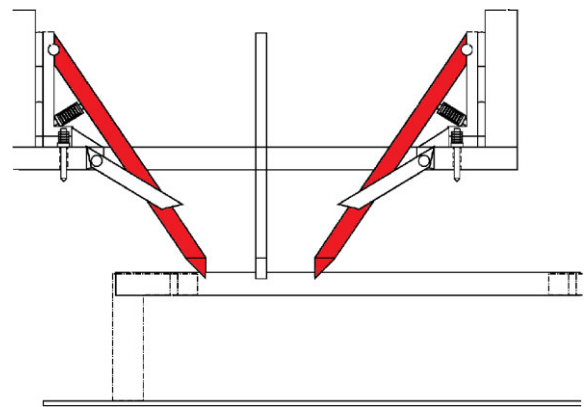


Figure 3-9 Patent for an alignment system, adapted by the author from (Spence & Russell, 2013)

Besides those theoretical ideas and inventive patents, one solution for a centralisation device has already been used in practice: plastic guide cones, which were put around the flange connection of a met mast (Forewind, 2013). Figure 3-10 presents some pictures of this human-free met mast installation.

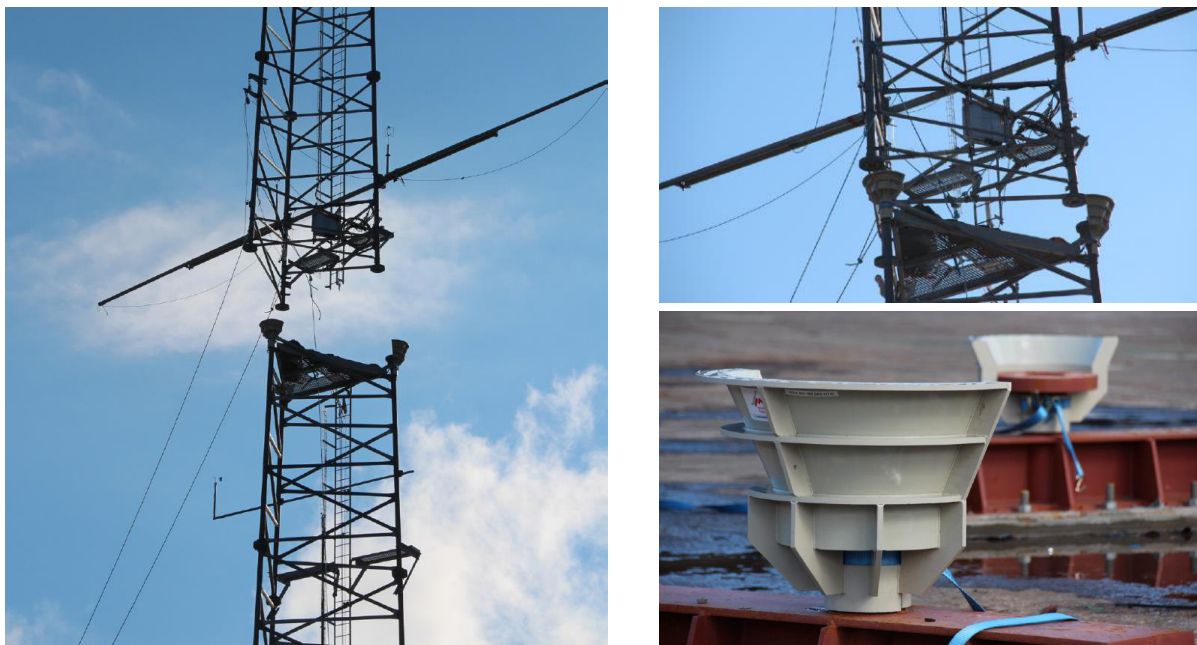


Figure 3-10 Guide cones for human-free met mast installation (Forewind, 2013)

3.1.2.2 Visual Guidance

Visual guidance via a suitably placed banksman giving clear orders to the crane operator is simple, effective and, assuming good protocol, safe. For the majority of industries and payloads, successful lifts can be achieved with the banksman close enough to the lifted object without being below the load. When installing offshore wind turbine components this is rarely possible due to the marine environment and nature of the structure, hence the need for banksmen in potentially dangerous positions. This section presents ideas for moving the banksman away from the load whilst keeping the visibility of a local field of view.

3.1.2.2.1 Mirrors

The most basic way to alter one's field of view is through mirrors. Mirrors, correctly placed, can be useful for crane operators to see behind or around corners without requiring movement. They are best used at near distance, however, so if dealing with large parts and large distances, may not be practicable. Accurate placement could also be difficult and even at the correct position use of a mirror may not be useful if the load is moving. Fixed mirrors, facing the connection of the already

installed part, combined with movable mirrors, controlled by tracking the load (similar to solar tracking systems for solar panels), could be helpful but this would be maybe too complex for real application

3.1.2.2.2 Multiple Cameras

Cameras, such as Closed Circuit Television (CCTV), provide a remote live feed of a chosen location. The field of view of the camera or multiple cameras can be easily transferred to a monitor in a chosen location wirelessly or hard-wired.

The use of cameras during lifting has been developed by companies such as 'HoistCam', a durable camera system that is attached magnetically to the boom of the crane to give operators visibility particularly during blind or far lifts. According to their website, these have mainly been used onshore but have been used on offshore oilrigs. (HoistCam, 2016).

Transferring the use to the offshore wind industry may encounter issues such as:

- Connectivity & power – Lifting operations may run 24 hours a day during safe weather windows and any delays cost substantial sums of money. For this reason, both connectivity and connection should be robust and reliable. If lost mid-way through a lift the whole lift might need to be aborted and cameras inspected. Wired connections or well-positioned wireless transmitters with a long-lasting power source would be needed.
- Limitations to fields of view – A Conventional camera gives only a single field of view. Multiple cameras will give further views but the problem remains. It might be confusing for banksmen causing inaccurate instructions and clash-points might be missed. The view may also be obscured by weather or light (if the weather window allows offshore operations will run through the night). Finally, an accurate idea of distance may be difficult to perceive.
- Fixing/Removing – Attaching and removing the cameras should be quick, simple and reliable.

3.1.2.2.3 Fisheye

Fisheye lenses increase the field of vision of conventional cameras using an ultra-wide lens. The result is a larger, albeit distorted, view which could be used in the same way as conventional

cameras however attracting much of the same issues. The distortion may even make interpretation and distance estimation more difficult, particularly around the edges of the image.

3.1.2.2.4 360 degree + VR

360-degree cameras record a full sphere of vision around the point at which the camera is placed. The user can then look in any direction around this feed, mimicking the choice of a view of someone in that position. This is often created using multiple cameras, which record all angles of a scene and then stitch them into a single video. VR (Virtual Reality) headsets present this video through a headset, which uses the movement of the user to select the angle of view and can run in real time.

Although not used in lifting operations yet, VR crane simulators have been developed by companies such as 'ITI' and 'GlobalSim' for use in training of operators (ITI, 2016; PTI, 2016).

Access to a wide field of views might help to avoid clashes and the VR headset could give banksmen an easier 'feel' of directions and distances. The camera would have to be fixed in a single position, however, which limits the freedom of visibility, particularly for the accurate fine hoisting stage. Equally, due to the nature of the 'stitched' footage, there is often a few positions, which are blind spots or are distorted.

3.1.2.2.5 Drones with cameras

Drones with cameras fitted to them can be used to provide a video feed of almost anywhere on a site, particularly areas at a height that may not be easily accessed. This has been well used for the inspection of damage to blades and is expected to grow (Lorenz, 2017).

These have the benefits of flexibility of location so could be used to aid banksmen when trying to avoid clashes during global hoisting. Dynamic positioning (see Section 3.1.2.4.4) could be used to control their location with respect to the payload providing a consistent and stable view and many are capable of stable flight even in high winds (Hambling, 2014). This may require an additional trained controller and may not be able to get close enough to assist with accuracy during the fine hoisting.

As the cost of technology falls and usage grows all of the above options are becoming increasingly cost-effective. 360-cameras can be purchased from £200 and camera drones from around £500. Clearly, the prices rise with quality but when compared to the cost of offshore operations they are orders of magnitudes less.

3.1.2.3 Sensorial Guidance

Visual guidance could move the banksman to a location from which they may safely give signals to the crane operator. Sensorial guidance could assist with these directions and potentially quantify required movement. It could also be used to warn of potentially clashes particularly outside of the field of vision.

3.1.2.3.1 Lasers

Laser distance tools send out a high-energy beam of light, measuring the time taken and phase shift of the response. Used for a wide variety of applications, they are cost-effective and very accurate.

Used in conjunction with cameras these could aid with depth perception. However, they are limited by the single direction of the beam.

3.1.2.3.2 Proximity Sensors

Proximity sensors are able to detect the presence of nearby objects without physical contact. Often emitting an electromagnetic field, ultrasonic waves, or a beam of infrared (electromagnetic radiation), the sensor then looks for any changes in the return signal. Again, this technology is widely used from parking sensors to smartphones. Within the industry, they are used for dynamic positioning of vessels, pitch and yaw measurements, and distance measurement to locate defects in bearings, shafts etc. (Pepperl+Fuchs, 2016)

Again, this could be used in conjunction with cameras to aid depth perception or applied to avoid clashes.

3.1.2.4 Automated Guidance

The human could also be removed from being under the load by automating the offshore lifting process. In the following some possible concepts are presented.

3.1.2.4.1 Image Guidance

Template matching is used in several areas, such as medicine or robotics, in order to detect motions or recognise patterns or images (Kadhm, 2014). Kaur, Watkins, Moss, & Luechtefeld (2009) also studied the positioning of a load and a vehicle by means of image processing and template matching. The bolt holes of a wind turbine element flange connection could thus be used as pattern, based on which the counterpart could be positioned correctly. However, different scales, such as varying distances to the object, rotational and angular misalignments, make this technique very complex and expensive (Kadhm, 2014). Additional motions due to offshore lifting conditions make it more difficult to achieve accurate results.

3.1.2.4.2 Smart Cameras

Smart cameras are already used in robotic guidance for position detection and rotation of elements. Those cameras not only capture images, but can also extract further information from them, describe the situation, make decisions and work within an automated system. In this way, smart cameras could be used in the fine hoisting stage for automated fine control of the lift. The repetitive connections and lifts during an offshore wind turbine and wind farm installation would also enable machine learning. In total, the lifting process could be faster with the help of smart cameras. However, their use would require a full automation of control of the crane, which is questionable if this is possible.

Rahman (2015) and Rinner & Guggi (2010) have used smart cameras to map workshops and control cranes, whilst Kyung (2016) presents a full overview of their possibilities.

3.1.2.4.3 Remote Control

Piloting a small aircraft without a pilot (Marshall Cavendish Corporation, 2003) or driving a small tractor (RCT, 2012) and a compact loader-tramper (Ruff, 1992) without a driver can be made feasible by the use of remote control. Different navigation, guidance, and control systems are

currently available for remote control applications. Using remote control in offshore lifting operations could remove the human from dangerous areas, as lifting tools could be connected remotely to the load. However, depending on the technologies used, the offshore environment, in which one often has to deal with clouds, rain, or other precipitation, could make it difficult to obtain reliable and accurate data for positioning.

3.1.2.4.4 Dynamic Positioning

Dynamic positioning systems are already common practice for station keeping in the offshore industry. Vessels or other floating devices can maintain their position by controlling the drive unit based on measured position data. The precision of station keeping, however, depends on how accurate position data can be obtained. As wind turbine elements are being lifted and thus moving, there would be only a possible application of dynamic positioning for drones carrying a camera, which should stay in a certain position with respect to the moving body. This idea is further elaborated in Section 3.1.2.2.5. With some adaptations, dynamic positioning may also be used to stabilise the load in the global hoisting.

3.1.2.5 Fine Tuning Control

Controlling the fine motion of payloads has historically been done using taglines, which run to the ground and can be controlled by workers below. This becomes difficult during offshore operations where, if controlled by people who are not directly beneath the load, the taglines are limited to the location of the vessel or jack-up platform. This has led to numerous systems, which aim to control the fine motion and reduce the sway.

3.1.2.5.1 Highwind ‘Boom Lock’

The ‘Boom Lock’ system, shown in Figure 3-11, helps to control large movements during lifting. Mounted onto the crane, the payload is free to move until Boom Lock is required at which point the boom is clamped. This reduces sway movement by reducing the free-length of the winch line. At this point, boom in-out movement is controlled by the Boom Lock gaining finer control.



Figure 3-11 High Wind ‘Boom Lock’ (Nielsen, 2016)

Its first trial use was in January 2015. Monitored by the University of Leuven and watched by 'GeoSea', it kept a 6MW turbine blade steady in wind speeds of 20m/s. It has since been used for Kentish Flats Extension. (Nielsen, 2016)

Ability to work in higher wind conditions, suitable for use on all OWT (Offshore Wind Turbine) components and finer, automated control are all benefits, which allow the movement of tagline control from beneath the load. However, this does not control all movements so may be required as part of a suite of options.

3.1.2.5.2 AH Industries – Tagline Master & C-Yoke

Another option for movement of tagline control is to control them remotely. AH industries 'Tagline Master' (Figure 3-12) is attached to the crane tower and automatically controls the tension in a set of taglines. The advantage of this is again two-fold; controlling tension in the lines avoids the risk of breakage and damps the effects of sway whilst the control joysticks can remotely control rotation to a high accuracy and with full control.

Used in conjunction with suitable yokes this can control the rotation of any turbine part. Again only controlling one degree of freedom (rotation) this should be used in conjunction with others.

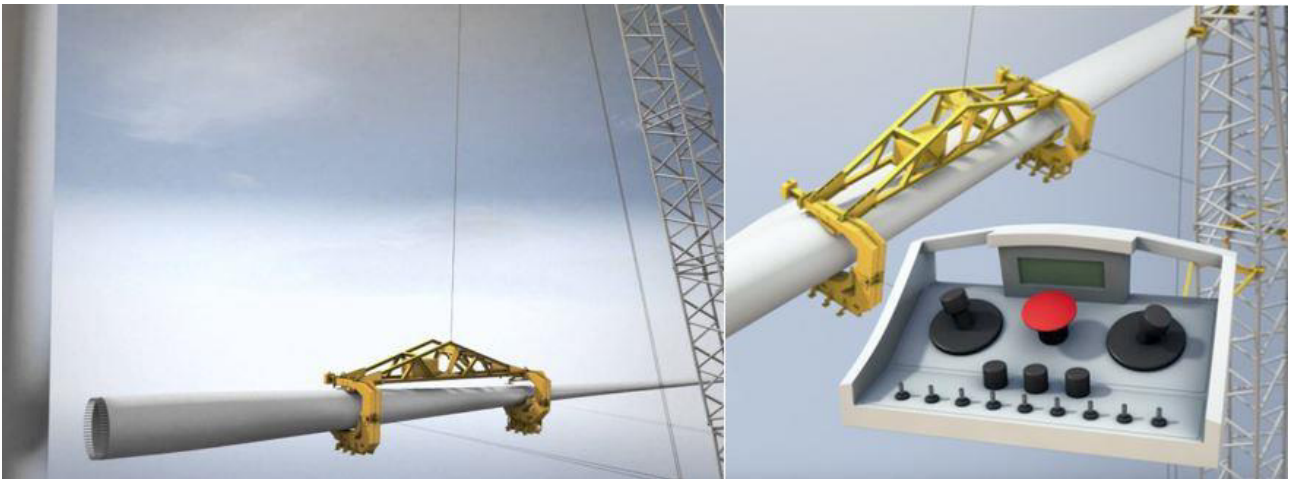


Figure 3-12 Tagline master with the Blade Yoke by AH Industries, showing the remote control set-up (AH-Industries, 2016)

3.1.2.5.3 Liftra Blade dragon



Figure 3-13 Liftra products. Left - Blade Dragon, Right - Self-hoisting crane (Liftra, 2016)

The blade dragon, Figure 3-13, is similar to the tagline master in that it controls the movement of payload independently from the crane. This remote controlled blade yoke can rotate the blade about its perpendicular axis allowing for installation to the hub in any position. Limitations here are that it is only suitable for blades.

3.1.2.5.4 Self-Hoisting Crane

The self-hoisting crane also made by Liftra, Figure 3-13, is mainly for use during maintenance. Mainly reducing mobilisation costs, it can be brought to the site by a vessel rather than jack-up and climbs up its own lifting wire onto the top of the nacelle. Used both off- and onshore it is useful for replacing large parts such as generators and bearings. Where this could be useful from a safety point of view is that the crane can be controlled locally close to the place in which the component is to be landed. This gives the operator a close view without having to be under a load controlled from elsewhere. This is limited to the use of replacing parts in the nacelle but two in conjunction have been used to replace small rotors onshore (Liftra, 2016).

3.1.2.5.5 Smart Cranes



Figure 3-14 Image displayed in the cabin, which shows the position of the target and the correct vertical position as an overlaid circle (Wilson, 2012)

Smart cranes have been used to offload containers from ships. Using imaging software to reduce the amount of sway of containers (Wilson, 2012). Antisway systems such as that developed by 'Matrox Imaging' (Matrox Imaging, 2017), automatically compensate for any sway with slight movements of crane controls whilst ensuring that the spreader is optimally positioned. Using machine vision, a smart camera (see Section 3.1.2.4.2 for more details) is mounted to the boom (trolley) which interprets images of two light sources on the container, continually calculating the centre point of the two markers. A signal is then passed to the electronic control system, which

regulates the movement of the crane, reducing sway. Figure 3-14 shows a similar system, which uses a contrasting coloured target.

A similar system has been used for bridge cranes in warehouses. Rather than an operator using the control pendant to move the payload the crane can be controlled by moving a hand-held wand. An image-processing system tracks the reflective end of the wand and its position is used to control the crane (Peng & Singhose, 2009). Light sources or reflective/contrasting elements are often used for robustness against changes in light.

A system similar to those mentioned could certainly be used for the placement of OWT components, either with targets at the centre of the camera's view or using the bolt holes as a target.

3.1.3 Selection of Most Promising Solutions

In order to refine the concepts discussed in Section 3.1.2 the group have employed a Multi-Criteria Decision Analysis (MCDA) based on results from a survey sent to industry. This has been used to aid the choice of potential solutions to take forward within this project by judging the suitability of each solution on a number of criteria. More information on the process can be found in Section 4. The output of this analysis is a rating of each concept as a 'C value', which indicates the closeness to ideal solution (between zero and one, with one being ideal). Table 3-1 shows C values for the concepts introduced in Section 3.1.2, the concepts in bold are those that are to be taken forward into the next section and investigated further. Clearly the closer to the top of the table the more suitable the concept. However, some have been pursued because it suits experimentation or further study. For instance, if we are to investigate camera systems it makes sense to investigate more than one type. Remote control indicates any system that can be controlled away from the lifted load, all options in Section 3.1.4 will have this attribute.

Table 3-1 MCDA results for guidance and control

Concepts	C value	Concepts	C value
Guide Pins	0.7124	Liftra - Blade Dragon	0.5512
Remote Control	0.7099	Proximity sensor	0.5292
Taglines/Tagline winches	0.6668	Self-hoisting Crane (Maintenance only)	0.5211
Highwind – Boom Lock	0.6389	Mirrors	0.4628
Funnels/Cones	0.6318	Smart Cameras	0.4236
Multiple Cameras	0.6268	Machine Vision + Smart Cranes	0.4183
Fish Eye	0.594	Electromagnetic Guidance Systems	0.4157
Lasers (Distance measurement)	0.5884	Image Guidance	0.3907
DP System	0.5802	Drones with Cameras	0.3687
360° camera + VR	0.5553		

3.1.4 Development of Solutions in Detail

3.1.4.1 Global Hoisting

As mentioned in Section 3.1.1.1 the lifting process can be broken down into global and fine hoisting. Once hoisted the load is subject to forces, which can cause undesirable movements. Within global hoisting, we are aiming to control large-scale movements and maintain a well-controlled lift. Onshore this is often provided by conventional, manually controlled taglines, particularly in open spaces where people can stand clear of the load multi-directionally about the payload. Offshore this is more difficult as the structures are not located close to land, limiting the position of the manual taglines to below the load and on the jack-up. ‘Boom Lock’ and remote taglines featured high on the MCDA results and both aim to control the load without direct human interaction. In this section, we present how the two could be used in conjunction to gain full control of the load.

This control is needed for two reasons. Firstly, to reduce the lateral sway of the load that may arise from inertial forces and gust forces, keeping the payload in a safe, secure orientation. Secondly, to

achieve fine control when attempting to locate the payload in its final position, this involves manoeuvring the component to a space with very small clearances and hence additional deflections become comparatively large. The second point is particularly important if banksmen are to be moved from under the load and therefore cannot provide any manual guidance. Whilst this technically falls under fine hoisting, better control globally will give more room for manoeuvre when considering human-free fine hoisting solutions.

Sway control The 'Boom Lock' system locks the hook securely against the boom of the crane. At this point, the lateral movements of the hook are restricted by the arms (Figure 3-15b), reducing the free length of the winch line and therefore reducing the movement. The system can then lock the hook completely against the frame (Figure 3-15d), restricting movement in/out from the crane again reducing the sway. At this point the hook becomes completely fixed within the 'Boom Lock' system.

This, however, does not eliminate unwanted movement. The hook is still free to rotate and if the payload is large (such as a tower section), the base is still free to move. Some control of the base appears to be possible with the boom lock on smaller sections, see Figure 3-15f, where lines are passed around the nacelle and back into the frame.

This is where employing the tagline master could prove beneficial. Taglines could be attached to the extremities of the blades (shoulder and tip), tower (diametrically opposed at the base) or nacelle (at the hub and rear) and passed into the tagline master system. This system automatically controls the tension in the taglines; fixing the tension in both lines will eliminate unwanted rotation. The payload cannot rotate anti-clockwise (boom at 6:00) as the right hand (3:00) tagline will not allow outward movement. Equally it cannot rotate clockwise as the left hand (9:00) tagline will not allow outward movement. The tension will also stop the payload from moving away from the boom and soften movement if it begins to move towards the boom.

Fine Movement Fine movement of the payload is also made more precise by this system. The Boom Lock can control up and down movements, as well as in/out from the boom (Figure 3-15e & f). Whilst the slew of the crane can still control the left/right movements. Rotation of the payload is

then controlled completely by the tagline master increasing the tension on one tagline whilst reducing the other (this is automated by sharing a percentage of tension to each line). The system is now highly controlled remotely from the lift, ensuring there is no longer a requirement for manual control of the movement.



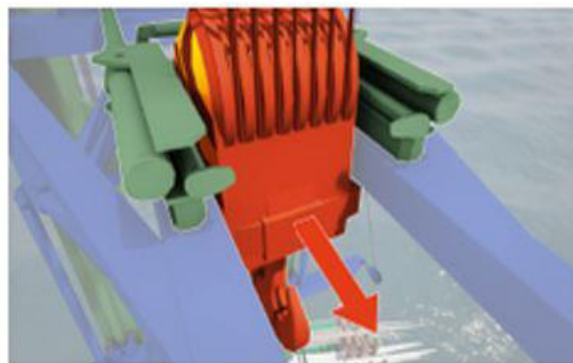
a)



b)



c)



d)



e)



f)

Figure 3-15 Boom Lock system; red arrows indicates restricted movement, green arrows indicate allowable movement. (High Wind, 2014)

Employing both of these systems means that unwanted sway will be greatly reduced. Equally, both systems can be used for all large turbine elements. There is an initial outlay to purchase the hardware but once a jack-up is equipped, they can be used for every lift. Both can be controlled remotely and use simple systems which could be controlled by the crane operator or by specialist workers. There may also be a distinct advantage in that by reducing sway: the operable weather window could be increased, as lifts are made possible in higher wind speeds.

3.1.4.2 Fine Hoisting

3.1.4.2.1 Visual Guidance

As discussed in Section 3.1.2.2 visual guidance via the use of cameras could be used in offshore operations to move the banksman from beneath the load to a safe location. Costs of a system of cameras are magnitudes less than the cost of installation with vessel charter costs alone of £130k/day (The Crown Estate, 2010, sec. 17.1) and there have been some recorded uses on offshore lifts (albeit for documenting the lifts, example see (Windcarrier, 2016)).

The MCDA analysis referenced in Section 3.1.3 has shown that amongst others feasibility, reliability of operation, and time of operation were highly important criteria. It is with a view to evaluating the criteria that experiments have been undertaken mimicking the use of various cameras in an offshore operation.

3.1.4.2.1.1 Experimental Aim

The aim of the following experiments was to test the accuracy of a variety of configurations of cameras when used to assist the visibility of a lift in offshore wind turbines. For simplicity focusing on tower and nacelle connection lifts such as those shown in Figure 3-16 in which a vertically oriented cylindrical flange is to be positioned atop a similar sized cylinder about the same axis, the bolt holes on the respective flanges must align to ensure the connection is possible. This experiment does not aim to recreate conditions offshore but rather attempt to quantify changes in accuracy, operability and time of similar lifts when the fields of vision of the operator and banksman are removed and exchanged for cameras.

Experiment set A only measured the accuracy of the centralisation of the tower, i.e. the tower flange is in the correct position but the boltholes may not align. Experiment set B also measured the accuracy of the positioning rotationally (bolts aligning), as well as testing a novel mechanical guidance system which is discussed in Section 3.1.4.2.2

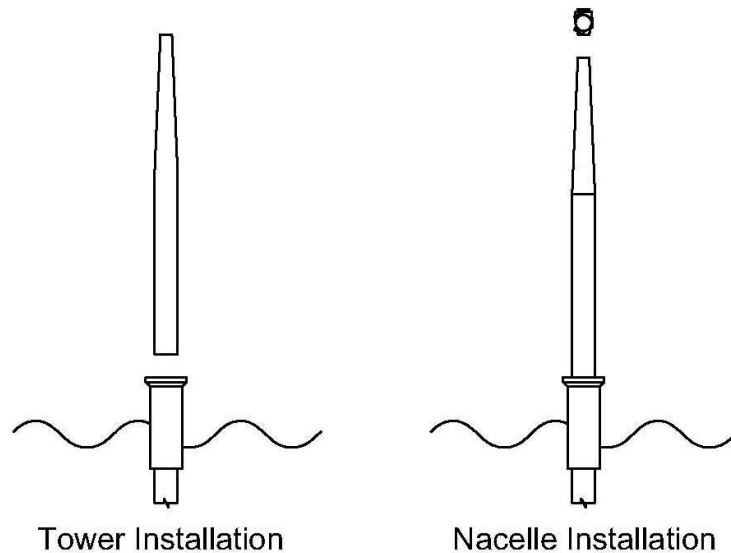


Figure 3-16 Tower and Nacelle installation of an offshore wind turbine

3.1.4.2.1.2 Experiment A

Method and Set-up

Tests were undertaken in the lab using a standard gantry crane with three axes of movement (x, y, and z) and a freely rotating boom. A cylindrical steel section of 1.27 m internal diameter, 0.55 m height and 22 mm wall thickness was used to represent a typical tower section. Equidistant holes around the circumference were drilled and lifting shackles attached, see Figure 3-17. The size of the section was chosen to be as large as feasibly and economically possible to minimise the scaling effects discussed at the end of this section. The cylinder was lifted to a known position and the section traced onto the lab floor, this marked circle representing the bottom, fixed section of the tower/transition piece.

The centre of the 'ideal position' was found using three diametrically opposed pairs of points marked on the side of the cylinder (measured using half the circumference) and then onto the

ground. The cylinder was then removed and centre marked atop a sprayed white rectangle on the lab floor as shown in Figure 3-17.

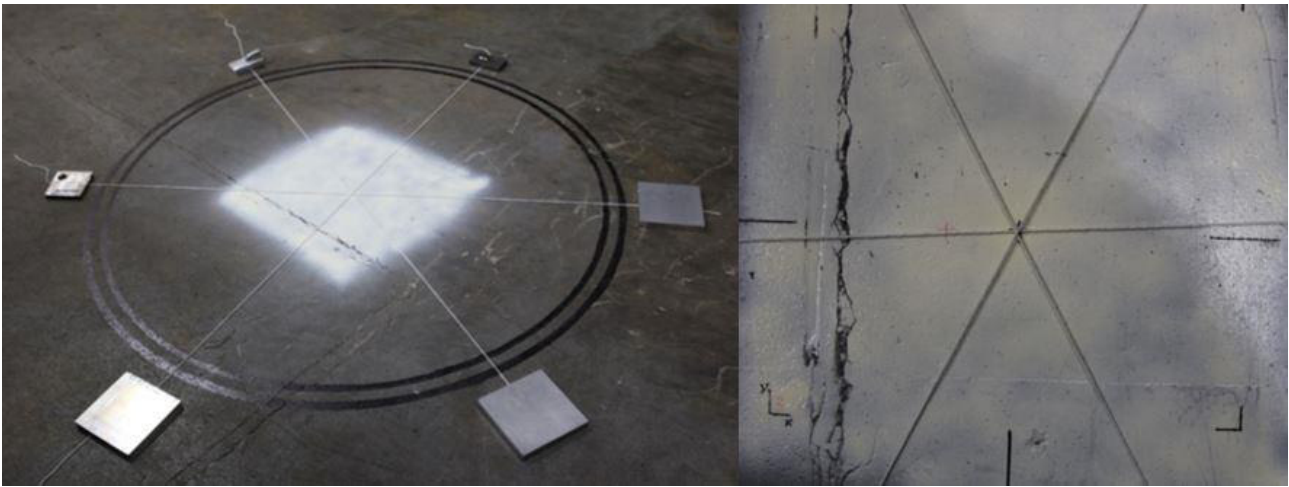


Figure 3-17 Left) Marked 'Ideal Position' representing the bottom fixed tower/transition piece. Right) Measurement of the centre-point, marked as a cross beneath the intersection.

Two types of cameras were used in the set-up. The first was a set of four standard Swann 650TVL (Television Lines) CCTV (Closed Circuit Television) cameras with night vision and a field of vision of 55°. The cameras were wired to a monitor via a DVR (Digital Video Recorder). The second was a Samsung gear-360 camera. This streams live 360 degree stitched video footage directly to a phone app via Bluetooth. The user is then able to zoom and scroll across the live footage.

Figure 3-18 shows the set-up of the lifting equipment and cameras. The 360-degree camera was located in the middle of the 'ideal' position raised to approximately 50 *cm* above the ground. Cameras 1, 2 and 3 were clamped equidistant around the top circumference of the lifted cylinder looking downwards towards the ground; the field of view was positioned to ensure the banksman could see both the cylinder it was connected to and what was below. Camera 4 was attached to the top of the lifting chains approximately 80 *cm* below the hook, which, when chains are taught, is about 2 *m* above the base of the payload. This gave an approximately central view of the majority of the edges of the lifted cylinder along with a clear view of below. Ideally, this position would have included the full circumference but an unobscured view of this was not possible with the rigging that was available.



Figure 3-18 Left) Set-up of the cameras and crane system. Top right) typical view of 360 camera feed and monitor. Bottom right) Monitor feed of cameras 1, 2, 3 & 4.

The Cases

In order to test the suitability of each type of camera, seven cases were investigated. Details of each can be found in Figure 3-19 and Table 3-2. The control cases are tests 1 & 2 with one representing a local lift and 2 representing current practice offshore. Cases 3-7 form the test.

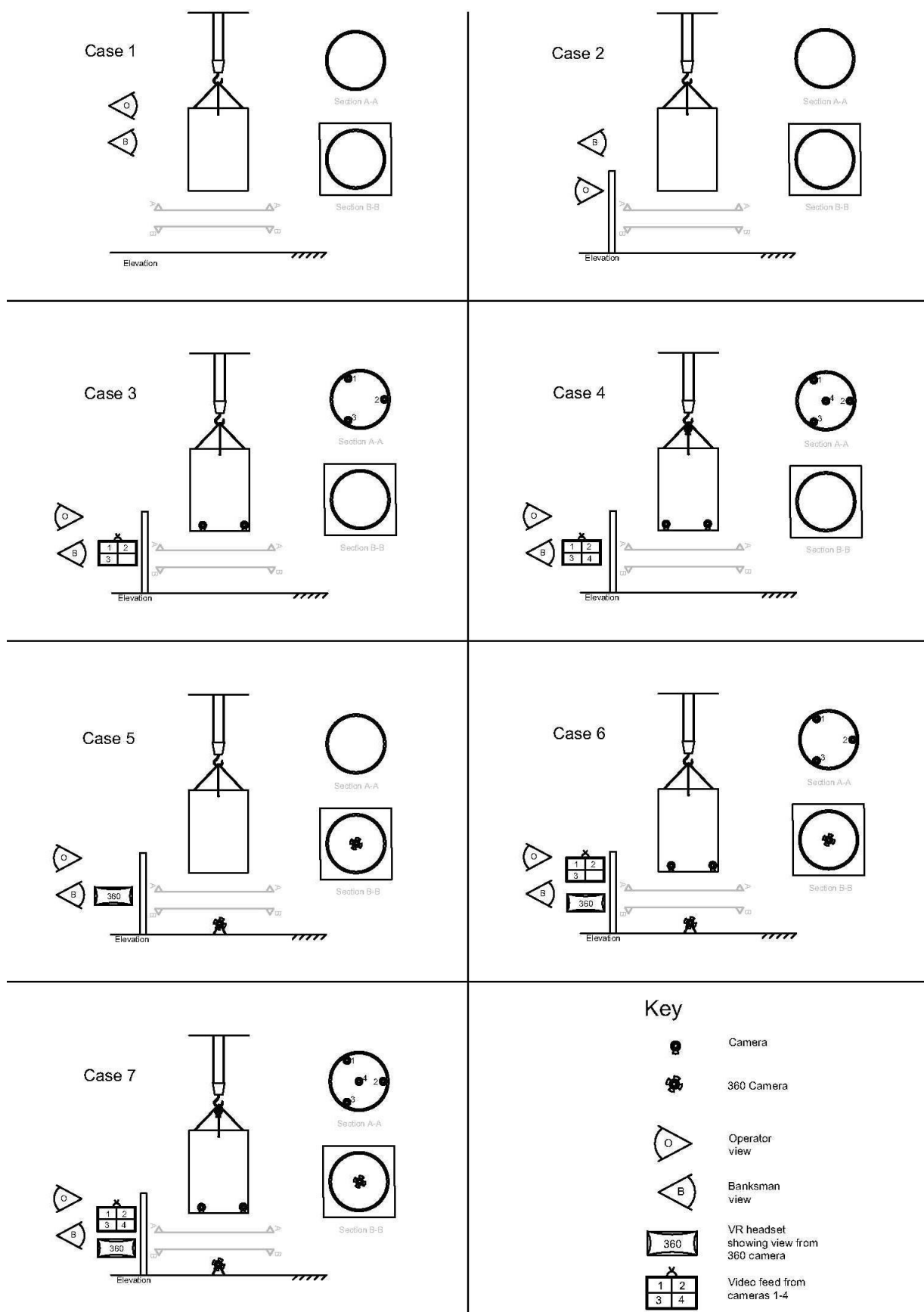


Figure 3-19 Experiment A - Representation of cases of camera configurations

Table 3-2 Experiment A - Description of cases of camera configurations

Case	Name	Description
1	Control – Operator and Banksman under load	Crane operator and banksmen as close as possible to payload and location with visual freedom.
2	Control - Banksman under load	Crane operator is blind (no direct view of payload). Banksmen as close to payload as required with visual freedom.
3	3* fine cameras	Crane operator is blind. 1 * Banksman has access to the video feed from cameras on payload but is blind to the physical lift.
4	3* fine cameras + 1* hook camera.	Crane operator is blind. 1 * Banksman has access to the video feed from cameras on payload but is blind to the physical lift.
5	360° camera	Crane operator is blind. 1 * Banksman has access to video feed on the app, is free to move around virtually but is blind to the physical lift.
6	360° camera + 3* fine cameras	Crane operator is blind. 1 * Banksman has access to video feed on app and monitor, is free to move around virtually but is blind to the physical lift.
7	360° camera + 3* fine cameras + 1* hook camera	Crane operator is blind. 1 * Banksman has access to video feed on app and monitor, is free to move around virtually but is blind to the physical lift.

Controls

For each case, five tests were undertaken, in which the starting and end positions were the same and 3.05 m apart. The same crane operator was used for each lift and barring the control cases was behind a screen, listening for instructions. Two banksmen (BM1 and BM2) were used; barring the control cases one had access to the monitors showing video feed (BM1) whilst the other stayed close to the load for safety (BM2). Each banksman (ML-Mareike Leimeister and TB-Toby Balaam) performed 2 to 3 tests in each case as BM1. The sway of the cylinder during global hoisting was controlled by BM2 by hand until the bottom section was in view and large motions had stopped (this mimicked the use of remote taglines).

Accuracy was measured as the eccentricity from the centre-point of the drawn ideal position to that of the final position of the landed cylinder. Six diametrically opposed points were marked permanently on the cylinder, these were marked on the ground and the landed section removed. The centre point of the landed section was found at the intersection of diameters, as shown in Figure 3-20, using weights and taught strings. A measure of the distance between ideal position and final dropped position was measured indicating accuracy as well as the time taken from the first call to touchdown and qualitative comments from operators and banksmen.

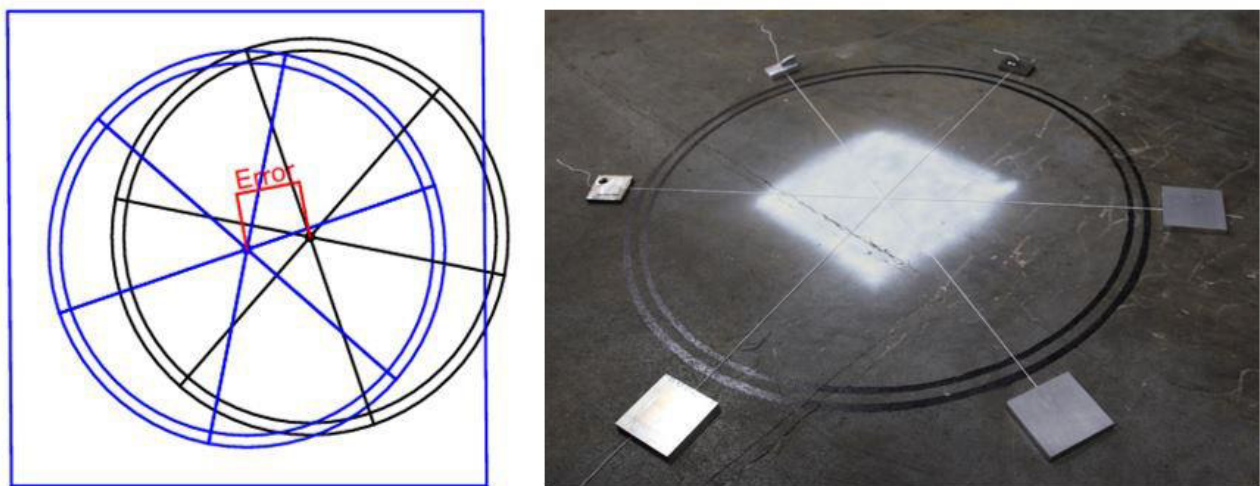


Figure 3-20 A) Measurement of Error – Blue indicates drawn ideal section on ground with the centre point marked. Black indicates the landed section. Red indicates the measured error. B) Example of this in practice

Results

Figure 3-21 shows the average results (time taken and accuracy) for the different cases. (5.5Appendix B contains the raw data and graphs of the tests within each test). It is clear that the two control cases are the fastest. This may be related to reduced uncertainty in the direction of movement required and the ability to control the load by hand (reducing sway more quickly). Within the camera systems, it seems that using the 360-degree camera speeds up the operation, ease of orientation might well play a key role here. The freedom to move the field of vision gives rise to the opportunity to reference directions against locations around the room, whereas the fixed cameras are subject to rotation about the hook causing confusion as to where the global co-ordinate system is.

Accuracy of the tests do not follow the same trend. Having the operator and both banksmen able to see the load was not the best. Each person, positioned around the edge of the cylinder, only has a finite view and therefore cannot see the position of the load as a whole. The same can be said for both banksmen under load. In fact, the most accurate test was that of the three cameras and 360-degree camera (shown by the dashed line in Figure 3-21). Four cameras have a similar average error and fares better than control case 1. In both of these cases, a full view of the cylinder is possible for the banksman in control and once in a good position each of the three fine cameras can be used to locate the load more accurately.

Case 7 was not undertaken as it was found that the 360 camera and hook camera performed much the same function and therefore the banksmen were not actually using all five cameras. This is, however, useful concerning redundancy.

It was clear throughout the tests that there were disparities in accuracy concerning each banksman. This can be seen in Figure 3-22, time taken remains much the same between the two but accuracy varies. Interestingly Mareike Leimeister (ML) favoured the four cameras over the 360+3 cameras. Apart from this, the trends remain the same.

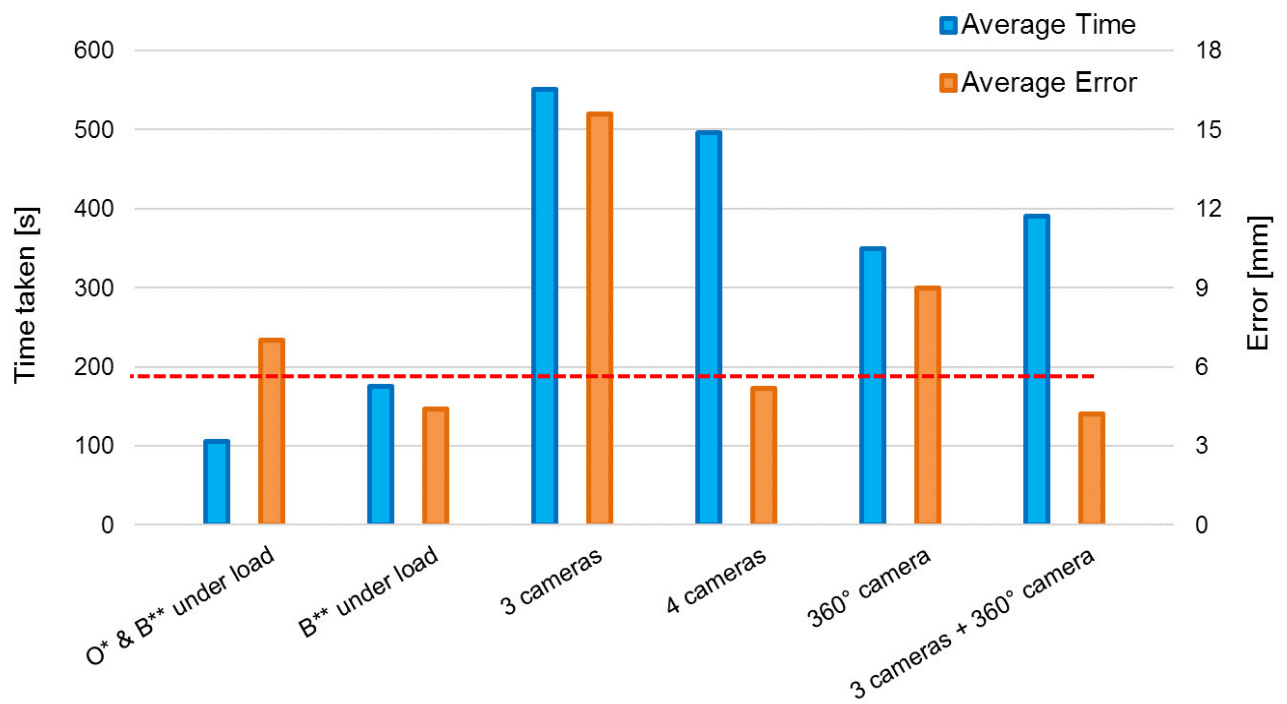


Figure 3-21 Average test results across the six tests for accuracy and time

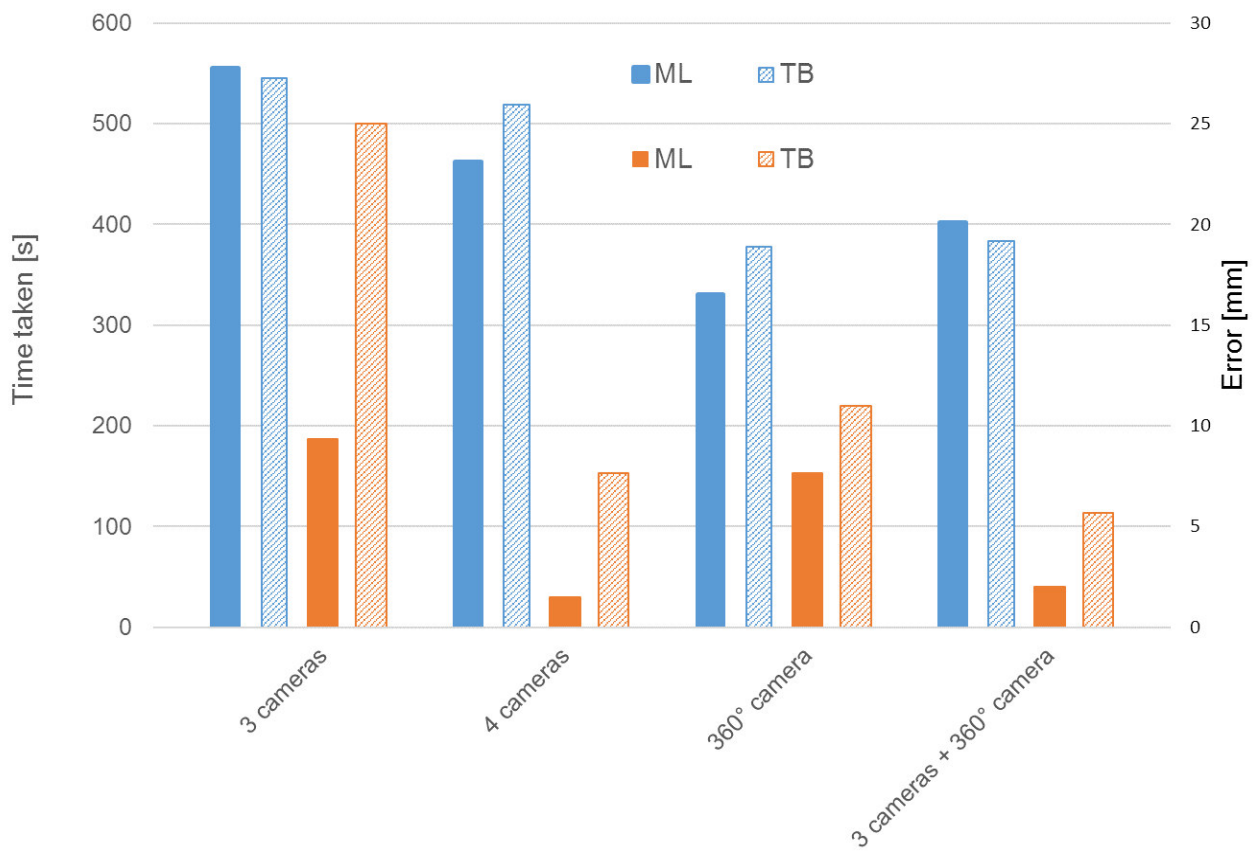


Figure 3-22 Comparison of time taken (blue) and accuracy (orange) for both banksmen

Video footage of all of the tests was saved and an example of 360 and global footage can be found of test A5.2 on YouTube. (Balaam & Leimeister, 2017a, 2017b)

3.1.4.2.1.3 Experiment B1&2

Method and Set-up

Rotational accuracy was not considered in the first set of experiments and is now considered. This is required if bolts are to be aligned with their respective boltholes. The method and set-up was largely the same as that in experiment set A, the same equipment was used although three small rods were welded on the internal face of the cylinder just above the base and equidistant about the circumference. These were used as points of reference when measuring rotational error.

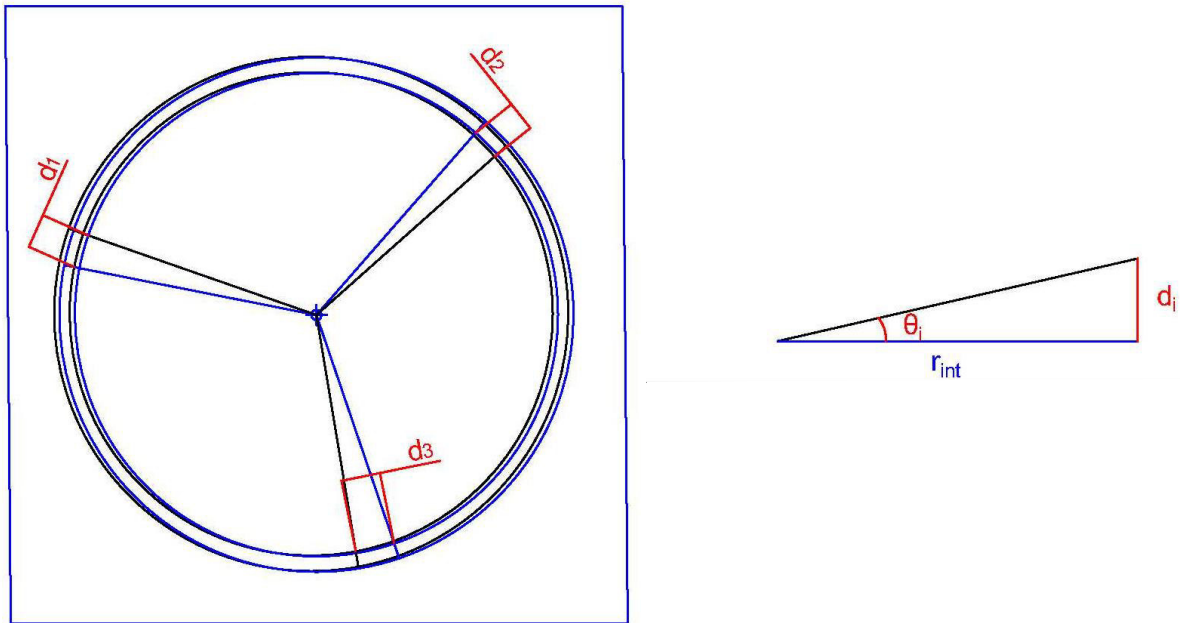


Figure 3-23 Measurement of rotational error - Blue indicates the drawn ideal section, black indicates the landed section and red measurements of error.

Rotational error was measured as shown in Figure 3-23; at three distinct locations, a distance (d_i) of error was measured. The angular error was then calculated assuming a right-angled triangle to the ideal centre-point such that:

$$\theta_i = \tan^{-1}\left(\frac{d_i}{r_{int}}\right) \text{ for } i=1,2,3 \quad (3-1)$$

Where $r_{int} = 635 \text{ mm}$.

Clearly, there will be some centralising error as well so this formulation contains some error; however, this should make a very small difference given that maximum centralising error will be less than 10 *mm* and the internal radius is 635 *mm*.

The rotational error (θ_i) is calculated as positive or negative if clockwise or anticlockwise respectively. Hence, the absolute value of rotational error for each test is calculated as:

$$\theta_{abs} = \frac{\Sigma(\sqrt{\theta_i^2})}{3} \text{ for } i=1,2,3 \quad (3-2)$$

Five tests are then undertaken for each case and the average taken.

The cases

Rather than testing each of the camera configurations again only two cases were tested, as shown in Figure 3-24 and Table 3-3. These form a control case (using banksmen under the load) and a case using all cameras.

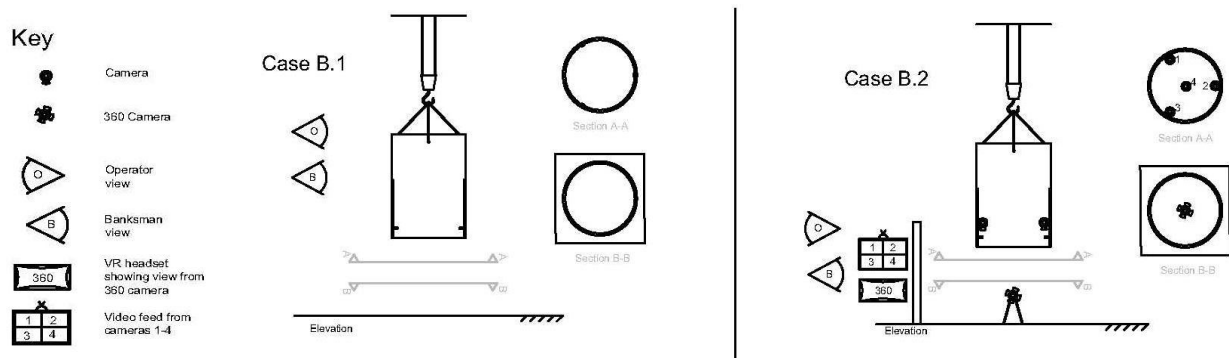


Figure 3-24 Experiment B - Representation of cases of camera configurations

Table 3-3 Experiment B - Description of cases of camera configurations

Case	Name	Description
B.1	Control	Crane operator and banksmen as close as possible to payload and location with visual freedom. Rotation is also required.
B.2	Cameras	Crane operator is blind. 1 * Banksman has access to the video feed from cameras on payload but is blind to the physical lift. Rotation is required.

Results

Figure 3-25 shows the average results of the two tests along with the best camera configuration from experiment set A (A.5). Time taken is shown in blue, centralising error in orange and rotational error in green. Clearly, test A.5 is not a fair comparison as rotational accuracy was not required. By following the top two dashed lines, it is clear that looking at both centralisation and rotational alignment makes it more difficult and takes more time compared to only looking at centralisation. Centralising accuracy is also affected although test B.2 is still centrally more accurate than test B.1 (with banksmen). Whereas the camera system is less accurate in rotational alignment compared to using banksmen beneath the load. The problem is considered in Section 3.1.4.2.2.

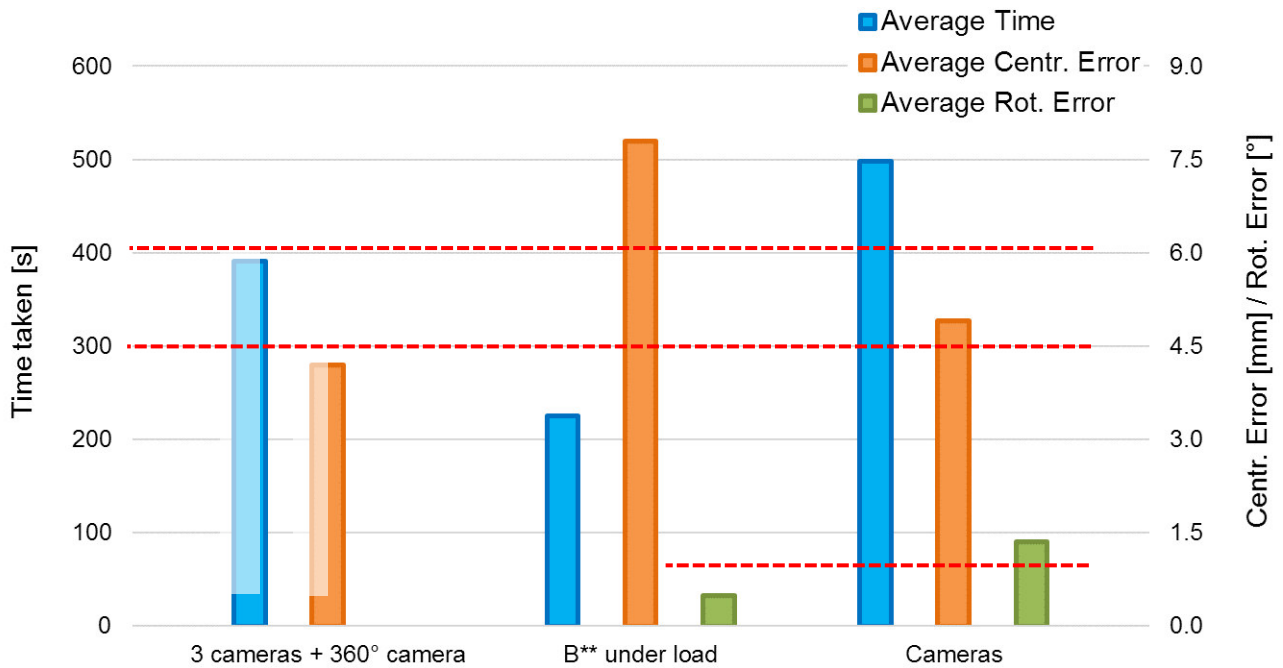


Figure 3-25 Average test results for rotational alignment

Limitations

There are, of course, some limitations to the results shown and some inherent errors, which are quantified in this section. Firstly, the accuracy of the gantry crane. This is a standard overhead lab crane, which is not designed for fine movements. In order to gauge the precision of the crane, tests were undertaken in which the smallest movement was attempted in both degrees of freedom (noted as East-West and North-South) 6 times. The results are shown in Figure 3-26. The N-S direction appears to be less precise with a mean value of 16 *mm* compared to 10 *mm* (E-W) although there is a considerable outlier (40 *mm*) which was an unrealistically long press, but this could easily occur during the experimental tests. The minimum movement of each being 4 *mm* (N-S) and 6 *mm* (E-W).

The section used in the tests measured 1.27 *m* in diameter (internal). Clearly, there will be some scaling effects when the cameras are used on 3 *m* + sections of an OWT. It is true that the field of vision of the cameras is relative to the size of the cylinder. However, this can be fine-tuned for larger cylinders, there may be a requirement for higher definition cameras to allow for zoom and in

particular, camera 4 (on the boom) may need to be positioned within the tower to allow for similar field of view.

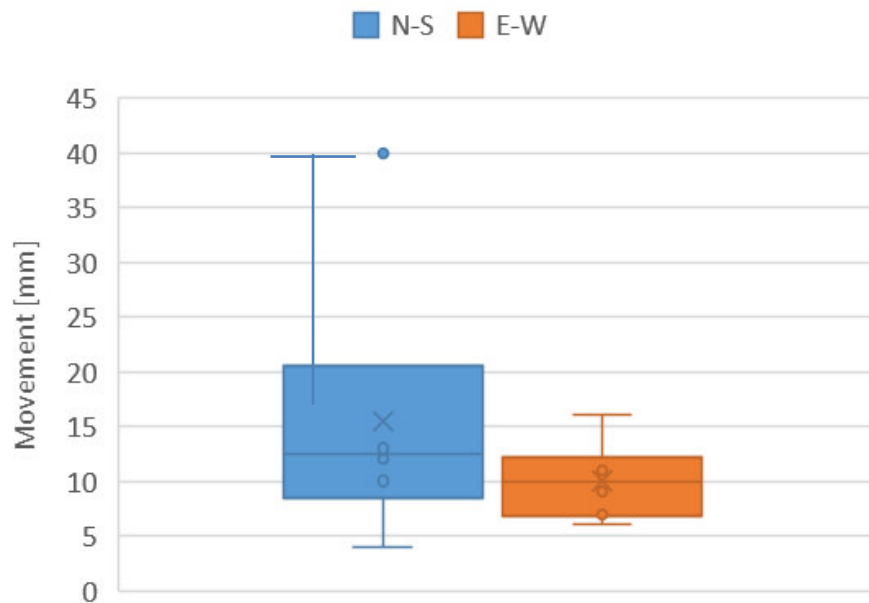


Figure 3-26 Box and Whisker Plot of Crane precision test. The cross indicates the mean.

Measurements of central accuracy were rudimentary so there is certainly some human/systemic error to be considered. In order to quantify the error when estimating the central point of the landed section, one landed position was measured five times. The points were marked and all fell within a range of 3 mm. Hence, the assumed error is approximately ± 1.5 mm.

Rotational measurements also have inherent inaccuracies but central and rotational error are inherently linked, it is therefore difficult to separate them as we did. Accuracy of landing due to sway is certainly a consideration although this was constant throughout the tests and was down to the banksman to await a steady load.

Key Learnings

Throughout the tests, a few key points were true across all tests. These are covered here; considerations for the application in industry are covered in Section 3.1.5.3.

- With regards to banksmen, clear orders & repetition was crucial. It was also found early on that it was easier if the banksmen gave orders rather than the crane operator having access to the

live feed (it was confusing for the operator during the single attempt in which both could look at screen)

- Whilst using the standard CCTV cameras (1-4), the night vision function was valuable. Despite the tests being under well-lit conditions, shadows caused problems at various points, these were mitigated once the night vision was employed but problems did occasionally rise with reflections on the ground.
- The three circumferential cameras (1, 2 & 3) were of no use until the edge of the ideal section could be seen; but from this point on, they were extremely useful for fine-tuning.
- The fourth camera located below the hook proved useful for global distance measurement and some fine tuning
- The 360-camera was used for global hoisting, distance, and depth measurement. The payload could be followed as it was moving helping to avoid clashes and quantify the up-down movement required. Blind spots occur around the circumference and particularly within around 20 *cm* of the lens.
- Due to limitations with the streaming of live footage, we were unable to live stream to the VR headset. However, we did attempt to use this posteriorly with video footage. Issues included seasickness and a lack of awareness of reality, as well as difficulty changing between various views/cameras

3.1.4.2.2 Mechanical Guidance

Due to limited fine control of the crane and remaining motions of the lifted element, because of the rigging ropes and wind loads or gusts, mechanical guiding elements would be a great support in offshore lifting operations. Furthermore, the experiments, presented in the previous Section 3.1.4.2.1, showed that matching centric and rotational alignment at the same time by just using visual guiding systems is quite complicated and not feasible without any further support. With guiding elements for centralisation and rotational alignment, the lifting procedure would be sped up from the time at which the upper element is in contact with the mechanical guiding system. Accurate positioning of the counterparts to each other could also be obtained without having humans involved under the load.

3.1.4.2.2.1 Initial Design Including Mechanical Guiding Elements

Funnels as a centring system, which are already used in practice, are presented in Section 3.1.2.1.2. These, however, are not applicable for the installation of offshore wind turbines, as the dimensions are too large. Thus, the group discussed having a coned shaped element on top of the already installed tower element, instead of having a funnel. Based on the different connection methods of wind turbine elements, proposed in (Stiesdal, 2011), the group came up with the idea of having an L-shape connection with the bolts going in radial direction and extending the top end of the bottom element with a conical ring, which would then align the top element centrically.

As this solution would still be a bolted connection, another mechanical guiding system for rotational alignment of the bolt holes is required. Thus, the idea of Bitsch & Baun (2012) was adapted and three guide pins, attached to the inner surface of the top element, as well as the corresponding socket sections on the outside of the bottom element, both equally distributed around the circumference, were included in this initial design.

The final version of the initial design including mechanical guiding elements for centralisation and rotational alignment is presented in Figure 3-27. The bolt connection in radial direction is represented by three bolt holes in both top and bottom element.

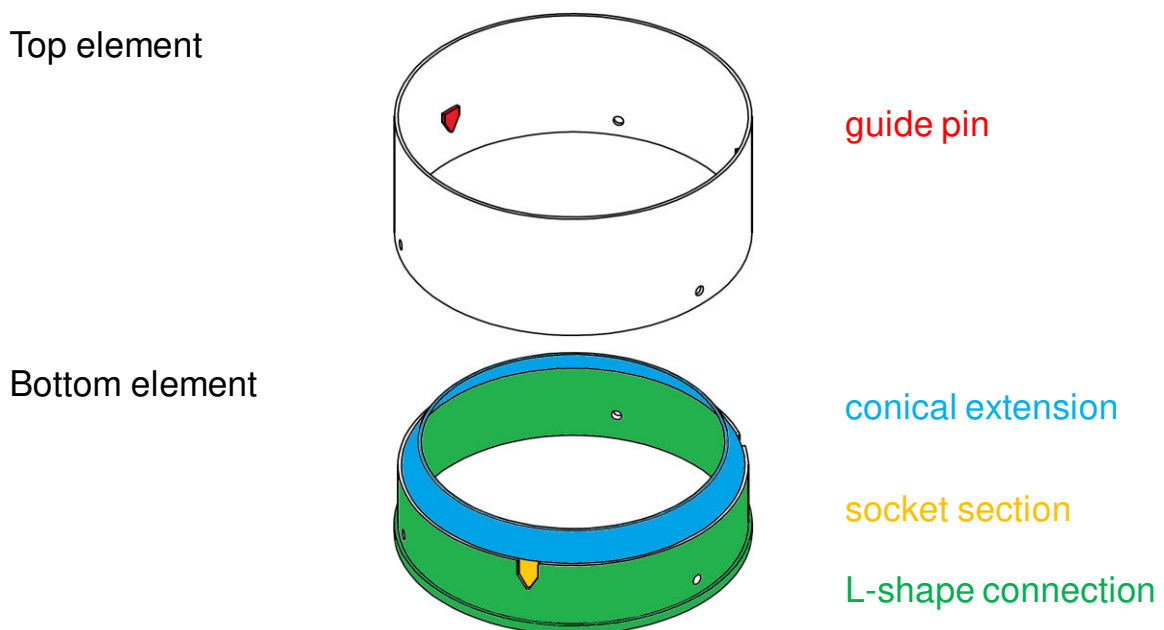


Figure 3-27 Initial design including mechanical guiding elements

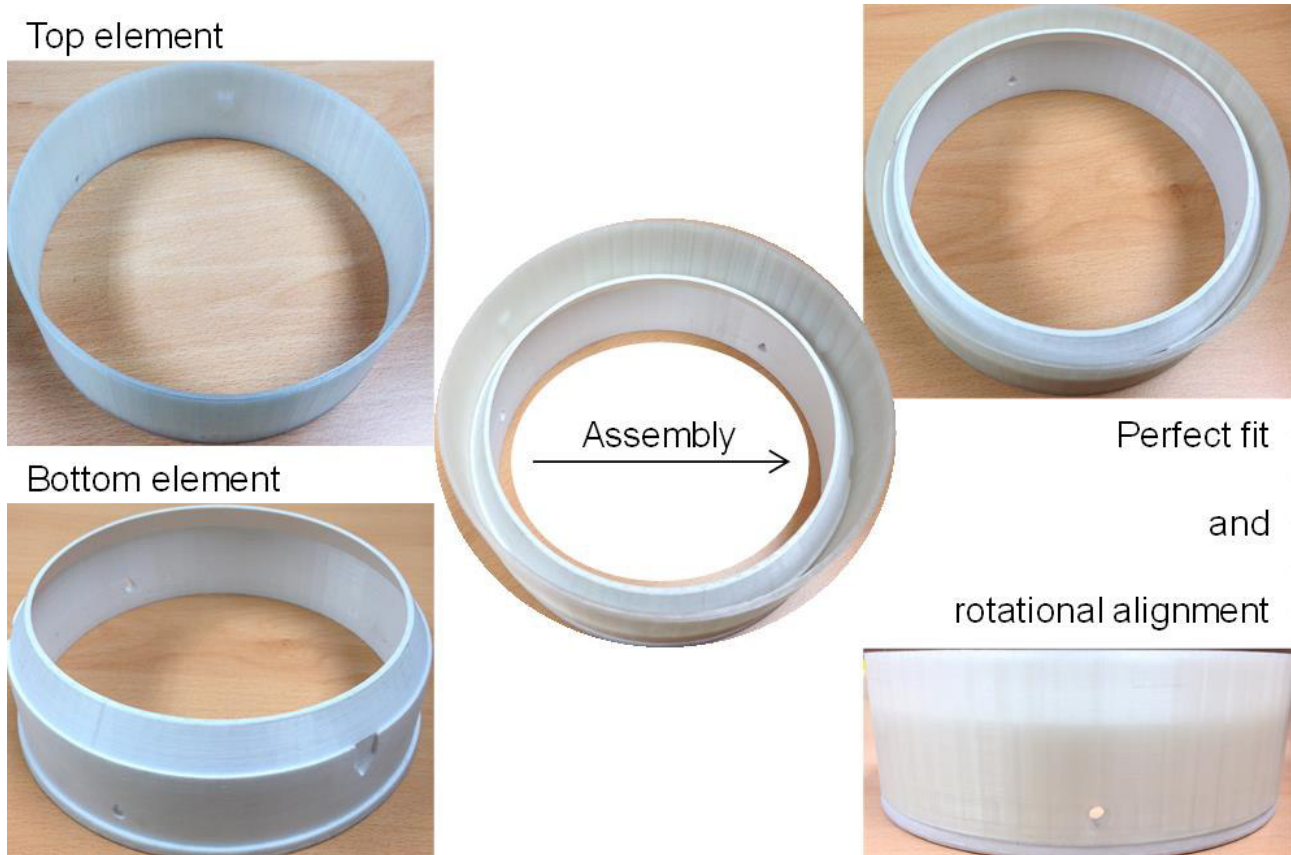


Figure 3-28 3D-print of the initial design

This design was 3D-printed (Figure 3-28 and Appendix 5.5C.1). The detailed drawings including all dimensions can be found in Appendix 5.5C.1. For those it has to be mentioned that the outer dimension, as well as the minimum thickness are predefined by the 3D-printer. Furthermore, the drop-shaped bolt holes and the inclined top end of the guide pins are just adaptations due to 3D-printing requirements. The 3D-printed model proves the functionality of the included mechanical guiding elements. However, this printed example also points out some drawbacks of this initial design. The main disadvantage is that two cylindrical elements have to be slid over each other. To allow this and also to include tolerances in fabrication, there has to be some clearance between inner diameter of the top element and outer diameter of the extended connection of the bottom element. This, however, decreases the accuracy of the centric positioning and requires completely upright installation to avoid snagging. In reality, however, the bottom section might not be 100 percent vertical. On the other hand, having such a tight fit of a cylinder over another cylinder would give some stability prior to bolting. But in addition, the entire design, using an L-shape connection

with bolts going in radial direction, as well as the conical extension on top of the bottom element, implies complete new design and manufacturing of wind turbine elements at their connection ends, and additional material would be needed, which would affect the cost factor negatively.

3.1.4.2.2 Revised Design Including Mechanical Guiding Elements

Due to the drawbacks of the initial design, the first ideas were amended. The main criteria for the redesign are:

- Use typical wind turbine elements with the traditional flange connection.
- Use several single mechanical guiding elements instead of one, which goes around the entire circumference.
- Use existing bolt holes for connecting the guiding elements to the turbine parts.
- Consider tolerances and allow enough clearance to adjacent components.

In general, the group aimed to design mechanical guiding elements which could be attached to typical wind turbine components, removed after the lifting operation and connection of the two elements, and thus reused again for installation of other wind turbines of the same kind. Furthermore, with just using single guidance elements instead of one full circular one, the amount of material needed, as well as the costs for the guiding system could be significantly reduced.

Thus, a top guide and a bottom guide were separately designed. The top guide is equipped with a rod, which is strengthened for stability reasons. This top guiding element can be screwed from above on the flange of the top wind turbine element, using two existing bolt holes of the flange connection, which are slightly modified by adding threads. The bottom guide is screwed from below on the flange of the bottom wind turbine element. The guide itself extends to the inside of the circular section with a conical surface, which is strengthened by three stiffeners. A socket is cut in the conical extension, which positions the rod of the top guiding element into its final correct rotational orientation. The rod is designed to be long enough to be guided by the cut out in the bottom element from first contact, even if the top and bottom cylindrical sections are horizontally displaced. Figure 3-29 shows the design of the single guiding elements, a cross section through

the connection of both in the final position, as well as the entire assembly, with the top elements coloured in grey and the bottom elements highlighted in orange.

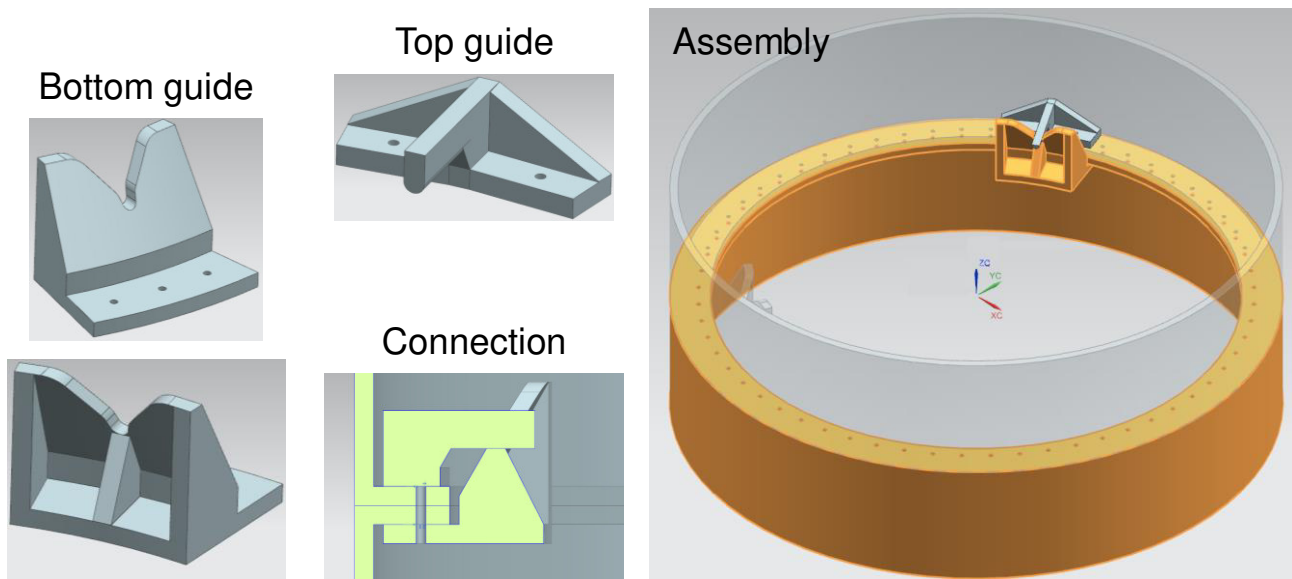


Figure 3-29 Revised design including mechanical guiding elements

The benefits of this revised design of the mechanical guiding system over the initial design are the following:

- The wind turbine elements do not have to be redesigned, as the typical flange connection can be used.
- The guiding system consists of three top guides and three bottom guides, which are positioned equally distributed around the circumference of the flange connection.
- The guiding elements are connected with two (top guide) or three (bottom guide) screws to the flanges of the wind turbine elements. The bolt holes can be used for this connection and only in those three times two/three holes a thread has to be cut. The screws have to be short enough so that they are not sticking out of the flange. With this screwed connection, the guiding elements can be removed after successful connection of the two turbine section, and thus reused again for another wind turbine installation.
- The guiding elements are designed with enough clearances to adjacent components, which can be clearly seen in the cross section of the connection in Figure 3-29.

For testing the functionality of this revised design, another 3D-print was made. The dimensions for those printed elements are given in Appendix C.2, whereby the outer dimension and minimum thickness were again prescribed by the 3D-printer. The printed elements are presented in Figure 3-30 and Appendix C.2.

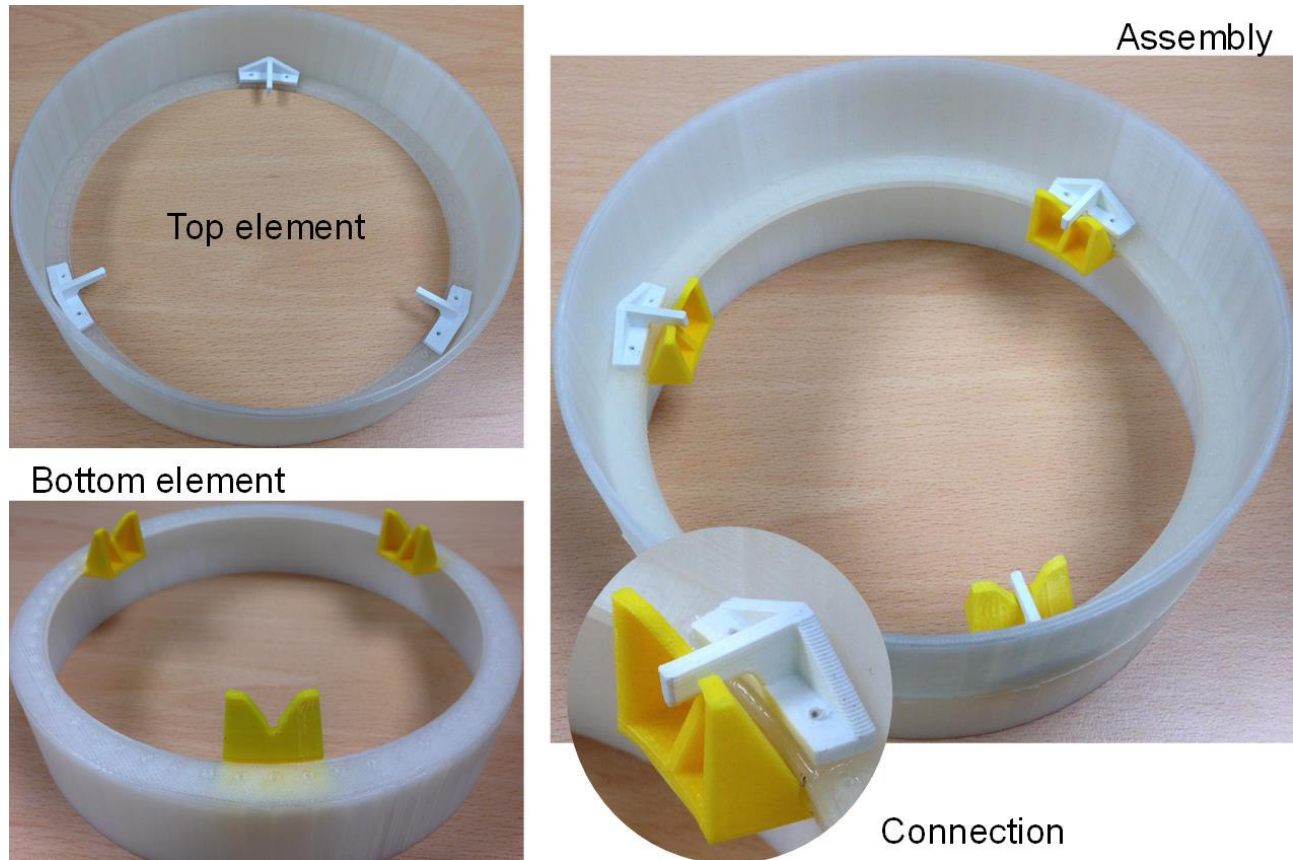


Figure 3-30 3D-print of the revised design

3.1.4.2.2.3 Simplified Design for Experimental Tests (C1)

In order to test experimentally the revised version of the mechanical guiding system, presented in Section 3.1.4.2.2.2, this design had to be simplified and adjusted based on existing material on the manufacturing site. As the cylindrical top section without any flange connection was already available from the first test cases, mentioned in Section 3.1.4.2.1 the rods were directly welded onto the inner surface. The bottom turbine section is again just represented by circular lines drawn on a plate, which was available at the manufacturing site. The bottom guiding elements were fabricated out of channels, which were cut conically at the top and into which the socket was cut. This, however, was only feasible to be cut into the straight vertical side, but still represents the

main idea and includes both guiding parts (centralisation and rotational alignment). These bottom guiding elements were welded onto the plate, similar to the guide rods, as both are equally distributed around the inner cylindrical circumference, but included some clearance. Furthermore, there was the need to drill and tap four holes in the edges of the plate to attach lifting eyes for transportation of the bottom-plate-assembly. Another four holes in the edges were required to fix the plate to the floor in the testing hall (Figure C-7 in Appendix C.3.4). This ensured that the bottom part would not move when the top cylindrical element would be lowered down. The drawings and dimension of this manufactured design for the experimental testing can be found in Appendix C.3. Some pictures of this setup are shown in Figure 3-31.

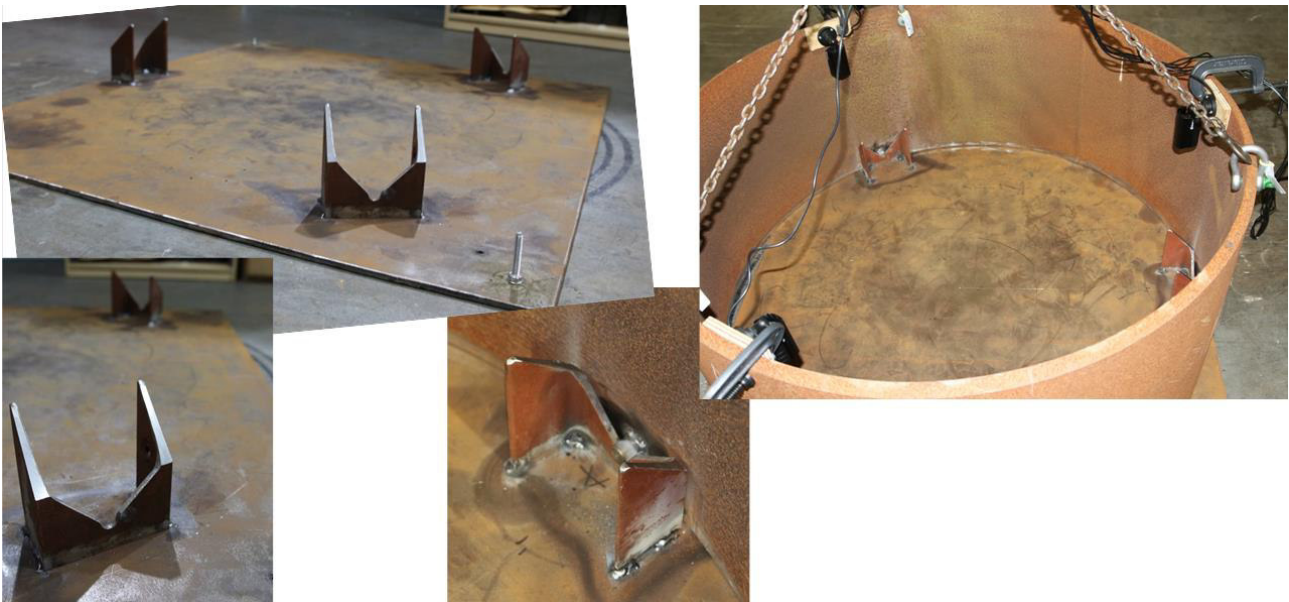


Figure 3-31 Manufactured simplified design

The tests performed with these mechanical guiding elements still used visual guidance. Based on the best solution, found from the previous tests in Section 3.1.4.2, three cameras on the circumference of the top cylindrical section, slightly shifted away from the rods, were used in combination with the 360° camera standing in the centre of the bottom cylinder. The entire setup is presented in Figure C-8 in Appendix C.3.4.

As the accuracy of the final positioning only depended on the precision of fabrication and included clearances, which made up in the end just maximum 3 *mm* of tolerance in total, the main interest

was aimed at the performance. The test realisation was similar to the previous tests, mentioned in Section 3.1.4.2.1: the tests were repeated five times and included a switch of the banksman. However, only the time, how long it took the banksman to guide the top element from the same starting position to the bottom plate in the final position, was measured. The results of those tests, named C1, are shown in Figure 3-32. It can clearly be seen that the speed depends on the banksman, but also on the number of lifts already performed. Based on this learning curve, even shorter times are expected after some training.

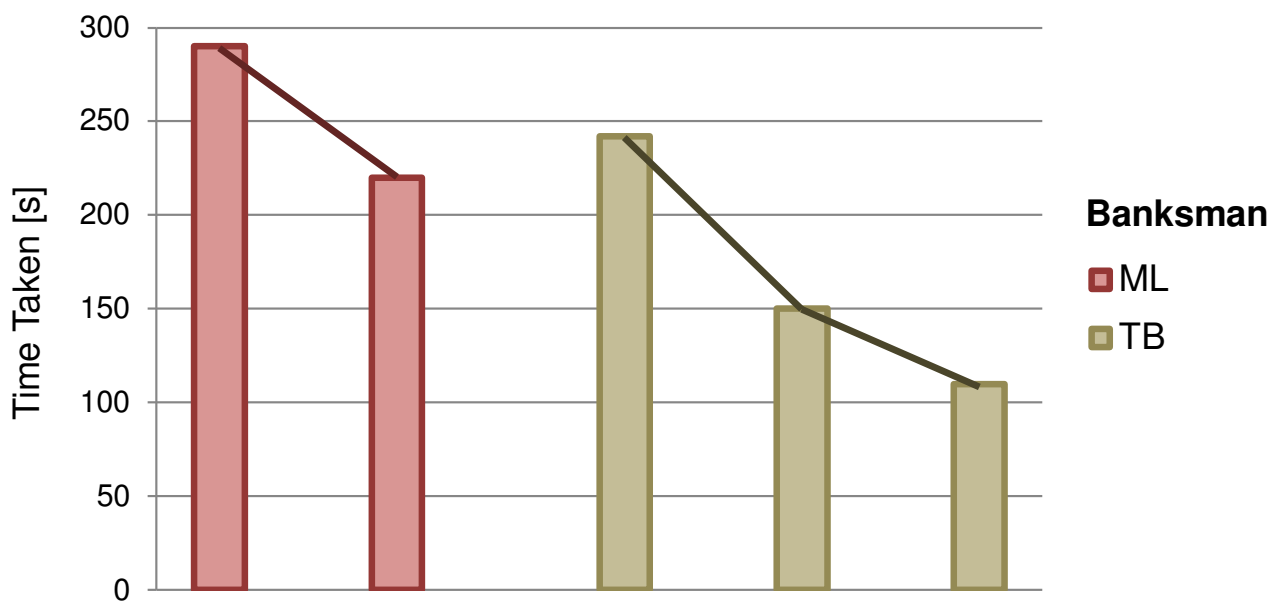


Figure 3-32 Individual times for the tests with mechanical and visual guidance (C1)

The average time of 202 s is compared to the previous performed tests, covered in Section 3.1.4.2.1, as shown in Figure 3-33. The first six tests (A1 - A6) cannot directly be used for comparison and are thus shaded, as they only focussed on centralisation and did not include the rotational alignment. Comparison with the other two tests (B1 and B2), which focussed on both central and rotational alignment, with or without having people directly involved, shows that the use of cameras and mechanical guiding elements allows for faster installation. With respect to the accuracy in positioning, the combined guiding system, without having people under the load, is unbeatable.

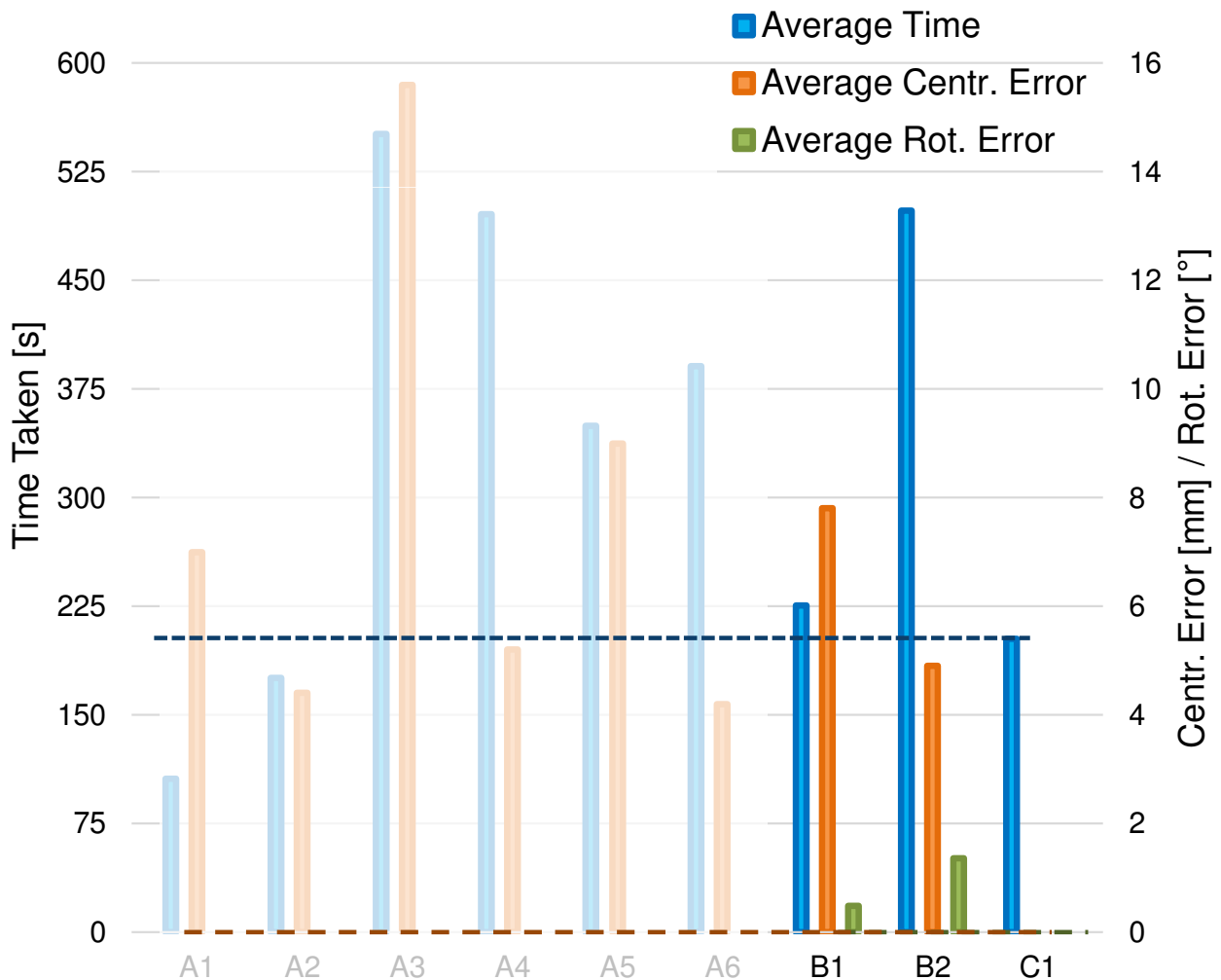


Figure 3-33 All test results in comparison

When carrying out the tests with the mechanical guiding elements, the performance of each camera became clearer. The 360° camera in the centre of the bottom element was quite useful for seeing all three guide pins and the corresponding bottom guiding elements, for which a normal camera mounted to the hook was too limited in the field of view. The three cameras on the circumference of the upper cylindrical element still gave the local view and the whole local arc could still be seen if the guide pin was not too thick, as it was the case in the design for the performed tests. The angular shift of the cameras on the circumference with respect to the guide pins, however, no longer had a negative impact, as very accurate positioning of the guide pins was not needed due to the socket sections in the bottom guiding elements.

The application of the guiding elements itself was quite simple. As soon as the load was just above the bottom element, the guide pins were already positioned rotationally by using taglines, represented by the other banksman in the test realisation. In this position the load was then lowered down step by step until the bottom guiding elements are employed. From this point on, no further alignment corrections by banksmen or crane operator were needed, as the final positioning was then taken over by the mechanical guiding elements. However, to avoid a rough landing and the risk of wedging, short stops were implemented in the lowering down process, to allow the top element for self-adjustment with respect to the bottom guides.

A 360 degree video of test C.1 can be found on YouTube (Balaam & Leimeister, 2017c).

3.1.4.2.2.4 Detailed Full-Scale Design for Real Wind Turbine

In order to ensure the design described in Section 3.1.4.2.2.2 would be suitable for use offshore we have undertaken a concept design of the part to check against potential load and, given the proposed reusable nature, check that it could be easily handled by a worker. This can be found in Appendix C.4.

3.1.5 Conclusion and Recommendations

Several ideas had been collected for human-free lifting solutions by making use of guidance and control systems. The detailed study yielded certain feasible concepts. The benefits of the presented mechanical guiding solutions are highlighted in more detail and compared to each other in Section 3.1.5.1, all presented ideas are collated and demonstrated in a holistic solution for guidance and control in Section 3.1.5.2, and the realisation and application of those systems in practice are finally further discussed in Section 3.1.5.3.

3.1.5.1 Mechanical Guiding Elements for Increased Tolerance Margin

Using mechanical guiding elements, such as stabbing guides, which are already applied for tower (Figure 3-2) and blade (Figure 2-5) installation, or the presented ideas for combined rotational and centralisation units, allow accurate positioning of two corresponding wind turbine elements. The degree of accuracy only depends on the tolerances applied in design and obtained during manufacturing. However, depending on the guiding element the tolerance margin, allowing for

having an initial misalignment at the first contact with the guiding element, may be different. The larger this tolerance margin, the faster and easier the lifting process and installation may be, which is especially under offshore conditions a welcome side effect in addition to the correct positioning.

Thus, the tolerance margins for centralisation and rotational alignment, both given as \pm values with respect to the correct final position, are calculated for the different designs presented in this study, as well as approximately determined for the current practices. For the sake of simplicity, the tolerance margins for centralisation and rotational alignment are considered separately.

For the designed guiding elements, as discussed in Section 3.1.4.2.2, the tolerance margin for centralisation is computed based on the distance from the top outer edge of the coned part to the inner wall of the cylindrical element, and then normalised by the outer radius of the cylindrical element. For the tolerance margin of the rotational alignment, first, half of the maximum opening angle of the socket section with respect to the centre of the cylindrical elements is determined. Based on this, the allowable arc length (at the position of the bolt holes), up to which a bolt could be misaligned from the bolt hole in both directions, is computed. This is then related to the bolt hole radius and used as measure for the rotational tolerance margin.

In order to compare the tolerance margins of the designed guiding elements with those currently achieved in practice by using stabbing guides, tolerance margins for centralisation and rotational alignment are computed on the example of the assumed dimensions for the LEANWIND 8MW wind turbine (Desmond, Murphy, Blonk, & Haans, 2016), which was also used for designing the full-scale guiding elements. The guide pin is assumed to have a 20% smaller diameter than the bolt hole has. Thus, with a used bolt hole radius of 18.75 *mm* (Table C-1) the approximated radius of a guide pin turns out to be 15.0 *mm*. The tolerance margin for centralisation is then directly obtained by the difference of those two radii, normalised afterwards with the outer cylinder radius. Due to the small dimensions, the difference of bolt hole and guide pin radii is then directly taken as the arc length at the position of the bolt holes. This value is then again related to the bolt hole radius to obtain the tolerance margin for the rotational alignment.

The detailed numbers of the described calculation of the tolerance margins can be found in Table C-4 in Appendix C.5. Based on those results, the tolerance margins are compared graphically in Figure 3-34.

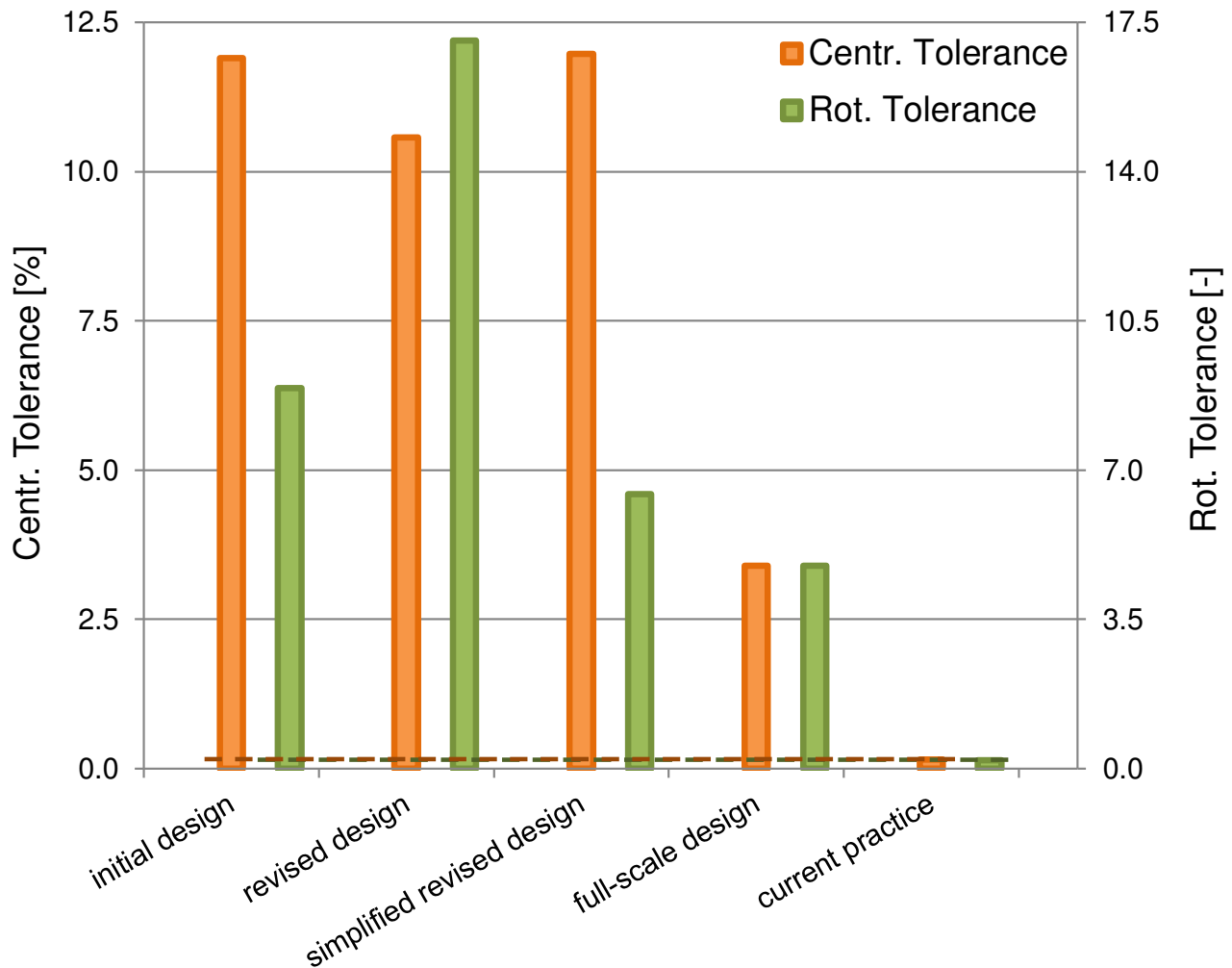


Figure 3-34 Tolerance margins in comparison

It can be seen that the tolerance margins vary for the different designed guiding elements and are smallest for the full-scale design. However, those values are still significantly larger than the tolerance margins which are currently achieved in practice by using just stabbing guides: by a factor of 22.67 for centralisation, and by a factor of 23.75 for rotational alignment. This shows that the designed mechanical guiding elements allow a much larger tolerance margin, which will definitely have a very positive effect on the time for the lifting and installation process. If even larger tolerance margins were required for further handling improvements, the width and/or

opening angle of the design could just be extended. Any changes to the design, however, always have to be recalculated with respect to structural integrity and weight.

3.1.5.2 Holistic Solution for Guidance and Control

All presented ideas; the final design of mechanical guiding elements, the visual guidance by means of cameras on the circumference and a 360° camera in the centre, as well as the Boom Lock system and taglines; can be combined to obtain a holistic solution for guidance and control which allows fast and precise human-free lifting operations. The combination of cameras and mechanical guiding element has already been tested in the experiments (C1). However, it was only possible to mimic the use and effect of Boom Lock and taglines by stopping large motions during the tests and rotating the lifted element manually (without looking at the aimed position). The control of taglines and Boom Lock can be realised remotely and maybe linked to the crane operator. Furthermore, the lifted element, the already installed wind turbine component, and also crane and ship could be equipped with proximity sensors as an additional alarm system for avoiding clashes and collisions. Finally, the number and position of cameras used should depend on the turbine dimensions and real conditions. Some more cameras for the sake of redundancy have to be included, too.

3.1.5.3 Realisation and Application in Practice

What has worked perfectly under laboratory conditions could still experience some difficulties in real life. The tests performed did not aim to represent the real offshore conditions during installation of a wind turbine, but rather attempted to quantify changes in accuracy, operability, and time of similar lifts, when the people are removed from being under the load.

Before testing those guidance and control systems in the field, offshore, some additional concerns have to be considered:

- Attachment of the cameras: How should the cameras on the circumference of the lifted element be attached to it? In the laboratory tests, the cameras were just clamped to the structure, which may be difficult in real life. A possible solution could be magnets, similar to the 'HoistCam' system, which is attached magnetically (HoistCam, 2016). Anyhow, a secure attachment of the

cameras has to be ensured, to avoid additional hazards coming from such guiding systems which should primarily reduce risks.

- Issues about the feed: In the laboratory tests it was not a problem to have cables running from the cameras via the hook to the power supply and desktop, and to charge the 360° camera ahead of the experiments and use Bluetooth connection. However, in reality it has to be made sure that the camera views are not cut off at any time during the offshore lifting procedure. It could be an option to use wireless systems, but having a receiver close to the cameras, for example at the crane hook, from which then cables can be running along the crane arm to the power supply and analysis unit. The 360° degree camera may receive power supply at the already installed turbine unit. Anyhow, independent on which type of connection is used in reality, redundant systems (some more cameras, but also different connection types) should be used.
- Offshore conditions: Weather and light conditions offshore could complicate the lifting procedure. Based on the performed experiments, the night vision functionality of the CCTV cameras turned out to be useful when operating in dark areas, such as shadows in the tests. Maybe additional light would be required for offshore lifting and installation work at night. However, any kind of reflections, which would again negatively influence the view obtained from the cameras, should be avoided.

Finally, some recommendations are to be given, based on the gained experience during the practical tests. Those are maybe already known and applied by the offshore workers and crane operators, but still important to be mentioned at this point:

- It is really crucial to have clear orders between banksmen and crane operators. Repetitions of the orders also ensure that the correct command was understood and also given as intended.
- With respect to the use of visual guiding systems, it would be easier if the banksman is looking at the view of the cameras and giving the orders to the crane operator. Otherwise, based on the experiences from the experiments, it would be quite confusing for the crane operator to look at the camera views and in parallel to operate the crane.

3.2 Concepts for Connections and Seafastening

3.2.1 Introduction

Bolted flange connections are used in a wide range of construction industries and are a very important part of offshore wind structures. The major components of an offshore wind turbine generator (WTG); the tower sections, nacelle, and blades are connected together through bolted, ring-flange connections. Often there can be a large number of bolts. On a typical tower section, where the flange runs along the inside perimeter, as shown in Figure 3-35, there can be well over 100 high strength, pre-stressed bolts. While bolts used in steel construction are usually M8-M30, so that the nominal major bolt diameter is 8 to 30 mm, offshore WTGs use much larger bolts, some as large as M64 or M72 at the base of the tower (Schaumann & Eichstädt, 2015; SKI, 2017).



Figure 3-35 View of bolts inside tower section during installation (Fred. Olsen Windcarrier, 2015)

Provided that the bolts are tightened to the correct pre-load, bolted flange connections can offer a great deal of strength; for example a 10.9 class M36 bolt, at its correct pre-load torque provides around 441kN of clamping force (Tribology-ABC, n.d.). While M8 or M10 bolts require only a small

amount of pre-load torque and can be tightened easily by hand with a torque wrench, as shown in Figure 3-36, due to the size of bolts in offshore WTGs the required pre-load torque is two orders of magnitude larger. This means that they cannot be tightened by hand and require special hydraulic tensioning or hydraulic torquing tools. The hydraulic tensioning tools require some length of bolt thread to be exposed so that the bolt can be grabbed and extended by a hydraulic system – while the bolt is extended the nut is turned which ensures the preload is applied (ITH, n.d.). The large number of heavy bolts and the special tools required result in a large amount of time needed to install all the bolts; as an example, it takes a crew of two personnel three hours just to tighten the bolts on a 4m diameter blade bearing (Müller et al., 2014).

Recommended Maximum Bolt Loads and Torque Values (Metric Coarse Threads)

	3.6		5.6		6.9		8.8		10.9		12.9		A/F
mm	Newtons	N.m	Newtons	N.m	Newtons	N.m	Newtons	N.m	Newtons	N.m	Newtons	N.m	mm
2	284	0.12	378	0.16	731	0.31	863	0.37	1216	0.52	1461	0.63	4
3	726	0.44	966	0.59	1863	1.13	2206	1.34	3109	1.88	3727	2.26	5.5
4	1255	1.00	1677	1.34	3226	2.60	3825	3.04	5374	4.31	6453	5.15	7
5	2059	1.96	2736	2.65	5286	5.10	6257	6.03	8806	8.48	10591	10.20	8
6	2903	3.43	3864	4.51	7453	8.73	8836	10.30	12405	14.71	14906	17.65	10
8	5315	8.24	7090	10.79	13680	21.57	16230	25.50	22751	35.30	27360	42.17	13
10	8473	16.7	11278	21.57	21771	42.17	25791	50.01	36284	70.61	43541	85.32	17
12	12356	28.4	16475	38.25	31773	73.55	37657	87.28	52956	122.60	63547	147.10	19
16	23340	69.6	31087	93.16	60016	178.50	71196	210.80	100027	299.10	120131	357.90	24
20	36481	135	48641	180	93849	384.1	111305	411.9	156415	578.6	187796	696.3	30
24	52563	230	70019	308.9	135331	598.2	160338	711.0	225552	1000	270662	1196	36
30	84043	466	112286	622.7	215745	1206	255952	1422	359902	2010	432471	2403	46
36	123073	814	164261	1089	316753	2099	374612	2481	527595	3491	432526	4197	55
42	169164	1304	225552	1746	435413	3364	515827	3991	725688	5609	870826	6727	65

P, S & T are the Material grade for unified inch and Whitworth fasteners (BS1768 & BS1083)
P = grade UTS of 35 tonf/in² and min. yield of 21 tonf/in², S = grade UTS of 50 tonf/in² and min. yield of 40 tonf/in²,
T = grade UTS of 55 tonf/in² and min. yield of 41 tonf/in²

Figure 3-36 Bolt loads and torque values (alfadoc, 2013)

Seafastening is intrinsically linked to the connection of the components because often the component is fastened to the ship in the same way in which it is fastened in construction. Flanges are welded to the grillage on the ship deck and the component, for example usually the tower section or nacelle, are bolted to the flange. Components can be seafastened in different ways, for instance the nacelle can sometimes be secured simply with corner stoppers (Siemens, 2015). One advantage of this link between seafastening and fixing is that potentially an idea for one can be extended for use in the other. This is something to keep in mind while reading this section.

Bolting and seafastening can lead to a number of potential health and safety issues which this section aims to address. Some examples of potential issues are:

- Unsecured loads while bolts are being applied
- Falling bolts during lifts
- Bolts in seafastening shaking loose and falling

3.2.2 Initial Ideas

3.2.2.1 Friction Connection

The use of a friction type connection for connecting tower sections together was proposed and investigated in (Heistermann, Husson, & Veljkovic, 2009) where it was also investigated and compared to a standards flange connection. The idea behind the friction connection is that it is fitted together as two concentric tubes which fit inside of each other. The bolts point radially outward and, in theory, clamp the surfaces of the two concentric tubes to each other. The bolts are installed prior to lifting and are lowered into vertical slots so that they only need to be tightened. This is demonstrated in Figure 3-37. It was found in the referenced study that a greater number of smaller bolts were required but that the connection would be stronger due to the way that force is transferred.

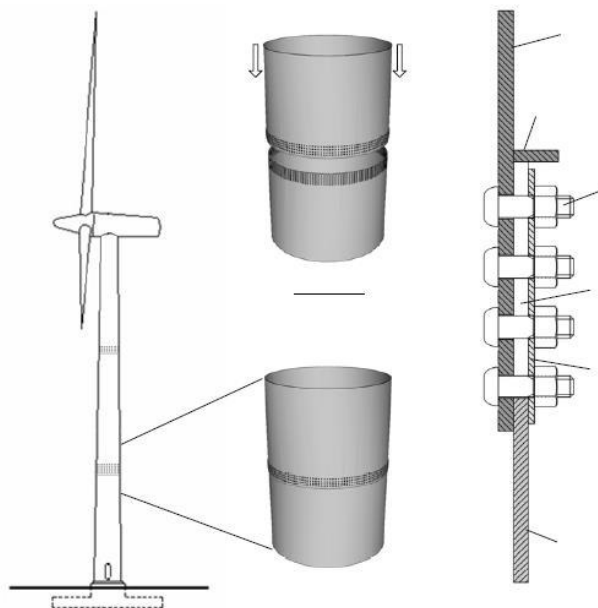


Figure 3-37 Friction connection (Heistermann et al., 2009)

This design is attractive from this project's perspective for a number of reasons:

- In the idea proposed, the bolts are pre-installed and lowered into vertical slots. This means that they don't need to be inserted by hand at the site.
- There can be some length when the two cylinders engage prior to the bolted area so that some guiding surface can be used to aid positioning which is discussed in Section 3.1.4.2.2
- There would be some level of the load being secured by the cylinders fitting into each other, as discussed in the referenced paper.

However, after brief consideration, there are also a number of potential drawbacks to the idea which would need addressing before it could be used:

- For a bolt to adhere two surfaces it must press the surfaces together, for two concentric cylinders to be pressed together there must be some deformation which, if achieved, would require force from the bolts reducing adhesion.
- If the two cylinders have a very tight fit, negating the previous point somewhat, then tolerance control as well as actually getting the cylinders into each other at the site would potentially be made much more difficult.
- A flange provides some stiffness due to area in the plane of stress, if there is no flange then the radius is weaker and more likely to deform in transit – deformation could lead to the tower sections not fitting on installation and would be difficult or impossible to resolve in situ.
- Instead of the key tolerances being with the flange surface and definition of hole positions, key tolerance is now roundness and smoothness of tower sections at joining area, also tower diameter at the area is very important – this is potentially much harder to achieve.
- In a flange connection, rotational and positional definition is achieved with dowels into datum holes – the friction fitting would require some other high-precision definition for rotation.
- Bolt corrosion on the exterior of the tower could be an issue if the coating is insufficient or is scratched.
- With the entire bolt assembly of the bolt, nut and washer lifted on the tower there is a risk of pieces falling.

- If the bolt or nut move between being placed in position prior to lifting and the tower being placed it could potentially cause an obstruction preventing the tower section from being installed which would be difficult to resolve.
- More bolts would take longer to tighten since they are not significantly different sizes and so the same method would still need to be used leading to more installation time.

As can be seen, there are a significant number of issues with the idea which may be hard to address, but potentially other designs may exist which offer the same potential positives without the negatives.

3.2.2.2 ConXtech Connection

ConXtech is a company which offers a number of building solutions aimed at the construction industry (ConXtech, 2015). The aim of their product is to speed up on-site construction by moving all welding operations to the shop floor where machines can perform them more quickly and repeatably. Modules, like rail type systems, are assembled onto the steel beam sections in the shop floor so that at the site these modules can be slid into each other. Once the sections have been slid together it is no longer required for the crane to hold them and they can be bolted together. There are also a number of similar connections (Bijlaard, Coelho, & Magalhães, 2009), but for the sake of brevity only the solution from ConXtech will be discussed here.

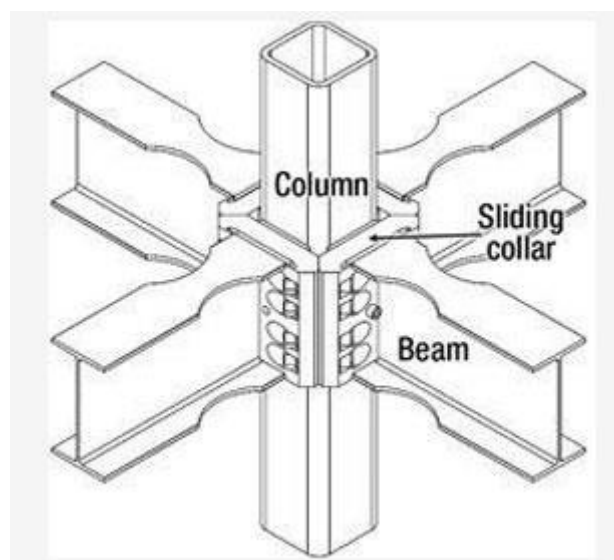


Figure 3-38 ConXtech connection drawing (Olson & Steel co, 2017)

This technology, as it exists for its current application, achieves some of the positive aspects of the friction connection in that it is partially secured once it is put into place. Additionally, with some redesigning, the bolts could be pre-positioned and slid into place with the rail system.

However, there are also some down sides to this design. While with steel beam construction the parts are bolted in a limited number of directions, in the wind turbine construction they would be bolted in completely around the radius of the tower to resist forces in all directions; this would lead to the same problem as mentioned in the Friction Connection' where the bolts are acting against each other rather than pressing the fastened members together.

With the large rail sections there will be less area for the bolts to act on within the same space, it will be more difficult to achieve the appropriate adhesion between the bolted components to resist service loads.

3.2.2.3 Single, Large Thread

The idea of single, large thread was one that this team had come up with and is proposed now. In this concept, rather than the thread being mounted to the two tower sections, there is a separate threaded collar which would rotate independently to the tower sections and clamp the two together. By having a separate collar for the thread this allows for the two tower sections to be located relative to each other with long dowels or other guides; in fact, these guides are necessary to prevent the top section from rotating with the collar. The collar would be rotated potentially via a motor and gear set or some hydraulic system located on the tower – either the motor could be external and used on each tower section in turn, or it could be internal and remain with the structure to retighten the threaded connection as necessary over time.

Potentially this might fully eliminate humans from the bolting process and there would be no small bolts which might drop. In terms of performance, for a quick first estimation the data from (alfadoc, 2013) is extrapolated using a line of best fit; a polynomial curve was used for compression and a power curve was used for torque. To meet the same compressive force of 120 times M36 class 10.9 bolts, a thread diameter of 300 millimetres would be needed, which is much smaller than the roughly 4 meter diameter flange which would accommodate 120 M36 bolts. However the torque

required to tighten this thread would be around 3.5 million Newton-meters, which might be impossible.

In addition to the massive amount of pre-load torque required there are a number of other issues which would need to be addressed:

- It may be difficult and expensive to manufacture such a large thread.
- The large torque required to tighten the thread could damage the structure, including the dowels which are used to locate the two tower sections and resist rotational moments during tightening. A study of loading values and structural resistance would be required.
- There is no redundancy if only one thread is used, if the one thread breaks then the connection itself breaks.

3.2.2.4 Hydraulic Seafastening

Hydraulic systems are already in use to sea-fasten a number of components to the ship deck, for example the system used in (Rolls Royce Marine AS, 2011) which talks about a system from Rolls-Royce which is used to secure items close to the ship deck. More specifically related to offshore wind industry, (Hoeksema, 2014) mentions a number of potential options for sea-fastening a transition piece (TP) to the ship deck. These options, as shown in Figure 3-39, generally secure the TP to the deck by applying some load to the flange either through a wedge system or directly. Although the aim of these seafastening methods is to secure the load for the entire duration of transporting the TP to the site, capital expenditure could be saved if they are only used temporarily while the bolts are being put into place and secured.

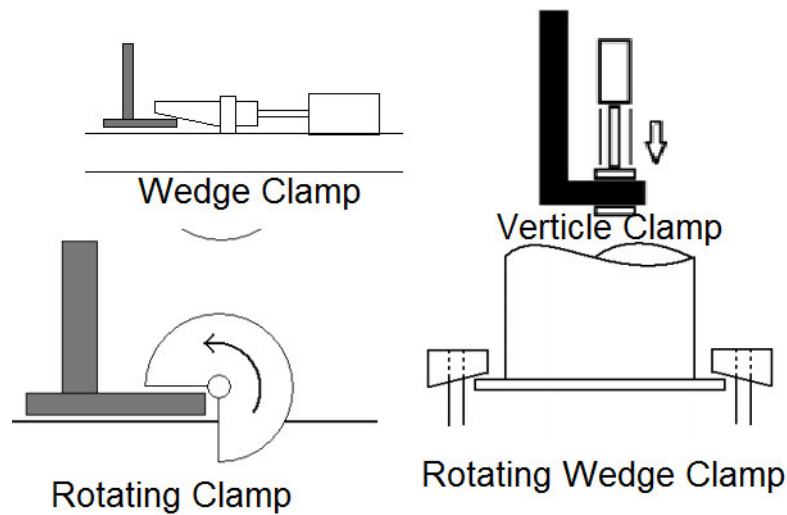


Figure 3-39 Various hydraulic seafastening options mentioned in (Hoeksema, 2014)

These systems are appealing because they are quick and reusable. Conventionally, there is some time when the load is unsecured, before the bolts are put into place.

However, there are a number of potential downsides to these options:

- In the case of the wedge type clamps, load is applied at the edge of the flange which, as mentioned in the referenced report, can apply a large moment to the weld.
- In the case of the direct systems such as the 'vertical clamp', there are space limitations and the system may need to be moved into position above the flange.

3.2.2.5 Internal Jack Seafastening

An internal jack system is proposed in (Hoeksema, 2014) for use in securing transition pieces to the ship deck. The final design, which was concluded in the referenced report was a hydraulic seafastening device, like a small tower, which went inside the TP and pressed outwards. The design proposed the use of eight pistons at two levels (a total of 16 pistons) which act on the internal surface of the TP to resist movement. The design included a rail system for positioning the TP to ensure clearance for the grout skirt. It was concluded in the referenced report that this method of seafastening can withstand a higher acceleration than a conventional bolted flange connection while being significantly faster and requiring no manual labour. The final design from the referenced report is shown in Figure 3-40.

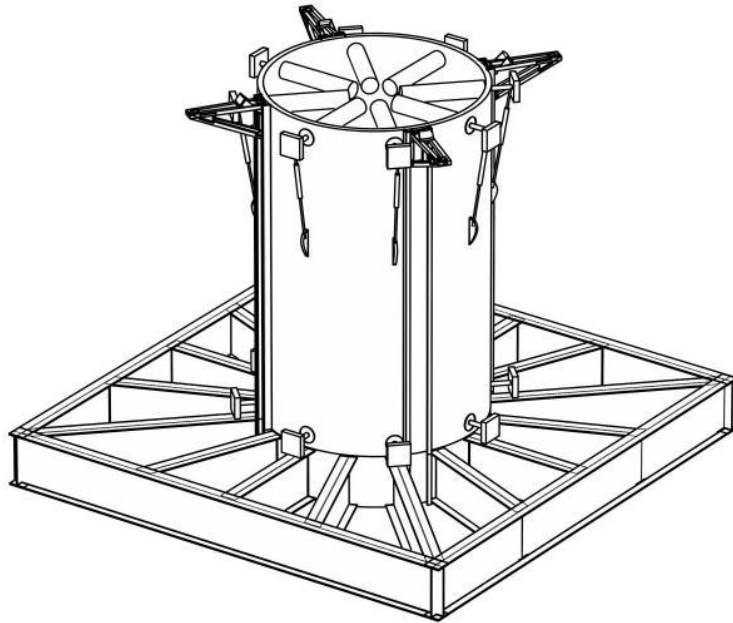


Figure 3-40 Hydraulic internal seafastening design proposed in (Hoeksema, 2014)

This design is very appealing because, apparently, it completely removes humans and bolting from seafastening of these components. It is potentially very fast, provided that the guides can be lined up quickly and there are no bolts which can shake loose.

The design does however depend on a single hydraulic system at each level so that it is self-centring and if it leaks there is potentially no redundancy. If there are internal features in what is being secured then this could create an obstacle preventing the device's use; for example, for a TP there is the grout skirt which is accommodated for in the report, but on a tower there could be floors, ladders or other features which might get in the way. The device could be very expensive compared to bolted seafastening and one unit would be required for each item that the user wants to transport each time – this would likely be a considerable capital expense.

3.2.2.6 Bolting Robot Arm

One obvious way to remove humans from the line of fire is to automate the tasks performed by humans. This is extremely common in factory manufacturing in a wide variety of industries where the speed, precision and repeatability of robot machinery have replaced human workers. There exist a number of automated systems specifically for bolting, for example Electroimpact

(Sydenham & Brown, 2015) have developed an automated system to deliver OSI bolts to the work specimen and tighten them with checks at each step to ensure they have been performed correctly. As mentioned previously, special methods of tightening are required to achieve the large pre-load necessary for the bolts; a method of applying this hydraulic tensioning method using a robotic arm has been developed in (Müller et al., 2014). These are all factory floor systems, so they would need to be developed for use in the operation site.

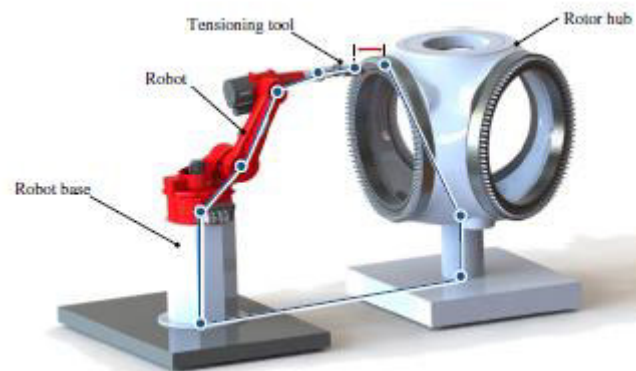


Figure 3-41 Rotor hub, bearing bolt tightening robot (Müller et al., 2014)

The advantages of such a system are potentially reduced installation time, the system in (Müller et al., 2014) performed the tightening task, which would normally require 3 hours work for two people, in only 2 hours with one person monitoring the controls. There is reduced risk to personnel from falling items or danger from high-pressure hydraulic lines as the system can be safely operated from a remote location. If the system can also position the bolts into the hole then there will be no need at all for humans to have any part directly in the bolting procedure.

There are some issues with the system which would require addressing, particularly in converting a shop floor system into an operational system. The system would need to be positioned inside wherever it is performing the operation, which would itself likely require some lifting and construction. Removal of the robot from where it has performed the operation may be even more difficult. There could be obstructions to the robot such as yaw motors in the hub or electronic components in the nacelle or tower which the robot would need to work around. The varied light conditions could cause issues for vision based systems. The robot itself is a complex system which

would require its own maintenance and repairs; it would need to be checked thoroughly prior to use to ensure it did not fail in operation and delay the procedure.

3.2.2.7 External Climbing Bolt Robot

A slightly more blue-sky type idea, which would remedy some of the issues mentioned in the bolting robot idea, would be a robot which could climb the outside of the tower and insert, and/or tighten the bolts from the outside. This would, initially, be restricted to fastening tower sections but could possibly be extended to other parts. It would also require a tower connection method where the bolts are accessible from the outside – this could be achieved either with horizontal bolts such as in a friction connection or simply by having the flange on the outside. The systems used in Section 3.2.2.6 could be used here in conjunction with some climbing technology. A way in which the robot could climb the tower is through wheels which are pressed tightly against the tower or perhaps some external crane.

This system would be very quick to get in and out of operation, it would only need to be assembled around the tower and then allowed to climb up and perform its task. If something should go wrong with the system it would not be very difficult to bring it back down to the TP for repairs or replacements.

The biggest issue with this idea is that it depends on changes to the connection design; friction connections may be infeasible and positioning the bolts on the outside would make it difficult for humans to perform any tasks, such as inspection, on the bolts. Bolts on the outside could also pose issues for corrosion and other wear. The system is limited in its capabilities and could initially only work on tower sections and potentially where the nacelle meets the tower as climbing off from the tower to other parts would pose a substantial challenge.

3.2.3 Selection of Most Promising Solutions

As a result of the MCDA analysis performed, discussed in Section 4.3 'Multi-Criteria Decision Method' the top ideas selected for further investigation, based on the needs and values of the industry personal surveyed, were the internal bolt tightening robot mentioned in Section 3.2.2.6

and a new seafastening method such as the internal hydraulic idea mentioned in Internal Jack Seafastening'. Due to this analysis, these ideas were deemed the most relevant for industry and thus were investigated further and will now be discussed.

3.2.4 Development of Solutions in Detail

3.2.4.1 Automated Bolting System

3.2.4.1.1 Application

As mentioned in Section 3.2.2.6 an automated system which combines a robotic arm, a vision based bolt hole identification system, a fastener feed system and a programmable logic control (PLC) could be used in conjunction to create an automated bolting system (ABS) which can insert and tighten the bolts necessary to hold large sections of the WTG together.

This ABS could be used in connection of tower sections or could be used to connect the blades to the hub or the hub to the nacelle as it has been developed for use on similar tasks on the shop floor (Leenhard Hörauf, Rainer Müller, Jochen Bauer, Holger Neumann Vette, 2013). It could be very difficult to use this to attach the nacelle to the tower because the nacelle is usually assembled with its inner components prior to being mounted to the tower (Sharpley, 2016).

Another potential use for an ABS is in seafastening, as shown in Figure 3-42, however it should be stressed that this is an original idea presented here which has not, to the author's knowledge, been developed. As the tower sections are usually bolted to the ship deck there is an amount of bolting and unbolting which is currently performed by human personnel. Fundamentally, the idea is that if the ABS is positioned in a recess underneath the grillage it could be mounted on a sled which can move between the individual flanges. The advantage of this is that one ABS can be used on the ship and will not require lifting and assembling like it would to connect tower sections. Power and hydraulics from the ship could potentially be used for the system rather than trying to source these on the tower.

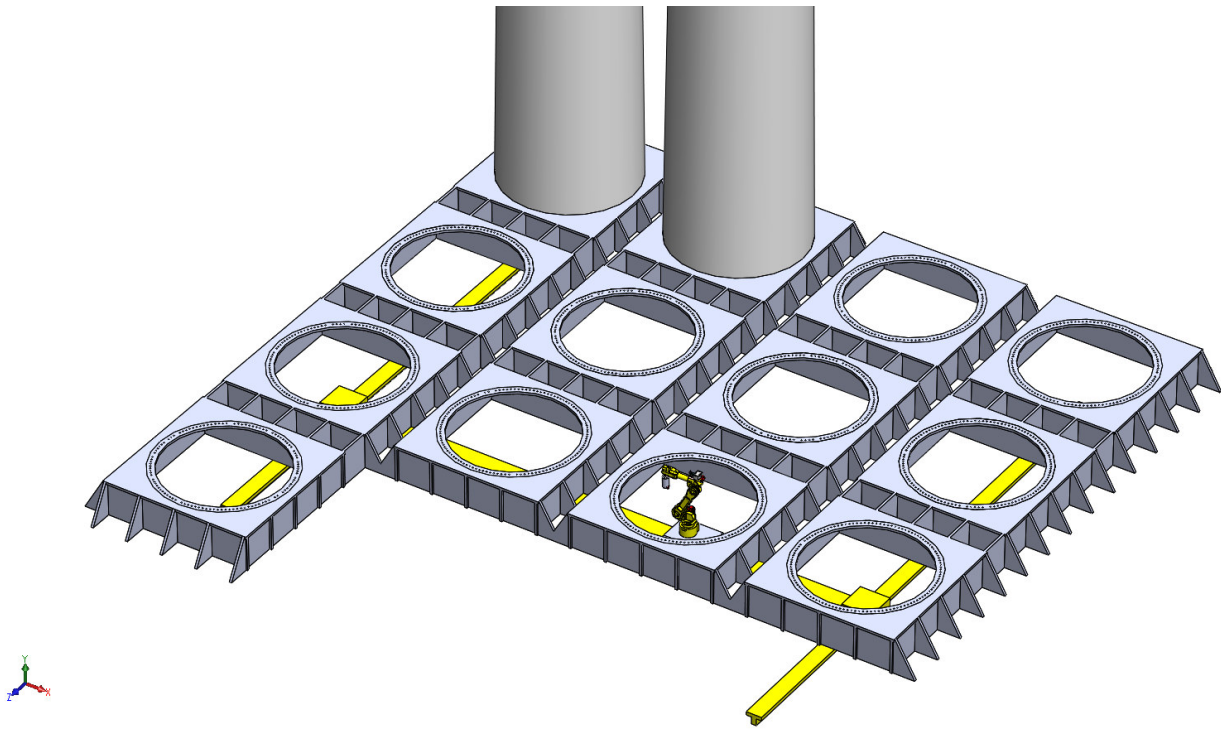


Figure 3-42 Automated bolted seafastening, concept illustration. CAD by M. Richmond

The following sections within 3.2.4.1, with some exceptions, can generally be applied to both of the previously discussed application and discuss the fundamentals of automation.

3.2.4.1.2 Mechanical Manipulator

The robot mechanical system generally used on a number of components is a 6-axis robot arm (Müller et al., 2014), this robotic arm can also be used on a sled to allow for it to be repositioned along a work piece (Sydenham & Brown, 2015). This allows for a great deal of flexibility which is necessary if the robot is not mounted directly to the work piece because there will inevitably be some misalignment between the two (Leenhard Hörauf, Rainer Müller, Jochen Bauer, Holger Neumann Vette, 2013). However, in some circumstances the robot can be connected to the flange section like in (Duan, Wang, Li, Kong, & Aliy, 2013) where a bolt tightening system is developed which secures flanges on nuclear energy steam pipes. The system from (Duan et al., 2013) uses a more simple robot which mounts directly to the flange and rotates about the central axis. In this way the system only requires 3 axes: angular rotation, θ , radial distance from the centre, r , and a third control for tightening mechanism height from the work piece, z .

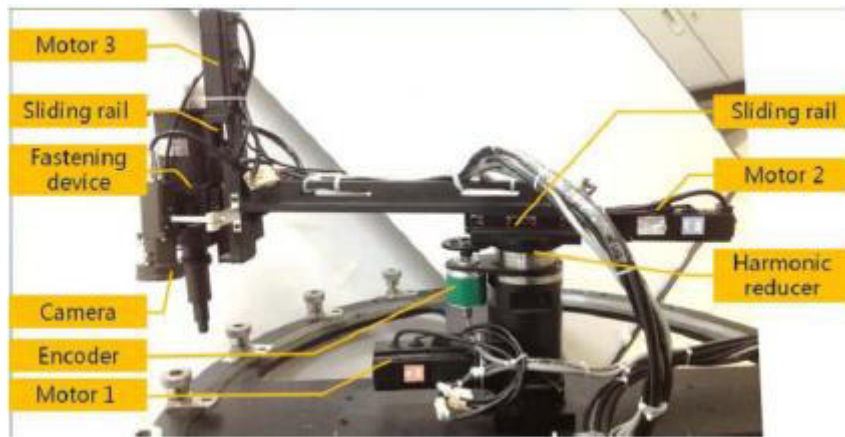


Figure 3-43 Mechanical manipulation robot discussed in (Duan et al., 2013)

Which system is most appropriate depends upon a number of factors, however it is worth considering that there are often components within the tower section or rotor hub which need to be worked around, so a radial system may not be appropriate in these situations. If capital expenditure is a concern then the simplicity of fewer axes could be cheaper. Fewer axes could simplify the bolt or bolt hole identification process as, if there is some connection between the ABS and the flange, several parameters can be determined more easily based on positioning relative to the connection.

3.2.4.1.3 Vision Systems

Machine vision and image analysis is a wide and substantial field in and of itself with a great many journals devoted to it; a list of some of these journals can be found in (guide2research, 2017). The machine vision process consists of taking the image, pre-processing, analysis and then sending the data. The basic analysis process can be pixel counting where the sum of a region of pixels is determined, threshold limit, edge finding, blob analysis and many more (SICK IVP, 2006).

Of course, there has also been a fair amount of research on bolting systems. Once the edges of an object have been found, possibly through pixel gradients, it needs to be determined if the object is what the system is looking for (a bolt hole or head) and its orientation and position need to be evaluated. In (Choe et al., 2009) a bolting robot was created which identified bolt holes using circular Hough transforms (CHT), their pre-processing consisted of 1.) Compensation for lens distortion, 2.) Noise filtering, 3.) Histogram equalization, and 4.) Edge definition. In (Duan et al.,

2013), the authors' objective was identifying the hexagonal hole in the head of bolts for tightening, which they accomplished using 'Canny algorithm' for binary realization and 'hexagonal spatial moment' to find the centre of the bolt.

Additional sensors and a priori knowledge of the work piece can be used to simplify the problem, whilst complexity is added if there is a question of where and at what orientation the bolts are relative to the robot. For example, in (Choe et al., 2009) the author uses a laser range finder and knowledge of the size of the bolt holes to simplify the analysis to two dimensions. In references (Hörauf, Müller, Bauer, Neumann, & Vette, 2013) (Müller et al., 2014), which discuss an adaptive process for tightening off shore wind turbine blade hub bearing bolts, there is a tolerance chain between the bolt and the tensioning tool due to tolerances in manufacturing as well as the robot's kinematics. These tolerances were reduced in two steps: 1.) by moving the robot inside the hub and using a laser triangulation sensor to determine the position of the bearing ring. 2.) Use of a camera system to determine the bolts positions, within the now determined bearing plane, relative to their nominal positions.

3.2.4.1.4 Fastener Feed

A fastener feeding system was discussed in (Sydenham & Brown, 2015) which was a study by Electroimpact to feed a variety of OSI bolts for use in an aircraft wing on the shop floor. The feed system had two sources; either the bolts were fed from hangers where orientation was already achieved or from hoppers where the output of the hopper oriented the bolts. In this system, the fastener is pushed by an air blast which sends it to an end effector. The bolt is checked at various stages to ensure that it is the correct bolt and that it has been positioned correctly. If the wrong bolt is sent then it can be returned along the same path and rejected.

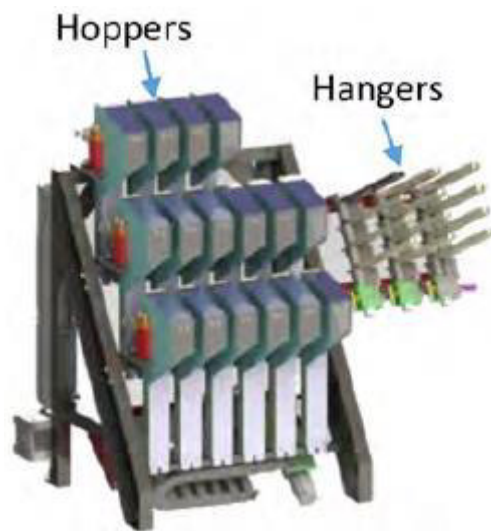


Figure 3-44 Fastener feed system discussed in (Sydenham & Brown, 2015)

If a system like this was used in offshore wind turbine installation then humans could be completely removed from the fastening process. However, this bolt feed system could potentially be challenging due to the size of the bolts, which are much larger than the bolts used in (Sydenham & Brown, 2015). A significant air blast would be needed to move the weight of the bolts. Also, the reference states that hangers were used for the larger bolts, the bolts would need to be loaded onto the hangers prior to the machine being put in operation.

3.2.4.1.5 Conclusion

A series of technologies have been presented which could be used in conjunction to accomplish the task of automating the bolting procedure, however there are some aspects which need to be further developed to make feasible.

The bolts used in the Electroimpact system are far smaller than the ones in offshore wind structures and the fastener feed system would need to accommodate that. The vision systems discussed were in controlled, shop floor environments and further work would be needed to ensure it could still work reliably with the varied lighting conditions offshore. The robot bolting systems are developed for the shop floor where they can easily be assembled and can be provided with power and hydraulics – this would be far more challenging offshore.

However, if these challenges are overcome then the technology looks promising to be able to perform the task in an automated fashion.

3.2.4.2 Hydraulic Seafastening

3.2.4.2.1 Introduction

Hydraulic seafastening is already in some use and has been design approved by DNV (Siemens, 2015), however, it is difficult to discuss the topic a great deal due to the lack of available information on the subject. Red Marine are developing a hydraulic seafastening solution which they say should reduce the time and cost of operations (AJP Recruitment, 2016). (Hydro International, 2017) mentions that IHC was using a hydraulic sea fastening system in 2009 and (Izzo, 2014) discusses a hydraulic seafastening system from IHC which is light weight and can clamp tower flanges together with a force of 25 tons by acting through and against 3 consecutive bolt holes.

In 2014, Wouter Hoeksema proposed a hydraulic sea fastening system for transition pieces which fully replaces bolting (Hoeksema, 2014). This system uses eight hydraulic pistons at two levels for a total of 16 pistons to act against the inside of the TP and secure it. A guide system was also proposed to avoid interference with internal components such as the grout skirt. It was concluded that this system could withstand twice the acceleration as conventional bolting and would require no manual labour, however existing grillage was insufficient to withstand the loads and would need reinforcing. This promising concept does not appear to have been developed further than this.

In conclusion, based on the limited availability of information on the subject, hydraulic seafastening appears to be a very promising means of reducing the risk and also time involved in seafastening. There are a wide range of methods to accomplish hydraulic seafastening and which one is chosen can be based on a balance of the level of capital expenditure one is willing to invest and the performance required.

3.3 Concepts for Assembly

3.3.1 Introduction

The different offshore pre-assembly transportation and installation methods are the major driving force for a successful wind farm installation. However, as outlined Section 1.2, the human presence beneath heavy lifts is the current most adopted procedure and most hazardous aspect of offshore wind turbine installation operations.

Installation pre-assembly concepts can be applied as a positive path towards achieving human free lifting operations offshore, thereby minimizing the number of lifts and reducing the human exposures to lifting hazards. Therefore, the aim of this section is to present different pre-assembly as well as assembly transportation and installation solutions and analyse their possible optimization and their pros and cons when employed to reduce or even cut out of human presence in the offshore heavy lift operation.

Some of the assembling and pre-assembling installation methods of bottom-fixed offshore wind turbines on already installed foundation are shown in Figure 3-45. The turbine system can be transported offshore and installed in:

- six lifting operations, transporting the turbine single pieces (SP), pre-assembling only the hub on the nacelle and lifting each component separately
- five lifting operations, performed in the same way for the six-lifts method but splitting the tower into two tower elements (2T): this solution can be employed where limitations in the design/operating capacity of equipment, or the stability of the installation unit (either vessel or barge) do not allow the entire tower (1T) to be lifted and transported;
- from three to four lifting operations, such as for bunny-ear (BE) and rotor (ROT) pre-assembly methods;
- from two up to a single lifting operation.

Other pre-assembly configurations are still possible depending on the particular combination of turbine and installing units' capacities.

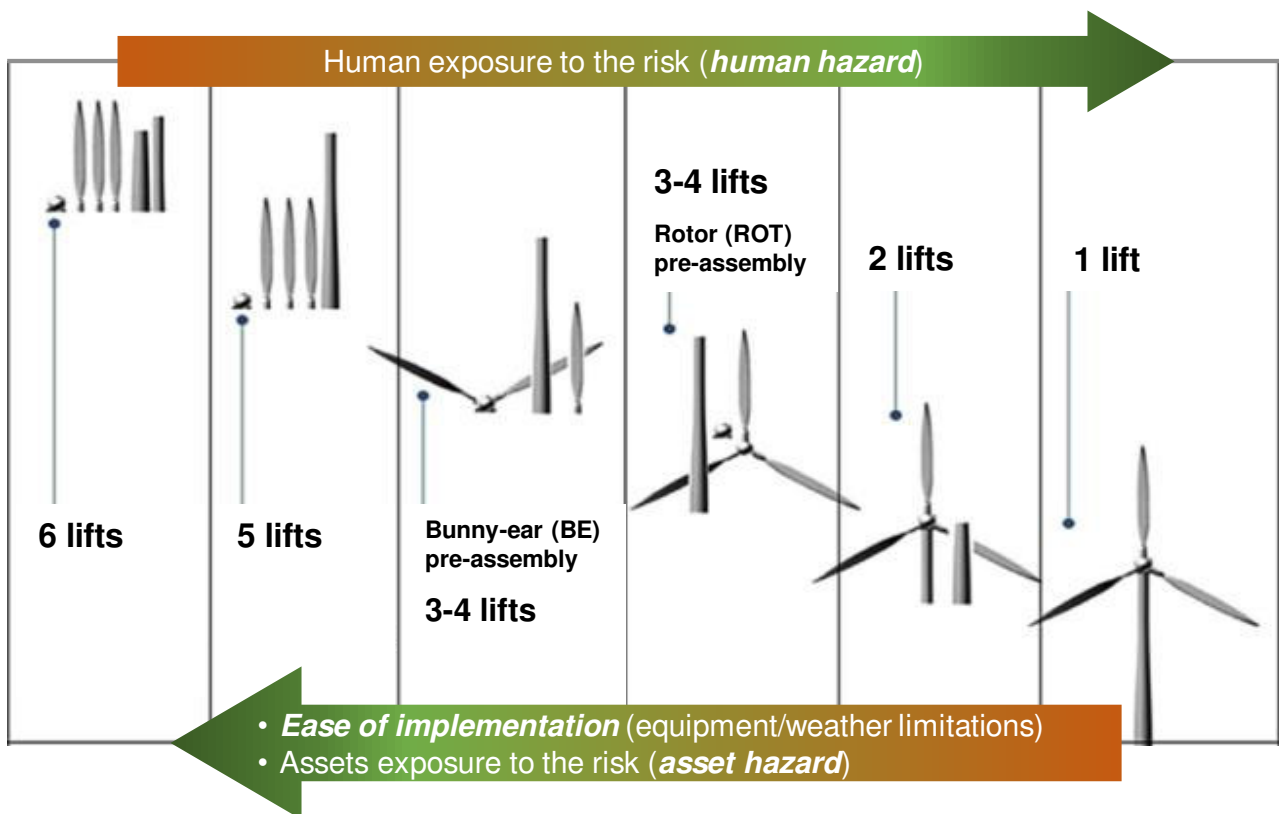


Figure 3-45 Offshore wind turbine current used and proposed installation methods. Adapted from (Ahn, Shin, Kim, Kharoufi, & Kim, 2016)

However, by looking at the procedures current employed (Section 2.1), it is observable that a minimum of three lifts is preferred to the more complicated and more strictly weather-limited two- and one-lift methods. An overview of the actual assembly methods used for North Sea wind farm installation is provided in Table 3-4, showing the relationship between the installation method, dimensions of the turbines, and the number of turbines to install and units (vessels and/or barges) in the wind farm.

Moreover, the choice of the method is highly dependent on the vessel and its equipment capacities;

Figure 3-46, shows some of the commonly used barge and vessel units in offshore installations, Turbine Installation Units (TIU).

Table 3-4 North Sea Wind farm installation requirements and characteristics. Adapted from (4C Offshore, 2017c),(C-power, 2017) and (Uraz, 2011)

Project	MW class	No. turbine in the farm	No. units to install	Duration [days]	Method	No. lifts per turb.
<i>Horns Rev.1</i>	2	80	2	110	BE-1T	3
<i>Prinses Amalia</i>	2	60	2	330*	BE-1T	3
<i>North Hoyle</i>	2	30	2	90	BE-2T	4
<i>Nysted</i>	2.3	72	1	78	ROT-2T	4
<i>Lillgrund</i>	2.3	48	1	73	ROT-2T	4
<i>OWEZ</i>	3	36	1	67	BE-1T	3
<i>Thanet</i>	3	100	1	197	SP-1T	5
<i>Greater Gabbard</i>	3.6	140	2	515*	SP-2T	6
<i>Lynn & Inner Dowsing</i>	3.6	54	1	122	SP-2T	6
<i>Thornton Bank (phase.I)</i>	5	6	2	70*	ROT-2T**	6

* Approximatively derived days from data available online (4C Offshore, 2017c). The exact dates from the first to the last turbine erection involve also working breaks for foundation installation, weather window availability and unplanned issues.

** Tower(s) and nacelle components separately pre-installed with respect to the rotor pre-assembly



a) Towed barge



b) Shear-leg crane barge



c) Semi-submersible heavy lift vessel



d) DP2 heavy lift cargo vessel



e) Towed jack-up crane barge



f) Self-propelled jack-up vessel

Figure 3-46 Offshore wind farm installation vessels (Ahn et al., 2016)

Indeed, choice of the TIU type and number for specific installation requirements, is dependent on several factors, from the maximum water depth (limiting the use of jack-up units and requiring the employment of dynamically positioning ones) to the cost for hiring the unit. In particular the TIU market current availability for turbines' single-lift installation is still at a feasibility study point of view (Vuyk Engineering Rotterdam b.v., 2017), being their use is highly reliant on the turbine's dimension and strictly restricted by weather conditions.

Therefore, even if single lift installation methods could potentially reduce the installation duration and improve overall project costs by 0.5% (Scottish Enterprise, 2004), to maintain a balance in the cost-effectiveness of the wind farm installation, it could be worthwhile investigating different ideas (patents and designs) and new concepts of offshore wind turbines, learning from the current or suggested solutions for onshore installations.

3.3.2 Initial Proposed Solutions

3.3.2.1 Onshore Pre-Assembly Solutions: Bottom-Fixed Wind Turbines

3.3.2.1.1 Introduction to the Methods: Main Factors and Limitations

The offshore assembly of wind turbines systems on pre-installed foundations (either monopiles, tripod, tripile, jacket, gravity based or suction bucket support structures) has many constraints, which can be especially addressed to:

- equipment's lifting capacities and TIUs' stability limitations, and
- ease of implementation of the pre-assembled piece(s) for encumbrance and/or lifting procedure limitations.

Therefore the onshore pre-assembling approach, aimed to reduce the offshore lift number up to single-lift operations, need for onshore facilities and offshore units able to deal with the port-loading and transporting and installing phases (Figure 3-47).

TIUs' market currently offers the employment of either jack-up vessels (JUV) and barges (JUB), dynamically positioning vessels (DPV), or semisubmersible barges for the requirements of the wind offshore industry (Figure 3-46). Since even a small movement of the vessel can cause meters of error at the hook height, DPVs used could cope with the need for high accuracy movements of the floating vessel, by reducing the position keeping excursion tolerance through the use of an high classes vessel (Germanischer Lloyd SE, 2013).

On the other hand due to the high cost of their renting and the inability to deal with air gap (Burton, Jenkins, Sharpe, & Bossanyi, 2011), those performing offshore heavy lifting for turbine installations usually prefer to employ jack-up units (Figure 3-48).

Moreover, JUV can be chosen over the JUB depending on the specific farm and installation timing necessities, offering generally faster design speed but lower deck area availability (due to the encumbrance of the engine casing and the crew manoeuvring bridge house).



Figure 3-47 Example of onshore pre-assembly site (harbour) for offshore wind farm installation (Asgarpour, 2016).



Figure 3-48 Jack-up vessels and barge comparison (during lifting and installation phases of BE pre-assembly) (Fred. Olsen Windcarrier, 2013; Uraz, 2011)

With regards to the semi-submersible barge, after being widely used in offshore oil and gas field, they have been employed by the wind industry (Atlantic Area Transnational Program, 2010) for fully pre-assembled transportation solutions (see chapter 3.3.2.1.3).

Although, even when the most suitable TIU type has been selected (usually jack-up units, for partially pre-assembled turbine method), the deck free area availability and structural characteristic (thus, deck loading capacity) vary depending on different companies' know-how and historical

shipbuilding profile. The JUV usually range between about 3,000 m² to 4,000 m² (A2SEA, 2009; MPI Offshore, 2017) for free deck area and reach a maximum net weight on deck of about 8,000 tons (Fred. Olsen Windcarrier, 2017). On the other hand, what is common between all of them, and distinguish offshore lifting operations from onshore ones, is the possibility to easily use higher capacity lifting equipment, able to lift up to about 1,000 tons (MPI Offshore, 2011a).

Despite this, there is a limit to transportation and lifting procedure when using pre-assembly, not only due to the installing unit characteristic, but also because of safety reasons. It is important to consider that the recommendations and rules for safe lifting operations become more restrictive by the increase of the weight and/or the exposed area to the wind. For instance, the DNV-GL offshore lifting operation standards, define and account for a dynamic amplification factor, which, together with a combination of other parameters (such as wind speed and crane characteristics) limit the crane operational condition (DNV, 2014a).

In particular, current and possible solutions for onshore pre-assembling and offshore transportation are presented in this section, dealing with, in details, their pros and cons and the specific requirements.

3.3.2.1.2 Currently Pre-Assembly Practice

The so called “bunny-ear” (BE) method consists of the onshore pre-assembly of the nacelle with the hub and two blades, while the single third blade and the tower piece(s) are positioned separately on the deck. Therefore during the offshore transportation the configuration lays on the deck either on the nacelle base (Figure 3-49, right) or on an in-situ designed structure for the deck reinforcement and/or encumbrance optimization (Figure 3-49, left).

This method has already been implemented for the installation of 2.0MW and 2.3MW classes wind turbines’ farms (see Table 3-4) and was chosen for the installation of the Haliade150-6.0MW demonstration project (Figure 3-49, right). However, as it can be expected and has happened for the Fred. Olsen commissioned project (4C Offshore, 2017a), this configuration installation can easily delay the farm completion due to adverse operating conditions.



Figure 3-49 BE configuration offshore transportation examples (Fred. Olsen Windcarrier, 2013; Uraz, 2011)



Figure 3-50 ROT configuration offshore installation examples (C-power, 2017; offshoreWIND.biz, 2015)

The star-array or rotor (ROT) pre-assembly configuration (Ahn et al., 2016), as suggested by the name itself, is the onshore pre-assembling of all the blades in the on the hub structure and their transportation on the hub diameter plane, mounted, as for the BE, on a reinforced deck support or specifically designed structure for the offshore transportation.

In particular this method requires low encumbrance installation units (ideally 3 jack-up legged or barges units), having to move and rotate the pre-assembly before its installation. Below are ROT pre-assembly installation examples of the 2.3MW-Siemens turbines in the Nysted wind farm

Moreover, the new tower-blade pre-assembly (see Figure 3-51) does not drastically affect (in terms of encumbrance, lifted weight, and operating accepted conditions) the solution already suggested by the normal BE method. However, as observable from Figure 3-51, the use and design of a particular temporary mechanical component, for the connection of the third blade to the respective tower, has to be introduced.



Figure 3-52 Conceptual designs for fully pre-assembled turbines transportation and installation on pre-installed bottom-fixed foundation (Ulstein Offshore Wind Team, 2017; Vuyk Engineering Rotterdam b.v., 2017)

The concept of fully pre-assembled turbine is the logical and direct consequence to the aim of the reduction of the number of lifts. However, even if the offshore installation units can easily achieve the capacity required for an entire turbine lift, a limitation of the single-lift procedures is the on-deck transportation and stability (Figure 3-52), nonetheless the severe weather condition constrains: for instance, transportation and installation significant wave height tolerance is reduced to not more than 2.5 meters for the Vuyk's proposed vessels below (Vuyk Engineering Rotterdam b.v., 2017). Therefore, only feasibility-study-level designs are currently available for this proposed solution, as the use of these ad-hoc vessels is expensive and limited to the project phase and over-designed for the farms' ordinary maintenance procedures and through-life operation.

For these reasons, and aiming to maintain the seabed-fixed structure for farms' limited water depth, the possibility to push further the designs of gravity based and/or suction bucket foundation designs could also be taken into account. In fact, several projects are presently looking for “float-out-and-sink” offshore installation method, in order to allow the floating transportation of the fully pre-assembled turbines and their in-situ sinking (4C Offshore, 2017b). Within the summer 2017 the approved project for the gravity based foundations (Figure 3-53, left) developed by BAM's Group for EDF's Blyth offshore wind demonstration project (BAM Nuttal, 2016) will be concluded, thus paving the way for fully pre-assembled “self-installing” (with the aid of semi-submersible barge, if needed) wind turbines (Figure 3-53, right).

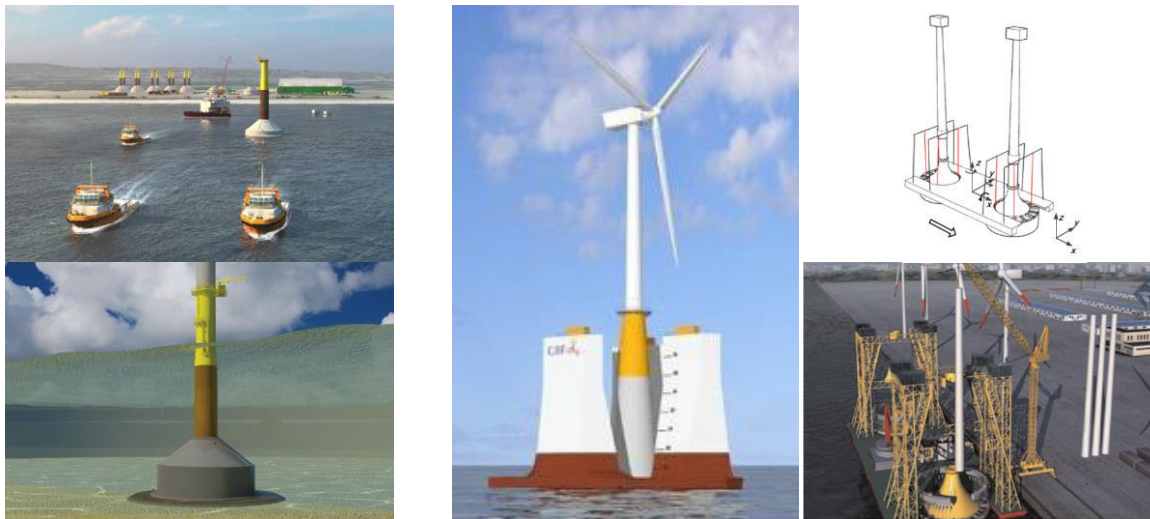


Figure 3-53 Left) BAM's Group gravity based design for EDF's Blyth demonstration project (4C Offshore, 2017b; BAM Nuttal, 2016; theconstructionindex, 2017). Right) Gravity based (middle right) and bucket (extreme right) foundations feasibility designs (4C Offshore, 2017b; P. Zhang, Han, Ding, & Zhang, 2015)

3.3.2.2 Onshore Pre-Assembly Solutions: Floating Wind Turbines

In order to deal with the transportation of fully pre-assembled wind turbines, the offshore wind market is moving toward the implementation of floating wind turbines solutions. Three classes, in which they can be subdivided, distinguish them in term of stability (Figure 3-54).

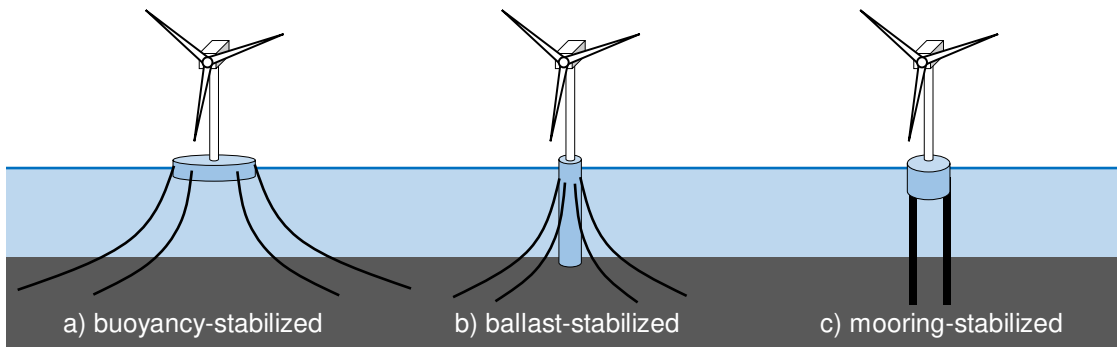


Figure 3-54: Floating wind turbines stability classes

While buoyancy stabilised support structure are suitable for a vertical towing transportation solution, ballast (spar) and mooring (TLP) –stabilised structure can be placed into their position in the farm only through the aid of semisubmersible and/or tilting barge (Figure 3-55).

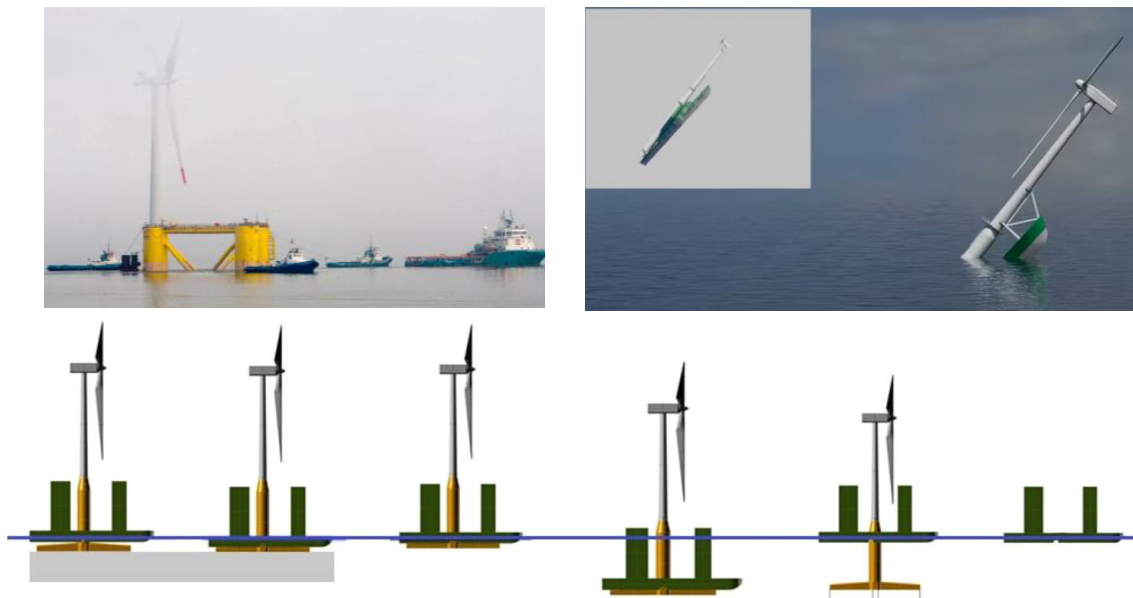


Figure 3-55: Floating wind turbine transportation possibilities. Top-left) Tri-floater top-right) spar , bottom) TLP (Amate, Sánchez, & González, 2016; Principle Power, 2011)

3.3.2.3 Offshore Assembly Solutions

By considering the possible adaptability of some in-use technologies adopted in the onshore wind production, it could be worth it to look at new installing ideas and crane designs for offshore application. These can be offered, for instance, by the adoption of different cranes layout, or new concepts of turbine, able to either partially (requiring the use of a crane) or fully (through the

employment of mechanical devices at the tower base level) self-erecting on their tower and foundations.

3.3.3 Selection of Most Promising Solutions

As previously anticipated in the other sections (Section 3.1-3.2), in order to refine the concepts discussed in Section 3.3.2, the group have employed a Multi-Criteria Decision Analysis (MCDA) based on results from a survey sent to industry. This has been used to select the most promising solutions within the three conceptual sections. More information on the process can be found in Section 4.3. The output of this analysis is a rating of each concept as a 'C value', which indicates the closeness to ideal solution (between zero and one, with one being ideal). Table 3-5 shows C values for the best 4 concepts that are worth to be investigated further in the next section (Section 3.3.4)

Table 3-5: MCDA results for assembly

Alternatives	C value
Current pre-assembly practise	0.7187
Bottom fixed WTS (partially Self erecting WTs)	0.5277
Bottom fixed WTS (Fully pre-assembled transportation)	0.5078
Offshore assembly (single pieces) installation	0.5072

3.3.4 Development of Solutions in Detail

3.3.4.1 Optimising Current Pre-Assembly Practice

3.3.4.1.1 Research Motivation

As reasonable, and confirmed by the MCDA, the most promising and easy implementable way to improve the safety of lifting operations, and reducing the hazard of human present beneath the heavy lifted loads, can be represented by the adoption of pre-assembly solutions and, thus, the reduction of the number of lifts required. Even if these solutions have been already used for existing wide scale wind turbine installations (for a maximum of 3.0MW-scale systems), they have now to face the demand for increasing higher power-output class turbines. Only few small-scale demonstration projects (4C Offshore, 2017a; C-power, 2017) actually selected these practises for

their turbine installation (Figure 3-49 and Figure 3-50, on the right), preferring them over to the more reliable single-component lifts, only in case of logistic benefits and time saving.



Figure 3-56: JUVs working together on the tower-nacelle and the rotor pre-assembly installations at the Global Tech I wind farm (offshoreWIND.biz, 2014)

Due to the existing TIUs' little deck-area availability with respect to the extensive encumbrance of the high-MW classes, multi-vessel charting and/or tower and nacelle separated pre-installing phases can be required to get the installation on schedule, as it happened in the case of the Global Tech I (offshoreWIND.biz, 2014). However, the installation of turbines must remain cost-effective. Thus, possible use of alternative configurations for safety reasons must be balanced against the cost of installation.

Therefore, looking for a balance between the reductions in the number of lifts equal or lower farms total installing times, an installation-simulating program has been created and developed in order to find the optimal match between turbines, TIU and pre-assembly method for the different wind farms' specific requirements.

3.3.4.1.2 Wind Farms' Installation Simulation Programs

The currently available and in use programs in this sector are either commercial or in-house specifically designed for and by the offshore installation companies (Wind Power Engineering & Development, 2016). Needing for detailed scheduled procedure for the lifting operations, this simulation tools usually implement weather conditions forecast and turbines' supply and delivery

times, without focusing on implementing sub-codes for on-deck fitting of the systems; see below (Figure 3-57) the modelling solution suggested by EOSIM (Petcu, 2009).

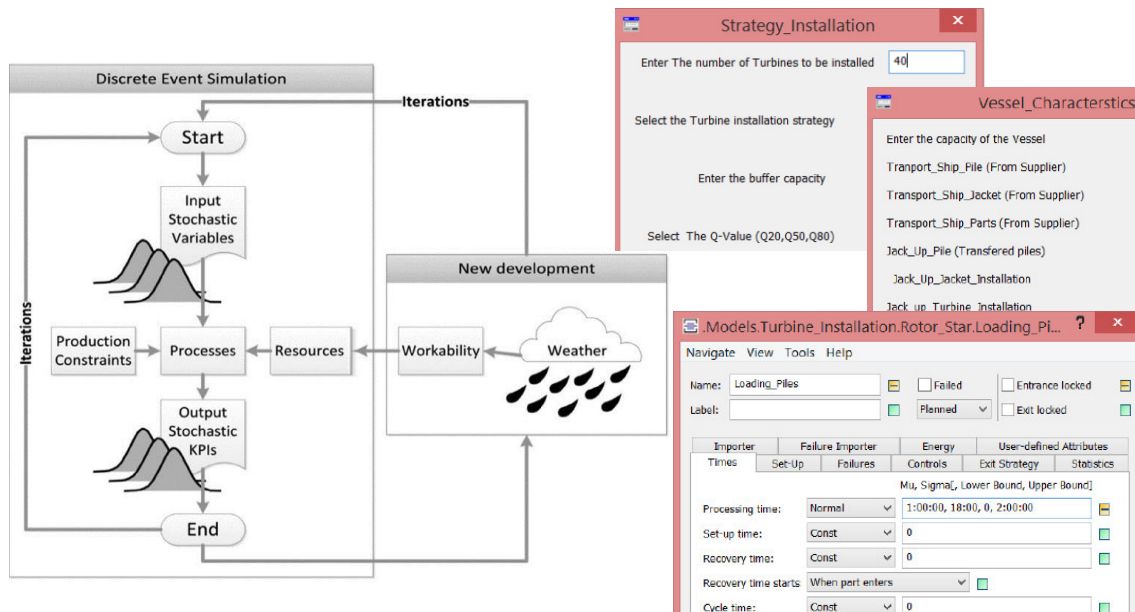


Figure 3-57: EOSIM installation-simulating program example (Petcu, 2009)

For what concerns the prediction of turbines' area occupied on deck, some simplified and academic-use program tried to generalise the turbines main dimensions and encumbrance by deducing them from their MW-class, and assuming the TIU characterised only by its maximum weight capacity (Ahn et al., 2016; Faiz, 2014; Uraz, 2011). Moreover, this models focus their attention on cost estimation and optimization (reduction) during the installation phase of the farm. As the present work is concerned with a lift reduction for safer operations, the program, presented here, deals with more specific and detailed transportation input and conditions, in order to be used as a practical and user-friendly interface to understand the best pre-assembly transportation and installation solution. However, needing for a quantity to measure the feasibility of the suggested practises in economic terms, the program has been integrated with rough time rough estimation for the complete farm installation.

Once verified and validated against case study for particular combination of vessel and turbine (existing wind farms case study), the program is supposed to deal with the pre-assembly optimal solution for future big-scale turbines requirements. Thus, rather than simply verify the configurations' pros and potentially cons, this simulation tool has been thought to be the first step

to the implementation of batch of simulations for the forecasts of the trend of the vessels'/barges' equipment and characteristics requirements (by its integration with up-scaling laws for the turbines dimension input).

3.3.4.1.3 Program Set-up

The program, written in MATLAB language, consists of the collection of fitting, time estimation, and number of lifts counting functions, able to be accessed and launched by users through a MATLAB GUI interface. As initially anticipated in Section 3.3.2.1.2, this pre-assembly concepts can be applied, in the project area, for the mounting of the turbine systems on pre-installed fixed-bottom foundations.

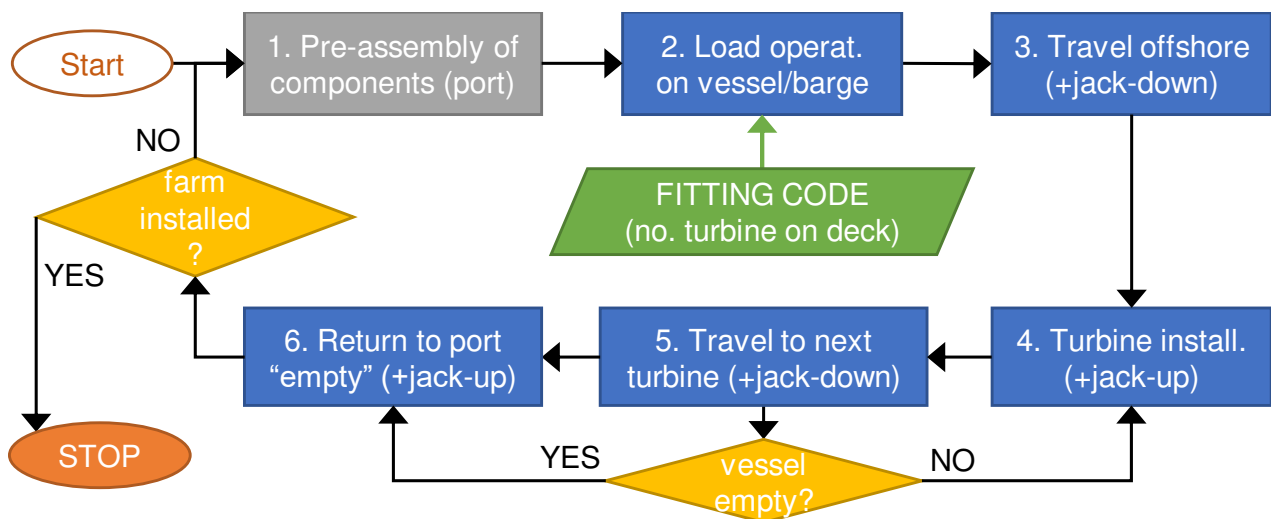


Figure 3-58: Flowchart of the program for the installation phase simulation

In order to have an easy understandable and controllable tool, different assumptions have been made:

- Same types of turbine designs (dimensions and weights), TIU characteristics, installation method, and loading and installing time for the entered number of turbines in the farm
- Every pre-assembly happens onshore, without accounting for turbines construction and/or delivery waiting times; the port temporal gap is quantified only in terms of waiting time for the turbines components and pre-assembly loading on the TIU
- It does not account for weather conditions, thus, it does not ask in input any kind of information about wind and wave and their probability distribution. It only considers an average of daily

weather window (see Figure 3-60) and equipment operative hours, assuming within this value the total working hours available per day during the farm installation

- It does not take into account the TIU stability during transportation, but it only accounts for the minimum stability requirements of: maximum weight on deck, and inboard loading of the single/pre-assembled components.
- It is designed for one jack-up units (JUV or JUB) operating per time loading on the deck an integer number of turbines system per voyage

Moreover, as it is observable from Figure 3-59, the program has been organised in three different blocks:

1. Main input entering phase and submission, asking for information about the turbines, the jack-up unit and the sites (port and farm) data,
2. Main data check for the minimum initial requirement satisfaction and/or initial suggestions for specific transportation practise (e.g. tower split for transportation). Additionally, time input variables, on-deck transportation issues and/or space optimising possibilities have to be assumed.
3. Running of pre-assembly (BE and ROT) and single pieces (SP) assembly specific simulation. By launching the respective fitting code, the total time to install the farm is determined by knowing the number of turbine transported and installed per voyage (see Figure 3-58).

It is important to observe that the SP transportation and installation solution has been integrated as comparative term and possibly validate the results against the real procedure and time values (e.g. Table 3-5). As regards the pre-assembly concepts, different loading solutions of the BE and the ROT configuration have been considered (Section 3.3.4.1.6)

Inputs

WIND TURBINE SYSTEM DATA

Tower
 Height [m]: 80
 Base diameter [m]: 3.98
 Top diameter [m]: 2.3
 Base section thickness [mm]: 35
 Top section thickness [mm]: 25

Hub
 Length [m]: 4.4
 Diameter [m]: 3.6

Nacelle
 Length [m]: 9.65
 Width [m]: 3.65

Blade
 Length [m] (root to tip): 44
 No. blades: 3
 Maximum chord [m]: 3.5

Weight [tons]
 Tower: 160
 Nacelle: 68
 Hub: 20
 Blade: 6.6

JACK-UP VESSEL/BARGE DATA

Main dimension
 Length [m]: 130
 Beam [m]: 38
 Free deck space [m²]: 3200
 Deck load [tons/m²] (max. concentrated load): 10
 Total net deck load [tons] (depending on stability): 4000

Operating parameters
 Service speed [kn]: 11
 Maximum water depth [m]: 32.25
 Jacking speed [m/min]: 0.5
 Crane max. capacity [tons]: 600
 Crane boom length [m]: 93.3
 Crane max. aperture angle [deg]: 82.5

SITE (FARM/PORT) DATA
 No. of turbines: 100
 Distance port/farm [naut. miles]: 7.5
 Distance between turbines [m]: 650
 Water depth at the farm site [m] (account for seabed penetration): 27.5
 Port water depth [m]: 20
 Port crane max. capacity [tons]: 600

Submit & check data Go to simulations Clear all data

Transportation specific inputs

BUNNY EAR (BE) PRE-ASSEMBLY METHOD

BE transportation modes
☒ Transverse ☐ Longitudinal
 Transv. overboard limit [m]: 40
 BE yCoG on jack-up unit [m]: 0

No. of blades per layer (assumed disposition of 3rd blades in the cage structure): 3

Simulate Clear

ROTOR (ROT) PRE-ASSEMBLY METHOD

ROT transportation modes
☒ Mode 1 ☐ Mode 2
 Transv. overboard limit [m]: 40
 Long. overboard limit [m]: 10

Reinforced support structure [m] (assumed main dimension): 5
 No. maximum of overlying rotors (for stability/height issues): 5

Simulate Clear

SINGLE PIECES (SP) ASSEMBLY METHOD

No. of blades per layer (assumed disposition of blades in cage structure - see below): 10

Simulate Clear

TIME VARIABLES

Port loading operations [hrs/turb]
 "Bunny ear" pre-assembly: 2
 Rotor pre-assembly: 2
 Single pieces assembled: 2

Working hours per day [hrs] (average of weather window and cranes operat. availab.): 10

Offshore lift/installation [hrs]
 Tower (1 element): 3
 Nacelle: 3
 Blade: 3
 "Bunny ear" pre-assembly: 3
 Rotor pre-assembly: 3

TOWER TRANSPORTATION
☐ one piece ☒ two pieces
 Height of tower base [m]: 40
 Upper piece weight [tons] (insert 0 if unknown): 0

Outputs

BUNNY EAR (BE) PRE-ASSEMBLY METHOD

Jack-unit capacity usage
 Deck area occupied [m²]: 2700.40
 Net total load on deck [tons]: 1071.2
 Number of turbines on deck per voyage: 4

Safety related results
 Total number of lifts: 400
 Maximum lifted load [tons]: 101.2
 Time required to install the farm [days]: 165.1

ROTOR (ROT) PRE-ASSEMBLY METHOD

Jack-unit capacity usage
 Deck area occupied [m²]: 850.34
 Net total load on deck [tons]: 1339.0
 Number of turbines on deck per voyage: 5

Safety related results
 Total number of lifts: 400
 Maximum lifted load [tons]: 97.2
 Time required to install the farm [days]: 163.3

SINGLE PIECES (SP) ASSEMBLY METHOD

Jack-unit capacity usage
 Deck area occupied [m²]: 2617.76
 Net total load on deck [tons]: 3749.2
 Number of turbines on deck per voyage: 14

Safety related results
 Total number of lifts: 600
 Maximum lifted load [tons]: 97.2
 Time required to install the farm [days]: 220.3

BE/ROT pre-assembly

SP assembly

Time variables

Figure 3-59: Program complete user-interface (e.g. after the three blocks use)

3.3.4.1.4 Input

Turbine, jack-up unit and sites data

The 3-blade horizontal axis wind turbine (HAWT) system is characterised in terms of main dimensions and weights (see Figure 3-60). The additional inputs regarding the tower wall thickness along the tower height have to be considered only in the case of tower split transportation (Section 3.3.4.1.6) when the upper tower piece weight is unknown, and then it is estimated by the program through a volume proportion with the tower total weight.

Moreover, the program is able to switch to 2-blades turbines configuration; however this additional capability has not been used and validated in the present work, due to lack of data (Section 3.3.4.1.8).

The jack-up unit is characterised (implicitly distinguishing vessels from barge adoption) by:

- deck capacity parameters: loading usable length (m), beam (m), free deck space (m^2), maximum net deck load (tons), and maximum concentrated load (tons/m^2)
- crane maximum capacity (tons) for assigned boom length (m) and maximum crane aperture angle (deg)
- operational parameters: service speed (kn), maximum operating depth (m) and jacking speed (m/min)

Therefore the jack-up unit's number of the legs is understandable and deductible from the loading deck area available (compared to the one approximately deduce by the unit dimensions). However when it has to be decided between the pre-assembly configuration, their number (together with their approximate emerged encumbrance), needs to be taken into account; the ROT practise, for instance, needs enough air-space for the rotation to the vertical position, during its ascent.

Finally, the loading and installation sites are then described in terms of:

- port and farm (with respect to its centre) distance (in nautical miles)

- water depth (m), which, for both, has to be incremented (when manually entered) of an additional seabed penetration depth for the jacking, in a range of about 2.5 to 5 meters (MPI Offshore, 2017)
- average distance between two consecutive turbines, at the farm
- lifting capacity (tons), at the port

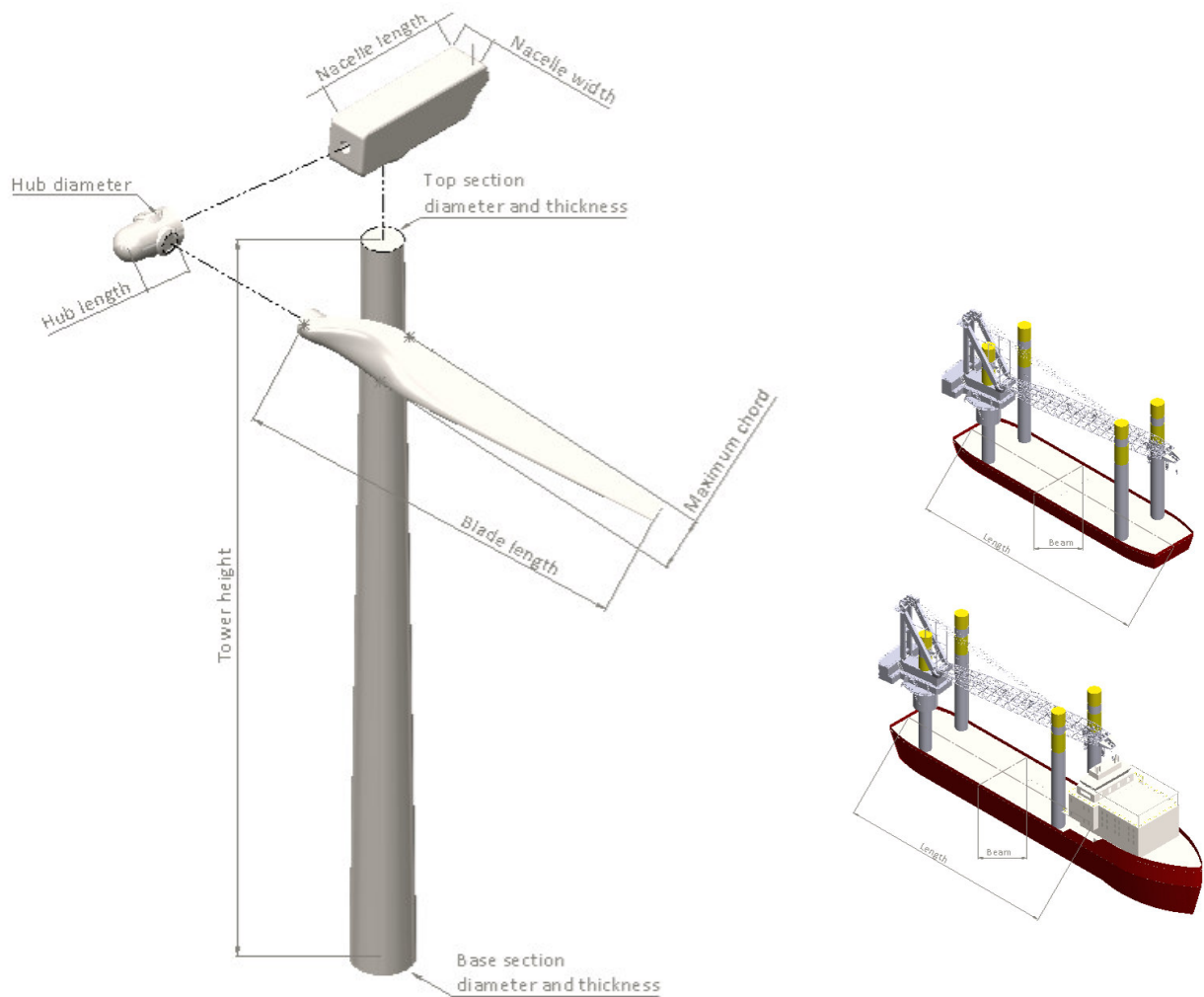


Figure 3-60: Turbine characteristics (left) and jack-up units (right) schematics. CAD adapted by M. Richmond

All the above mentioned parameters are directly used in the calculations, except the cranes (of the port and the jack-up unit) and deck capacities. While the firsts are used in term of lifting feasibility check for every components, and in particular for the entire tower piece transportation, the latter

are implemented either for direct checks or as thresholds depending on the specific fitting algorithms (see Section 3.3.4.1.6).

Loading and installing time variables

The most sensitive and difficult to predict variables are time estimations for the onshore loading and for the offshore lifting and installation operations. They are functions of the weather-conditions, the lifted component type, and constructor delivery and/or in-situ pre-assembly phases. A suspended tower element, for instance, behaves differently from either a single blade or a rotor pre-assembly (for aerodynamic profile and wind exposed surface), needing, at the same time, different loading and transportation sea-fastening timings (see Section 3.2).

Therefore the port and farm related operations are divided to account for these different aspects. For what concerns the jack-up loading, the input are required as time to load a turbine, differentiating for configuration method. On the other hand the offshore operations consider each element or assembly lifting and installing times (Figure 3-61).

TIME VARIABLES

Port loading operations [hrs/turb]

"Bunny ear"
pre-assemble

Rotor
pre-assemble

Single pieces
assembled

Working hours per day [hrs]
(average of weather window
and cranes operat. availab.)

Offshore lift/installation [hrs]

Tower (1 element)

Nacelle

Blade

"Bunny ear"
pre-assembly

Rotor
pre-assembly

Figure 3-61: Time variables input section

3.3.4.1.5 Ouputs

Since, as anticipated in section 3.3.4.1.1, the program aims to offer a pros and cons overview for the different methods selection, the outputs have been divided into two groups:

- Safety related: total number of offshore lifts and maximum lifted weight

- Economical related: fractional usage of the jack-up unit capacity and total time to install the farm

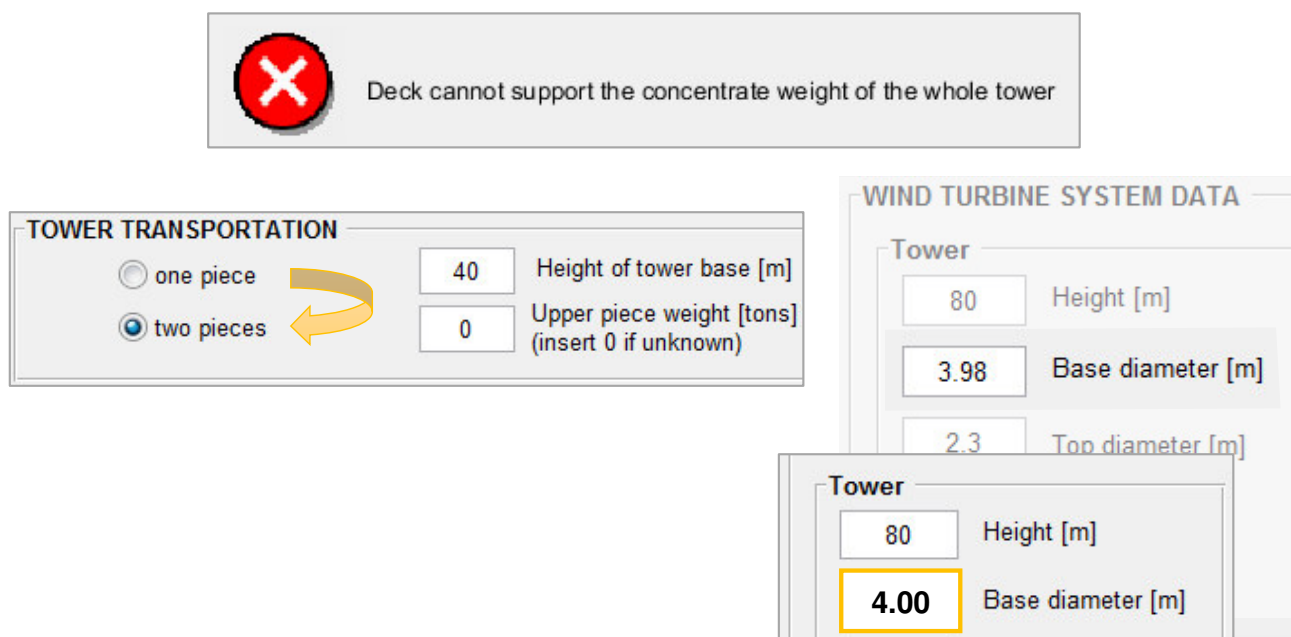
3.3.4.1.6 Pre-assemblies Transportation Specific Requirement

Turbine split transportation

Although transportation of the tower in one-element is preferred, some cases could require that the tower is split for transportation. In particular, this happens in case of exceedance of:

- the deck acceptable concentrated loads
- crane capacity (height and suspended weight limits)

While, in the second case the error appearance force the user to switch to the two-pieces transportation solution, the first error type can be also adjusted by small changes in the input for the contact deck area estimation (thus, the turbines element diameter), actually representing, in the reality, the adjustments in the support structures required on the deck.



The image shows a software interface with an error message and two input panels. The error message, located at the top, features a red circle with a white 'X' icon and the text: "Deck cannot support the concentrate weight of the whole tower". Below the error message are two panels. The left panel, titled "TOWER TRANSPORTATION", contains two radio buttons: "one piece" (unselected) and "two pieces" (selected). To the right of these buttons are two input fields: "Height of tower base [m]" with the value "40" and "Upper piece weight [tons] (insert 0 if unknown)" with the value "0". A yellow curved arrow points from the "two pieces" radio button to the "Upper piece weight" field. The right panel, titled "WIND TURBINE SYSTEM DATA", contains two sub-sections for "Tower" data. The top sub-section has input fields for "Height [m]" (80), "Base diameter [m]" (3.98), and "Top diameter [m]" (2.3). The bottom sub-section has input fields for "Height [m]" (80) and "Base diameter [m]" (4.00). The "4.00" value in the bottom sub-section's "Base diameter" field is highlighted with a yellow border.

Figure 3-62: Possible solution to be adopted when the entire tower transportation is not possible (error); split (left) and adjustment of the tower base/support structure dimensions (right). From Thanet Wind Farm case study.

SP assembly

For this base-configurations the tower piece(s), vertically transported, have a contact area on the deck (assumed support structure presence) corresponding to the entered (or local estimated) diameter to the power of two. Analogue is the loading and transportation of the nacelle with the pre-installed hub. More interesting, is the use of a blade “cage” structure, for the gathering of the blades on the deck during transportation. This solution has been adopted because it represents the currently in use practise to reduce the blades encumbrance on the deck.



Figure 3-63: Blade “cage”, transportation gathering structure examples (Fred. Olsen Windcarrier, 2017; Lawson, 2012)

However, for the other SP components, the SP method has been set up not to involve any overboard extension allowances (as actually could be happen for the cage transportation), only considering the loading of the pieces on the deck, until the lack of available space prevents the loading of the entire turbine.

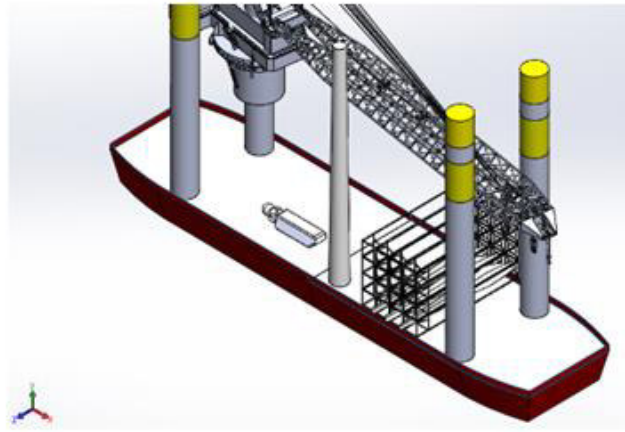


Figure 3-64: Schematic example of a SP transportation solutions. CAD adapted by M. Richmond

BE pre-assembly

The BE fitting code has been integrated with different transportation possibility for the deck area usage optimization and/or jack-up unit limitations (Figure 3-65). The main issues with this configuration are indeed related to its encumbrance (for the hub pre-installed blades horizontal and vertical extension) and the deck concentrated load for the laying condition on the nacelle base. To overcome the latter, a similar solution to the tower transportation can be used (by increasing the support structure/nacelle dimensions), the first induce the user to use the more suitable transportation depending on the jack-up unit overboard limits.

Thus, the loading condition has been distinguished in two user-selectable options

- BE transverse transportation, with the centre of gravity loading for each pre-assembly unit, on the vessel/barge centre line ($Y=0$ m). It, thus, requires a transverse overboard limit in the case of the BE overextension out of the vessel/barge beam.
- BE longitudinal transportation, with the loading of the centre of gravity of each pre-assembly unit along a vessel/barge length selected position (X coordinate), taking also into account the encumbrance and/or overboard limits (for longitudinal overextension out of the vessel/barge aft side).

Additionally, the possibility to implement the blade-cage (Figure 3-63) structure for the on-deck third blades transportation has been kept.

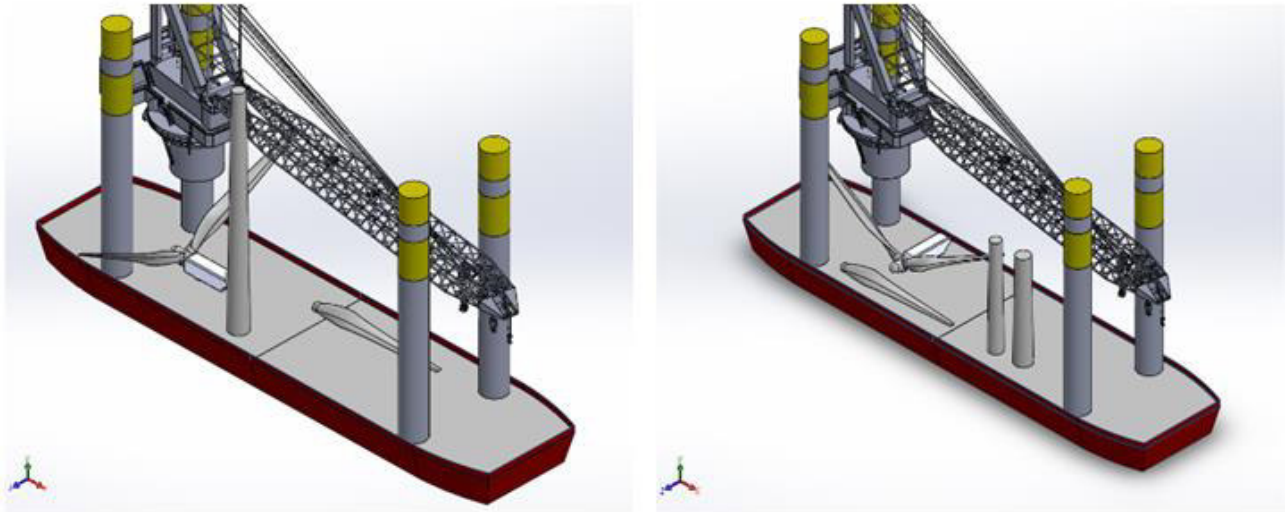


Figure 3-65: Schematic examples of BE transportation solutions; transverse-1T (left) and longitudinal-2T (right). CAD adapted by M. Richmond

ROT pre-assembly

As for the BE configuration, the ROT assembly has been integrated with different loading conditions. However, these are again limited to the pre-assembly unit loading on the vessel/barge centre line ($Y=0$). As regard the along length positioning (X coordinate), it is suggested to be set dependently on the overboard limit and jack-up legs positions on the ship (for the space necessity during the rotor ascent and rotation). The two the loading modes available are following visually shown (Figure 3-66).

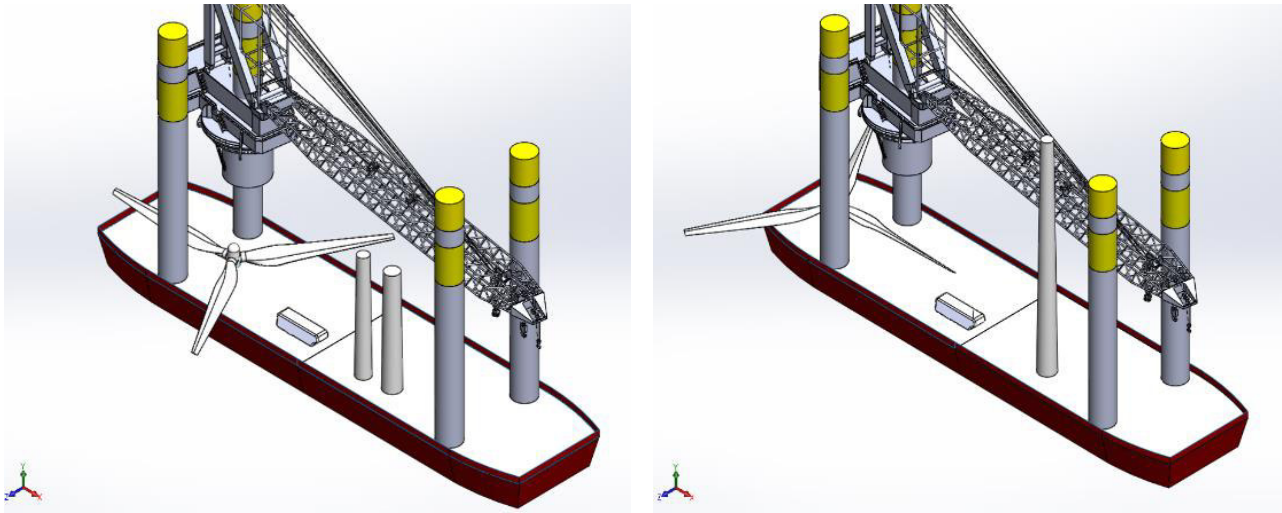


Figure 3-66: Schematic examples of BE transportation solutions; mode1-2T (left) and mode2-1T (right). CAD adapted by M. Richmond

3.3.4.1.7 Verification

In order to verify the program, simulations of existing wind farm installations, with the actual applied procedures, have been performed.

In particular, the case study of Thanet wind farms have been selected and following reported, due to the complete availability of the Vestas V90-3.0MW turbine (Figure 3-67) specifications sheets (Vestas, 2004; Vestas Wind Systems A/S, 2017).

With concern to the time variables assumed for this first stage of the analysis, Uraz (2011) study results for the installation phases of Lillgrund, Thanet itself, and Horns Rev II projects were used as references and averaged in terms of hours per offshore lift (about 3hrs per component or pre-assembly). As regards to the port loading time, instead, the suggested quantity has been decrease to 2hrs per turbine system boarding on the deck, considering the higher reliability and processes stability of the port operation compared to the offshore ones.

On the other hand, the averaged (through the entire wind farm installation) working hours' variable has been specified as of two-hours, to perform a rough first level sensitivity analysis.

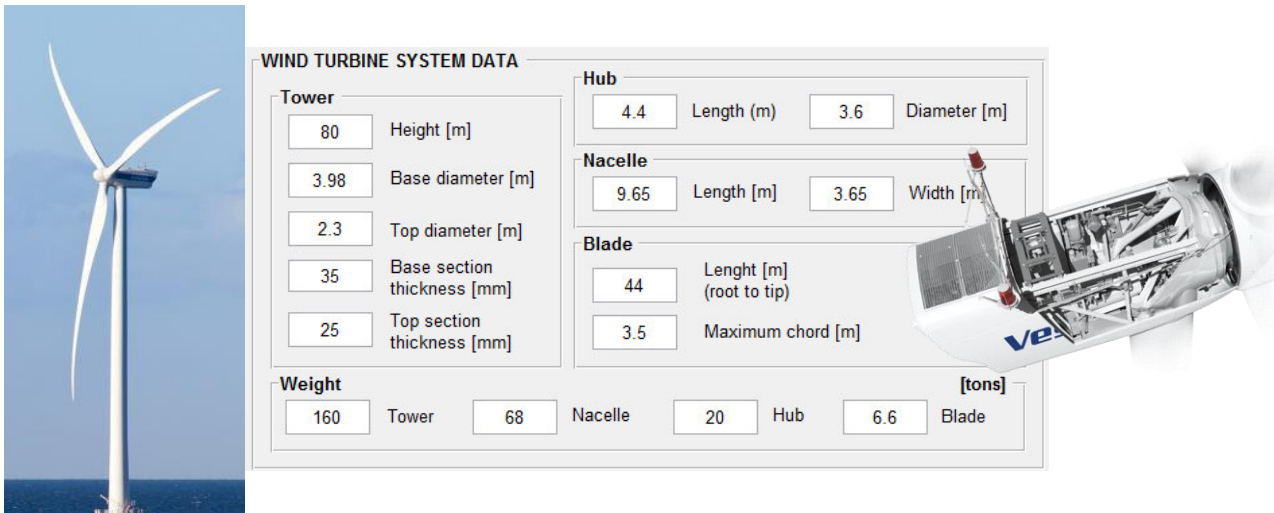


Figure 3-67: Vestas V90-3.0MW characteristic (Vestas Wind Systems A/S, 2017)

Thanet wind farm case study

As mentioned in Table 3-4, the wind farm was installed in 197 days, with a SP-1T configuration, leaving from Ramsgate port and commissioning the transporting and installing procedure to MPI Resolution JUV (MPI Offshore, 2017; Vattenfall, 2014).

To afford the transportation on the deck of the entire tower element, the support structure (initially assumed of the same dimensions of the tower) has been increased to a 4.0 meters sides' length (Figure 3-62).

Then the results have been compared to the suggested pre-assembly optimal solution (table). The BE-1T transportation configuration, indeed, is shown to be the best solution out of the three presented. The ROT configuration has not been taken into account, since the particular kind of vessel used (6-legged jack-up), would have not allowed its easy handling in the installation phase.

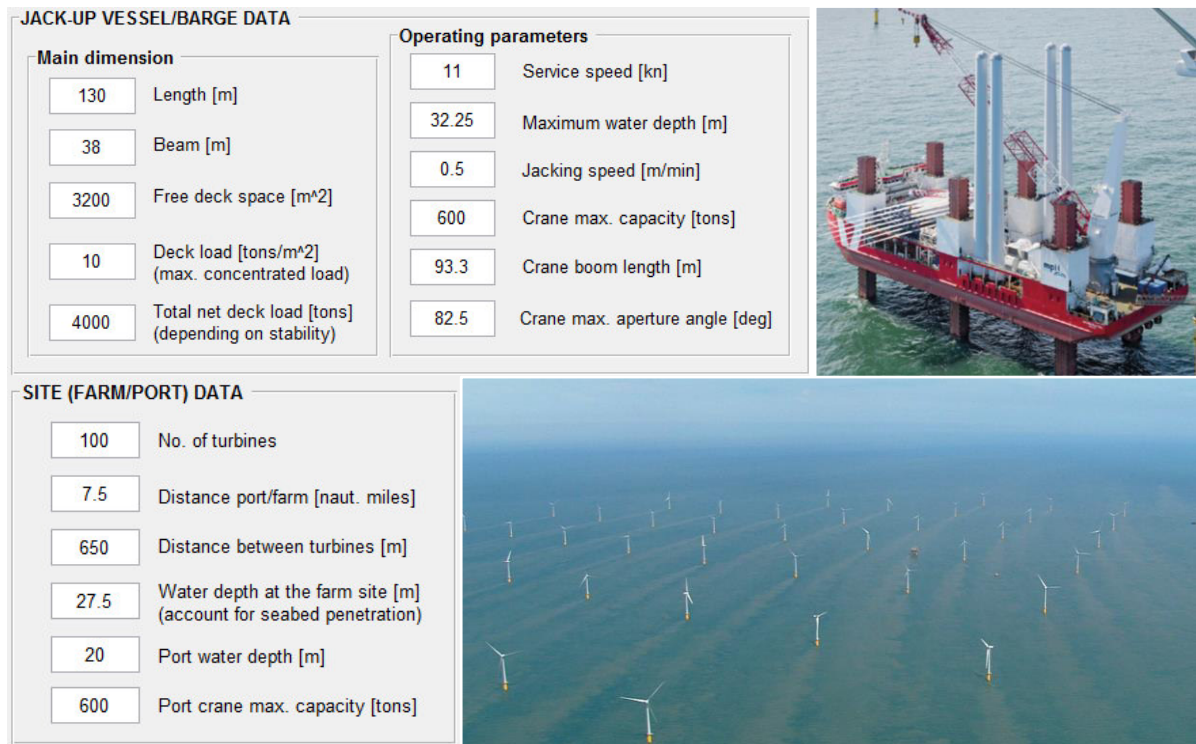


Figure 3-68: JUV, port and farm characteristics (MPI Offshore, 2011b; Vattenfall, 2005, 2014)

Table 3-6: Results table for Thanet case study

		Averaged working hours per day [hrs]	Deck area occupied [m²]	Net load on deck [tons]	No. of turbines on deck per voyage [-]	Total no. lifts [-]	Maximu m lifted load [tons]	Total installing time [days]
SP-1T	Farm report	-	-	-	-	-	-	197
	Simulated	8	2481.95	3749.2	14	500	160	238.1
	(10 blades at cage base)	10						190.3
		12						158.4
BE-1T	• Transverse (30m transv. overboard)	8	3057.50	1339.0	5	300	160	167.1
	• Longitudinal (40m long. overboard)	10						133.3
		12						111.3

3.3.4.1.8 Conclusions and further works

As it is observable from the results of the case studies, the use of pre-assembly solutions offer a reduced number of lifting operations for the installation procedure, for generally the same entities

of maximum lifted weight (usually represented by the entire tower, and thus independent from the pre-assembly configurations considered).

The next step and further development of the program can be:

- Improve the loading configuration possibility of the currently implemented pre-assembly ($Y \neq 0$ loading possibility)
- Implementation of other pre-assembly solutions (such as the suggested solution in the patent US20100281820A1)
- Verify the program against more case studies for different MW-classes wind farm case study and with more reliable time input variable
- Validate the program for the next generation of wind turbines MW-classes (from 5MW above) identifying the optimal assembly solution and/or the new requirements for the vessels.

3.3.4.2 Novel Assembly Concepts

These novel assembly concepts are some of the human free lifting solutions which would help to minimize the number of lifts in the offshore wind turbine installations. Majority of the offshore wind turbine projects are executed at water depths below 30 meters on support foundations such as monopiles, jackets or tripods, the suitability of these bottom fixed support structures are determined by the water depth (National Renewable Energy Laboratory, 2011). The monopile and tripod will support up to a water depth of 50 meters as shown in Figure 3-69. The offshore wind industry is currently adapting the tension leg platform, a semi-submersible structure moored and anchored to the seabed for additional stability for water depths greater than 50 meters. The spar buoy concept is used for water depths greater than 120 meters and the semi-submersible for water depths greater than 50 meters. The centre of gravity of the spar buoy lies below the centre of buoyancy, which gives the floater the stability (European Wind Energy Association, 2013), Figure 3-70 depicts all these cases.

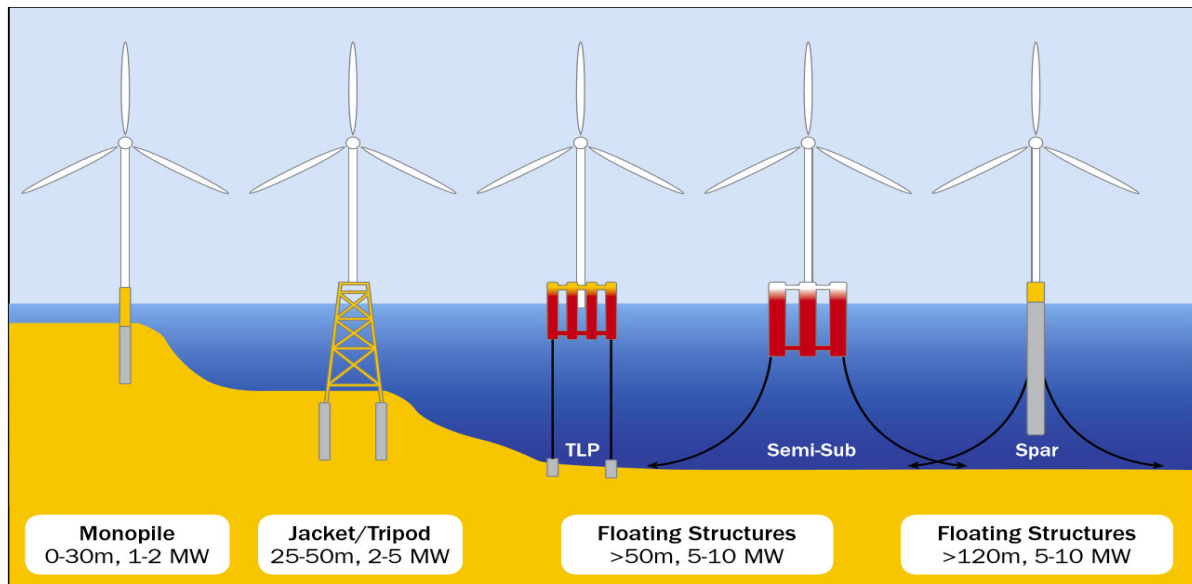


Figure 3-69 Trends in offshore wind foundations (European Wind Energy Association, 2013)

This novel assembly concept is categorised into two major concepts, the bottom fixed concept and the floating concept as shown in Figure 3-71. The bottom fixed wind turbines are normally erected on a foundation to carry the fixed structure while the floating wind turbines are normally anchored to the seabed with much degree of movement.

The floating wind turbine possesses some key attributes that really make it a unique installation process. Apart from the elimination of lifting risk and the reduction of the need to hire special heavy lifting and support vessels, because they are assembled at the quay side and towed by a barge to the point of installation, they are also a driver to the reduction of cost in wind turbine installation projects offshore (Myhr, Bjerkseter, Ågotnes, & Nygaard, 2014). The quantities of steel needed for fabrication of this floating wind turbines are far less than what is needed for the conventional turbine and elimination of the monopile foundation with its heavier tonnage is a plus to this concept. This concept reduces cost by eliminating the much-needed special marine engineering expertise as it is not required because no foundation is needed. The floating wind turbines are capable of generating more power than the bottom fixed wind turbines because of the more consistent winds further offshore where waters are deeper (Cordle & Jonkman, 2011). The floating concept is also suitable for water depths where the bottom fixed cannot be utilised, it poses low

environmental impacts to the environment and aquatic life, less risk to commissioning, and finally easier construction and assembly at lower heights.

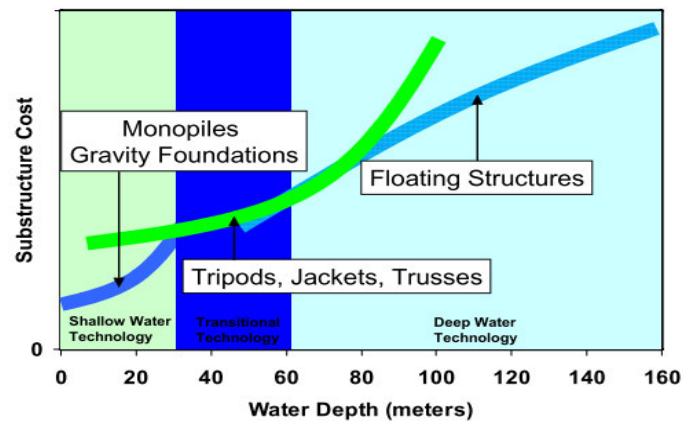


Figure 3-70 Cost of offshore wind turbine structures with respect to the water depth (W. Musial et al., 2006)

A recent study by Walter Musial, Butterfield, & Boone (2004) showed that for a single 5-MW turbine production cost estimates are \$7.1M for the Dutch tri-floater and \$6.5M for the NREL TLP concept. Despite the potentials of the floating wind turbines concept, the long-time reliability has not been proven yet.

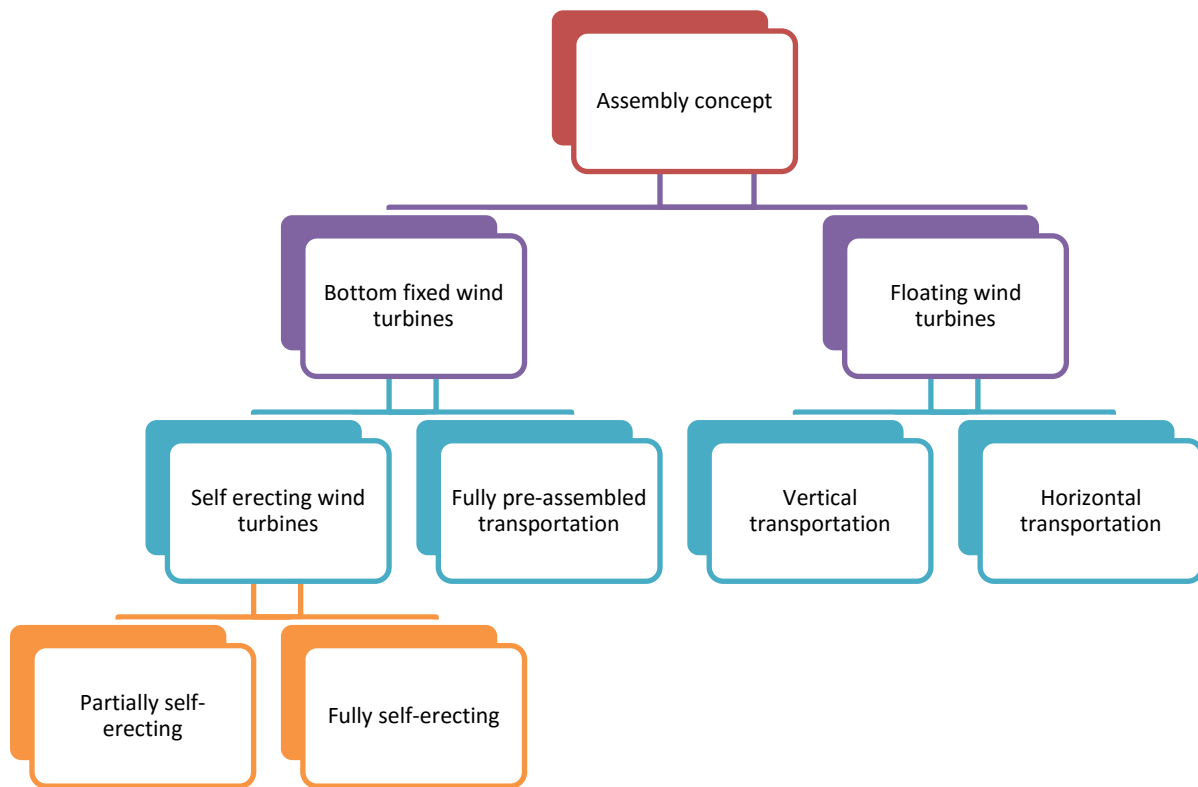


Figure 3-71 Wind turbine novel assembly concepts

3.3.4.2.1 Bottom Fixed Wind Turbines

3.3.4.2.1.1 Self-Erecting Wind Turbines

Self-erecting wind turbines comprise of partially self-erecting and fully self-erecting wind turbines. The partially self-erecting are installation methods where some of the components are installed by the combination of telescopic crane mechanism and a small ground crane as shown in Figure 3-72. This method is designed for onshore installation of tower and nacelle. It was patented in the USA by (Mehring & Waukesha, 1997)MISSING REFERENCE. The telescopic crane is attached to two tower elements hinged together at the top and at the base, as shown in Figure 3-72(a), the telescopic crane lifts the lower tower section as shown in Figure 3-72(b) and adjusts its position to lift the upper tower segment which has been installed with the nacelle at the lower height with the aid of another small crane as shown in Figure 3-72 (c & d). The telescopic crane finally booms up to complete the lifting simultaneously in a single lift as shown in Figure 3-72(e & f).

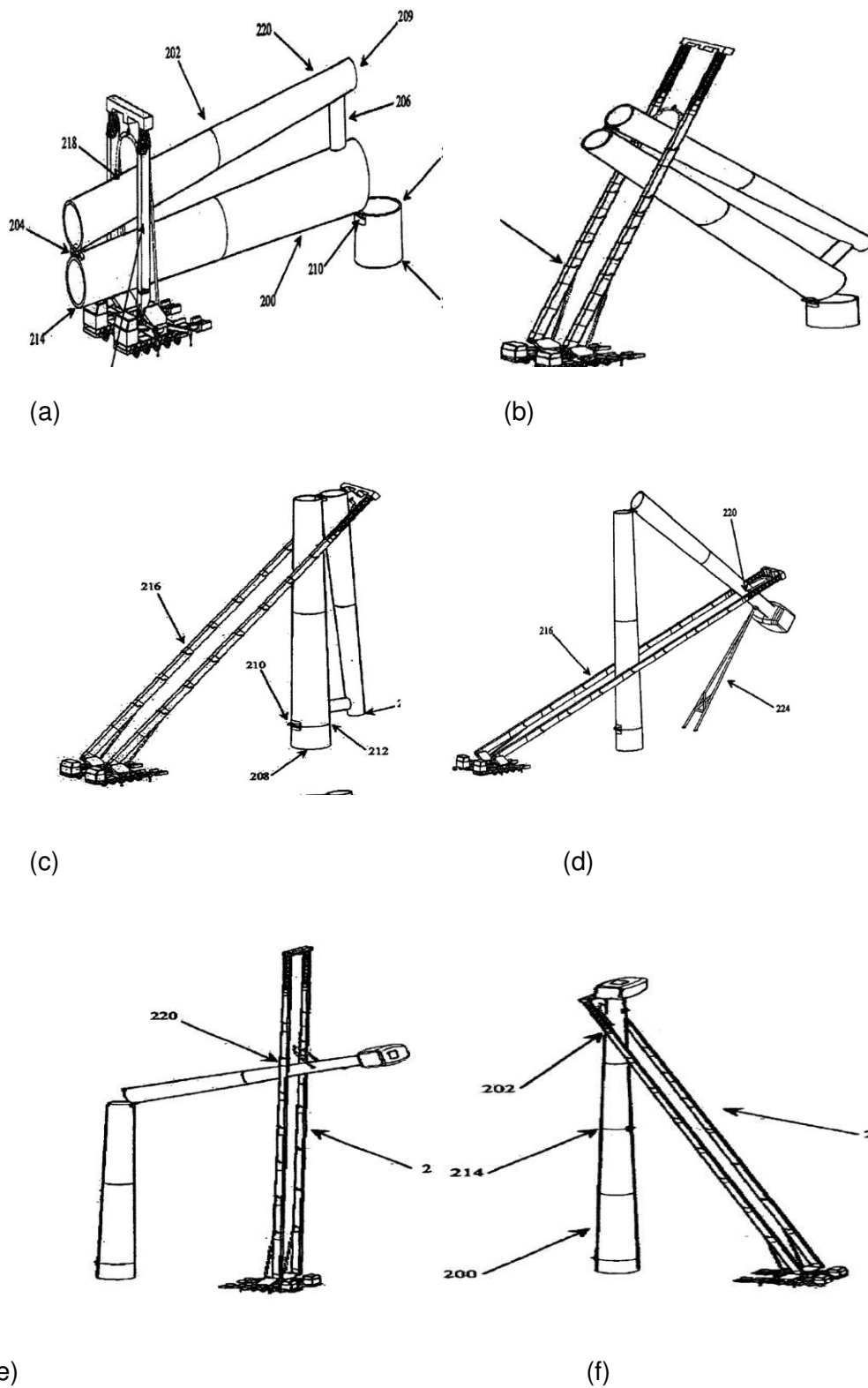


Figure 3-72 Partially self-erecting wind turbine tower (Dehlsen & Mikhail, 2005)

The partially self-erecting wind turbine has the potential to be barge mounted and used for offshore work locations. Its method of raising the tower, the nacelle and drivetrain is easier and less risky compared to other bottom fixed wind turbine concepts. Lastly, the technicalities of lifting and

arrangements are superior and even give more control on high wind speeds unlike others. (Dehlsen & Mikhail, 2005)

The second self-erecting wind turbine concept is the fully self-erecting wind turbine method, which was patented in the USA (Gee & FL, 2011). The tower is installed at low height with the aid of a telescopic pylon with three plurality legs.

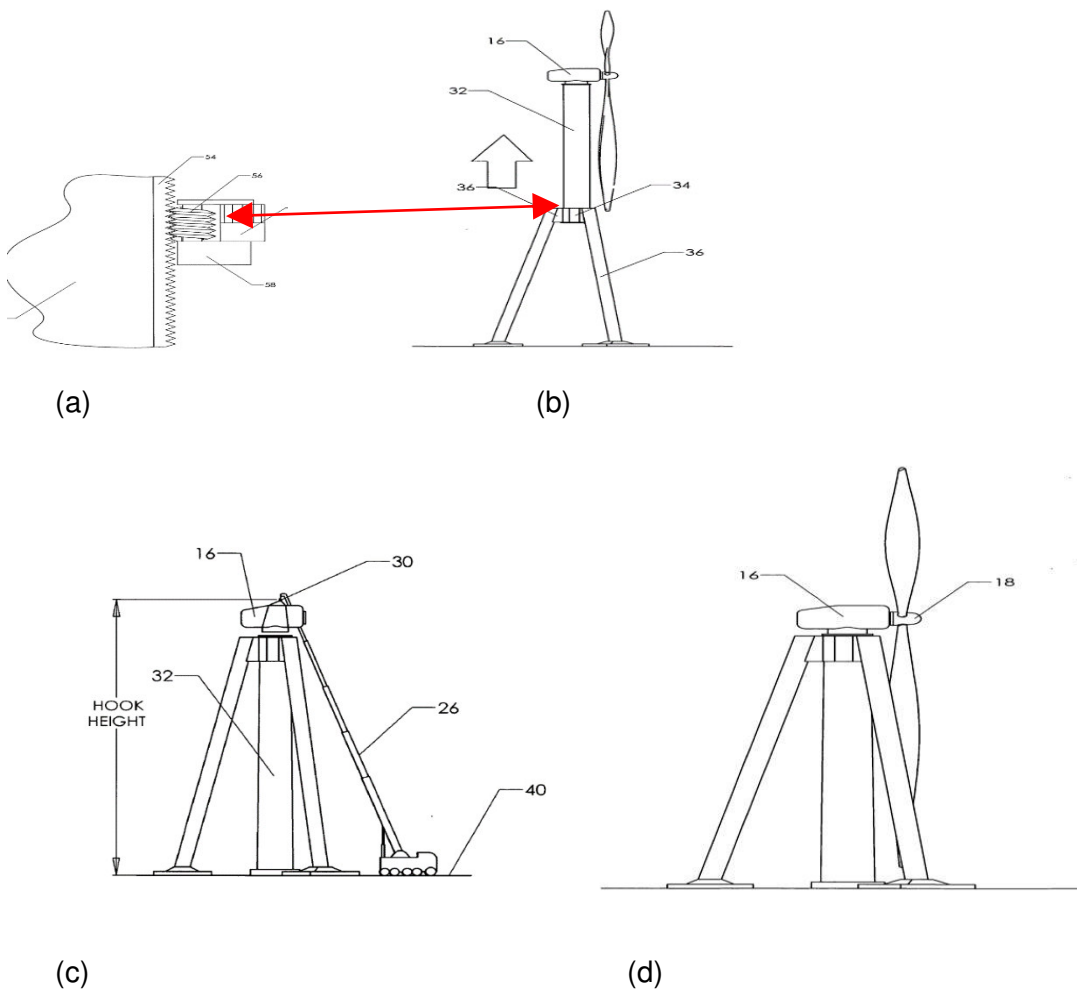


Figure 3-73 Fully self-erecting tower and method for raising the tower (Gee & FL, 2011)

The blades and nacelle are also installed at low height on the telescopic pylon, as shown in Figure 3-73 (c & d), and the entire assembly is driven up the telescopic pylon with the aid of a special worm gear train arrangement powered electrically as shown in Figure 3-73 (a & b). One of the drawbacks of this concept is the fact that additional support foundation is required for the multiple legs. This concept is suitable onshore for wind turbine installations up to a height of 100 -120

meters (Gee & FL, 2011). The key benefit of this system is to reduce the number of lifts required to complete the whole installation of the wind turbine and to reduce the risk of working at height since the nacelle, drivetrains and blades are installed at lower height. Some other drawbacks of this system are the limitation to the size of wind turbine installations onshore and the need for special support foundation to be deployed offshore. Other factors like the height of installation, and additional cost for making temporary foundation for the telescopic pylon are certain issues to be addressed with this patent.

Some other partially self-erecting methods are using hydraulic pulling devices as shown in Figure 3-74. This shown example was erected without the aid of any crane, the entire turbine with assembled parts was pulled into position (Hau, 2008). This method poses some integrity challenges to the turbine components. Other partially self-erecting methods are shown in Figure 3-75 (a & b) the nacelle, hub and blade were coupled to the base of the tower and they were propelled through the tower by the aid of a mechanical pulling rig mounted at the top of the tower into their position. This is a good method for erecting huge turbine components if the load cases will not be possibly supported by any crane. This method was used in the Growian farm installation which was the largest turbine then as shown in Figure 3-75 (b). (Hau, 2008) It was also used in the AEOLUS II installations, where the completely assembled hub, nacelle and blades were slid up the tower top with the aid of sliding rails erected on the concrete tower from the bottom to top and also with the aid of a pulling device installed at the tower top. All these partially self-erecting concepts help in reduce installation cost but do not totally eradicate the risk of objects falling off during lifting operations but minimize the number of lifts and minimize lifting hazards. They are mostly economically feasible in the onshore wind industry. Other partially assembled methods using cranes to install component wise are shown in Figure 3-76 (a & b) where each component is installed as the capacity of the crane limit permits.



(a)



(b)

Figure 3-74 Partially self-erecting wind turbine using hydraulic pulling device (Hau, 2008)



(a)



(b)

Figure 3-75 Partially self-erecting wind turbine using tower as track (Hau, 2008)



(a)



(b)

Figure 3-76 Partially pre-assembly using crane (Hau, 2008)

3.3.4.2.1.2 Fully Pre-Assembled Transportation

This single lift installation method uses a floating wind turbine installation vessel for the installation as it can be seen in Figure 3-77. This special floating vessel is dynamically positioned and

equipped with a special fully motion controlled overhead gantry crane of huge capacity (80t) to assist in the load out at quayside and installation. This installation method fully takes away human intervention in the lifting process and the risk of falling objects during lifting is reduced to a minimal. The vessel also has the capability to carry up to six pre- assembled wind turbines and connect the base of the tower to the transition piece. Weather conditions and installation capacity will be a limiting factor of this concept. This concept is a prototype being worked on by Vuyk Engineering Rotterdam b.v., (2017).



Figure 3-77 Fully pre-assembly using special vessel (single lift) (Vuyk Engineering Rotterdam b.v., 2017)

3.3.4.2.2 Floating Wind Turbines

3.3.4.2.2.1 Vertical Transportation

Professor William E. Heronemus of the University of Massachusetts was the first to push the boundary for industrial floating wind turbines (Walter Musial et al., 2004). The floating concept started in 1970s and since then lots of researches and prototypes were being deployed to the sea for data collection. The first world commercial vertical axis floating wind turbine called the Hywind was installed in Norway in the year 2009 with installed capacity of 2.3MW (European Wind Energy

Association, 2013), while the second large scale vertical axis floating wind turbine called the WindFloat was installed in 2011 in Portugal with generation capacity of 2MW and was finally commercialised in 2017. Other floating wind turbines are shown in Table 3-7, stating their designers, manufacturers, substructure, turbine capacity and year of commercial installation (European Wind Energy Association, 2013).

Table 3-7 Current floating wind turbine manufacturers and concepts (European Wind Energy Association, 2013)

Design name	Manufacturer	Substructure	Turbine capacity	Commercial installation
Wind Float	Vestas	Semi-Submersible	5-7MW	2017(Portugal)
Hywind	Siemens	Spar-buoy	3-7MW	2016(Norway)
Blue H TLP	Blue H	Submerged Deepwater platform	5-7MW	2016(Netherlands)
Floating Haliade 150	Alstom	Tension Leg Buoy & TLP	6MW	USA
WinFlo	Nass & Wind	Semi-submersible	2.5MW	2016(France)
Pela star	The glisten Associates	TLP	2.5MW	2017(USA)
IDEOL	IDEOL	Concrete floater	5-6MW	2014(France)
Hexicon Energy design	Hexicon	Floater	15MW	2015(Sweden)

The vertical transportation is one of the concept grouped under the floating wind turbines, these novel ideals are paramount in achieving human-free lifting solutions in the offshore wind energy industry. In these concepts the wind turbines are fabricated and installed at the dock side on their foundations, either tension leg platforms or semi-submersibles, and tugged to the installation location. The tri-floater concept, as shown in Figure 3-78, is one of the vertical floating concepts where the wind turbine components are installed on three stand at the quay side at a low elevation, thus eliminating the high risk of falling objects, and pulled by a tugged vessel to the installation site. The key similarities of these vertical transportation solutions are that they eliminate physical lifting

of any parts at the offshore base, thus eliminating all lifting risks. Other newly developed floating wind turbines are shown in Figure 3-79.



Figure 3-78 Tri-floater vertical transportation concept (Principle Power, 2011)

3.3.4.2.2.2 Horizontal Transportation

The horizontal transportation concept (WindFlip) is one of the floating wind turbine installation concepts, in which the turbine is fully assembled at the quay side and mounted horizontally on a special barge that has 29 ballast tanks with sea fastening capabilities, as shown in Figure 3-80 (a) (Anders Soe-Jensen, 2010). The barge is towed with another small vessel to the location of installation, as shown in Figure 3-80 (d), and with the aid of buoyancy and self-tilting mechanism that sucks in water into the ballast tank which gradually sinks the barge into the water until the barge and the attached turbine flipped 90 degree with the turbine in the upright position as shown in Figure 3-80 (c & d). Afterwards the barge is gradually detached from the assembly and, with the aid of compressed hot air in its system, the water in the ballast tanks is ejected back into the sea thus allowing the barge to return horizontally on the sea. The key benefits of this method as a human-free lifting alternative is the low risk exposure to people, since physical connections are designed out. The only challenging side of this method is the additional vessel needed to tow the special barge arrangement to the point of installation which might translate to more cost implication on the project.

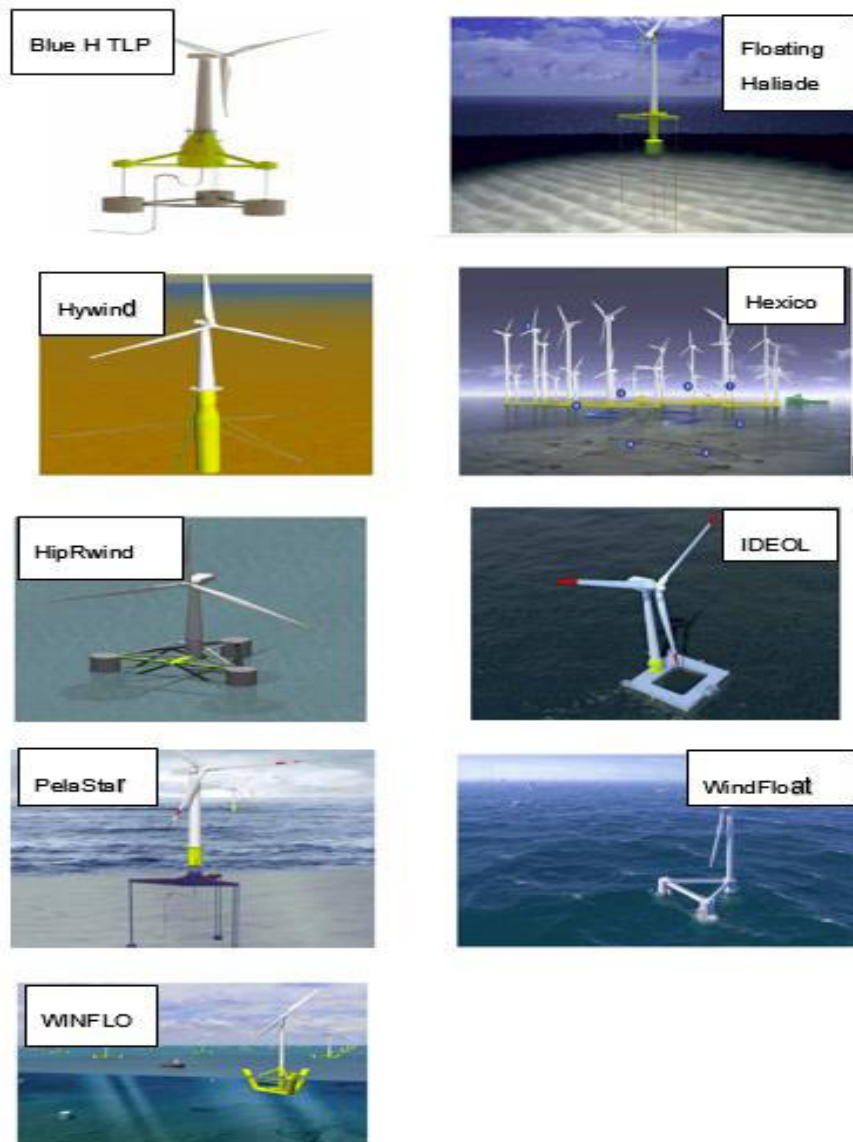


Figure 3-79 Other concepts of floating wind turbines (European Wind Energy Association, 2013)

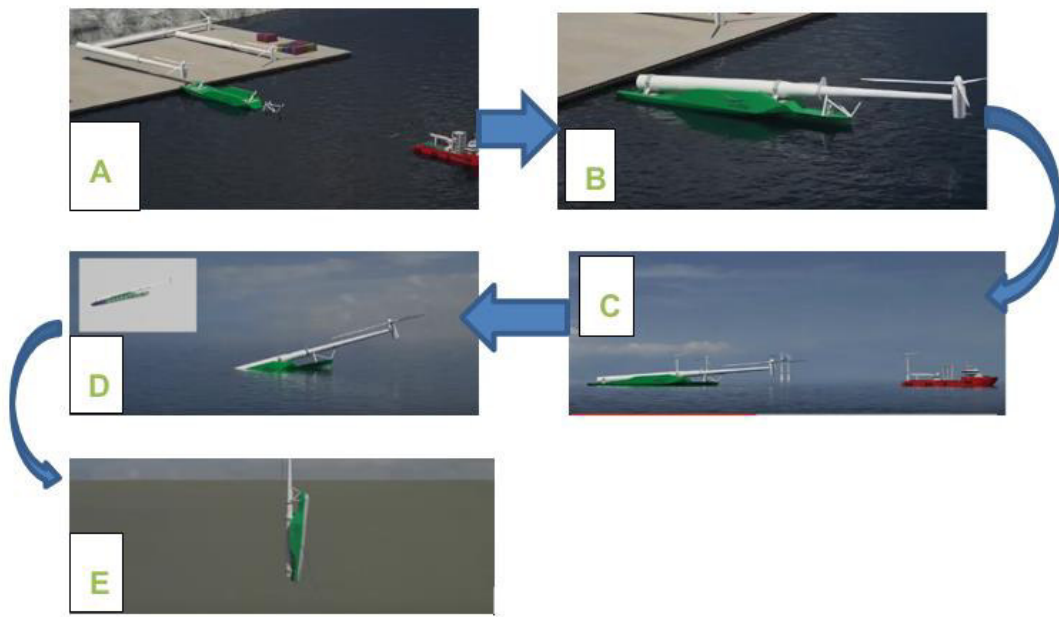


Figure 3-80 WindFlip, horizontal transportation concept with a fully self-erecting wind turbine (Barker, 2012)

4 MULTI-CRITERIA DECISION ANALYSIS

Numerous ideas have been presented in this report, all of which aim to reduce the risk to workers. The selection of the optimum solution, however, cannot simply be based on a single criterion. A fully automated crane system, which can position blades into the hub without any human intervention, would eliminate the risk but it would also be costly to develop and has little track record in offshore conditions. This presents a multi-dimensional problem lending itself to Multi-Criteria Decision Analysis (MCDA). MCDA divides a decision into smaller parts, analysing each and then combining through a logical process to present an overall picture. MCDA methods can be applied to any decision with complexity and have been employed in the sustainable energy industry as a whole (J. J. Wang, Jing, Zhang, & Zhao, 2009), and within the offshore wind sector (Lozano-Minguez, Kolios, & Brennan, 2011) amongst others.

The process for an MCDA can be defined as follows (Dodgson, Spackman, Pearman, & Phillips, 2009):

1. **Establish the Decision Context** - Identify the aims and context of the MCDA, the key stakeholders and experts, and a system for how all groups will contribute
2. **Identify the options to be appraised** - Collate all possible options to be considered
3. **Identify criteria** - Interpret the consequences of the options, identifying high-level objectives and categories within each.
4. **'Scoring'** - Assess the expected performance of each option against a set of criteria.
5. **'Weighting'** - Assign weights for each criterion, which reflect their respective importance.
6. **Combine weights and scores** - Use a multi-criteria decision method to combine.
7. **Examine Results** - Rank solutions to inform decision
8. **Sensitivity Study** - Investigate the disparity between scores and weightings; create new options that may fair better than the first set.

4.1 Decision Context: Aims, Stakeholders and Key Players

The purpose of this MCDA is to rank the viability of equipment and processes to reduce the need for people beneath loads during construction stage lifting operations of offshore wind turbines at

sea. Two distinct MCDA's will be undertaken: the first will rank all options with a view to defining a list of the 'most viable options' which are then researched further in this report; the second stage being to rank final options (or suites of options) which are to be recommended to industry.

The stakeholders are all those who may work in the design or operation of offshore heavy lifts for wind turbines. Key players include experts related to each of the options presented. Ideally, stakeholders would be included throughout this process, from collating and scoring options to defining and weighting criteria. This could take the form of workshops in which key players and stakeholders are led through the process. It is, however, at this stage that the confines of this project should be mentioned. The offshore wind industry is an international business and although it is supported by industry, this project has neither the funding nor the time to bring together groups for the full process.

Instead, the group have decided to utilise their industry contacts remotely through an online survey, this is discussed further in 4.3. All other aspects of the MCDA were undertaken at group meetings and with guidance from supervisors.

4.2 Criteria

The criteria were collected in two brainstorming sessions by the group, from this a shortlist of 21 were chosen based on votes from the group. When considering implementing a new technology we reflected upon the full timeline of developing and operating. Hence splitting the criteria into high-level groups of 'Research + Development', 'Operational', 'Manufacturing' and 'Other'. Each variable is described below and is either positive or negative. For instance, when scoring an option on cost (negative variable) a lower value represents a more cost-effective option, ie. Cost of cameras 2, cost of self-erecting turbine 8, showing that the cost of installing cameras is less and therefore more viable. These criteria are presented in Table 4-1 and Figure 4-1 Criteria to be considered.

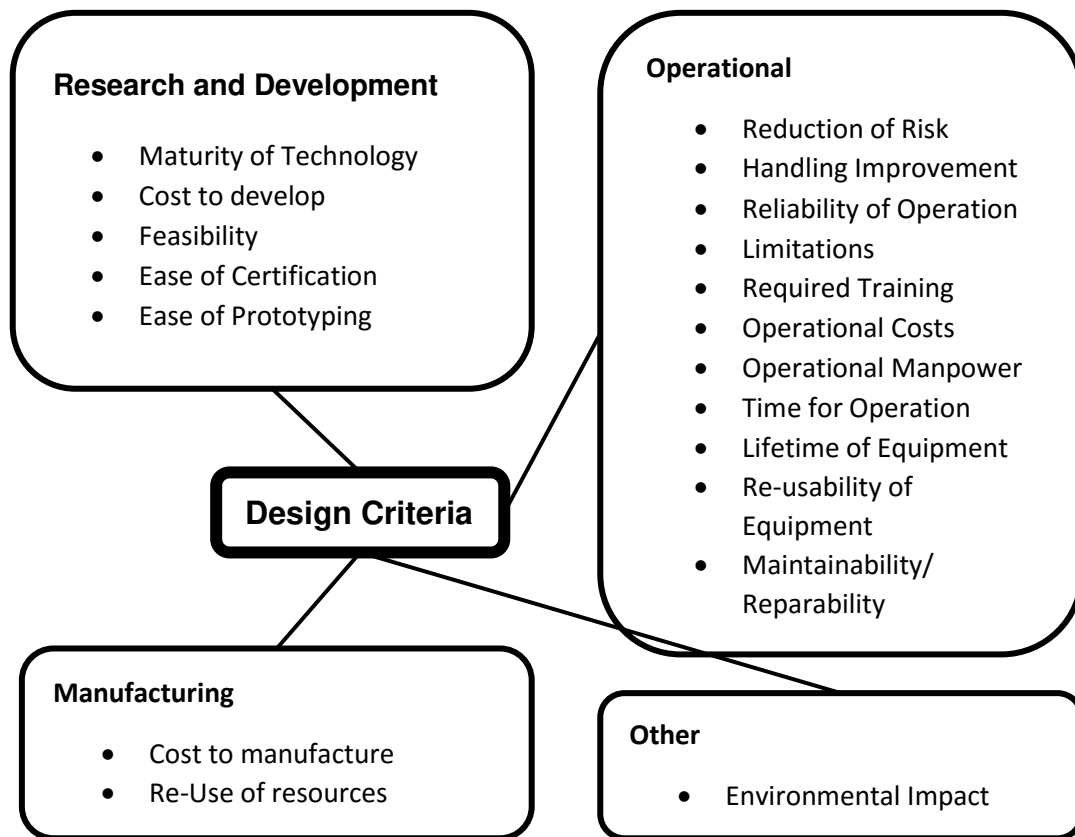


Figure 4-1 Criteria to be considered

Table 4-1 Description of criteria

Criteria	Type	Description
Maturity of Technology	Positive	Qualitatively describes how widely used the technology is and therefore how much R + D would be required to develop further.
Cost to Develop	Negative	A qualitative estimate of the expenditure required to bring this technology to industry-wide use.
Feasibility	Positive	A qualitative estimate of feasibility, how realistic is the development of this technology.
Ease of Certification	Positive	A qualitative estimate of how easily this technology could

		be certified by a related body.
Ease of Prototyping	Positive	Ease of prototyping and field-testing.
Cost to manufacture	Negative	Qualitative estimate of the upfront cost of manufacture
Re-use of resources	Positive	How well could this technology re-use previously owned resources?
Reduction of Risk	Positive	Qualitative estimate of the reduction of risk to the safety of personnel using technology
Handling Improvement	Positive	Qualitative estimate of improvement of handling using the technology
Reliability of Operation	Positive	Qualitative measure of the ability of the technology to perform without failure or problems
Limitations	Negative	How much does the use of this technology limit design and/or construction sequence possibilities?
Required Training	Negative	Level of training required for workers to implement technology
Operational Costs	Negative	Qualitative estimate of the cost to acquire and operate the technology (not including R+D)
Operational Manpower	Negative	Manpower required to safely and efficiently operate technology
Time for Operation	Negative	Time needed for complete lift with new technology
Lifetime of Equipment	Positive	Quantitative estimate of number of years that the equipment is likely to remain fully operational
Re-usability of	Positive	Qualitative estimate of the number of lifts for which the

Equipment		equipment could be re-used
Maintainability/Repairability	Positive	Qualitative estimate of how easily the equipment can be maintained/repared
Environmental Impact	Negative	Qualitative estimate of environmental impact to surroundings and of carbon footprint

4.3 Survey

A survey was sent out by us through G+ and other company contacts via a link to an online portal 'surveymonkey.com' and all information entered by respondents has been kept anonymous. In total, there were 38 respondents from industry and 2 from academia. The survey questions began with respondents being asked their job title, how many years they have worked in industry and their perceived level of expertise. Their job title has been used to gauge the level of spread across fields within the industry; we were aiming for senior to junior and from design to contracting. Ultimately, we had a bias towards HSE managers and managers in general; this is probably due to the network in which the link was shared. Both perceived experience and number of years have been used to weight the results and this is discussed further in Section 4.7. Next, the respondents were asked to weight each of the criteria discussed in the previous section from 1-9 (1 being not important and 9 being extremely important). There was also an option to include any criteria that, in the respondent's opinion, was omitted from the survey. A few key examples of these are included below.

Firstly, there seemed to be an overriding feeling that removing the human from beneath the load was important and that if the correct tool could be found cost would not be an issue:

'The aim should be to eliminate people under loads (not just reduce)'

'Within the UK para 230 of the ACOP for the Lifting Operations and Lifting Equipment Regulations states that where "practicable" loads should not be carried or suspended over areas occupied by people. Practicable is a legally defined term and is higher than "reasonably practicable" and hence cost is not a factor'

However, this tool should be simple and reliable:

‘....focus on the actual equipment complexity, some of the devices used are extremely complex and are a burden to maintain.’

‘.. increase operational limitation (less waiting on weather) together with [fool-proof], sound, and safe system (reduce risks)’

4.4 Evaluation of Criteria Satisfaction

One of the most challenging parts of this multi-criteria analysis is the determination of how well each alternative satisfies the criterion. If the technology is at a comparatively mature level of development, for example wind turbine support structures, then an empirical method can be used to determine criteria satisfaction, as was the case in (Lozano-Minguez et al., 2011). However, the technologies investigated in this study are not mature and, particularly in the initial stage of investigation, it may even be unclear what exactly the system or combination of systems consists of. Additionally the technologies cover a broad range and are fundamentally very disparate; while an empirical method may be suitable to determine criteria satisfaction for one technology, the method may not be suitable for another and an alternate method may not be comparable. The actual numbers themselves are not even comparable if the technologies accomplish very different tasks, for example, one technology may cost significantly more than another but if it accomplishes a very different task it may be better value for what it does.

The criteria satisfaction was based on personal judgement as this is the only method which could be used. At the initial stage, members of the group evaluated their own technologies that they had researched as they would be best placed to make that judgement. Team members gave scores, from 1 to 9, for each criterion to evaluate how well, or to what extent, that criterion was satisfied. The different sections were not compared to each other at this stage as the judgments of individuals are not comparable.

In the final stage, team members gave criteria satisfaction values to all of the technologies presented and these values were averaged. This was performed after the final group presentation

because it would ensure that everyone had an understanding of each other's sections. The average value was used to produce the final ranking.

This method of evaluation was deemed sufficient due not only to the inherent limitations but also in light of the objective of the MCDA. Initially, the MCDA was used to guide our own work, this was important so that the limited time available could be spent more efficiently and thoroughly evaluating the ideas at this stage would be counter to that. The second stage was to provide a recommendation to industry for future development. The method used for the final stage was not entirely different from the method used to elicit criteria weightings – those knowledgeable on the subject were asked. For the early nature of this report, it was decided that this was sufficient to accomplish the intended aims, however future work developing technologies further should use an empirical method to evaluate them.

4.5 Methods

There are a wide range of methods which can be employed for decision problems and whichever one the decision maker (DM) chooses to use has some impact on the results. A good comparison of methods for use in renewable energy technologies is made by Mateo (Mateo, 2012) and other such comparisons are made by various authors (Pohekar & Ramachandran, 2004). However, a brief overview of some of the most common methods which could be employed in the selection of a new technology are presented here.

The fundamental underlying principles of these methods can be somewhat disparate; while some methods compare each action or alternative in a pair-wise manner and rank the actions accordingly, others can ascribe absolute values to the actions which can then be ordered. Preferences of the DM, or those for whom the decision is being made, can be taken into account in a number of ways, for example, using thresholds or weightings. Uncertainty in the data can be considered in a number of ways which include by augmenting it with another function (Polatidis, Haralambopoulos, Munda, & Vreeker, 2006), by considering the inputs stochastically (A. Kolios, Mytilinou, Lozano-Minguez, & Salonitis, 2016) or using 'fuzzy' logic. The DM must decide, based on these differences, which is the most appropriate method for their particular problem.

4.5.1 Weighted Sum and Weighted Product Methods

4.5.1.1 Weighted Sum Method

Weighted sum (WSM) and weighted product (WPM) methods are two similar and simple methods.

Weighted sum method, which is discussed in (Mateo, 2012) and (Pohekar & Ramachandran, 2004) calculates the value of each alternative as the sum of the product between the weight of each criterion, w_j , and how well each alternative, from 1 to M, satisfies that criterion, a_{ij} . The simple equation is as follows, for $i=1,2,3...M$:

$$A^* = \sum_i^j a_{ij} * w_j \quad (4-1)$$

Where A^* is the value of the alternative, M is the number of alternatives which have N criteria.

While simple to apply, this method depends on the additive utility function, which may not always be valid. WSM does not incorporate any normalisation, so if any of the values are within different ranges to each other then it will not be appropriate to use. Due to the wide range of things to consider in the very different technologies which will be discussed, WSM was quickly ruled out as a suitable method.

4.5.1.2 Weighted Product Method

Weighted product method (WPM) is a very simplistic method like WSM, however the weights are applied as powers in a multiplicative utility. WPM was used in (Adriyendi, 2015) to compare food choices and (M. Wang, Liu, Wang, & Lai, 2010) used it to decide on bidders for a contract. The method is explained in further in (Evangelos Triantaphyllou & Mann, 1989).

WPM compares each alternative to another individually by determining the following product for alternative A_K to alternative A_L (Evangelos Triantaphyllou & Mann, 1989):

$$R\left(\frac{A_K}{A_L}\right) = \prod_{j=1}^N \left(\frac{a_{Kj}}{a_{Lj}}\right)^{w_j} \quad (4-2)$$

If the product, R , is greater than 1 then alternative K is preferable to alternative L . By dividing the criteria satisfaction value for one alternative by the other this eliminates the units – therefore a wide range of criteria can be compared.

4.5.2 Analytical Hierarchy Process

The Analytical Hierarchy Process (AHP) was developed by Saaty and presented in (Saaty, 1980). The process is similar to WSM in that it uses an additive utility function (Cinelli, Coles, & Kirwan, 2014) however it is far more complex and allows for a consistency check.

The basic process, as discussed here, is based on references (Saaty, 1980) and (Mateo, 2012). The first step is to determine weights for each alternative through a pairwise comparison of how important each criterion is to another using the Saaty scale of 1 to 9 where 1 is equal preference and 9 is absolute preference; the use of different scales is discussed further in (E. Triantaphyllou, Shu, Nieto Sanchez, & Ray, 1998). This weight matrix is normalised through each column and then averaged for each column to produce a weight vector, w .

For each criterion, the same procedure for the weight vector is used. This time one matrix for each criterion, j , comparing how well alternative, i , satisfies the criterion relative to alternative, h . This is all then used to produce a criteria satisfaction matrix.

Additive utility is then used to rank the alternatives. There is also a consistency check where a consistency index (CI) is compared to a random index (RI).

This method could be useful in comparing different, immature technologies if the basis for how well each criterion is satisfied is only known qualitatively. However if the values used for weights and criteria satisfaction depend on a group of people who are not personally invested in the project, for example a survey sent to industry, then a pairwise comparison for so many things may be too much to ask of them and responses may not be forthcoming.

4.5.3 PROMETHEE

There are a number of different types of PROMETHEE, which stands for: 'Preference Ranking Organisation Method for Enrichment Evaluations'. PROMETHEE I compares alternatives in a

pairwise manner where the preference for each alternative is given in a preference function, of which Brans et al (Brans & Vincke, 1985) proposed 6 generalised functions. As part of this comparison the DM uses preference and indifference functions to account for slight preferences being important or unimportant respectively (Pohekar & Ramachandran, 2004).

The comparison is used to create 'outranking indexes' Φ . The positive outranking index, Φ^+ , for alternative a is effectively the outranking power of that alternative over the others (Greco, Ehrgott, & Figueira, 2016). The negative outranking index, Φ^- , is how much the alternative is outranked. This gives a partial ranking of alternatives; PROMETHEE II expands on this to give a complete ranking by computing the net flow, or the difference between positive and negative outranking indexes, for each alternative. However this method in PROMETHEE II loses some resolution and is perhaps not as reliable. Weights are also used to determine the relative importance of the criteria themselves (Cinelli et al., 2014) as with the other methods.

4.5.4 ELECTRE

ELECTRE was introduced in 1968 by Roy (Roy, 1968) and has been developed into a number of iterations since. Fundamentally, ELECTRE works on the principles of concordance and discordance. For concordance, when comparing alternative a to alternative b , for a to be preferable to b (aSb), the majority of the criteria in a outrank b . At the same time, for non-discordance, none of the instances where b outranks a are significant enough to refute the claim, aSb (Greco et al., 2016).

ELECTRE I determines the concordance and discordance levels of the comparison of alternatives which yields a system of outrankings (Pohekar & Ramachandran, 2004). However, only one of these outrankings is absolute and so graphical methods are used to create a kernel where items that do not belong in the kernel are outranked by at least one item in the kernel. Other ELECTRE methods use concepts such as veto thresholds and pseudo-criteria for more complete rankings.

4.6 TOPSIS

TOPSIS method, which stands for Technique for Order of Preference by Similarity to Ideal Solution, was presented by Hwang and Yoon in 1981 (Hwang & Yoon, 1981). TOPSIS is a simple method which utilises concepts of theoretical ideal positive and negative solutions and ranks alternatives by their Euclidian distance to these solutions (Mateo, 2012).

The method was employed by a number of researchers, for example by A.J. Kolios et al (A. J. Kolios, Rodriguez-Tsouroukdissian, & Salonitis, 2016), who used stochastic inputs to evaluate wind turbine foundations. It has also been used to evaluate different energy generation technologies in (Sarkar, 2013) where an AHP methodology was used to evaluate the relative importance of criteria.

4.6.1 TOPSIS Method

The TOPSIS method is explained in references (A. Kolios et al., 2016) and (A. Kolios et al., 2016) but will also be explained here for reference with the following steps:

1. A decision matrix is created holding the values for how well each alternative solution, m , satisfies each criterion, n .
2. The decision matrix is normalised by dividing each value by the square root of the sum of all values in the matrix squared, as shown in the following equation:

$$r_{ij} = \frac{x_{ij}}{\sqrt{\sum x_{ij}^2}} \quad (4-3)$$

Where r_{ij} is the weighted value in the decision matrix at point (i,j) , x_{ij} is the original value at that point.

3. The decision matrix is weighted by multiplying each value in the matrix by the criterion's corresponding weighting, as in the following equation:

$$v_{ij} = w_i * r_{ij} \quad (4-4)$$

Where v_{ij} is the weighted, normalised value and w_i is the weight value for that criterion.

4. A Positive Ideal Solution (PIS) and a Negative Ideal Solution (NIS) are created from the decision matrix. The PIS is the maximum of all of the 'good' criteria for which the DM wants to maximise, and the minimum of all of the 'bad' criteria. The NIS is the converse of this. These solutions are purely theoretical and are used only for comparison.
5. For each alternative, the geometric distance to the PIS and to the NIS is determined. This is shown simply in the following equations:

$$D_j^{PIS} = \sqrt{\sum_{i=1}^n (v_{ij} - v_i^{PIS})^2} \quad (4-5)$$

$$D_j^{NIS} = \sqrt{\sum_{i=1}^n (v_{ij} - v_i^{NIS})^2} \quad (4-6)$$

Where D_j^{PIS} is the distance of the j th alternative to the PIS, D_j^{NIS} is the distance of the j th alternative to the NIS and v_i^{PIS} and v_i^{NIS} are the weighted, normalised values of the i th criterion for the PIS and NIS respectively.

6. How close each alternative is to the PIS relative to the NIS, C_j , is evaluated with the following equation:

$$C_j = \frac{D_j^{NIS}}{D_j^{PIS} + D_j^{NIS}} \quad (4-7)$$

This can be illustrated graphically as shown in Figure 4-2:



Figure 4-2 Illustration of the idea of 'Closeness'

Using this closeness value, which will range from 0 to 1, the alternatives can finally be ranked. The closer the alternative is to 1 the better the alternative and the higher it is ranked.

4.7 Methodology

MATLAB was used to implement the procedure described in Section 4.6.1 and the code used is given in the appendix. The weightings for the relative importance of each criterion was derived from the survey discussed in Section 4.3 and values for how well each alternative satisfies each criterion was discussed in Section 4.4.

4.7.1 Weights Used and Evaluation of Survey Data

The weight values used for each criterion were the averages of the values given by respondents to the survey. As part of the survey, the number of years of relevant experience as well as perceived levels of expertise were requested and these were used to weight the value of the response. The weight values used are now given in the following graphs:

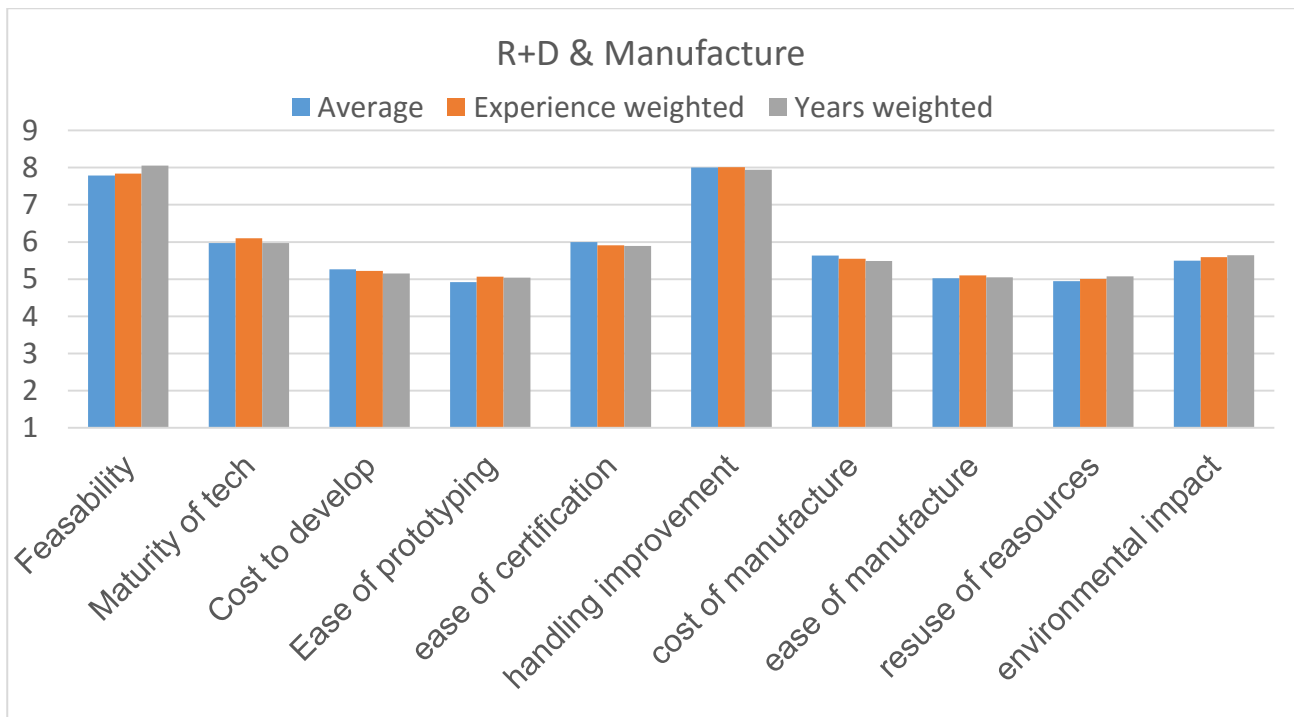


Figure 4-3 Averaged responses to the section 'R+D & Manufacture'



Figure 4-4 Averaged responses to the section 'Operational'

Figure 4-3 and Figure 4-4 show the averaged responses from the survey which were used as weights for the MCDA. The blue bars are simply the averages of all of the responses while the orange and grey bars are weighted by perceived level of experience and by years of experience respectively. While these weights have some effect on the values the effect is only minor. In this instance there is no significant correlation between experience by either measure and perceived level of importance of each criterion.

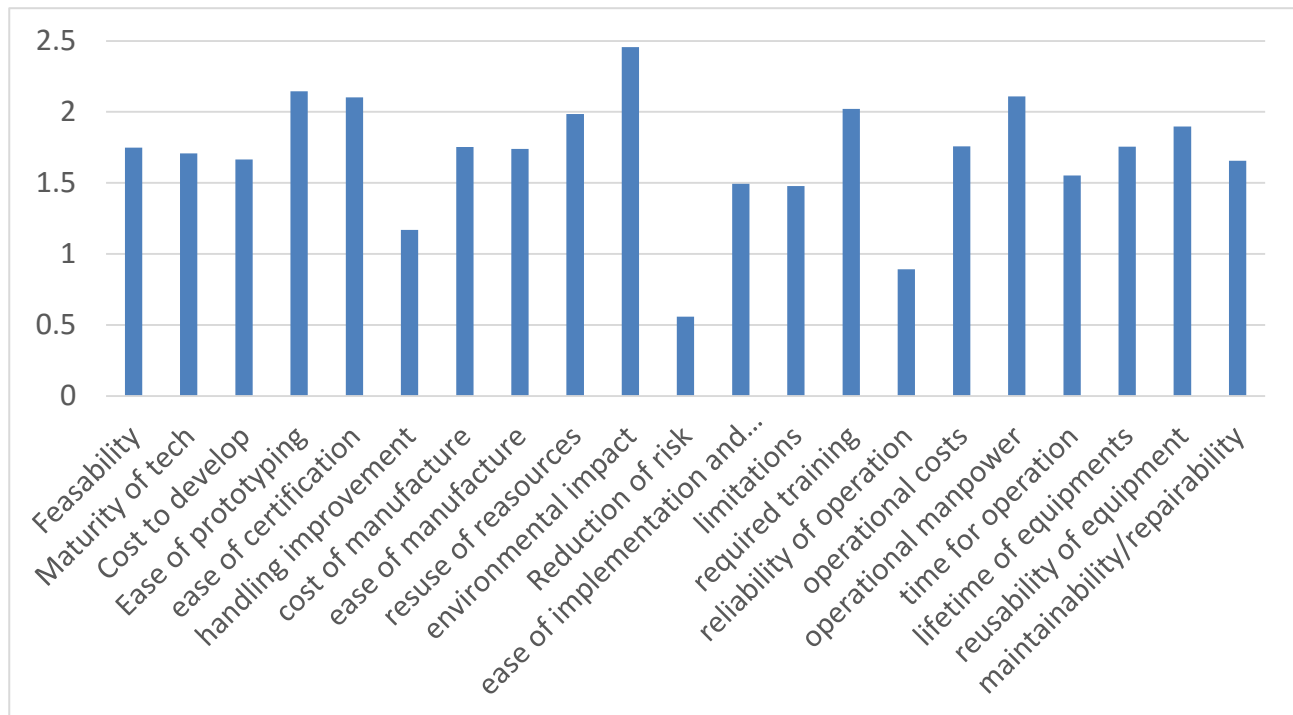


Figure 4-5 Standard deviation of responses

The responses were somewhat varied as is shown by the standard deviations given in Figure 4-5. While items such as 'Reduction of risk' had a very low standard deviation of 0.56, indicating good agreement by all respondents, other items had a significantly larger standard deviation, for instance 'Environmental Impact'. The mean value was 1.70.

The distribution of the responses varied between the different criteria. While most of the distributions appeared similar in shape to a normal or Weibull distribution, as shown in Figure 4-6 and Figure 4-7, 'Environmental Impact' was very close to an even distribution shown in Figure 4-8 and some criteria, such as 'reduction of risk' in Figure 4-9, were very close to a single value. This supports the approach used by A.J. Kolios et al (A. Kolios et al., 2016) where Monte Carlo

simulation was used to perform the analysis and evaluate confidence in the output. Given the way responses varied in the survey conducted for this study, the use of Monte Carlo simulation should be explored in future work. Histogram plots for all criteria, as well as a table of response numbers, are given in Appendix E.

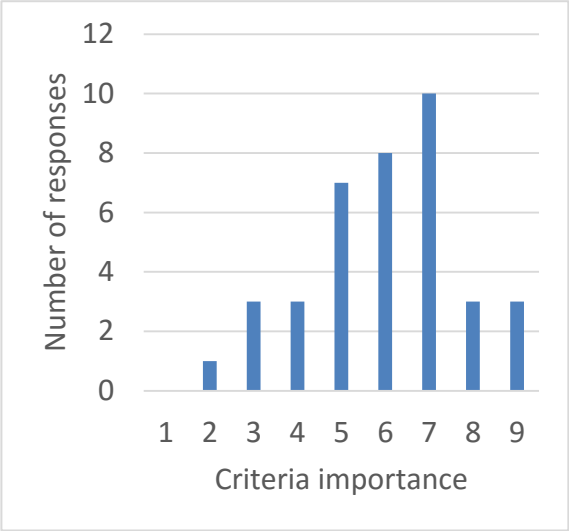


Figure 4-6 Maturity of technology

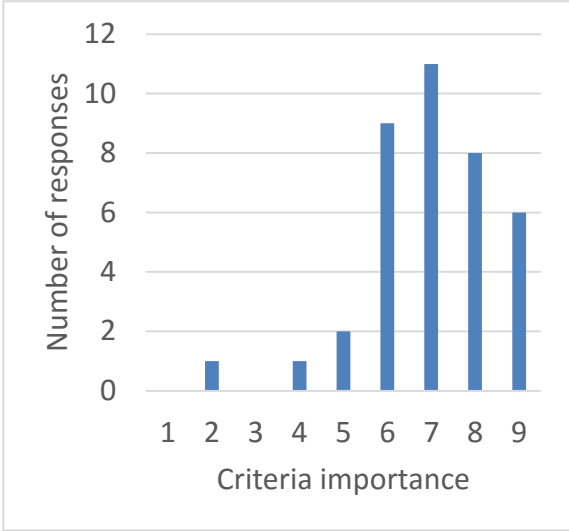


Figure 4-7 Limitations

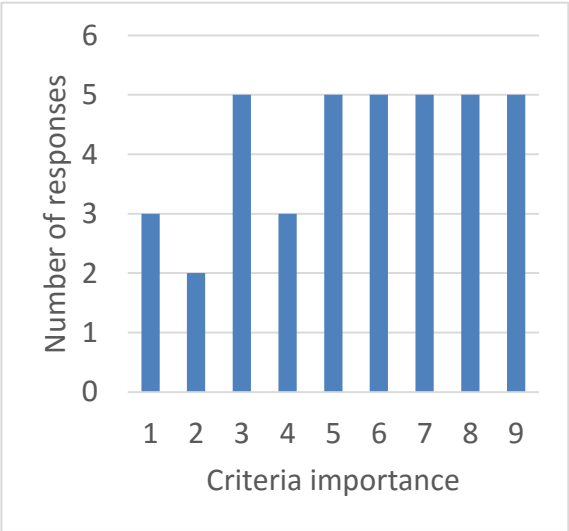


Figure 4-8 Environmental impact

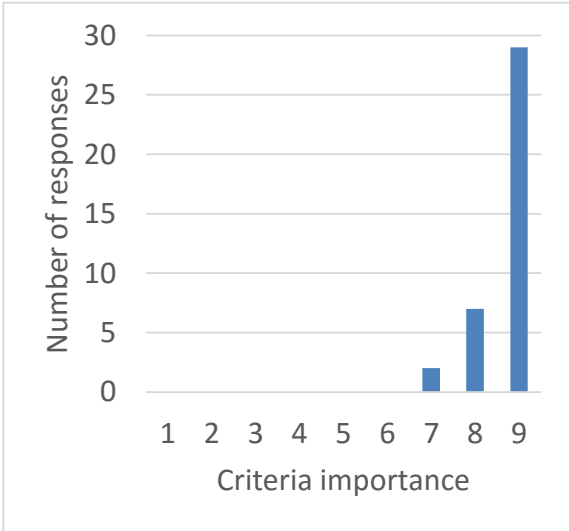


Figure 4-9 Reduction of risk

4.8 Results and Discussion

4.8.1 First Stage TOPSIS Analysis

The top results from the initial TOPSIS analysis stage are presented in Table 4-2 to Table 4-4. Complete tables including all ideas are presented in the appendix.

Table 4-2, Table 4-3 and Table 4-4 show the top results from all of the ideas initially investigated. These results can be compared within each table but cannot be compared between different tables due to the fact that the criteria satisfaction values were determined by different people and that they are separate TOPSIS analysis.

Table 4-2 shows the results from the guidance and control section, more on these ideas can be found at Section 3.1. Existing ideas such as guide pins and Boom Lock perform well due to the confidence in these comparatively simple ideas. Camera systems is at the bottom of these top ideas, possibly due to the uncertainty at this stage.

Table 4-3 shows the results from 'connections and seafastening', more information on these ideas can be found at Section 3.2. The top idea is automation of the bolting procedure followed by two novel seafastening methods and finally a new connection type.

Table 4-4 shows the initial results for the 'Assembly methods' section, which is further described at Section 3.3. Current pre-assembly methods, for example 'bunny ear' method, ranks top followed by two full pre-assembly methods and finally the conventional method of constructing individual pieces at the site.

This initial analysis served as a guide to the research team rather than a fixed prescription, therefore the concepts chosen for each individual section may differ from those presented here.

Table 4-2 First stage TOPSIS results for 'Guidance and Control'

Alternative	TOPSIS C	C, exp weighted	C, Year weighted
Guide Pins	0.7124	0.7108	0.7126
Remote Control	0.7099	0.7097	0.7077
Taglines/Tagline winches	0.6668	0.6681	0.6694
Highwind – Boom Lock	0.6389	0.6409	0.64
Funnels/Cones	0.6318	0.6307	0.6297
Multiple Cameras	0.6268	0.6257	0.6299

Table 4-3 First stage TOPSIS results for 'Connections and Seafastening'

Alternative	TOPSIS C	C, exp weighted	C, Year weighted
Bolting robot arm	0.6475	0.6495	0.6489
Hydraulic Seafastening	0.6125	0.6127	0.614
Internal Jack Seafastening	0.6125	0.6127	0.614
Friction connection	0.5647	0.5645	0.5631

Table 4-4 First stage TOPSIS results for 'Assembly Methods'

Alternative	Topsis C	C, exp weighted	C, Year weighted
Current pre-assembly practise	0.7187	0.7178	0.7203
Bottom fixed WTS(partially Self erecting WTs)	0.5277	0.5293	0.5268
Bottom fixed WTS(Fully pre-assembled transportation)	0.5078	0.5087	0.5076
Offshore assembly (single pieces) installation	0.5072	0.5069	0.5035

4.8.2 Second Stage TOPSIS Analysis

Of the ideas developed further, the final ranking of these ideas as determined through a TOPSIS analysis are presented here.

Here, all ideas developed in each section are compared directly. Based on the research of the team and their assessment of the concepts in combination with the criteria importance from industry. All of the final concepts are presented in Table 4-5.

The top five recommendations based on this analysis are:

1. Boom Lock and tag lines
2. Camera system with mechanical guidance
3. Automated bolt installation/fastening used for seafastening
4. Boom Lock, tag lines, mechanical guidance and cameras
5. Current pre-assembly practice of partially assembled components carried to the site for installation.

Table 4-5 Final ranking of all proposed ideas

Technology	Topsis C	C, exp weighted	C, Year weighted
Boom Lock and tag lines	0.6719	0.6719	0.6734
Camera system + mechanical guidance	0.6166	0.6159	0.6169
Robot arm for seafastening	0.6137	0.6139	0.616
Boom Lock, tag lines, mech guidance and cameras	0.5952	0.5942	0.599
Current pre-assembly practise	0.5949	0.5954	0.5922
Camera system (3* fine tune 1* 360 + redundancy)	0.5887	0.5873	0.5894
Robot arm for bolting in construction	0.5633	0.564	0.5652
Completely hydraulic seafastening	0.5562	0.555	0.5564
Offshore assembly (single pieces) installation	0.5506	0.5497	0.5455
Partial hydraulic seafastening	0.5471	0.5452	0.5448
Bottom fixed WTS(fully pre-assembled transportation)	0.3856	0.3862	0.3895
Bottom fixed WTS(partially self erecting WTs)	0.2349	0.2346	0.2355

4.9 Conclusions

In this section, a multi-criteria decision method was used to evaluate concepts in an effort to spend time more efficiently but also to give a final recommendation for further development. A survey was distributed to industry personnel with relevant experience which was used to elicit weighting values for use in the MCDA. Technologies were evaluated qualitatively in two stages for criteria

satisfaction values. The results of the survey showed not only which criteria were most important but also how opinion varied across the industry on some criteria as there was not always general agreement among respondents. Our final analysis proposes the ideas most worth developing further are: 1) Boom Lock and tag lines, 2) Camera system with mechanical guidance, 3) Automated bolt installation/fastening used for seafastening, 4) Boom Lock, tag lines, mechanical guidance and cameras and 5) Current pre-assembly practice of partially assembled components carried to the site for installation.

5 CONCLUSIONS

5.1 Summary of Report

This report, as part of the REMS-CDT group project at Oxford and Cranfield University and guided by contacts at G+ and DONG Energy, has looked into the health and safety issue of humans beneath suspended loads during the installation of offshore wind turbines. This appears to be common practice in the field and the lifting process was analysed along with guidelines and standards for health and safety in offshore lifts. Our direction was then guided by our contacts at DONG Energy with whom we discussed industry practice and areas of interest. Statistics regarding the reasons, areas, and consequences for incidents during lifting operations in offshore wind turbine installation processes, resulting from incident reports provided by G+, were then analysed and show the importance of safer and improved handling in offshore lifting operations. Ultimately, this appeared to show that the majority of issues were down to human error or equipment failure and the transition piece and nacelle are highly incident prone areas. With a large number of these incidents due to dropped objects, the focus remained on moving people from beneath suspended loads and it was decided that the focus of this report would lie in the project sites and more specifically the offshore operations.

Different concepts for human-free offshore lifting operations in the categories of guidance and control, connections, and assembly were proposed after a comprehensive literature review. The most viable solution to this issue is not only the one that reduces the risk to workers the most but is rather a multi-dimensional problem of many criteria. Thus, a multi-criteria decision analysis, using experts' opinions for the importance of defined criteria was obtained by conducting a survey and using the TOPSIS method. This method helped to define the concepts to be taken to a detailed study. The final ideas included the following:

- Holistic guiding systems linked with control instruments, which were investigated further by conducting lab experiments to study various configurations of cameras and novel mechanical guidance systems.

- Automatic bolting and hydraulic seafastening systems, both existing designs and a novel seafastening solution developed by the team.
- Optimisation of the preassembly and installation methods that may now be critically analysed by a program developed by the team.
- Finally, looking to the future of the industry, novel assembly concepts and the possibility of floating structures have been analysed.

Those recommended concepts were finally ranked by applying the same multi-criteria decision analysis with renewed scores and are discussed further in Section 5.4.

5.2 Drawbacks of Human-Free Operations

There are still some drawbacks which need considering before human-free operations become the norm in industry. These are mainly apparent due to the infancy of the technology/systems; this will bring about new challenges arising from teething problems and the requirement for additional and special training. Although some of the systems presented in this report would have little effect on the overall cost of offshore operations (for instance camera systems), others may have a substantial initial or ongoing investment (particularly if new vessels or fabrication are required). Equally, there may be mechanical complexity that should be considered. Finally, there may need to be consideration given to the effects to the lifting culture once people are removed from beneath the lifts. There may be less of a human connection, and with fewer risks maybe work would be pushed to be quicker and cause additional risks elsewhere.

5.3 Benefits of Human-Free Operations

The main benefit of human-free lifting is, of course, the reduction of risk to personnel. The placement of people beneath suspended loads is a risk that should no longer be accepted in the industry and developing solutions to make this a reality should be paramount. This change in a key health and safety area could change the culture in offshore wind turbine installations, encouraging further developments and safer work. Depending on the solution, it may also result in work that is more efficient and potentially open up the weather window to greater allowable working time. In

most cases the installation remains as precise, if not more so, compared to before and could result in a similar economic efficiency (although more costly, potential savings in time should be considered).

5.4 Recommendations

A wide variety of concepts have been presented in this report. Which, if any, a company or individual chooses to develop, if any, should depend on their own needs and resources. However, based on our MCDM analysis, discussed in Section 4, there are a number of options and suites of technologies which the authors are confident will be worth development.

The top results from our MCDM are:

1) Boom lock and tag-lines

A Boom Lock holds the hook against the bottom of the crane, this reduces the free oscillatory distance and increases control. Tag-lines can help mechanically in much the same way as when manually held by personnel, however, remote controlled tag-lines increase control over the load without the need to place personnel at risk.

2) Camera system with mechanical guidance

Mechanical guidance, such as stabbing guides, rails and other systems, act to reduce the tolerance margins in installation which can reduce installation time and remove the need for fine guidance control from personnel. Camera systems can be used, in conjunction with the mechanical guidance, to give equipment operators visual access from afar.

3) Automated bolt installation/fastening used for seafastening

There exist a range of technologies in sensors, robotics, feed systems, etc, which could be used in conjunction to perform bolting procedures in a fully automated way. The area identified as most promising for this is in seafastening where it can save operational time and reduce risk.

4) Boom lock, tag lines, mechanical guidance and cameras

While it is more complex, a full suite of guiding technologies can provide a higher level of control, accuracy, redundancy and safety.

5) Current pre-assembly practice of partially assembled components carried to the site for installation.

It is current practice, in some situations, to use some level of pre-construction in the assembly of OWTs. For example having the tower as one part, rather than sections, or 'bunny ears' where the nacelle, hub and two blades are pre-installed. The best combination of pre-assembly is not always obvious, therefore in this project a logistics program was developed to estimate construction time of different options.

5.5 Outlook and Future Work

This research team believe, from our analysis of available data and also from survey responses and other interactions with industry, that there is both a need and a strong drive to reduce the risk inherent in offshore lifting in the renewable energy industry. A number of solutions, particularly the technologies recommended in Section 4.8.2, showed a great deal of promise in the aim of removing humans from the areas of risk.

The implementation of these technologies into operations may not necessarily be easy or immediate, as many of the ideas still require further development. However, due to the growth of the industry and the strong desire among those within the industry to reduce risk, it is perhaps inevitable that some of these technologies, or technologies like them, will find their way into operational use in the future.

REFERENCES

- 4C Offshore. (2017a). Belwind Alstom Haliade-Demonstration Project. Retrieved March 15, 2017, from <http://www.4coffshore.com/windfarms/belwind-alstom-haliade-demonstration-belgium-be11.html>
- 4C Offshore. (2017b). Gravity Based Support Structures. Retrieved April 4, 2017, from <http://www.4coffshore.com/windfarms/gravity-based-support-structures-aid8.html>
- 4C Offshore. (2017c). Wind Farm Installation Specification. Retrieved April 4, 2017, from <http://www.4coffshore.com/windfarms>
- A2SEA. (2009). SEA INSTALLER specification sheet.
- Adriyendi. (2015). Multi-Attribute Decision Making Using Simple Additive Weighting and Weighted Product in Food Choice. *International Journal of Information Engineering and Electronic Business*, 7(6), 8–14. <https://doi.org/10.5815/ijieeb.2015.06.02>
- AH-Industries. (2016). Tagline Master. Retrieved March 16, 2017, from <http://www.ah-industries.com/lifting-equipment/>
- Ahn, D., Shin, S., Kim, S., Kharoufi, H., & Kim, H. (2016). Comparative evaluation of different offshore wind turbine installation vessels for Korean west–south wind farm. *International Journal of Naval Architecture and Ocean Engineering*, 9(1), 45–54. <https://doi.org/10.1016/j.ijnaoe.2016.07.004>
- AJP Recruitment. (2016). RED MARINE LOOKING TO CUT OFFSHORE WIND FARM INSTALLATION COSTS WITH NEW GEAR. Retrieved April 2, 2017, from <http://www.ajprecruitment.com/news/news/red-marine-looking-to-cut-offshore-wind-farm-installation-costs-with-new-gear/print>
- alfadoc. (2013). Why You Don't Want to be Superman with your Alfa Romeo. Retrieved March 16, 2017, from <https://alfadoctor.wordpress.com/2013/06/11/why-you-dont-want-to-be-superman-with-your-alfa-romeo/>

- Amate, J., Sánchez, G. D., & González, G. (2016). Development of a Semi-submersible Barge for the installation of a TLP floating substructure. TLPWIND[®] case study. *Journal of Physics: Conference Series*, 749, 12016. <https://doi.org/10.1088/1742-6596/749/1/012016>
- Anders Soe-Jensen. (2010). Method for establishing a wind turbine on a site, transport of a wind turbine tower, wind turbine tower and vessel suitable for transporting a wind turbine tower. DK. Retrieved from <https://www.google.com/patents/US20100281820>
- Asgarpour, M. (2016). *Assembly, transportation, installation and commissioning of offshore wind farms. Offshore Wind Farms: Technologies, Design and Operation*. Elsevier Ltd. <https://doi.org/10.1016/B978-0-08-100779-2.00017-9>
- Atlantic Area Transnational Program. (2010). Vessels and platforms for the emerging wind and wave power market.
- Balaam, T., & Leimeister, M. (2017a). *REMS_Group Project_A5.2_360 View*. Retrieved from <https://www.youtube.com/watch?v=nASOm9QKLcU&t=4s>
- Balaam, T., & Leimeister, M. (2017b). *REMS_Group Project_A5.2_Global View*. Retrieved from <https://www.youtube.com/watch?v=mme1c4Kr4tU&t=2s>
- Balaam, T., & Leimeister, M. (2017c). *REMS_Group Project_C1.5_360 View*. Retrieved from <https://www.youtube.com/watch?v=oOL1FNmdcZ4>
- BAM Nuttal. (2016). BAM's contract with EDF signals a worldwide first for leading edge Gravity Base Foundation Solutions.
- Barker, P. (2012). A flipping good idea for floating turbines. *Maritime Journal*. Retrieved from <http://www.maritimejournal.com/news101/marine-renewable-energy/a-flipping-good-idea-for-floating-turbines>
- Beardmore, R. (2008). Table of Bolt Sizes. Retrieved April 3, 2017, from http://www.roytech.co.uk/Useful_Tables/Screws/Hex_Screws.htm

- Bijlaard, F. S. K., Coelho, A. M. G., & Magalhães, V. J. D. A. (2009). Innovative joints in steel construction. *Steel Construction*, 2(4), 243–247. <https://doi.org/10.1002/stco.200910033>
- Bitsch, M. L., & Baun, T. F. (2012). An apparatus for and method of mounting wind turbine blades on a wind turbine tower.
- Bøe, T., & Nestegård, A. (2010). Dynamic Forces during Deepwater Lifting Operations. *The Twentieth International Offshore and Polar Engineering Conference*, 7, 500–507.
- Brans, J. P., & Vincke, P. (1985). A Preference Ranking Organisation Method: (The PROMETHEE Method for Multiple Criteria Decision-Making). *Management Science*, 31(6), 647–656. <https://doi.org/10.1017/CBO9781107415324.004>
- British Standards. Code of practice for safe use of cranes - Part 11: Offshore cranes, BS 7121-11:1998 (1998).
- British Standards. Code of practice for safe use of cranes - Part 1: General, BS 7121-1:2006 (2006).
- Burton, T., Jenkins, N., Sharpe, D., & Bossanyi, E. (2011). *Wind Energy Handbook* (2nd ed.). John Wiley & Sons Ltd.
- Bush, E. (2015). Nation's first offshore wind farm under construction, opportunity in NW. Retrieved March 20, 2017, from <http://www.seattletimes.com/seattle-news/northwest-could-get-its-own-offshore-wind-farm-by-2017/>
- C-power. (2017). Thornton Bank Wind Farm Specification. Retrieved April 4, 2017, from <http://www.c-power.be/index.php/project-phase-1/effective-works>
- Cairney, J. (2015). Offshore Wind Farm Case Study - How to Achieve Cost Reduction at Offshore Wind Farm Construction Projects. In *Offshore Technology Conference*. Offshore Technology Conference. <https://doi.org/10.4043/26037-MS>
- Choe, Y., Lee, H. C., Kim, Y. J., Hong, D. H., Park, S. S., & Lim, M. T. (2009). Vision-based

estimation of bolt-hole location using circular hough transform. In *ICROS-SICE International Joint Conference* (pp. 4821–4826). Retrieved from <http://www.scopus.com/inward/record.url?eid=2-s2.0-77951110745&partnerID=40&md5=00ce10c276c2741bd3b7d6f4fa600534>

Cinelli, M., Coles, S. R., & Kirwan, K. (2014). Analysis of the potentials of multi criteria decision analysis methods to conduct sustainability assessment. *Ecological Indicators*, 46, 138–148. <https://doi.org/10.1016/j.ecolind.2014.06.011>

ConXtech. (2015). ConXtech. Retrieved March 16, 2017, from www.Conxtech.com

Cordle, A., & Jonkman, J. (2011). State of the Art in Floating Wind Turbine Design Tools. In *Proceedings of the International Offshore and Polar Engineering Conference* (pp. 367–374). Retrieved from <http://www.scopus.com/inward/record.url?eid=2-s2.0-80052781492&partnerID=40&md5=4eb652a02cf3d5f1e16e8107398cdcfe>

Dehlsen, J. G. P., & Mikhail, A. S. (2005). Self-erecting tower and method for raising the tower.

Desmond, C., Murphy, J., Blonk, L., & Haans, W. (2016). Description of an 8 MW reference wind turbine. *Journal of Physics: Conference Series*, 753, 92013. <https://doi.org/10.1088/1742-6596/753/9/092013>

DNV. (2013). *DNV-RP-C208 Determination of Structural Capacity by Non-linear FE analysis Methods* (Vol. DNV-RP-C20).

DNV. (2014a). *DNV-OS-H205 Lifting Operations (VMO Standard - Part 2-5)*.

DNV. (2014b). *DNV-RP-C205 Environmental Conditions and Environmental Loads*.

DNV GL. (2016a). *DNVGL-ST-N001 Marine operations and marine warranty*.

DNV GL. (2016b). Rules and standards. Retrieved April 6, 2017, from <https://www.dnvgl.com/rules-standards/>

Dodgson, J. S., Spackman, M., Pearman, A., & Phillips, L. D. (2009). *Multi-criteria analysis: a*

manual. London. <https://doi.org/10.1002/mcda.399>

Duan, X., Wang, Y., Li, M., Kong, X., & Aliy, S. A. (2013). A fastening bolt method based on image recognition. In *International Conference on Robotics and Biomimetics (ROBIO)* (pp. 2709–2714). <https://doi.org/10.1109/ROBIO.2013.6739883>

European Wind Energy Association. (2013). *Deep water*.

EWEA. (2016). *The European offshore wind industry*. Retrieved from <http://www.ewea.org/fileadmin/files/library/publications/statistics/EWEA-European-Offshore-Statistics-2015.pdf>

Faiz, T. I. (2014). *Minimization of Transportation , Installation and Maintenance Operations Costs for Offshore Wind Turbines*. Graduate Faculty of the Louisiana State University and Agricultural and Mechanical College. Retrieved from http://etd.lsu.edu/docs/available/etd-04112014-091556/unrestricted/Faiz_thesis.pdf

Forewind. (2013). *HSE case study 2: The “ human free ” met mast installation*.

Fred. Olsen Windcarrier. (2013). Case Study: Alstom Haliade™ Demonstrator. Retrieved March 30, 2017, from <http://windcarrier.com/blog/case-studies/alstom-haliade/>

Fred. Olsen Windcarrier. (2015). Global Tech I wind turbine installation - Fred. Olsen Windcarrier short. Retrieved from <https://www.youtube.com/watch?v=88hu8l8WO4k&t=181s>

Fred. Olsen Windcarrier. (2016a). *Block Island Offshore Wind Farm*. www.youtube.com. Retrieved from <https://www.youtube.com/watch?v=p29MnJL4lIQ>

Fred. Olsen Windcarrier. (2016b). Case Study: Block Island. Retrieved February 16, 2017, from <http://windcarrier.com/blog/case-studies/block-island/>

Fred. Olsen Windcarrier. (2017). Lifting Offshore Wind - Fred Olsen fleet. Retrieved February 1, 2017, from <http://windcarrier.com/fleet/#jack-ups>

G9 Offshore Wind Health & Safety Association. (2014). *Good practice guideline - Working at height*

in the offshore wind industry.

- Gee, A. F., & FL, T. (2011). Patent(US20110314767) - Partially selferecting Wind turbine Towers.
- Germanischer Lloyd SE. (2013). Rules for classification and construction – ship technology (1 August 2). Hamburg: Germanischer Lloyd SE.
- Greco, S., Ehrgott, M., & Figueira, J. R. (Eds.). (2016). *Multiple Criteria Decision Analysis: State of the Art Surveys* (2nd ed.). New York: Springe.
- guide2research. (2017). Top Journals for Image Processing & Computer Vision. Retrieved March 21, 2017, from <http://www.guide2research.com/journals/computer-vision>
- Hambling, D. (2014). Moth drone stays rock steady in gale-force winds. *New Scientist*. Retrieved from <https://www.newscientist.com/article/mg22129524-300-moth-drone-stays-rock-steady-in-gale-force-winds/>
- Hau, E. (2008). *Wind turbines*. <https://doi.org/10.1533/9780857097286.3.387>
- Health and Safety Executive. (2012). *Manual handling at work. A biref guide. INDG143(rev3)*. [https://doi.org/10.1016/0003-6870\(89\)90067-7](https://doi.org/10.1016/0003-6870(89)90067-7)
- Health and Safety Executive. (2014). *Safe use of lifting equipment - Lifting Operations and Lifting Equipment Regulations 1998* (2nd ed.).
- Heistermann, C., Husson, W., & Veljkovic, M. (2009). Flange connection vs . friction connection in towers for wind turbines. In *Nordic steel and construction conference* (pp. 296–303). NSCC2009.
- High Wind. (2014). The Boom Lock. Retrieved January 25, 2017, from <http://www.high-wind.eu/boomlock/>
- Hobson Technical. (2007). *Hex Bolts Details*. Retrieved from <https://www.hobson.com.au/files/technical/htd-hxb-met-properties.pdf>
- Hoeksema, W. (2014). Innovative Solution for Seafastening Offshore Wind Turbine Transition

Pieces during transport Innovative Solution for Seafastening Offshore Wind Turbine Transition
Pieces during transport, (February).

HoistCam. (2016). HoistCam Visual Aid Technology Case Studies. Retrieved March 16, 2017, from <http://hoistcam.com/case-studies/>

Hörauf, L., Müller, R., Bauer, J., Neumann, H., & Vette, M. (2013). Development of an Intelligent Bolt Tensioning System and Adaptive Process for the Automated Pitch Bearing Assembly of Wind Turbines. In A. Azevedo (Ed.), *Advances in Sustainable and Competitive Manufacturing Systems* (pp. 651–663). Springer. https://doi.org/10.1007/978-3-319-00557-7_54

Hussain, S. A., Reddy, B. S., & Reddy, V. N. (2008). Prediction of Elastic Properties of FRP Composite Lamina for Longitudinal Loading. *ARP Journal of Engineering and Applied Sciences*, 3(6), 70–75.

Hwang, C.-L., & Yoon, K. (1981). *Multiple Attribute Decision Making: Methods and Applications*. Springer-Verlag Berlin Heidelberg.

Hydro International. (2017). IHC EB Technology at Offshore Wind 2009. Retrieved March 20, 2017, from <https://www.hydro-international.com/content/news/ihc-eb-technology-at-offshore-wind-2009>

IMCA Holdings Ltd, & IMCA Trading Ltd. (2017). ABOUT IMCA. Retrieved April 6, 2017, from <https://www.imca-int.com/about-imca/>

International Association of Oil & Gas Producers. (2006). *Lifting & hoisting safety recommended practice*.

ITH. (n.d.). Hydraulic, friction- and torsion-free tensioning with ITH Bolt Tensioning Cylinders. Retrieved March 20, 2017, from <http://www.ith.com/en/tension-and-torque-tools/hydraulic-bolt-tensioning-and-equipment/bolt-tensioning-cylinders.php>

ITH Bolting Technology. (2016). Examples of ITH project engineering - Automation. Retrieved February 6, 2017, from <http://www.ith.com/en/engineering/project-engineering-in-bolting->

technology.php

- ITI. (2016). VR Mobile Crane Simulator Announced. Retrieved March 16, 2017, from <http://www.iti.com/news/vr-mobile-crane-simulator-announced-by-iti>
- Izzo, G. (2014). *Sea-fastening of Wind Turbine Generators for assembled tower Transportation and Installation*.
- Jensen, M. J. S. (2013). An aligning tool in the field of wind turbines for aligning a hole with a fastener.
- Johst, K., Jagd, L., Bovin, J., & Marinitsch, G. (2013). Bolt mounting and tightening robot for wind turbines.
- Kadhm, M. S. (2014). *Pattern Recognition - Template Matching*. Baghdad. Retrieved from <https://de.slideshare.net/mustafasalam167/template-matching>
- Kolios, A. J., Rodriguez-Tsouroukdissian, A., & Salonitis, K. (2016). Multi-criteria decision analysis of offshore wind turbines support structures under stochastic inputs. *Ships and Offshore Structures*, 11(1), 38–49. <https://doi.org/10.1080/17445302.2014.961295>
- Kolios, A., Mytilinou, V., Lozano-Minguez, E., & Salonitis, K. (2016). A comparative study of multiple-criteria decision-making methods under stochastic inputs. *Energies*, 9(7), 1–21. <https://doi.org/10.3390/en9070566>
- Lawrie, G. A. (2010). Implementation of the OGP Lifting and Hoisting Recommended Practice. In *SPE International Conference on Health, Safety and Environment in Oil and Gas Exploration and Production*. <https://doi.org/10.2118/126607-MS>
- Lawson, J. (2012). Offshore Wind Turbines Transporters Rise to the Challenge. Part 1.
- Leenhard Hörauf, Rainer Müller, Jochen Bauer, Holger Neumann Vette, and M. (2013). Development of an Intelligent Bolt Tensioning System and Adaptive Process for the Automated Pitch Bearing Assembly of Wind Turbines. *Advances in Sustainable and*

- Li, L., Gao, Z., & Moan, T. (2016). Analysis of Lifting Operation of a Monopile Considering Vessel Shielding Effects in Short-crested Waves. *International Journal of Offshore and Polar Engineering*, 26(4), 408–416. <https://doi.org/10.17736/ijope.2016.tsr09>
- Liftra. (2014). Blade Dragon. Retrieved March 20, 2017, from <http://www.liftra.com/product/product-2/>
- Liftra. (2016). Liftra Products. Retrieved March 16, 2016, from <http://www.liftra.com/4563-2/>
- Lombardo, T. (2013). Climbing Robotic Wind Turbine Inspector. Retrieved March 20, 2017, from <http://www.engineering.com/ElectronicsDesign/ElectronicsDesignArticles/ArticleID/5652/Climbing-Robotic-Wind-Turbine-Inspector.aspx>
- London Array. (2013). *London Array foundation and Turbine installation*. Retrieved from <https://www.youtube.com/watch?v=O7b3Ev2Emyc>
- Lorenz, L. (2017). Revenue for Wind Turbine Unmanned Aerial Vehicles Sales Is Expected to Total Nearly \$6 Billion by 2024. Retrieved March 30, 2017, from <https://www.navigantresearch.com/newsroom/revenue-for-wind-turbine-unmanned-aerial-vehicles-sales-is-expected-to-total-nearly-6-billion-by-2024>
- Lozano-Minguez, E., Kolios, A. J., & Brennan, F. P. (2011). Multi-criteria assessment of offshore wind turbine support structures. *Renewable Energy*, 36(11), 2831–2837. <https://doi.org/10.1016/j.renene.2011.04.020>
- MacFarlane, C. (2016). Alexandra Dock - Siemens. Retrieved March 20, 2017, from <http://greenporthull.co.uk/projects/alexandra-dock/siemens>
- Marshall Cavendish Corporation. (2003). *How It Works - Science and Technology - Volume 13*. (W. Horobin, Ed.) (3rd ed.). Marshall Cavendish. Retrieved from <https://books.google.de/books?id=Pzun0xgvVuMC&pg=PA1747&lpg=PA1747&dq=remote+control+guidance+system&source=bl&ots=42GBqdur1g&sig=d0HQEBYCUDZ7tPcn->

YJ04NwxcT8&hl=de&sa=X&ved=0ahUKEwjVnfz97N3SAhVLB8AKHRn1BHoQ6AEIcDAM#v=onepage&q=remote%2520control%2520guida

Mateo, J. R. S. C. (2012). *Multi Criteria Analysis in the Renewable Energy Industry*. London: Springer. Retrieved from <http://www.springer.com/gb/book/9781447123453>

Matrox Imaging. (2017). Machine vision helps port terminals increase productivity. Retrieved March 28, 2017, from http://www.matrox.com/imaging/en/press/feature/heavy_industry/ship_to_shore_container_crane/

McMorran, P. (1998). Training for Safe and Efficient Lifting Operations. In *SPE International Conference on Health, Safety and Environment in Oil and Gas Exploration and Production*. Society of Petroleum Engineers. <https://doi.org/10.2118/46786-MS>

Moeller, J., Nielsen, J. G., & Svinth, K. H. (2016). Arrangement to align a part of a wind turbine.

Moestrup, H., & Westergaard, J. (2014). Tower assembly system for wind turbines and method thereof.

MPI Offshore. (2011a). MPI ENTERPRISE specification sheet. Retrieved February 10, 2017, from <http://www.mpi-offshore.com/>

MPI Offshore. (2011b). MPI Resolution specification sheet.

MPI Offshore. (2017). MPI offshore fleet. Retrieved February 2, 2017, from <http://www.mpi-offshore.com/>

Müller, R., Hörauf, L., Vette, M., Martin, J. L. S., Alzaga, A., Hohmann, J., ... Würdemann, H. (2014). Robot guided bolt tensioning tool with adaptive process control for the automated assembly of wind turbine rotor blade bearings. *Production Engineering*, 8(6), 755–764. <https://doi.org/10.1007/s11740-014-0557-8>

Musial, W., Butterfield, S., & Boone, A. (2004). Feasibility of Floating Platform Systems for Wind

Turbines. In *23rd ASME Wind Energy Symposium*. Retrieved from <http://www.nrel.gov/docs/fy04osti/34874.pdf>

Musial, W., Butterfield, S., & Ram, B. (2006). Energy From Offshore Wind. In *Offshore Technology Conference*. Offshore Technology Conference. <https://doi.org/10.4043/18355-MS>

Myhr, A., Bjerkseter, C., Ågotnes, A., & Nygaard, T. A. (2014). Levelised cost of energy for offshore floating wind turbines in a life cycle perspective. *Renewable Energy*, 66, 714–728. <https://doi.org/10.1016/j.renene.2014.01.017>

National Renewable Energy Laboratory. (2011). *New Modeling Tool Analyzes Floating Platform Concepts for Offshore Wind Turbines*. NREL/FS-5000-50856. Golden.

Nielsen, O. J. W. (2016). Reducing weather downtime in offshore wind turbine installation. Retrieved April 3, 2017, from <http://www.highwindchallenge.com/2016/06/13/reducing-weather-downtime-in-offshore-wind-turbine-installation/>

offshoreWIND.biz. (2014). Two rotor stars installed at Global Tech I. *10/03/2014*. Retrieved from <http://www.offshorewind.biz/2014/03/10/two-rotor-stars-installed-at-global-tech-i/>

offshoreWIND.biz. (2015). Royal HaskoningDHV Team Studies OW Financing Side. *06/07/2015*. Retrieved from <http://www.offshorewind.biz/2015/07/06/royal-haskoningdhv-team-studies-ow-financing-side/>

Øllgaard, B. (2014a). Method and device for aligning tower sections.

Øllgaard, B. (2014b). Tower section and a method for a tower section.

Olson & Steel co. (2017). ConX® Chassis Based Modular™ Building System. Retrieved March 17, 2017, from <http://www.olsonsteel.com/section.asp?pageid=28044>

Peng, K. C. C., & Singhose, W. (2009). Crane control using machine vision and wand following. In *IEEE 2009 International Conference on Mechatronics, ICM 2009*. IEEE. <https://doi.org/10.1109/ICMECH.2009.4957227>

- Pepperl+Fuchs. (2016). *Perfection by Precision - Sensors for Wind Energy Applications*.
- Petcu, C. (2009). *EOSIM – simulation tool for the assembly of offshore wind parks considering the weather conditions offshore wind turbines*. Retrieved from <http://www.anast.ulg.ac.be/index.php/en/search/software-developed/eosim>
- Pohekar, S. D., & Ramachandran, M. (2004). Application of multi-criteria decision making to sustainable energy planning - A review. *Renewable and Sustainable Energy Reviews*, 8(4), 365–381. <https://doi.org/10.1016/j.rser.2003.12.007>
- Polatidis, H., Haralambopoulos, D. A., Munda, G., & Vreeker, R. (2006). Selecting an Appropriate Multi-Criteria Decision Analysis Technique for Renewable Energy Planning. *Energy Sources, Part B: Economics, Planning, and Policy*, 1(2), 181–193. <https://doi.org/10.1080/009083190881607>
- Principle Power. (2011). *Principle Power's WindFloat Concept Animation*. Retrieved from <https://www.youtube.com/watch?v=IO7GXMLR4YUo>
- PTI. (2016). New Crane VR Unveiled. Retrieved March 16, 2017, from https://www.porttechnology.org/news/new_crane_vr_unveiled
- RCT. (2012). Remote Control Technologies (RCT) GuidanceSystem testing - Dorothy drives. Retrieved January 23, 2017, from <https://www.youtube.com/watch?v=DDhxZ35ndg0>
- renewableUK. (2013). *Guidelines for the Selection and Operation of Jack-ups in the Marine Renewable Energy Industry*.
- RenewableUK. (2015). Wind Energy in the UK, (October), 1–43. Retrieved from <http://www.renewableuk.com/en/publications/guides.cfm>
- Rolls Royce Marine AS. (2011). Rolls-Royce deck machinery, 2011.
- Roy, B. (1968). Classement et choix en présence de critères multiples (le méthode ELECTRE). *RIRO*, 8, 57–75.

- Ruff, T. M. (1992). *Development and Testing of a Computer-Assisted Remote-Control System for the Compact Loader-Tramper*.
- Saaty, T. L. (1980). *The Analytic Hierarchy Process*. Retrieved from http://www.dii.unisi.it/~mocenni/Note_AHP.pdf
- Sarkar, A. (2013). A TOPSIS method to evaluate the technologies. *International Journal of Quality & Reliability Management*, 31(1), 2–13. <https://doi.org/10.1108/IJQRM-03-2013-0042>
- Schaumann, P., & Eichstädt, R. (2015). Fatigue Assessment of High-Strength Bolts with Very Large Diameters in Substructures for Offshore Wind Turbines, 880653.
- SCHEUERLE Fahrzeugfabrik. (2012). Transport solutions for Offshore Wind Power Plants. Retrieved November 24, 2016, from <https://www.youtube.com/watch?v=oHXN9qq-S6Y>
- Scottish Enterprise. (2004). *Innovation in Offshore Wind installation, operation & maintenance*.
- Sharpley, N. (2016). How is a nacelle manufactured? Retrieved March 21, 2017, from <http://www.windpowerengineering.com/design/mechanical/nacelle/how-is-a-nacelle-manufactured/>
- SICK IVP. (2006). Machine Vision Introduction. *Industrial Sensors*, 12–27. Retrieved from http://www.sick.com/uk/en-uk/home/products/product_portfolio/Documents/Machine_Vision_Introduction2_2_web.pdf
- Siemens. (2015). Optimized concepts for loading & installing Offshore wind turbines, 1–19. Retrieved from <https://www.slideshare.net/IQPCGermany/siemens-optimized-concepts-for-loading-installing-offshore-wind-turbines>
- SKI. (2017). Ring flange connections - SKI. Retrieved March 15, 2017, from <http://www.ski-consult.de/1/verbindungstechnik/ringflanschverbindungen.html>
- Spence, R., & Russell, J. (2013). Tower section alignment apparatus and system.
- Statutory Instruments. (1998). *The Lifting Operations and Lifting Equipment Regulations 1998*.

Stiesdal, H. (2011). Wind Turbine Installation.

Sydenham, M. W., & Brown, T. (2015). Robotic Installation of OSI-Bolts.
<https://doi.org/10.4271/2015-01-2512>. Copyright

Szulecki, K., Fischer, S., Gullberg, A. T., & Sartor, O. (2016). Shaping the “Energy Union”: between national positions and governance innovation in EU energy and climate policy. *Climate Policy*, 16(5), 548–567. <https://doi.org/10.1080/14693062.2015.1135100>

Technical Design Guide for FRP Composite Products And Parts. (2017), 25. Retrieved from <http://www.moldedfiberglass.com/>

The Crown Estate. (2010). *A Guide to an Offshore Wind Farm*. Retrieved from http://www.thecrownestate.co.uk/guide_to_offshore_windfarm.pdf

theconstructionindex. (2017). Blyth debut for BAM gravity base foundations. 06/04/2017.

Trabish, H. K. (2016, October). Wind in the sails - Capitalizing on Asia's offshore power boom. *Breakbulk Magazine*, 44–51. Retrieved from <http://www.breakbulk.com/capitalizing-asias-offshore-power-boom/>

Triantaphyllou, E., & Mann, S. H. (1989). An Examination of the Effectiveness of Multi-Dimensional Decision Making Methods: A Decision Making Paradox. *Decision Support Systems*, 5(3), 303–312.

Triantaphyllou, E., Shu, B., Nieto Sanchez, S., & Ray, T. (1998). Multi-criteria decision making: an operations research approach. *Encyclopedia of Electrical and Electronics Engineering*, 15, 175–186. Retrieved from <http://univ.nazemi.ir/mcdm/Multi-Criteria Decision Making.pdf>

Tribology-ABC. (n.d.). Tightening torque to preload a bolt. Retrieved from http://www.tribology-abc.com/calculators/e3_6a.htm

Ulstein Offshore Wind Team. (2017). Getting the best from oil and gas to offshore renewables. Retrieved January 20, 2017, from <https://wind.ulstein.com/getting-the-best-from-oil-and-gas->

- Uraz, E. (2011). *Offshore Wind Turbine Transportation & Installation Analyses: Planning Optimal Marine Operations for Offshore wind turbines. Master Thesis*. Gotland University. Retrieved from <http://www.diva-portal.se/smash/get/diva2:691575/FULLTEXT01.pdf>
- Vattenfall. (2005). ThaneT OffshOre Wind farm. *Offshore (Conroe, TX)*, (November).
- Vattenfall. (2014). Thanet.
- Vestas. (2004). General Specification V90 - 3.0 MW. *Aviation*, (950010), 1–31. <https://doi.org/10.1007/s10661-011-2038-2>
- Vestas Wind Systems A/S. (2017). *Vestas V90 3.0MW Brochure*. Retrieved from <http://nozebra.ipapercms.dk/Vestas/Communication/Productbrochure/V9030MW/V9030MWUK/>
- Vis, I. F. A., & Ursavas, E. (2016). Assessment approaches to logistics for offshore wind energy installation. *Sustainable Energy Technologies and Assessments*, 14, 80–91. <https://doi.org/10.1016/j.seta.2016.02.001>
- Voormolen, J. A., Junginger, H. M., & van Sark, W. G. J. H. M. (2016). Unravelling historical cost developments of offshore wind energy in Europe. *Energy Policy*, 88, 435–444. <https://doi.org/10.1016/j.enpol.2015.10.047>
- Vuyk Engineering Rotterdam b.v. (2017). Floating Wind Turbine Installation Vessel. Retrieved from <http://www.vuykrotterdam.com/product-sheets-specials/>
- Wang, J. J., Jing, Y. Y., Zhang, C. F., & Zhao, J. H. (2009). Review on multi-criteria decision analysis aid in sustainable energy decision-making. *Renewable and Sustainable Energy Reviews*, 13(9), 2263–2278. <https://doi.org/10.1016/j.rser.2009.06.021>
- Wang, M., Liu, S., Wang, S., & Lai, K. K. (2010). A weighted product method for bidding strategies in multi-attribute auctions. *Journal of Systems Science and Complexity*, 23(1), 194–208.

<https://doi.org/10.1007/s11424-010-9337-5>

Webster, A. (2013). GE uses climbing robots to insect wind turbine blades. Retrieved March 20, 2017, from <http://www.theverge.com/2012/6/13/3083141/ge-wind-turbine-robot>

Wilson, A. (2012). Smart Cranes Ease Load Positioning. *Vision Systems Deisgn*. Retrieved from <http://www.vision-systems.com/articles/print/volume-17/issue-7/features/smart-cranes-ease-load-positioning.html>

Wind Power Engineering & Development. (2016). Wind Power Software. Retrieved January 15, 2017, from <http://www.windpowerengineering.com/design/wind-power-software/page/2/>

Windcarrier, F. O. (2016). *Block Island Offshore Wind Farm*. www.youtube.com. Retrieved from <https://www.youtube.com/watch?v=p29MnJL4IIQ>

Zhang, C., & Hammad, A. (2012). Improving lifting motion planning and re-planning of cranes with consideration for safety and efficiency. *Advanced Engineering Informatics*, 26(2), 396–410. <https://doi.org/10.1016/j.aei.2012.01.003>

Zhang, P., Han, Y., Ding, H., & Zhang, S. (2015). Field experiments on wet tows of an integrated transportation and installation vessel with two bucket foundations for offshore wind turbines. *Ocean Engineering*, 108, 769–777. <https://doi.org/10.1016/j.oceaneng.2015.09.001>

APPENDICES

Appendix A Project Management and Planning

The key to a successful project work is thorough project management and forward planning from the very start. Thus, in the early stage of this project, a management plan was developed, a risk assessment was performed, and a communication plan was set up. These are presented in the following and compared to the real course of the project.

A.1 Project Management Plan

The project management plan includes a schedule for the different stages within the project, the division of labour into several work packages, as well as the project team members and their roles and tasks.

A.1.1 Time Schedule

The main time for the group project was from January 2017 until end of March 2017, almost three months, while the preparations and setup of the project had been carried out in December 2016.

The project can be divided into three main stages and some additional elements, running in parallel. In stage 1, firstly (a), literature reviews covering human-free lifting operation solutions should be done and ideas for concepts collected in brainstorming sessions. Stage 1 closes (b) with the analysis of the proposed solutions and the final selection of those concepts, which should be further elaborated in detail. For those decisions, the results of the incident report analysis are required as input. Stage 1 should be completed until end of January so that stage 2 could start in February. This covers the detailed analysis of the selected concepts, in which the feasibility and the application of the solutions should be examined. This task may last until beginning of March and is followed by stage 3, the multi-criteria analysis. This final analysis is realised in March, however, the preparatory work of setting up a survey, carrying out the survey, and evaluating the survey should be done in January and February. In parallel to all those stages, writing up of the different group project topics and categories has to be done. The general chapters about introduction to lifting operations and review of existing guidelines can already be written up at the

beginning of the group project. The results of each stage should be written during the stage and completed by the end of the stage. Having all results collected and analyses performed, the final conclusions can be collated by the end of March. This planned time schedule for the group project is shown in Figure A-1.

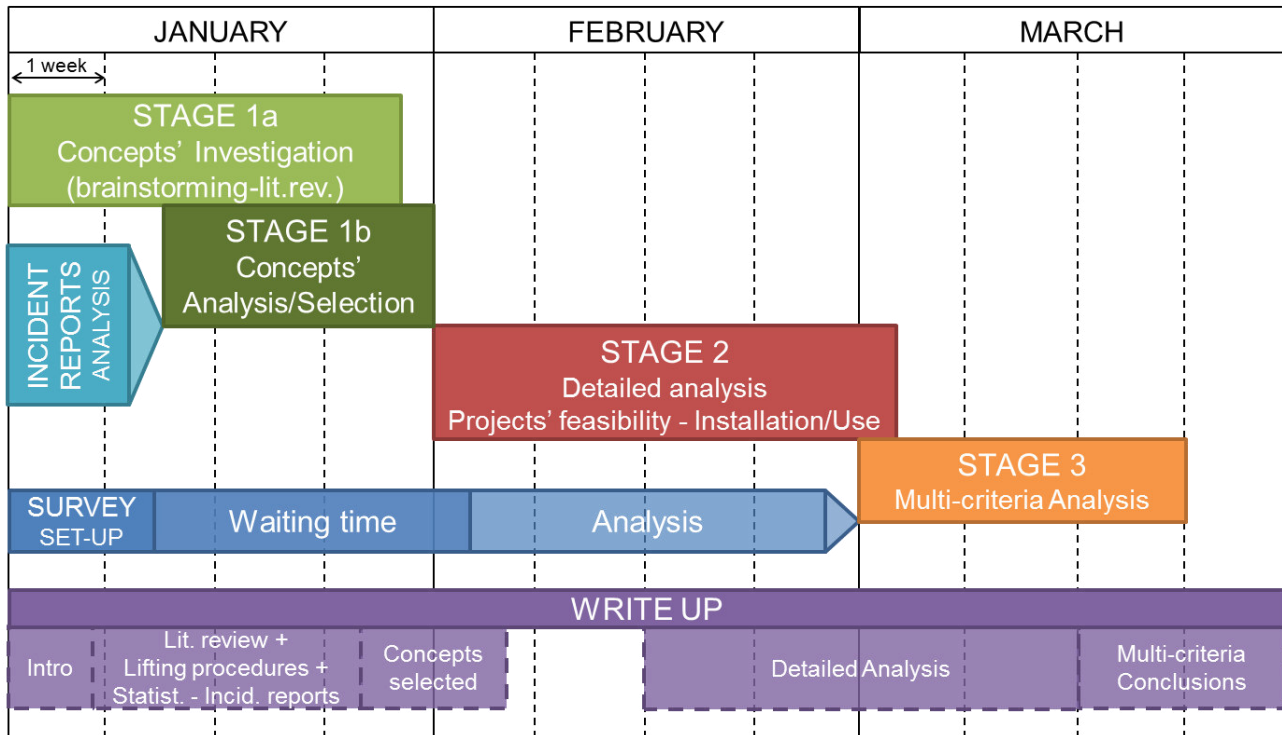


Figure A-1 Gantt chart for group project

At the time of setting up this Gantt chart, the final deadline for the group project was not yet known. But still, our planning was quite close, as the final presentation was set to end of March and the report submission in the first week of April. The plan remained as we had to have all the results ready by the presentation. We did, however, had some more time for writing up afterwards. By the end of January we had, for each concept category, selected solutions for stage 2. Furthermore, the incident reports had been analysed and evaluated and the survey for the multi-criteria analysis was already set up, ready to be sent out. The analysis was prepared whilst awaiting the survey responses and the survey was closed at the end of February. Stage 2 was extended and lasted until the week before the presentation. The main reason for this was external workload, but also the depth in which we carried out the detailed analysis. Furthermore, we realised the issue of timing when having more people from different sides involved, as it was for receiving the incident

reports, carrying out the survey, and preparing and performing some experimental tests. But still, with having stage 2 finished later than planned, there was still enough time for the final multi-criteria analysis, as this could already be prepared during stage 2. Finally, as already mentioned before, the deadline for the report submission in the first week of April allowed us a less stressful write-up and completion of the report.

A.1.2 Work Packages and Distribution

The individual tasks were defined based on the outline of our guideline report. Thus, every group member received one general topic, such as introduction, existing guidelines, effects of human-free operations, and conclusions. These could all, except the latter, be completed in the early stage of the group project in January. In addition to those general parts, we grouped the concepts for human-free lifting solutions into three categories, meaning that a group of two was working on each concept. This task, as well as everyone's writing up, extended during the entire project time. These work packages, together with the responsible people and the corresponding time schedule are presented in Figure A-2.

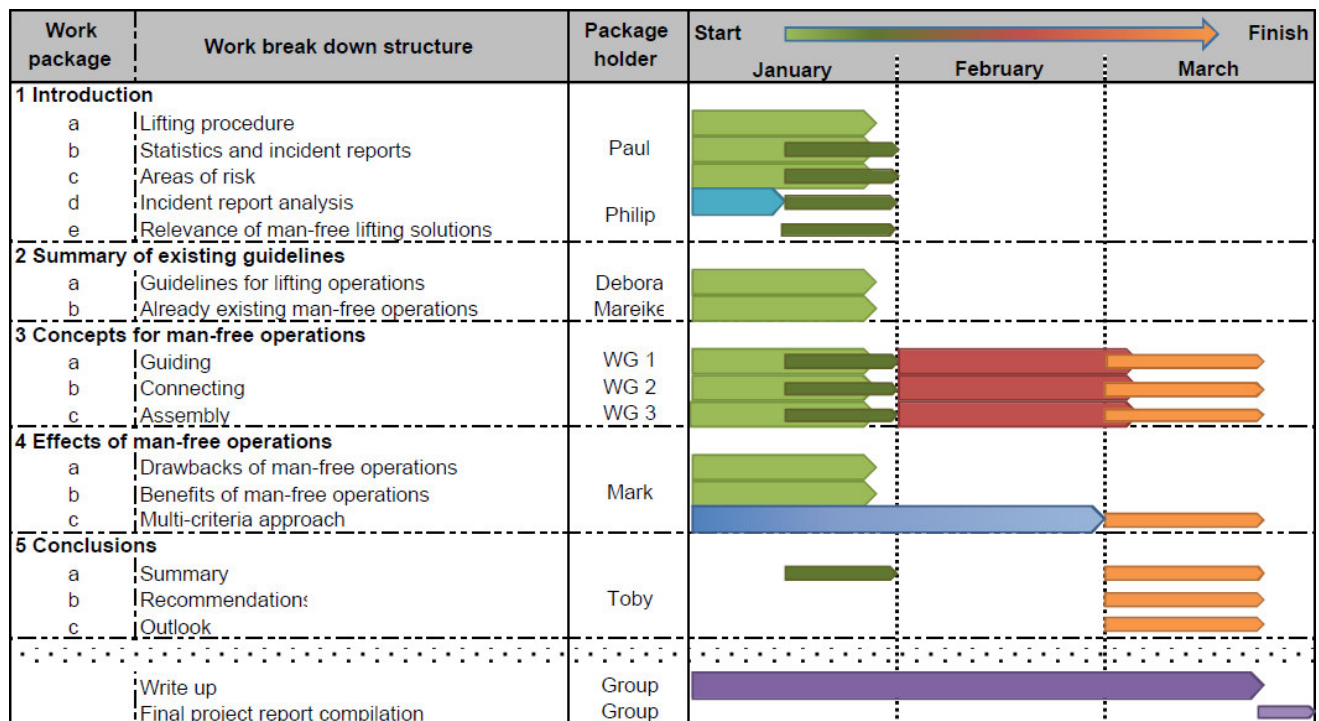


Figure A-2 Work packages, responsibilities, and time schedule

The people involved, as well as the composition of the three working groups, are shown in Figure A-3.

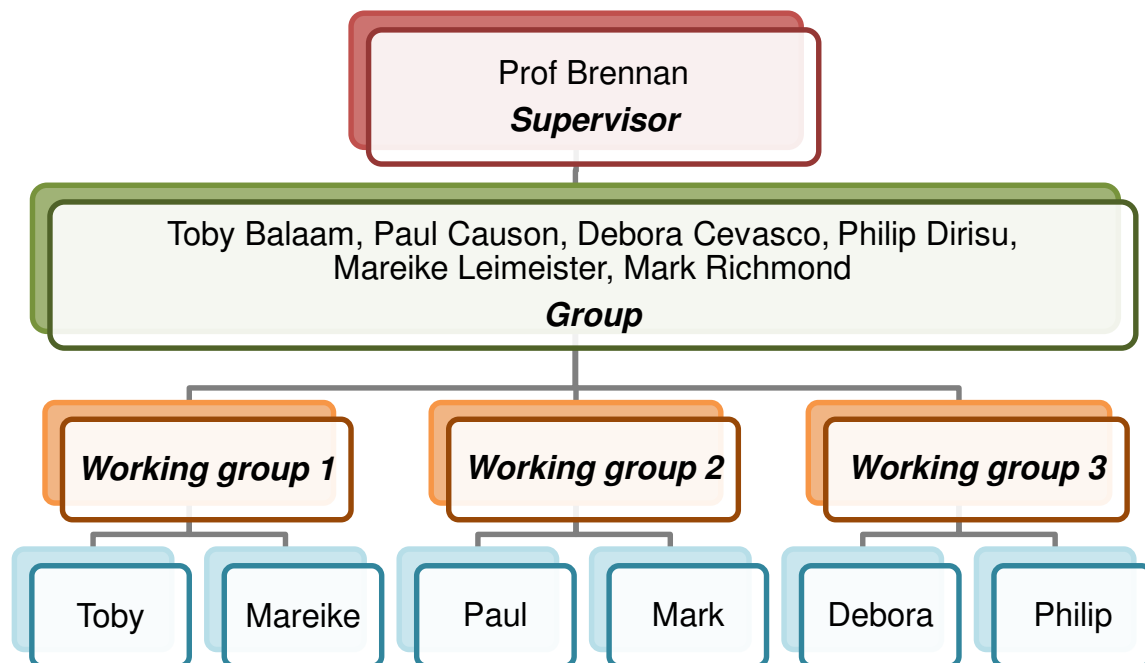


Figure A-3 Involved people and working groups

This initial definition of the work packages and responsibilities was almost wholly maintained. There was just a slight change in the structure of the introduction, as we realised that Paul has already covered the relevance of human-free offshore lifting solutions in his analysis of the incident reports. So we changed Paul's part into the relevance of human-free offshore lifting solutions, covering all work on the incident reports, as well as the overview of this guideline at the end of the introduction, and gave Philip the explanation of the lifting procedures in general at the beginning of the introduction. Furthermore, the summary of existing guidelines was no longer divided between two people, but now assigned entirely to Mareike. Finally, we decided that Mark and Toby work together on the multi-criteria decision analysis, and Philip assists both with the last chapter, so that not only one individual has to write up the conclusions alone at the final end of the project period. The other parts all remained as they had been planned and this was also very helpful, as it gave us a clear structure for our work and an overview of the extend of the work.

For the sake of clarity, especially regarding the assessment of the individual work and contribution to the group project, the outline of this document is reported in the following again, with having the names of the responsible group members added to each (sub)section. Furthermore, Table A-1 summarises the page numbers to which each individual has contributed.

ABSTRACT	Mareike Leimeister
ACKNOWLEDGEMENTS	Mareike Leimeister
1 INTRODUCTION	
1.1 Lifting Procedure	Philip Dirisu
1.2 Relevance of Human-Free Lifting Solutions	Paul Causon
1.3 Guideline for Human-Free Offshore Lifting Operations	Paul Causon
2 SUMMARY OF EXISTING GUIDELINES	Mareike Leimeister
3 CONCEPTS FOR HUMAN-FREE OFFSHORE LIFTING OPERATIONS	Mareike Leimeister
3.1 Concepts for Guidance and Control	Mareike Leimeister
3.1.1 Introduction	Mareike Leimeister
3.1.2 Initial Proposed Solutions	
3.1.2.1 Mechanical Guidance	Mareike Leimeister
3.1.2.2 Visual Guidance	Toby Balaam
3.1.2.3 Sensorial Guidance	Toby Balaam
3.1.2.4 Automated Guidance	Mareike Leimeister
3.1.2.5 Fine Tuning Control	Toby Balaam
3.1.3 Selection of Most Promising Solutions	Toby Balaam
3.1.4 Development of Solutions in Detail	
3.1.4.1 Global Hoisting	Toby Balaam
3.1.4.2 Fine Hoisting	
3.1.4.2.1 Visual Guidance	Toby Balaam
3.1.4.2.2 Mechanical Guidance	Mareike Leimeister
3.1.4.2.2.1 Initial Design Including Mechanical Guiding Elements	Mareike Leimeister
3.1.4.2.2.2 Revised Design Including Mechanical Guiding Elements	Mareike Leimeister
3.1.4.2.2.3 Simplified Design for Experimental Tests (C1)	Mareike Leimeister
3.1.4.2.2.4 Detailed Full-Scale Design for Real Wind Turbines	Toby Balaam
3.1.5 Conclusion and Recommendations	Mareike Leimeister
3.2 Concepts for Connections and Seafastening	Mark Richmond
3.3 Concepts for Assembly	
3.3.1 Introduction	Debora Cevasco & Philip Dirisu
3.3.2 Initial Proposed Solutions	Debora Cevasco
3.3.3 Selection of Most Promising Solutions	Debora Cevasco
3.3.4 Development of Solutions in Detail	
3.3.4.1 Optimising Current Pre-Assembly Practice	Debora Cevasco
3.3.4.2 Novel Assembly Concepts	Philip Dirisu

4 MULTI-CRITERIA DECISION ANALYSIS	Toby Balaam
4.1 Decision Context: Aims, Stakeholders and Key Players	Toby Balaam
4.2 Criteria	Toby Balaam
4.3 Survey	Toby Balaam
4.4 Evaluation of Criteria Satisfaction	Mark Richmond
4.5 Methods	Mark Richmond
4.6 TOPSIS	Mark Richmond
4.7 Methodology	Mark Richmond
4.8 Results and Discussion	Mark Richmond
4.9 Conclusions	Mark Richmond
5 CONCLUSIONS	
5.1 Summary of Report	Toby Balaam
5.2 Drawbacks of Human-Free Operations	Philip Dirisu
5.3 Benefits of Human-Free Operations	Philip Dirisu
5.4 Recommendations	Mark Richmond
5.5 Outlook and Future Work	Mark Richmond
APPENDICES	
Appendix A Project Management and Planning	Mareike Leimeister
Appendix B Experimental Results	Toby Balaam
Appendix C Mechanical Guidance	
C.1 3D-Printed Initial Design	Mareike Leimeister
C.2 3D-Printed Revised Design	Mareike Leimeister
C.3 Simplified Design for Experimental Tests	Mareike Leimeister
C.4 Full-Scale Design	Toby Balaam
C.4.1 Calculating Loads	Toby Balaam
C.4.2 CAD Drawing of Full-Scale Design	Mareike Leimeister
C.4.3 FEA Analysis	Toby Balaam
C.5 Mechanical Guiding Systems in Comparison	Mareike Leimeister
Appendix D Program Code for the Optimisation of the Assembly	Debora Cevasco
Appendix E MCDA Appendix	Mark Richmond

Table A-1 Contribution of each group member to report, indicated by means of page numbers

Group member	Page numbers
Toby Balaam	35-38, 40-62, 71, 135-140, 155, 156, B-17-B-23, C-43-C-48, C-50-C-54
Paul Causon	10-19
Debora Cevasco	93-121, D-56-D-103
Philip Dirisu	1-9, 93-96, 121-133, 156, 157
Mareike Leimeister	i, iii, 20-27, 29-35, 39-40, 62-75, A-1-A-16, C-24-C-42, C-49, C-55
Mark Richmond	76-92, 140-154, 157, 158, E-104-E-109

A.2 Project Risk Assessment

Very essential in a meaningful project management plan is the risk assessment. Not only the identification of potential risks should be included, but also mitigation strategies should be mapped out to be prepared in the case of something happening during the project period.

The risk assessment was performed based on the risk matrix shown in Figure A-4. Thus, the risk was defined by two factors: the occurrence and the impact. The occurrence (O) describes the likeliness of the event happening. The impact (I) is defined in terms of lost work days. Based on the different categories, listed in Figure A-4, numbers between 1 and 5 were assigned to the occurrence and impact of each identified risk event, and the exposure (E) was then computed by multiplying those two numbers. The events themselves were grouped into four problem areas: data, human, ideas, and communication.

			OCCURRENCE (O)				
			Very unlikely	Unlikely	Possible	Likely	Certain
			1	2	3	4	5
IMPACT (I) Lost work day	Few days	1	1	2	3	4	5
	~ 1 week	2	2	4	6	8	10
	> 1 week	3	3	6	9	12	15
	~ 1 month	4	4	8	12	16	20
	> 1 month	5	5	10	15	20	25

Figure A-4 Risk Matrix

A.2.1 Problem Area: Data

The risk assessment of the problem area data is presented in Figure A-5. It has to be pointed out that a delay in the provided data or even missing data was expected to be the event with the highest risk.

RISK	DESCRIPTION	O	CAUSES	TIME	I	E	MITIGATION STRATEGY	CONTINGENCY PLAN
Storage	Loss of data	3	Y-drive failure	Jan-Mar	5	15	Back-ups of individual work	Weekly back-ups in Cranfield, Oxford, Germany
Delay/ Missing	Incident reports	4	Confidentiality problems	Jan-Feb	5	20	Remind G+ contacts	Company workers' survey (qualitative) - within Jan
							Use only G+ statistics (public data)	
	Expert survey (for MC analysis)						Remind DONG contacts	Send survey to other companies and academical experts - within Jan
							Fill in survey ourselves - within Feb	
Knowledge	Lack of understanding	4	New concepts	Jan-Feb	1	4	Ask DONG for workshop with Siemens or Vestas	Contact other companies or academical experts
			Company policy					
			Confidential data					

Figure A-5 Risks in the problem area data

Based on our experience during the group project, we realised that the dependency on others for receiving information and data was quite critical, but in the end we were really lucky and received most of all required data and had a high response from our survey. However, the university drive turned out to be more a problem, not in terms of losing data, but in terms of accessing it. Sometimes the drive was not available and we had to send our working files via email. By the end of the project period we could still access the drive but were not able to upload anything. This was a significant restriction, as especially at the end of the group project we had to share a lot of files for organising the writing up and set up of the final presentation. Still we managed this issue, as we used email for sharing the information, however, it was quite annoying and more time consuming.

A.2.2 Problem Area: Human

The risk assessment of the problem area human is presented in Figure A-6. The risk events scored in general less than in the category data, but still additional work load and delivery of the individual tasks not on time were some relevant points.

RISK	DESCRIPTION	O	CAUSES	TIME	I	E	MITIGATION STRATEGY	CONTINGENCY PLAN
Health	Illness or injuries (≥ 1 week)	3	Unknown	Jan-Mar	3	9	Watch your health!	Inform group asap Re-arrange responsibilities (if it lasts longer)
Time	Additional work load (other commitments)	4	Other projects' priority	Jan-Mar	3	12	Two people for each main part: 1 main and 1 shadow person Plan ahead	Inform group asap Delegate to the shadow person (for limited time period) Re-arrange responsibilities (if it lasts longer)
Delay	Delivery not on time	4	Personal/ Unknown	Jan-Mar	3	12	Be aware of your obligations Plan ahead	Inform group asap Delegate to the shadow person (for limited time period) Add resources

Figure A-6 Risks in the problem area human

As expected, the punctual delivery was one critical issue. Luckily, we had no late deliveries although some were quite critically timed. For example, the presentation slides had to be changed shortly before the presentation time slot, as still some comments were sent on the day of the presentation. Furthermore, we also set internal deadlines for the deliverables, which were some days before the official deadline and thus gave us some time buffer for merging the individual parts, making some corrections, and applying final changes.

Another big issue was the additional work load we all had, due to other submission deadlines, tasks, appointments, and individual research work. However, our structure of having individual work packages for the general topics and groups of two for the concepts allowed us to organise our time quite flexible dependent on our availabilities. In the main working periods, the individual working groups managed their process themselves and we only had to schedule a meeting all together at intervals of about three weeks for exchange about the current status and discussions about the further procedure. In the meantime we exchanged all essential information via email, which everyone could read and answer at a time that worked for each individual.

A.2.3 Problem Area: Ideas

The risk assessment of the problem area ideas is presented in Figure A-7. We were most worried about having not feasible concepts after stage 1, so that we would not have a basis to work on further in stages 2 and 3.

RISK	DESCRIPTION	O	CAUSES	TIME	I	E	MITIGATION STRATEGY	CONTINGENCY PLAN
Amount	Too much spread	3	Too many ideas collected in first brainstorming	Jan	2	6	Focus on stage 1b	Report actual state of discarded ideas after stage 1b Select a few concepts for stages 2 and 3
Feasibility	Concepts not feasible	5	Insufficient investigations Concepts not practicable	Feb-Mar	4	20	Focus on stage 1a	Report all findings Try to find new ideas Further elaborate existing technologies

Figure A-7 Risks in the problem area ideas

Those fears were not confirmed, as we had collected a lot of ideas in stage 1, so that we still found some feasible concepts to work further on with in the other stages. However, it was more difficult to limit the extension to detailed analysis of those ideas. But we decided, due to time reasons and the fixed schedule for the final presentation and project report submission, that we would work out our concepts up to a certain level of detail and then just mention our further ideas for more detailed elaborations of our proposed solutions.

A.2.4 Problem Area: Communication

The risk assessment of the problem area communication is presented in Figure A-8. The problem of having misunderstandings and lacking clarity in communication was ranked quite high, while IT issues were expected less critical than poor communication in group meetings.

RISK	DESCRIPTION	O	CAUSES	TIME	I	E	MITIGATION STRATEGY	CONTINGENCY PLAN
Meeting	Poor communication	3	Unjustified absences	Jan-Mar	4	12	Schedule regular meetings (latest every second week) Define agenda for next meeting at end of each meeting	Minutes of each meeting, available to all group members in the shared folder, to catch up with the progress and work done
Clarity	Misunderstandings	5	Not 1st language Fail of communication resources	Jan-Mar	3	15	Repeat topic in own words Summaries at beginning (actual status) and end (further work) of meetings	
IT issues	Bad/No internet connection	3	Group members at different locations	Jan-Mar	3	9	List with contact details for flexibility	

Figure A-8 Risks in the problem area communication

It turned out to be slightly different than assessed at the beginning. The group meetings were mostly well structured and very effective, maybe due to our separation into single working groups. However, misunderstandings appeared despite carrying out our formulated mitigation strategies. But still some definitions of tasks were not accurately understood, which in the end gave us some more additional work. Problems with the internet connection also turned out to have a higher rate of occurrence, as sometimes the internet signal and connection was quite bad, or the quality of the sound made talking and understanding in the meetings difficult. We tried to solve this with sharing the screens and sending summary emails, as well as the minutes after the meetings, so that this could be read at the time when the connection was working again.

A.3 Communication Plan

The communication plan is divided into the communication of the group with the contacts and supervisors at the industries (G+ and DONG energy), and the communication within the group.

A.3.1 Communication with the Industry

For the communication with the industry we appointed Mark (MR) as the main point of contact (PoC). For our project work, we required some input from both G+ and DONG energy, which were the incident reports, the survey for the multi-criteria decision analysis, and some additional technical information about the offshore lifting practices. Furthermore, we wanted to present and discuss our project status and objectives with the supervisors at the industries and our academic supervisor Prof Feargal Brennan. The detailed plan for the communication with the industry is shown in Figure A-9.



	OBJECTIVES	MEDIUM	FREQ.	AUDIENCE	OWNER	DELIVERABLE
	Incident Reports and/or Workers' Survey	Email	<i>Once (reminders)</i>	Group	Designated PoC (*MR)	Paper (confidentiality)
	Review project's objectives and approach	Email (Conference call)	<i>Monthly</i>	• Group • Prof Brennan	Group	Project status presentation
	Experts' Survey (for MCDA)	Email	<i>Once (reminders)</i>	Group	MR	Paper (confidentiality)
	Further technical information		<i>As needed</i>	Group	MR	-
	Review project's objectives and approach	Conference call	<i>Once</i>	• Group • Prof Brennan	Group	Project object. presentation

Figure A-9 Plan for the communication with the industry

The decision of nominating one point of contact, who then mainly communicates with the industrial supervisors, turned out to be a really helpful idea, as this simplified the communication. Mark shared the information he received from the companies with the group, we discussed all together further steps and questions to be asked, and Mark got in contact with the industry partners again. The supervisors at G+ (Kate Harvey, Bir Virk, and Andrew Sykes) and DONG energy (David Delamore, Peter Geddes, and Joe O'Toole) were really cooperative and gave us a lot of support in

our group project work. It was also really helpful to have a project status and objective presentation at the initial stage of the project work, as this simplified the first contact to the industry partners and also gave us some relevant feedback about different ideas of defining the scope of the project.

A.3.2 Group Meetings

For the internal communication within the group we decided to have weekly regular meeting for reviewing the status of the project and two weeks meeting together with the industry. Furthermore, we left the option for extraordinary meetings if particular reasons required additional meetings outside the time schedule. The detailed plan for the group meetings and communication within the group is presented in Figure A-10.

	OBJECTIVES	MEDIUM	FREQ.	AUDIENCE	OWNER	DELIVERABLE
Regular	Review status of the project with the group	<ul style="list-style-type: none"> • Face to face • Skype/ WebEx • Call 	<i>Weekly</i>	Group	Each group member (Chair/Minute-taker)	<ul style="list-style-type: none"> • Agenda • Individual work presentations • Minutes
Extra-ordinary	Solve particular issues and/or individual/group questions		<i>As needed</i>	<ul style="list-style-type: none"> • Group (• Prof Brennan) 	Group	<ul style="list-style-type: none"> • Agenda • Minutes
Project Status	Review status of the project with the industry	Conference call	<i>~ 2 weeks</i>	<ul style="list-style-type: none"> • Group • Prof Brennan • Industries' PoC 	Group	Project status presentation

Figure A-10 Plan for group meetings and internal communications

The schedule for the regular group meetings was slightly revised during the project period: we had more regular meetings within each working group, however, just approximately every three weeks a meeting with the entire group. More often full group meetings would not have been manageable due to individual work loads and availabilities. Furthermore, we only had a meeting with the industry at the beginning of the project and replaced the regular meetings with email threads. We also made use of the extraordinary meetings, when there was a particular question to be discussed directly or when plans just changed suddenly. In this case, having the opportunity to use Skype was really helpful.

A.4 Resources

In order to have an overview of the available resources, both personally and technologically, we gathered information at the initial stage of the group project.

A.4.1 Personnel

As already mentioned, we had some support from the industry: G+ and DONG energy. From G+ we wanted to receive incident reports, but also more detailed information about the lifting procedures and the incident data, which was not open to the public. Of course, we had to maintain confidentiality, but we got enough data to work with, which we could use as basis for our scope of the guideline report. The contacts to DONG energy were mainly relevant for obtaining technical information and experience and, as mentioned before, they were really willing to help us and provide us with as much as possible information. Both G+ and DONG energy were contacted regarding our survey for the multi-criteria decision analysis. They both shared the link comprehensively, hence we received plenty of feedback. We received further answers by sending the survey via our own contact we already had due to our studies or work experience.

Besides the industry we also had the support from the university. Prof Feargal Brennan was the main supervisor for the project work. He was mainly in the consultancy and advice role. In the initial planning we also thought that some other academic staff would be helpful for additional communication and requirements. And this was right. Especially Antony Charnley and Dr Supriyo Ganguly helped us quite a lot in organising our experimental tests. The detailed discussion about manufacturing and the fabrication itself were only possible with the help of Graham Hartwell and Derek Brown, and performing the tests only with the support by Flemming Nielsen and Nisar Shah. For the final structural analysis of our new design, Dr Ali Mehmanparast supported us with the load calculation and structural modeling. Furthermore, we made use of contacts to Oxford University for getting our guiding designs 3D-printed. In our multi-criteria decision analysis, Dr Athanasios Kolios gave us helpful advice. Finally, we received support by the IT service, as we already planned at the beginning of the group project work to use a shared folder in the Cranfield's intranet, which will also be mentioned in the next section about the technological resources.

A.4.2 Technological

As said before, we required a drive in the university intranet to share our data. This was set up at the beginning of the group project work. However, during the project period we had several issues with this drive, as it was either not accessible or data could not be uploaded to the drive. For safeguarding the data on the drive against loss, we planned to do regular back-ups on our personal laptops or USB sticks. This task was performed by everyone individually, but luckily we only had trouble with sharing data on the drive but not with losing data.

In our initial project planning we had considered that we would require some software. Those were PROMETHEE and ELECTRE for the multi-criteria decision analysis, CATIA and SOLIDWORKS as CAD software for presenting new possible designs and installation concepts, as well as Excel and MATLAB for design and basic calculations. In the end we used TOPSIS, written in MATLAB, for the multi-criteria decision analysis. The drawings for different assembly concepts were made in SOLIDWORKS, and our own design for guiding elements was constructed and drawn in Siemens NX 8.5, using access and licenses available at Fraunhofer IWES (Institute for Wind Energy and Energy System Technology, where Mareike is employed). The final load analysis was performed in Abaqus. Excel was indeed helpful for brainstorming and basic calculations, as well as the detailed load calculations for the full-scale design of the guiding elements. The setup of the program for determining the optimal solution for pre-assembly and installation methods was done in MATLAB/GUI. Finally, due to the experimental work on the mechanical and visual guiding elements, we also used four cameras of Swann DVR4-1525 four-channel security kit, as well as a 360-degree camera set, including a Samsung Gear 360 4k spherical camera with Gear VR and Samsung smartphone.

A.4.3 Financial

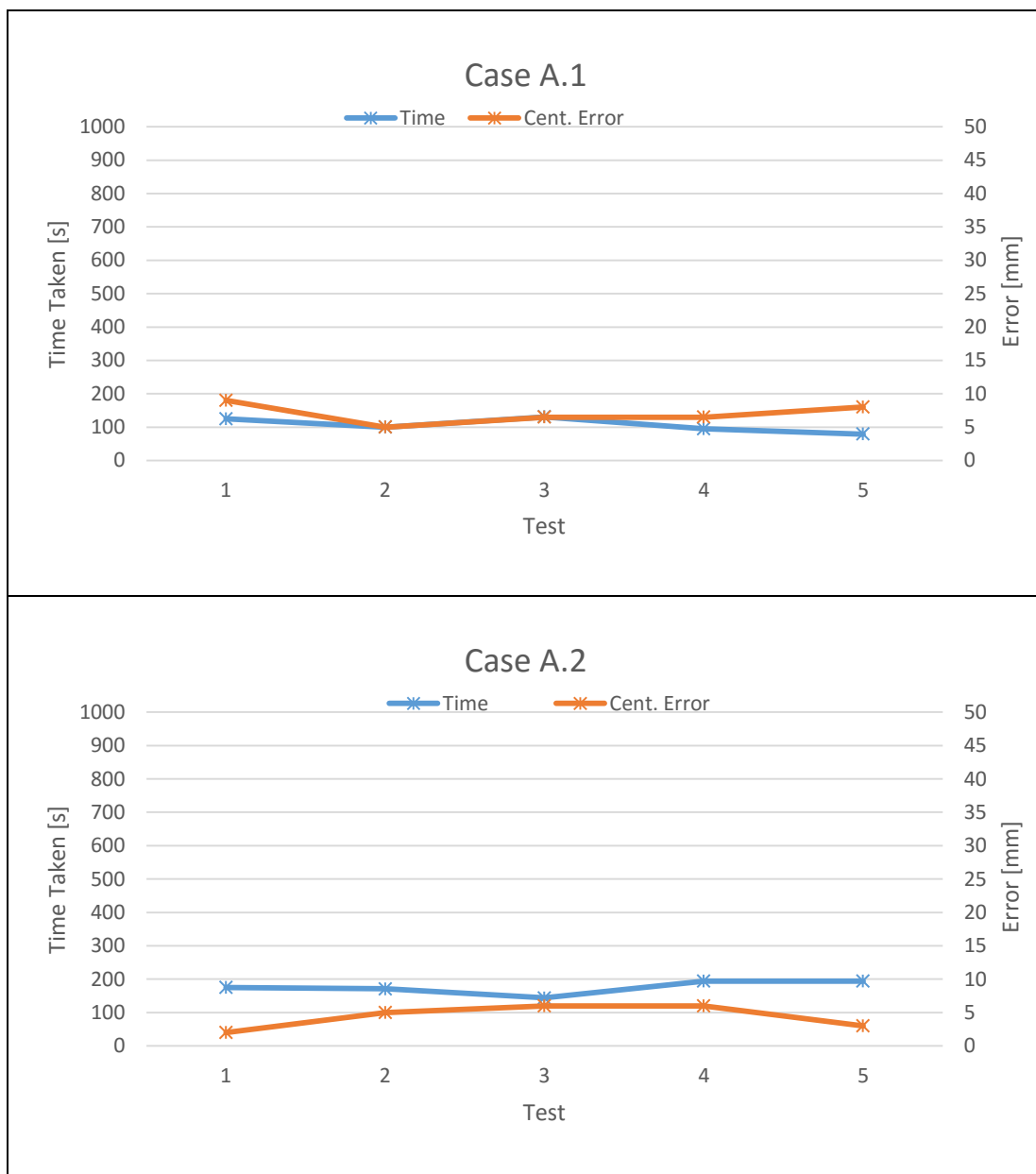
What was not included in the project management plan at the beginning, were financial resources, as, based on the first impression of the topic, the group project was judged to be rather theoretical than practical. However, during the brainstorming work, the group came up with their own ideas for guiding solutions, which could be tested. For those experiments security cameras by Swann were

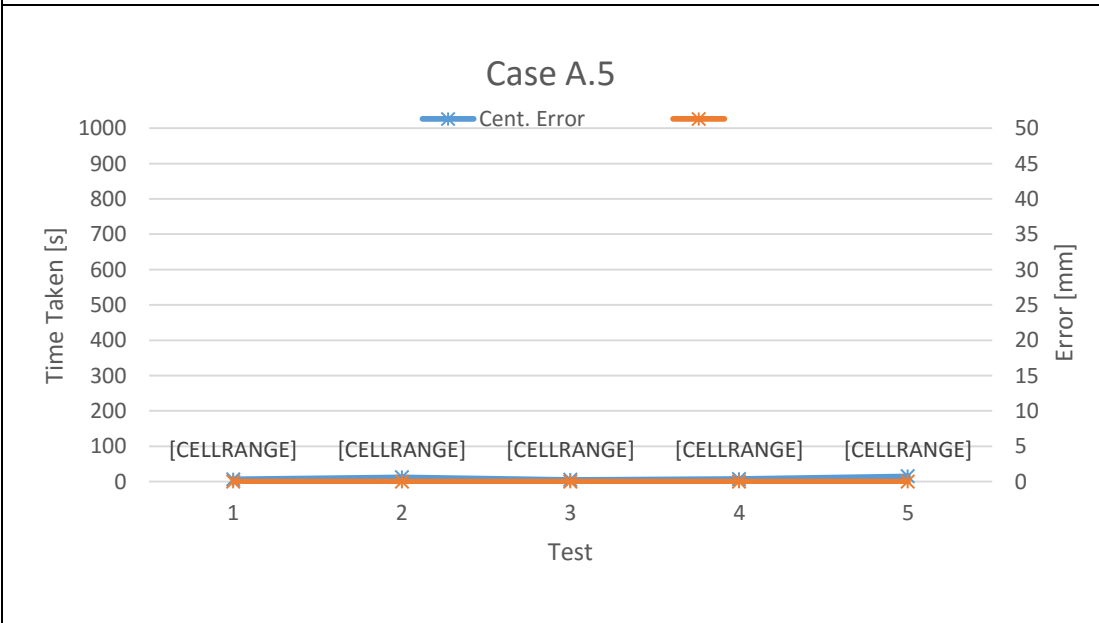
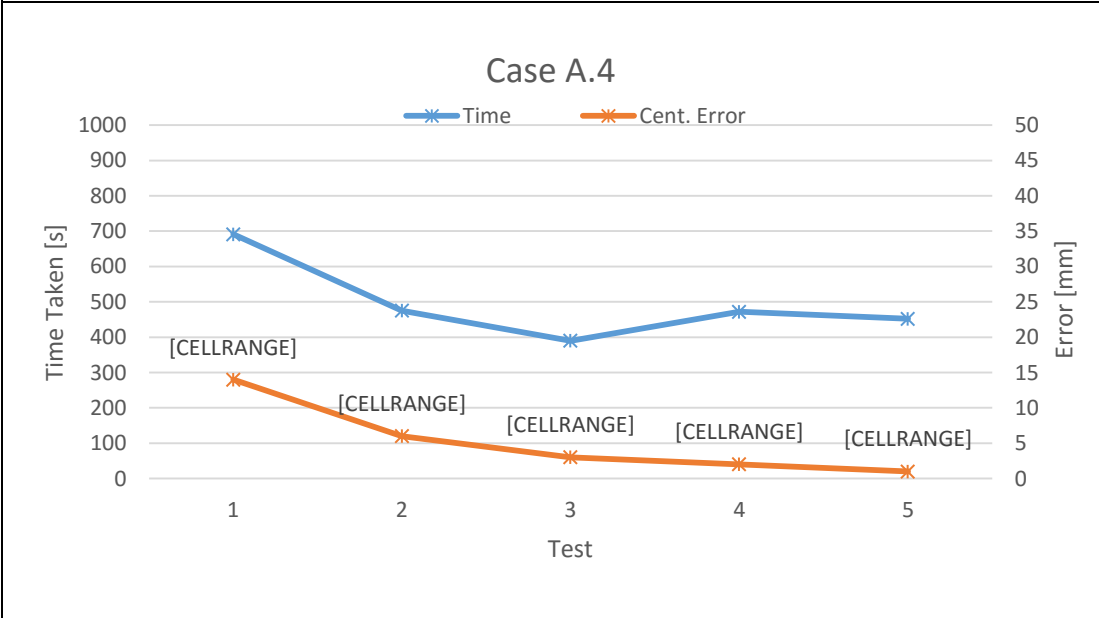
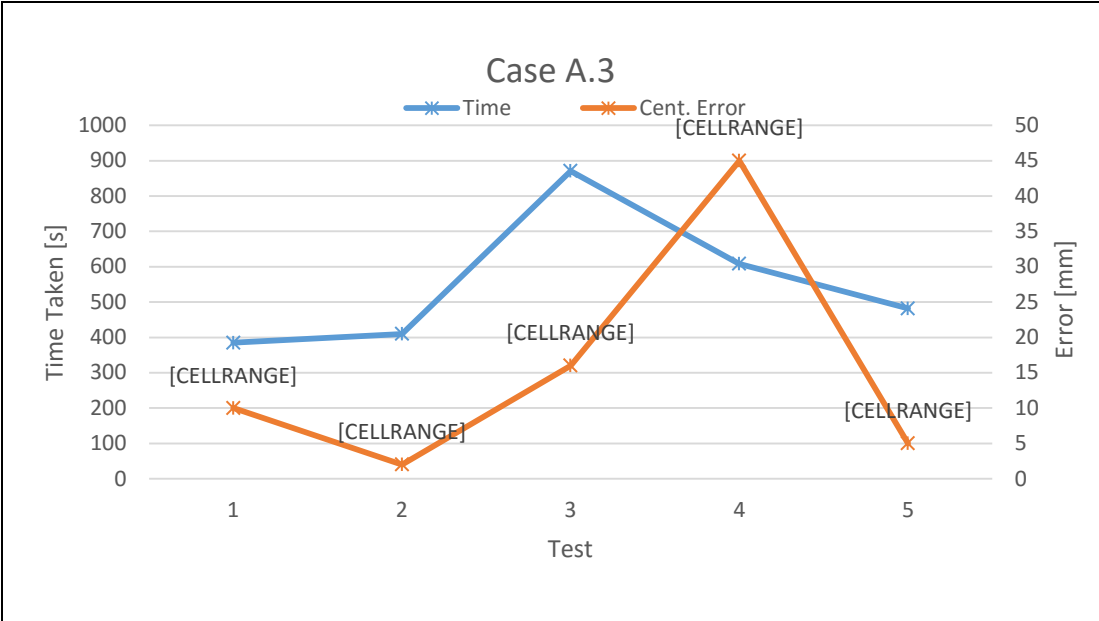
bought, the designed guiding elements were 3D-printed in small scale, and a similar simplified design of the mechanical guiding system was manufactured. Furthermore, we had traveling expenses refunded by REMS, as two of the group were not mainly based at Cranfield.

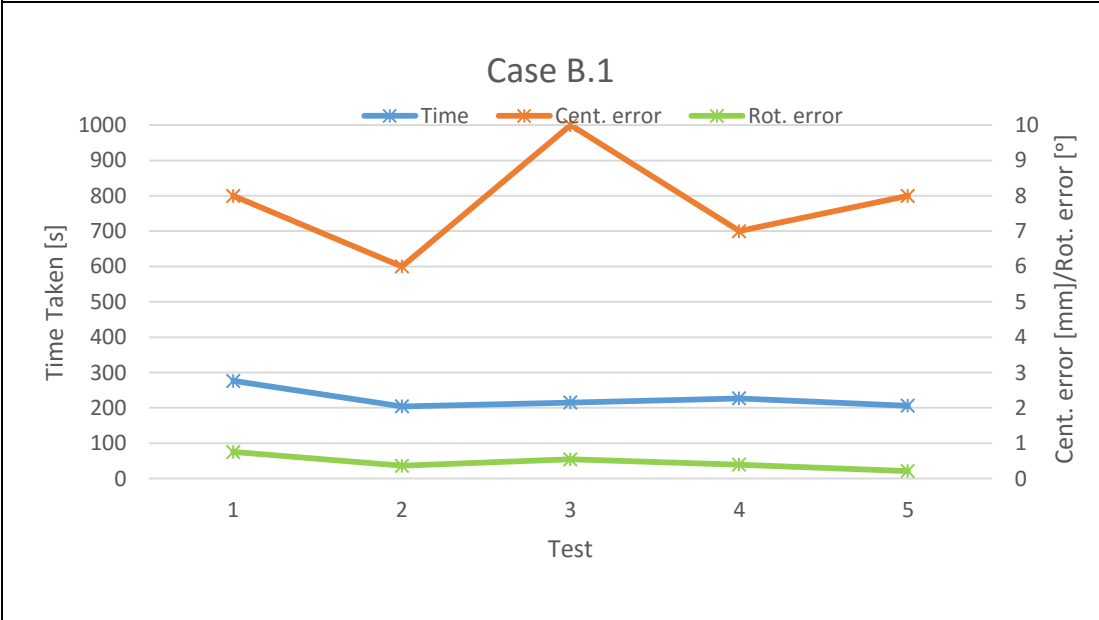
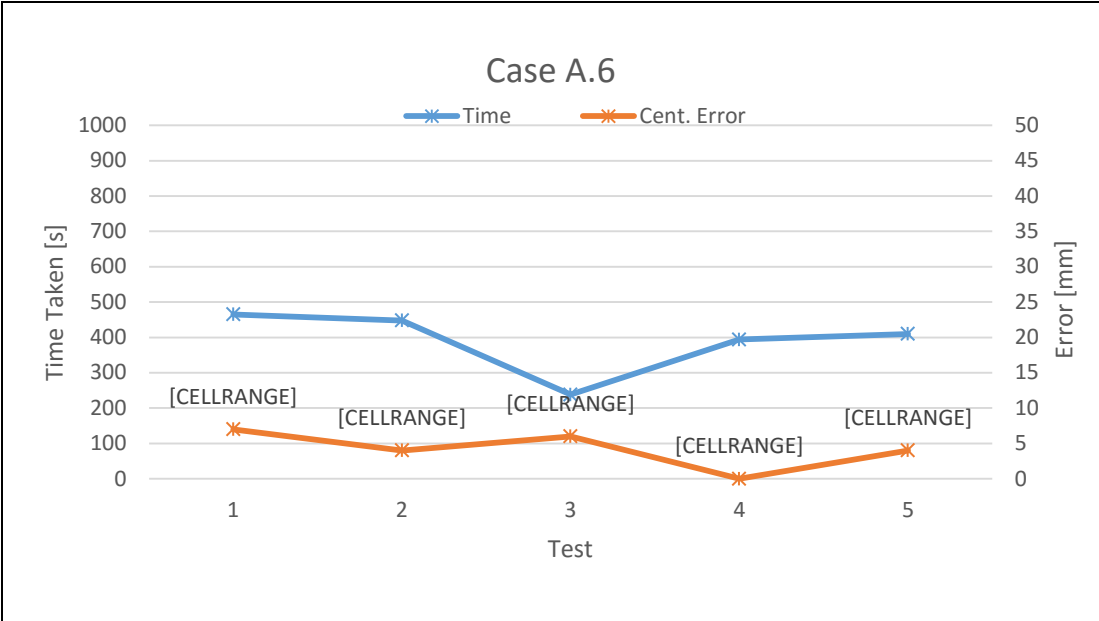
Appendix B Experimental Results

B.1 Graphs of Each Case

The graphs below show the results of each individual test within each case. Markers indicate the banksman in control where applicable (ML-Mareike Leimeister, TB-Toby Balaam). In many of the graphs, there is a clear learning process, case A.4 being a good example (both time and error reduce with increasing tests and practice).







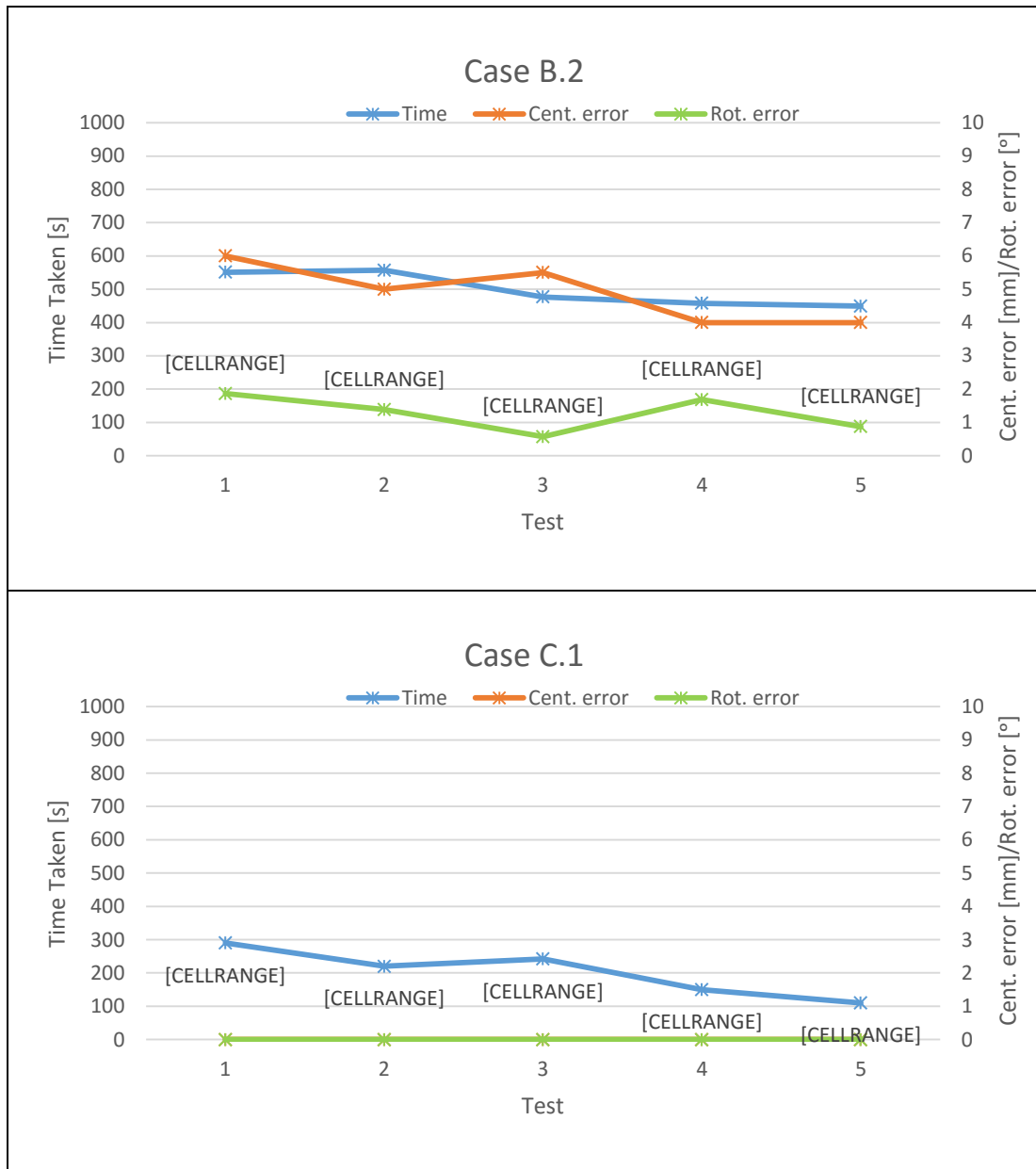


Figure B-1 Graphs of time and error for five no. tests undertaken for each case

B.2 Tables of Raw Data

Case	Test	BM1	BM2	Date	Time Start	Time of Test			Error	Comments
-	-	Control	Safety	dd/mm/yy	hh:mm	minutes	seconds	Total [s]	mm	-
A.1	1			06/03/17	12:26	2	5	125	9	
A.1	2			06/03/17	12:38	1	40	100	5	
A.1	3			06/03/17	12:46	2	11	131	6.5	
A.1	4			06/03/17	14:14	1	35	95	6.5	
A.1	5			06/03/17	14:20	1	19	79	8	
A.2	1			06/03/17	14:42	2	55	175	2	
A.2	2			06/03/17	14:59	2	51	171	5	
A.2	3			06/03/17	15:08	2	24	144	6	
A.2	4			06/03/17	15:15	3	14	194	6	
A.2	5			06/03/17	15:23	3	14	194	3	
A.3	1	ML	TB	06/03/17	15:56	6	25	385	10	<ul style="list-style-type: none"> - Operator and 1*Banksman looking at monitor - 1* Bankman controlling sway until within camera range and guiding (mimicing taglines and view) - Difficult to know which camera was in which position at first (should be known before) - Difficult to realise depth; how close to the ground
A.3	2	ML	TB	06/03/17	16:14	6	50	410	2	<ul style="list-style-type: none"> - Operator no visual access, BM1 watching monitor and BM2 guiding until cameras in view and controlling sway to this point. Orders relayed to operator only by BM1. - Although very successful it was difficult to envisage where real camera positions are. May be simpler if you could see the camera view with regards to the real position.
A.3	3	ML	TB	06/03/17	16:28	14	31	871	16	<ul style="list-style-type: none"> - Operator no visual access, BM1 watching monitor and BM2 guiding until cameras in view and controlling sway to this point. Orders relayed to operator only by BM1 - Section rotated a lot in this test - This meant camera positioning was changing a lot with respect to axes of crane control. The respective axes of the field of vision of each camera was changing relative to the crane movement axes. - It was also swinging more than prior tests, hence the time to test was longer - Due to the rotations there were many repeat orders i.e. 'forward no backward' - Helpful to know at least which order the cameras are in about the cylinder - Was swinging during touchdown which may have added to error.
A.3	4	TB	ML	07/03/17	08:45	10	8	608	45	<ul style="list-style-type: none"> - Difficulty reading depth and knowledge of where each camera was, hence it would be good to have orientation points
A.3	5	TB	ML	07/03/17	09:04	8	2	482	5	<ul style="list-style-type: none"> - Cameras remained in position - Helpful to drop cylinder down whilst seeing all lines in the picture - Key point: Either control rotation or have some way to know the location of each camera
A.4	1	TB	ML	07/03/17	09:26	11	31	691	14	<ul style="list-style-type: none"> - Easier with 4th camera - Swinging somewhat as it settled - Much easier to gauge distance - Orientation marks are helpful
A.4	2	TB	ML	07/03/17	09:45	7	55	475	6	<ul style="list-style-type: none"> - Less swing
A.4	3	TB	ML	07/03/17	09:58	6	30	390	3	<ul style="list-style-type: none"> - Much easier - Brought down whilst swinging but could easily tell distance. - Was able to guide lift from far earlier as 3D camera could see full lift from its position
A.4	4	ML	TB	07/03/17	10:10	7	52	472	2	<ul style="list-style-type: none"> - Fine control of crane is very important - Also calls to operator are difficult, not much idea of scale ie. touch forward (difficult to gauge distance)
A.4	5	ML	TB	07/03/17	10:24	7	32	452	1	None
A.5	1	ML	TB	07/03/17	11:16	6	15	375	6	<ul style="list-style-type: none"> - The 3D camera is maybe positioned slightly too high, should be above line but maybe not that much - Good to change from looking upwards to downwards and being able to move around - In reality may need to test for light, some difficulties in darker areas.
A.5	2	ML	TB	07/03/17	11:31	4	1	241	12	<ul style="list-style-type: none"> -Light reflecting in the South (Backwards) so was difficult to see
A.5	3	ML	TB	07/03/17	11:46	6	15	375	5	<ul style="list-style-type: none"> - BM1 took control from the beginning of lift - Camera may need to be exactly in the centre for accuracy (will test this)
A.5	4	TB	ML	07/03/17	12:02	5	50	350	7	<ul style="list-style-type: none"> - BM1 took control from the beginning of lift - Battery dies after this test - Could be an important point with regards to reality. If battery dies part way through a lift require some kind of redundancy.
A.5	5	TB	ML	07/03/17	12:33	6	46	406	15	<ul style="list-style-type: none"> - BM1 took control from the beginning of lift - Also tried off centre 360 camera which was far harder

Case	Test	BM1 Control	BM2 Safety	Date dd/mm/yy	Time Start hh:mm	Time of Test			Error	Comments
-	-					minutes	seconds	Total [s]	mm	-
A.6	1	TB	ML	07/03/17	14:29	7	45	465	7	- Many screens to consider
A.6	2	TB	ML	07/03/17	14:46	7	28	448	4	- Using 360 degree camera until approximately 10cm above ground, then moved to static cameras
A.6	3	TB	ML	07/03/17	15:49	3	58	238	6	- Maybe an issue with light in the South hence why results all contain errors in that direction
A.6	4	ML	TB	07/03/17	15:58	6	34	394	0	- Perfect lift - BM2 settled swing until fairly close
A.6	5	ML	TB	07/03/17	16:11	6	50	410	4	- Night vision was on on camera 1 and there was a large glare which made it difficult

Test of 4 cameras + 3D camera (Case 7)

A.7	1	ML	TB	08/03/2017	09:19	5	58	358	Similar	- If a view from the beginning of the lift until close to the location is required then the 360 degree camera is the best - However both central camera (#4) and 360 camera gives redundancy. During fine tuning you are really only looking at the 3 fine tune cameras and 1 other. - Trying to look at both can be confusing - ML would rather have 4 cameras, 3 different kind of views can get confusing.
A.7	2	TB	ML	08/03/2017	09:32	6	30	390	Similar	

Test of Redundancy (Cameras 1,2 & 4)

A test to see if accurate positioning is possible if a camera was lost (ie. one of the fine tune cameras)

				08/03/2017	09:46	7	37	457	Similar	- Still possible - However slightly more difficult (takes more time) - Focus on getting the distances at the remaining cameras to a similar distance (Concentric circles) - Do not rely on the 4th camera being directly in the centre (if it is not then this causes skew)
--	--	--	--	------------	-------	---	----	-----	---------	--

Case	Test	BM1	BM2	Date	Time Start	Time of Test			Cent.Error	Distances [mm]			calculated angle error [°]			Average	Comments
-	-	Control	Safety	dd/mm/yy	hh:mm	minutes	seconds	Total [s]	mm	1	2	3	1	2	3	[°]	-
B.1	1	-	-	24/03/17	10:06	4	36	276	8	-11	-4	-10	-0.99	-0.36	-0.90	0.75	- Whole view is crucial
B.1	2	-	-	24/03/17	10:26	3	24	204	6	-6	-3	-3	-0.54	-0.27	-0.27	0.36	- Error in centralisation effects rotational misalignment aswell (problem in both DoFs if one camera not working)
B.1	3	-	-	24/03/17	10:41	3	35	215	10	-7	-4	-7	-0.63	-0.36	-0.63	0.54	- More difficult to keep an eye on both (centralisation and rotational alignment) - Taglines mimicked by banksman, can only rotate and cannot look at lines (throughout all tests)
B.1	4	-	-	24/03/17	11:00	3	47	227	7	-8	2	3	-0.72	0.18	0.27	0.39	- Difficult with two people but three rods, this would be different with just a single guide pin - Free rotation of the hook gives a lot of room for error
B.1	5	-	-	24/03/17	11:28	3	26	206	8	2	3	2	0.18	0.27	0.18	0.21	- Negative effect on final position if load is not perfectly perpendicular/horizontal due to chains/ropes to hook (not exactly distributed between shackle holes or different chain/ropes lengths)
B.2	1	ML	TB	24/03/17	11:47	9	11	551	6	-24	-19	-19	-2.16	-1.71	-1.71	1.86	- Consideration of camera not directly above rod - this is a good position for the majority of the lift. However becomes confusing once going down - needs fine corrections close to touch down - importance of inclusion of this angle of eccentricity: must be put down at slightly "wrong" position, but hard to estimate how much
B.2	2	ML	TB	24/03/17	12:11	9	17	557	5	-18	-11	-17	-1.62	-0.99	-1.53	1.38	- B.2.2 Difficult view (2 cameras in night vision but a great deal of reflection)
B.2	3	ML	TB	24/03/17	14:11	7	57	477	5.5	-10	1	-8	-0.90	0.09	-0.72	0.57	- Best practice - first centralisation then (if in final centred position) rotational positioning - Took some time for banksmen to get used to how to mimick the taglines
B.2	4	TB	ML	24/03/17	14:44	7	38	458	4	-27	-12	-17	-2.43	-1.08	-1.53	1.68	- Used 360 camera for proximity, but side cameras for accurate rotational alignment
B.2	5	TB	ML	24/03/17	14:59	7	29	449	4	-1	18	10	-0.09	1.62	0.90	0.87	- B.2.4 BM1 found it very confusing for rotational orientation - Large effect of fine tuning of taglines for rotational guiding and final alignment
C.1	1	ML	TB	27/03/17	09:33	4	50	290	0							0	- Whole view of 360 camera would be helpful (didn't see all guiding elements until 4th camera was in view)
C.1	2	ML	TB	27/03/17	09:43	3	40	220	0							0	- Quite a rough landing (C.1.1) but system worked perfectly
C.1	3	TB	ML	27/03/17	09:50	4	2	242	0							0	- Mechanical guidance systems was already rotationally positioning when roughly above bottom element
C.1	4	TB	ML	27/03/17	10:02	2	30	150	0							0	- If the payload is not directly over the section can cause a difficult landing - C.1.4 relied on mechanical guidance and stopped once it was employed.
C.1	5	TB	ML	27/03/17	10:08	1	50	110	0							0	- It should be noted that in the final design the vertical 'edge' is not there - Camera position when guide pins are involved depends on thickness of the guide pin. So you can still see the whole section.

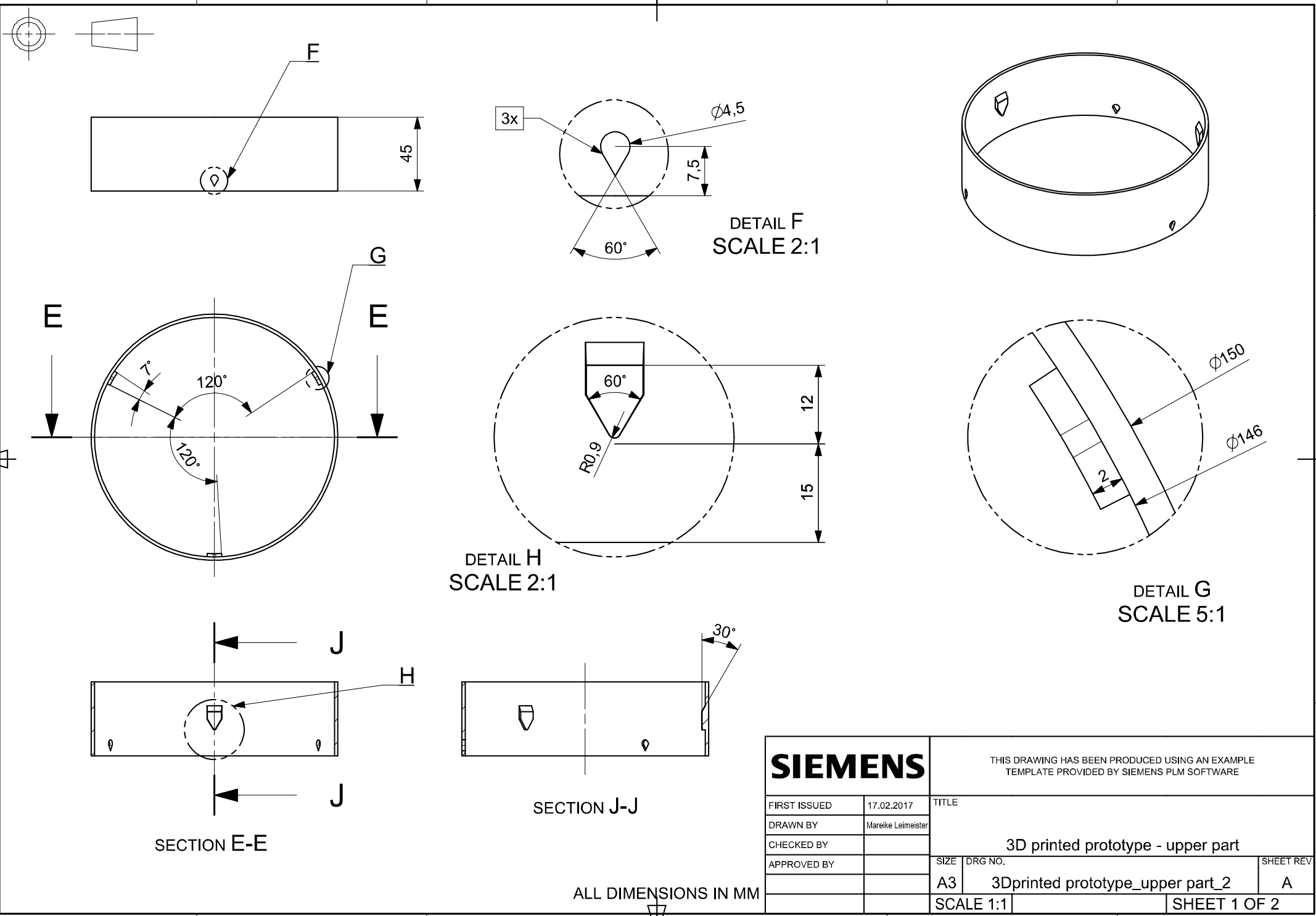
Appendix C **Mechanical Guidance**

C.1 **3D-Printed Initial Design**

C.1.1 **Top Element**



Figure C-1 Top element of the 3D-printed initial design



SIEMENS

FIRST ISSUED	17.02.2017
DRAWN BY	Mareike Leimeister
CHECKED BY	
APPROVED BY	

THIS DRAWING HAS BEEN PRODUCED USING AN EXAMPLE
TEMPLATE PROVIDED BY SIEMENS PLM SOFTWARE

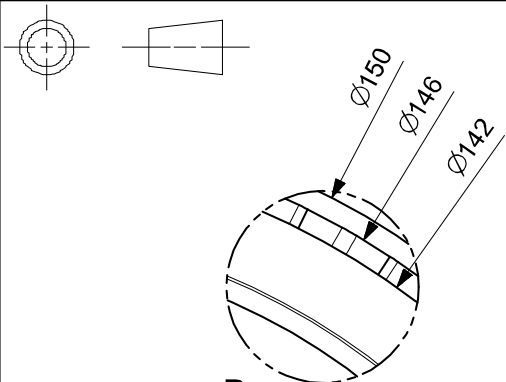
3D printed prototype - upper part

SIZE	DRG NO.	SHEET REV
A3	3Dprinted prototype_upper part_2	A
SCALE 1:1		SHEET 1 OF 2

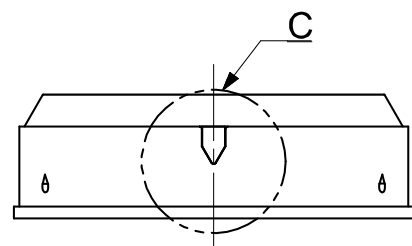
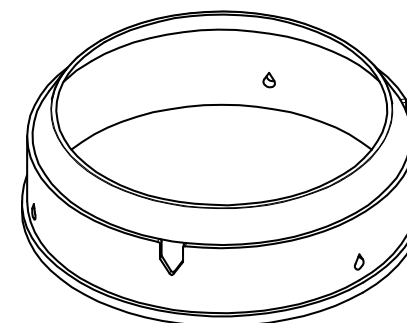
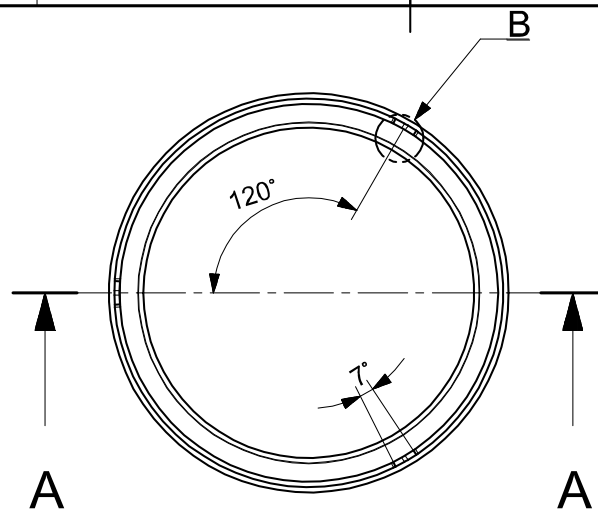
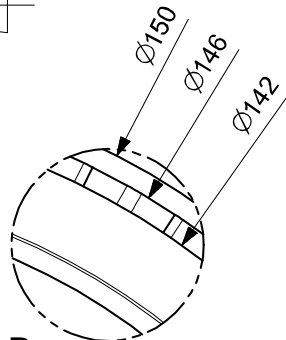
C.1.2 Bottom Element



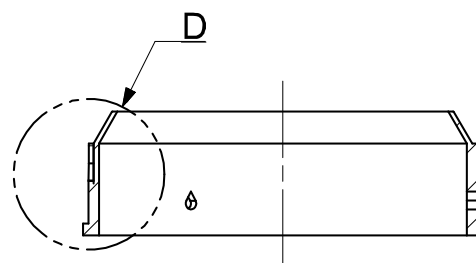
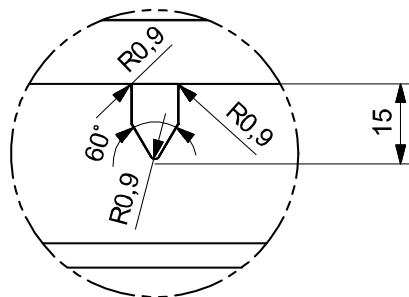
Figure C-2 Bottom element of the 3D-printed initial design



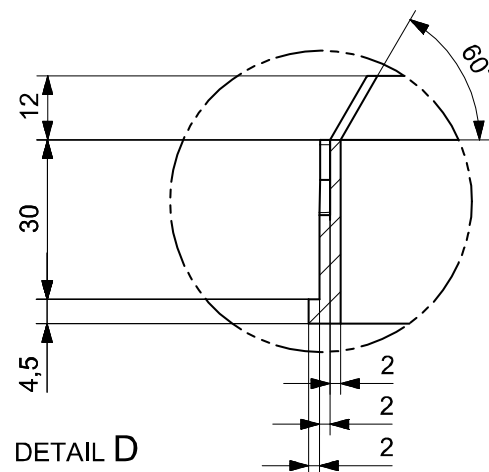
DETAIL B
SCALE 2:1



DETAIL C
SCALE 1:1

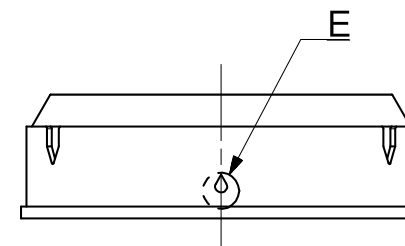


DETAIL D
SCALE 1:1

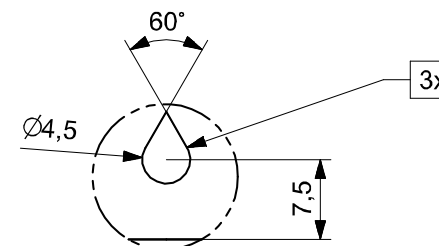


SECTION A-A

ALL DIMENSIONS IN MM



DETAIL E
SCALE 2:1



SIEMENS		THIS DRAWING HAS BEEN PRODUCED USING AN EXAMPLE TEMPLATE PROVIDED BY SIEMENS PLM SOFTWARE	
FIRST ISSUED	15.02.2017	TITLE	
DRAWN BY	Mareike Leimeister	3D printed prototype - lower part	
CHECKED BY			
APPROVED BY		SIZE	DRG NO.
		A3	3Dprinted prototype_lower part
		SCALE 1:1	SHEET 1 OF 2
			SHEET REV
			A

C.1.3 Assembly

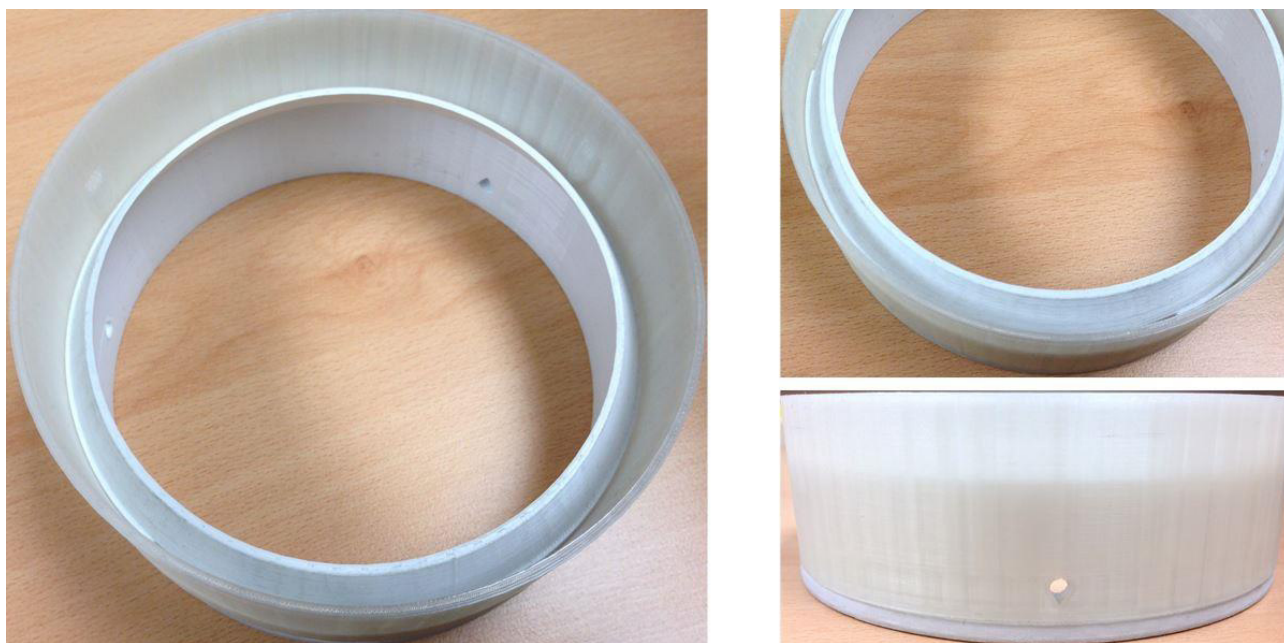


Figure C-3 Assembly of the 3D-printed initial design

C.2 3D-Printed Revised Design

C.2.1 Top Element

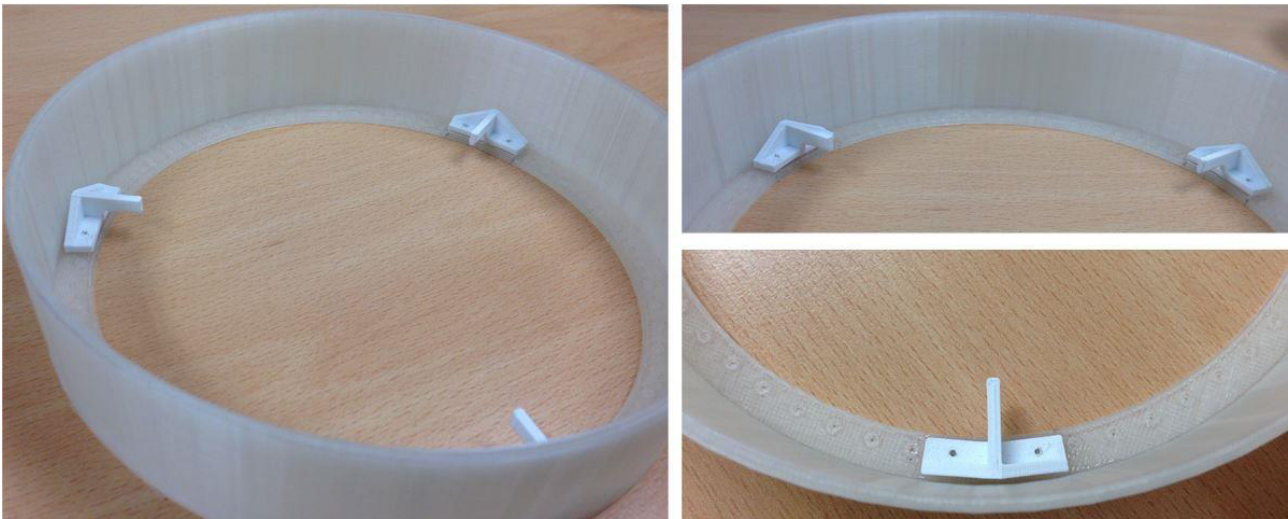
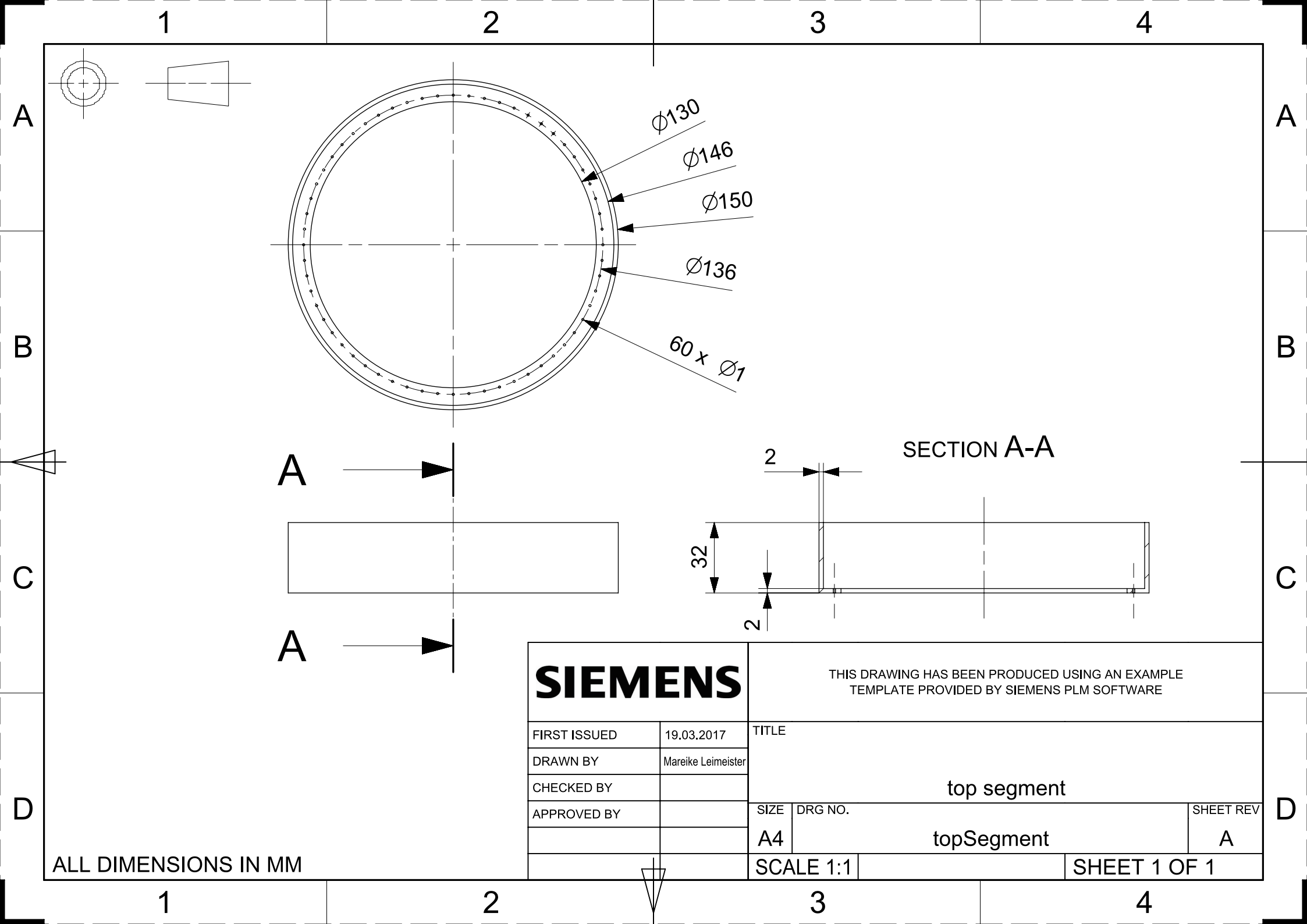
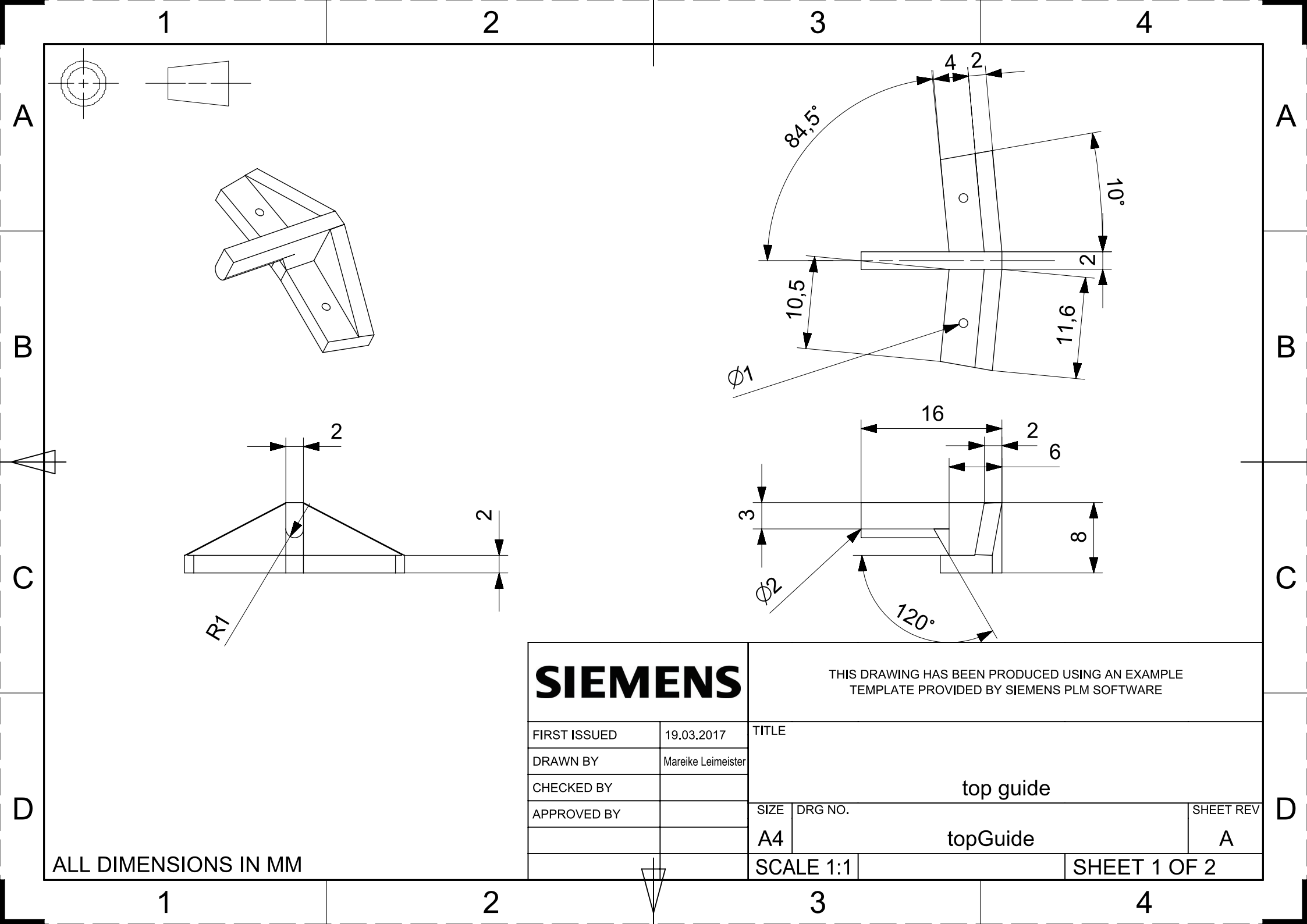


Figure C-4 Top element of the 3D-printed revised design



SIEMENS		THIS DRAWING HAS BEEN PRODUCED USING AN EXAMPLE TEMPLATE PROVIDED BY SIEMENS PLM SOFTWARE		
FIRST ISSUED	19.03.2017	TITLE top segment		
DRAWN BY	Mareike Leimeister			
CHECKED BY				
APPROVED BY		SIZE	DRG NO.	SHEET REV
		A4	topSegment	A
		SCALE 1:1		SHEET 1 OF 1

ALL DIMENSIONS IN MM



ALL DIMENSIONS IN MM

SIEMENS

THIS DRAWING HAS BEEN PRODUCED USING AN EXAMPLE
TEMPLATE PROVIDED BY SIEMENS PLM SOFTWARE

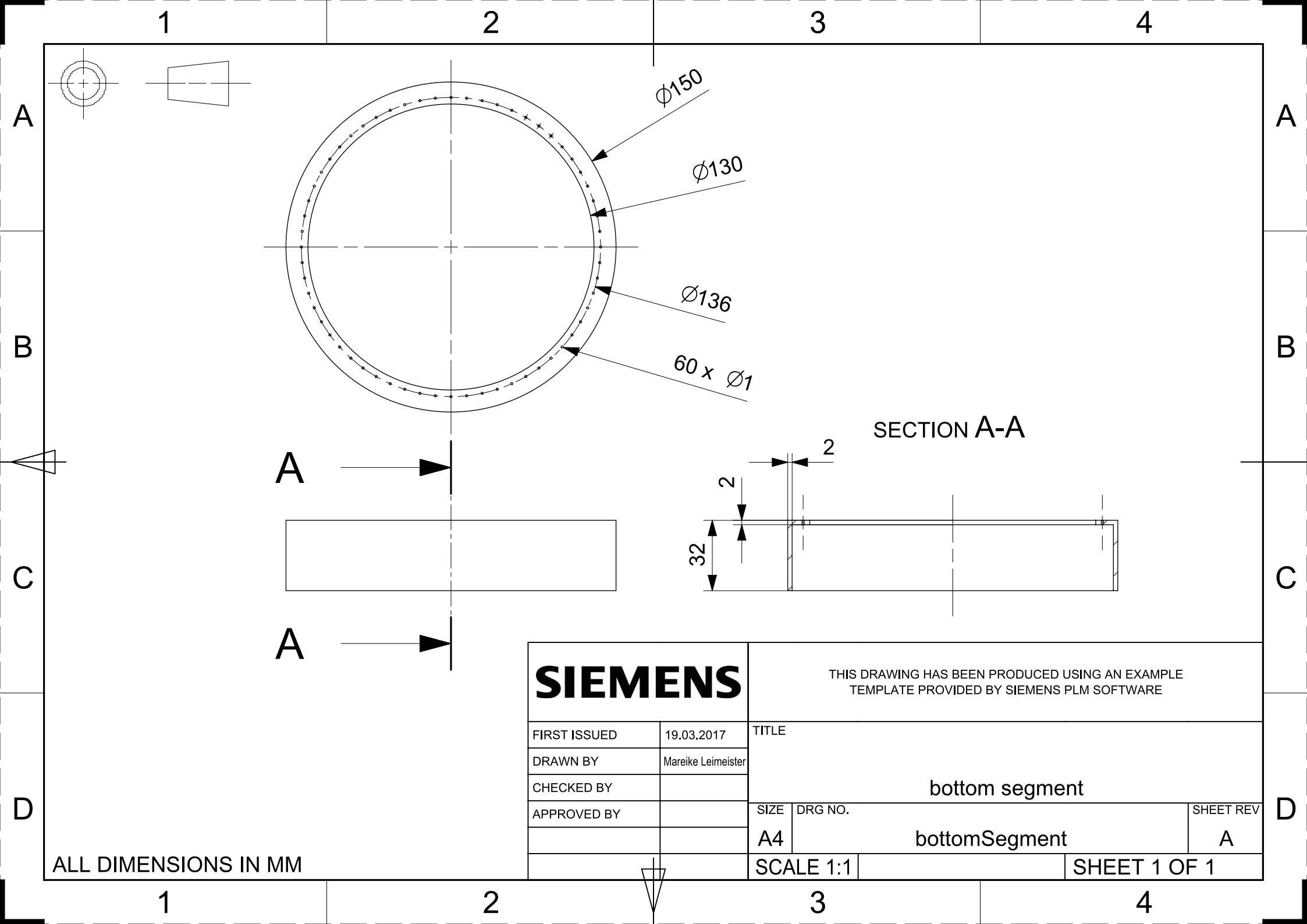
FIRST ISSUED	19.03.2017
DRAWN BY	Mareike Leimeister
CHECKED BY	
APPROVED BY	

TITLE		
top guide		
SIZE	DRG NO.	SHEET REV
A4	topGuide	A
SCALE 1:1		SHEET 1 OF 2

C.2.2 Bottom Element



Figure C-5 Bottom element of the 3D-printed revised design



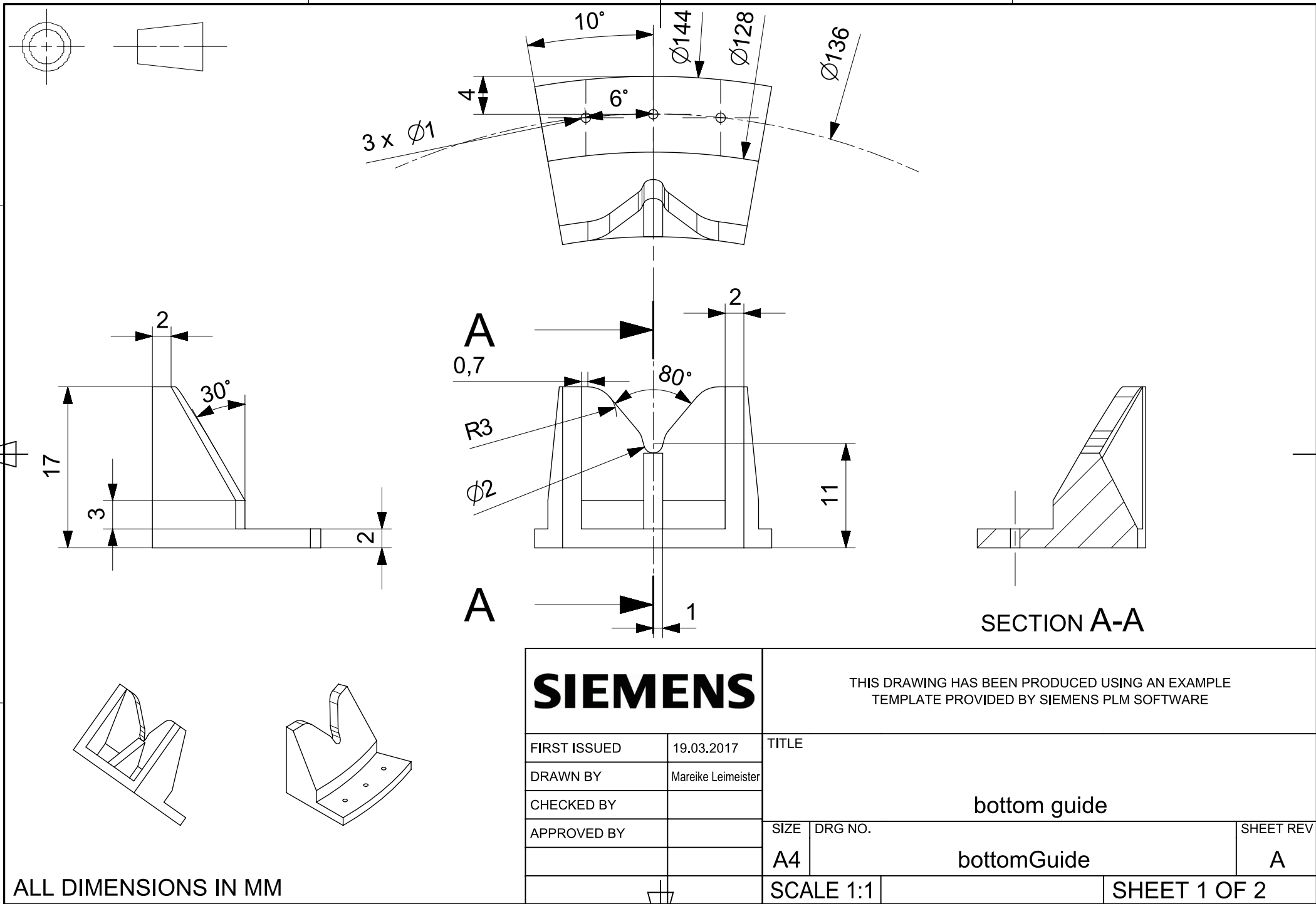
SIEMENS

THIS DRAWING HAS BEEN PRODUCED USING AN EXAMPLE
TEMPLATE PROVIDED BY SIEMENS PLM SOFTWARE

FIRST ISSUED	19.03.2017
DRAWN BY	Mareike Leimeister
CHECKED BY	
APPROVED BY	

TITLE			
bottom segment			
SIZE	DRG NO.		SHEET REV
A4	bottomSegment		A
SCALE 1:1		SHEET 1 OF 1	

ALL DIMENSIONS IN MM



C.2.3 Assembly

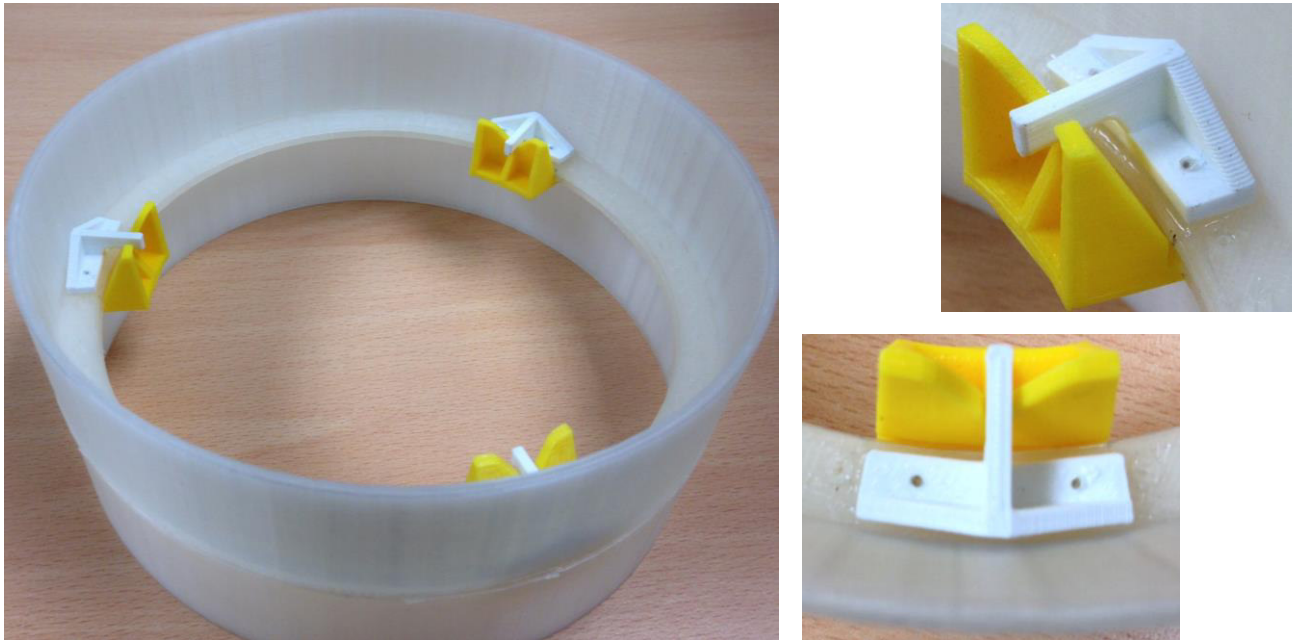
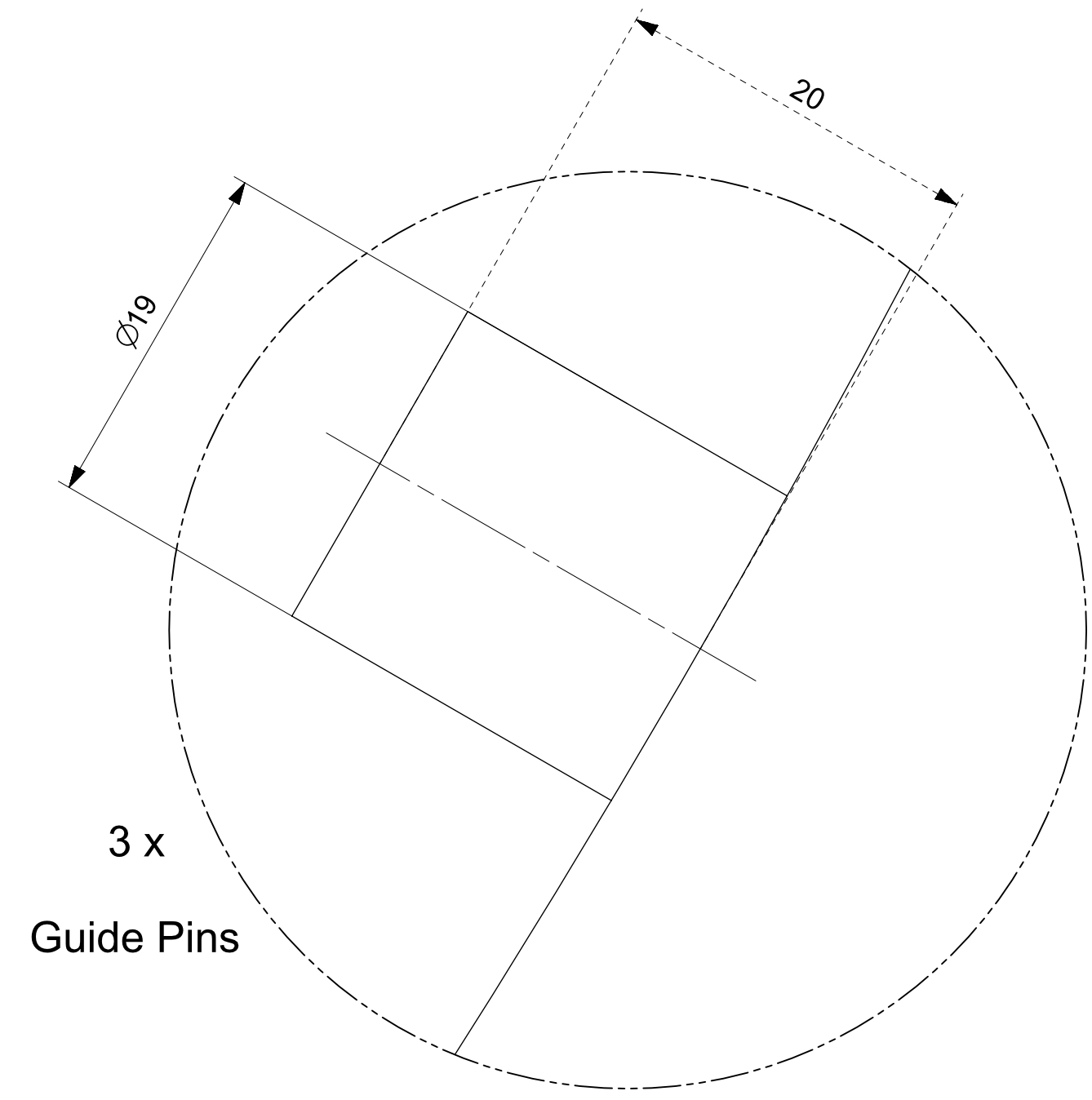
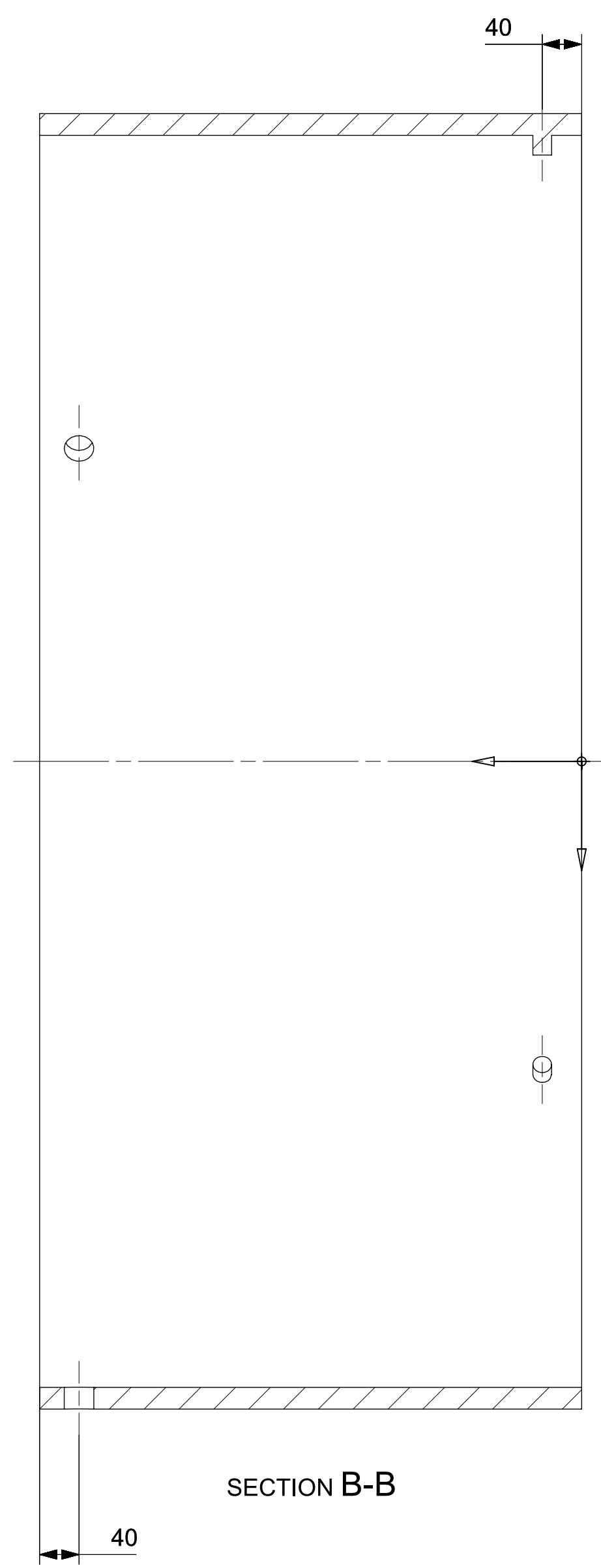
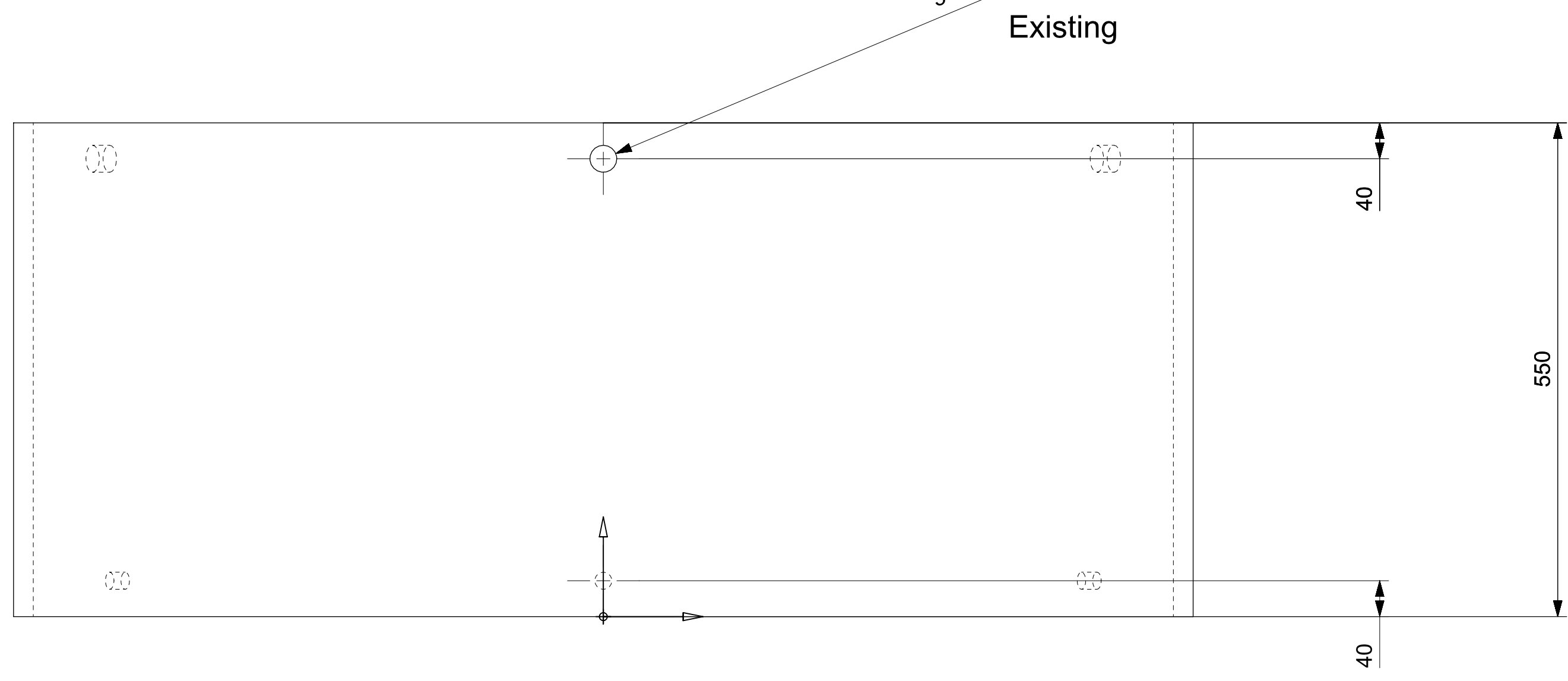
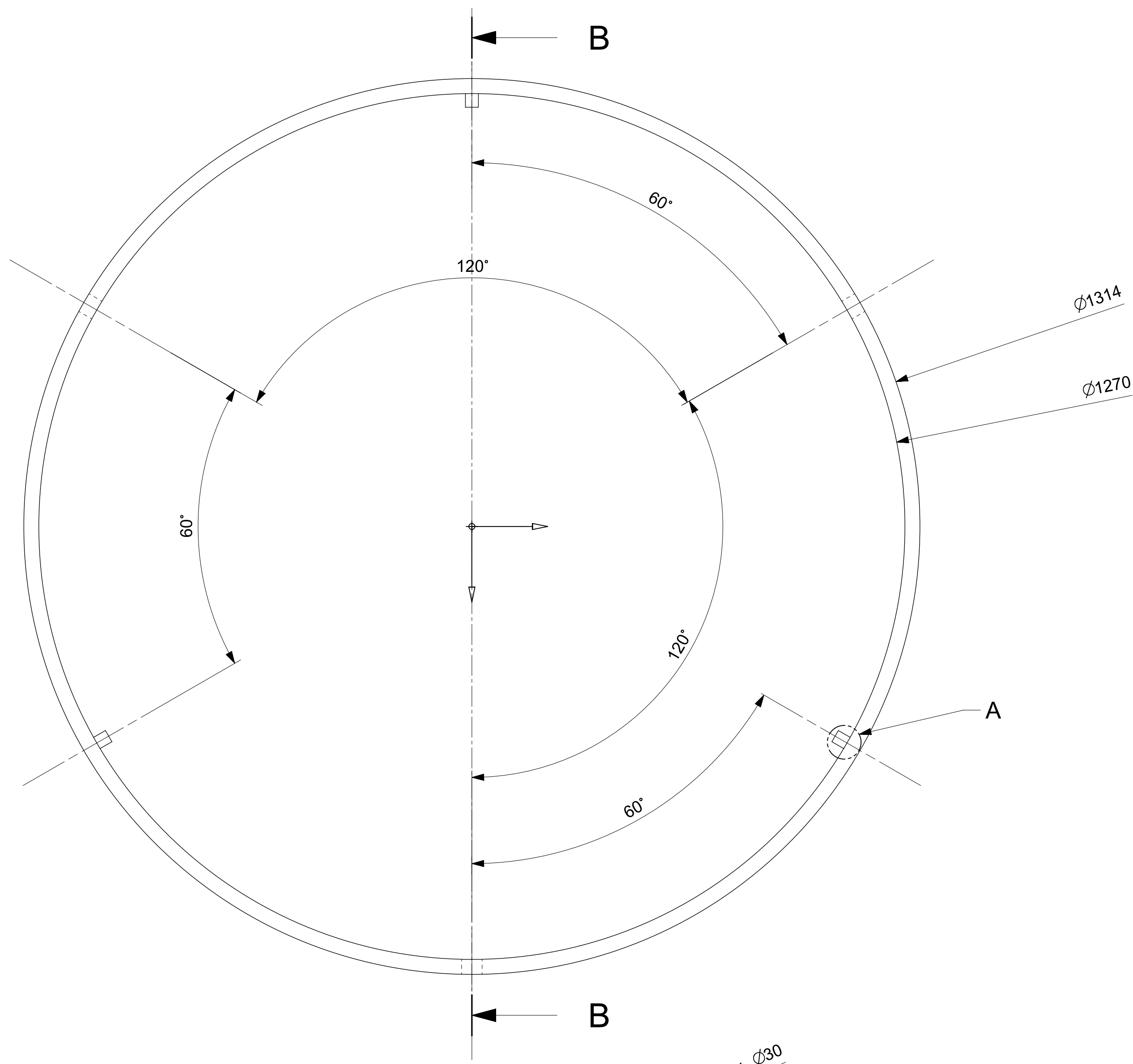
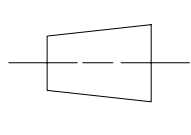
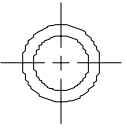


Figure C-6 Assembly of the 3D-printed revised design

C.3 Simplified Design for Experimental Tests

C.3.1 Top Assembly

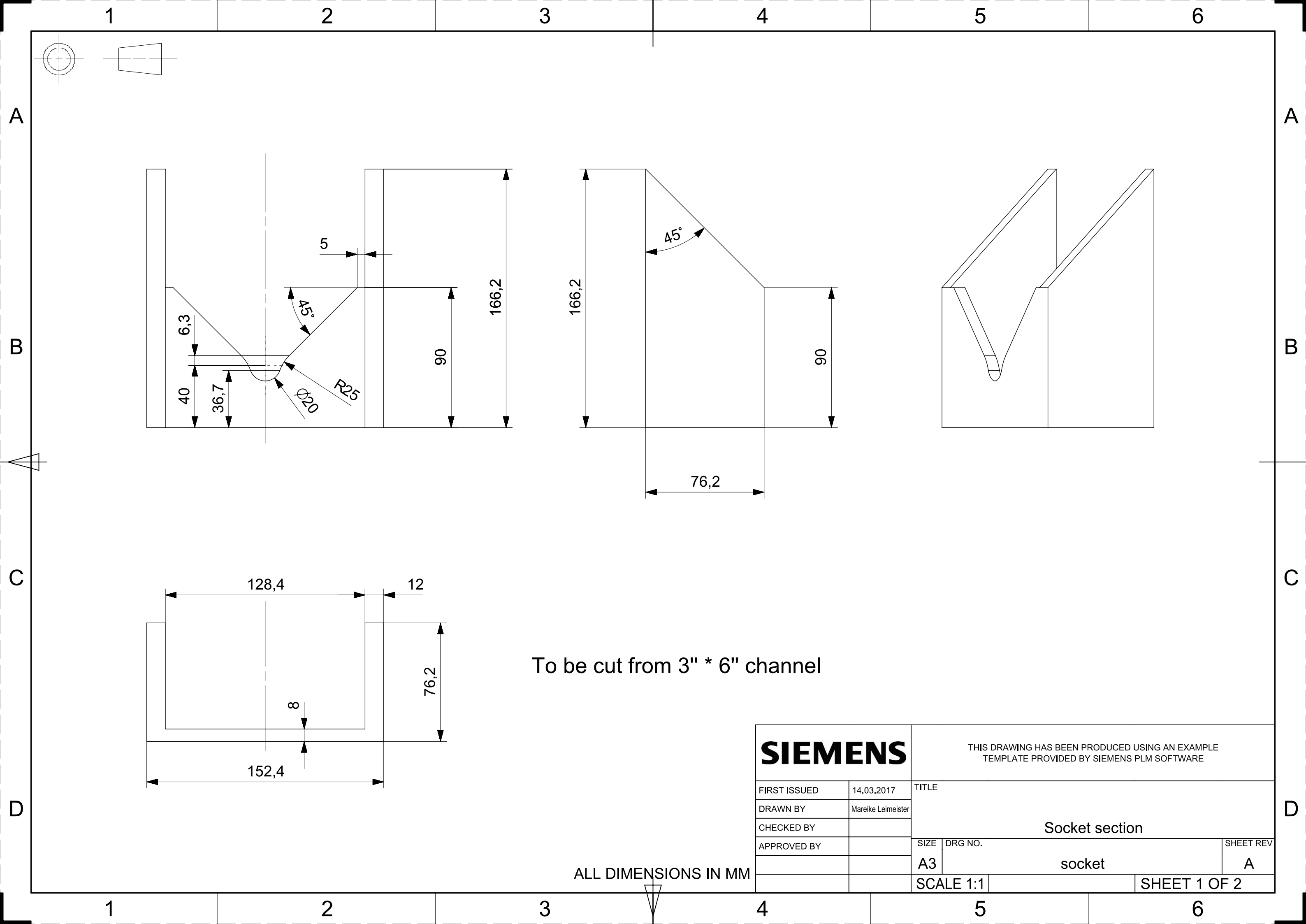


DETAIL A
SCALE 3:1

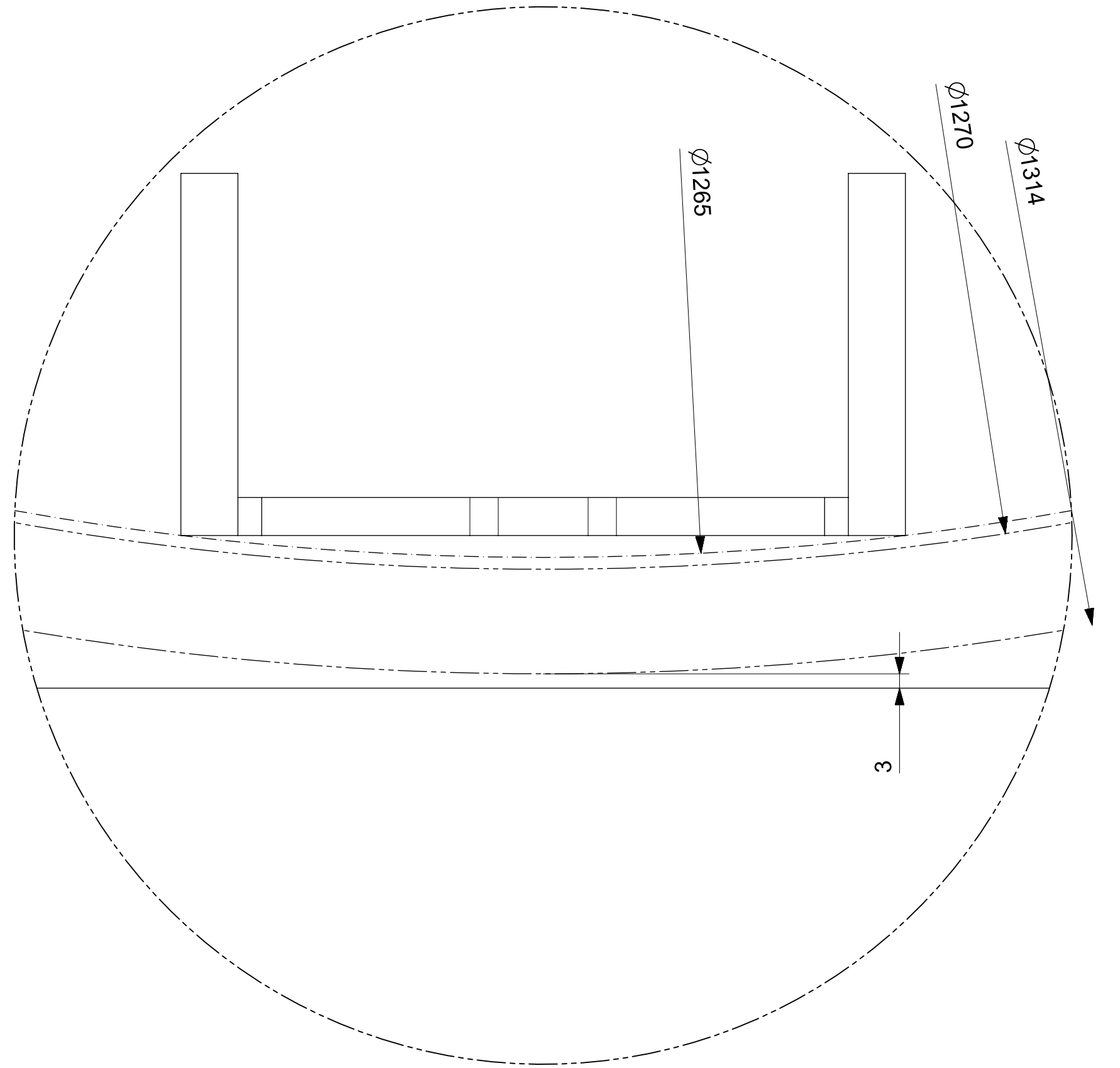
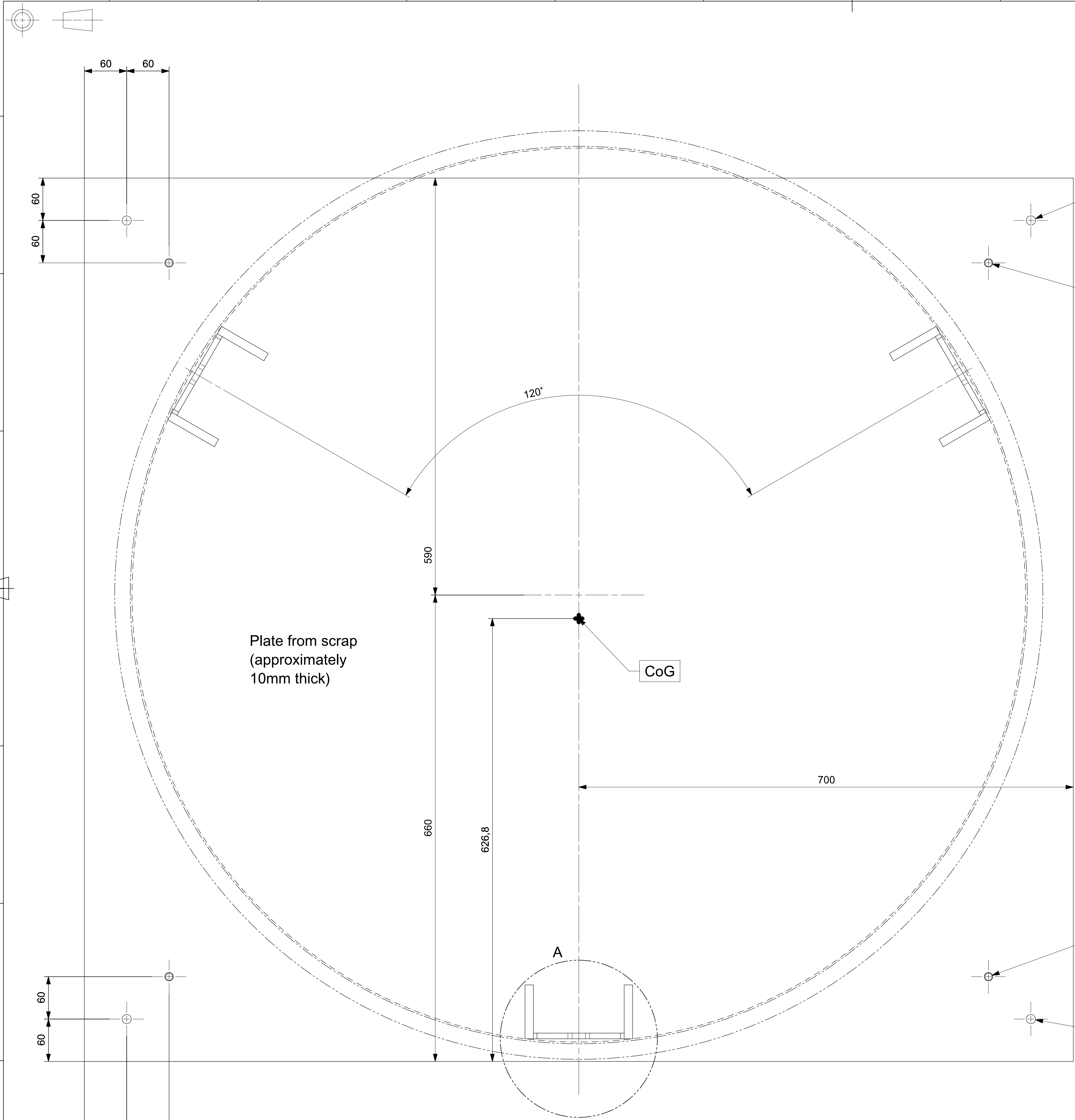
SIEMENS		THIS DRAWING HAS BEEN PRODUCED USING AN EXAMPLE TEMPLATE PROVIDED BY SIEMENS PLM SOFTWARE		
FIRST ISSUED	14.03.2017	TITLE		
DRAWN BY	Mareike Leimeister	Top element		
CHECKED BY		assemblyTop		
APPROVED BY		A		
SCALE 1:1		SHEET 1 OF 2		

ALL DIMENSIONS IN MM

C.3.2 Socket Section



C.3.3 Bottom Assembly



SIEMENS		THIS DRAWING HAS BEEN PRODUCED USING AN EXAMPLE TEMPLATE PROVIDED BY SIEMENS PLM SOFTWARE	
FIRST ISSUED	14.03.2017	TITLE	
DRAWN BY	Mareike Leimeister	bottom part	
CHECKED BY		assemblyBottom	
APPROVED BY		A	
SCALE 1:1		SHEET 1 OF 2	

ALL DIMENSIONS IN MM

C.3.4 Test Setup



Figure C-7 Fixation of bottom element to floor



Figure C-8 Setup of mechanical and visual guiding systems

C.4 Full-Scale Design

In order to ensure the design described in Section 3.1.4.2.2 would be suitable for use offshore we have undertaken a concept design of the part to check against potential loads and, given the proposed reusable nature, check that it could be easily handled by a worker.

The design considered is for the tower-top nacelle connection as shown in Figure C-9 and with the weights and dimensions shown in Table C-1.

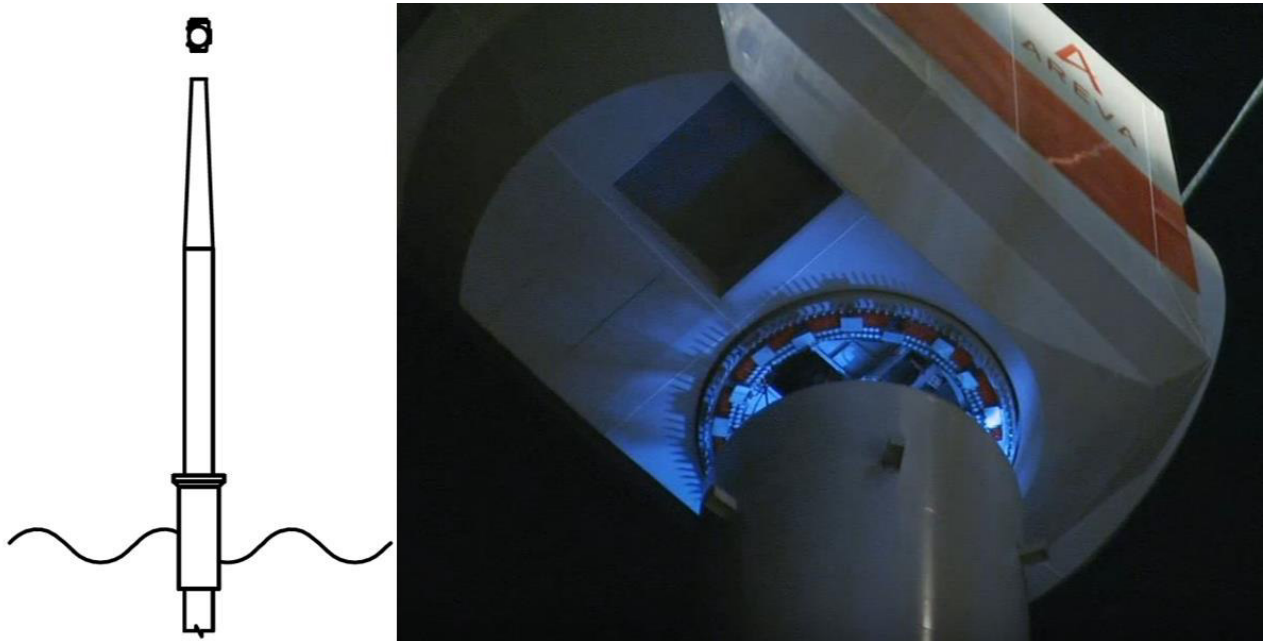


Figure C-9 Nacelle to tower connection. Right (Fred. Olsen Windcarrier, 2015)

In this section, the proposed guide pin and socket defined in Section 3.1.4.2.2.2 was scaled up to the appropriate size, (DNV GL, 2016a) was used find approximate loads before an FEA analysis was undertaken in ABAQUS. It should be noted that this is not a detailed analysis and design of the part but rather a check of the feasibility of the concept and review of the design.

Table C-1 Input data from the 8MW reference wind turbine (Desmond et al., 2016). *

indicates dimensions which were approximated based on realistic proportions

Tower/Flange	Unit			Nacelle	Unit	
Outer Diameter	<i>m</i>	5		Height	<i>m</i>	7.5
Internal Diameter at flange extremity*	<i>m</i>	4.6		Length	<i>m</i>	20
Tower wall thickness	<i>m</i>	0.022		Width	<i>m</i>	7.5
Thickness of flange*	<i>m</i>	0.022		Weight (including gearbox etc.)	<i>ton</i>	285
Number of bolts*	-	180				
Bolt diameter*	<i>m</i>	0.0375				

C.4.1 Calculating Loads (DNV GL, 2016a)

At an initial stage rather than using the analysis method in (DNV GL, 2016a, sec. 4.4) default characteristic impact forces for in-air lifts can be used as in (DNV GL, 2016a, sec. 16.14.4).

Table 16-6 in (DNV GL, 2016a) gives default guide forces. When lifting onto a fixed platform, such as a transition piece or already installed tower piece, pin/bucket guides are subject to a **horizontal force of 0.05W** and a **vertical force of 0.10W**. Where *W* is the hook load. The horizontal force in any direction along with the vertical force should be applied to any likely position to find the worst design case.

According to (DNV GL, 2016a, sec. 16.3.2.2), the static hook load, *SHL*, is equal to:

$$SHL = W_{UD} + W_{rigging} + Effect\ of\ special\ Loads \quad (C-1)$$

Where

W_{ud} = Upper bound design weight

$W_{rigging}$ = Rigging Weight (this is assumed negligible given the weight of the nacelle)

Upper bound design weight is referred to in (DNV GL, 2016a, sec. 5.6.2.2) as:

$$W_{ud} = W_{Report,Factored} * \lambda_{weight} \quad (C-2)$$

Where

$W_{Report,Factored}$ is the reported weight = 285,000 kg see Table C-1.

λ_{weight} is a factor for inaccuracy and as a lift sensitive to weight (class A) = 1.05 (DNV GL, 2016a) Table 5.2.

Hence:

$$SHL = (285,000 * 1.05) [kg] * 9.81 \left[\frac{m}{s^2} \right] = 2935643 [N] \quad (C-3)$$

+Effect of special Loads

Effect of special loads is covered in (DNV GL, 2016a, sec. 16.2.7.1), in which it is said that ‘where appropriate’ allowances for should be made special loads such as tugger line loads, guide loads, wind loads etc.

The components to be lifted (Nacelle/Tower Sections) are large and have solid projected areas thus wind loads will be substantial. This is covered in (DNV GL, 2016a, sec. 5.6.3) and is based on projected area and characteristic wind speed as defined in Section 3 of the same guide. The guide then refers to (DNV, 2014b, sec. 5.3.1) which calls for a wind force, F_W of:

$$F_W = C q S \sin \alpha \quad (C-4)$$

Where

C = shape coefficient

q = basic wind pressure

S = projected area of member normal to the force = $7.5 m * 20m = 150 m^2$

α = angle between the direction of wind and axis of member which in this case can be considered to be 90° thus $\sin\alpha = 1$

Basic wind pressure can be calculated as (DNV, 2014b, sec. 5.2.1)

$$q = 0.5 \rho_a U_{T,z}^2 \quad (\text{C-5})$$

Where

ρ_a = the mass density of air and is taken as 1.226 kg/m^3

$U_{T,z}$ = Characteristic wind speed

Current offshore lifting operations are only undertaken at wind speeds of 12 m/s or less (Nielsen, 2016). Therefore, 12 m/s will form the characteristic wind speed. However, if one could increase the working limits (potentially requiring better hoisting control) this design could be strengthened to cater for this.

Hence:

$$q = 0.5 * 1.226 \left[\frac{\text{kg}}{\text{m}^3} \right] * 12 \left[\frac{\text{m}}{\text{s}} \right]^2 = 88.3 \left[\frac{\text{N}}{\text{m}^2} \right] \quad (\text{C-6})$$

Shape coefficient is referenced to 'Eurocode EN 1991-1-4 General Actions – Wind Actions' but certain shapes are also covered in (DNV, 2014b, sec. 5). Considering the nacelle one could safely assume a rectangular section and therefore use (DNV, 2014b, sec. 5.4.2) & Table C-1. For an infinite rectangular section:

$$C_{s1} = 2K_R \sin\alpha \quad (\text{C-7})$$

Where

$K_R = 1$ for $r/b < 0.1$, r is the corner radius (assumed small compared to $b = 10 \text{ m}$). This assumption may be conservative if the nacelle is shaped.

Hence:

$$C_{s1} = 2 * 1 * 1 = 2 \quad (C-8)$$

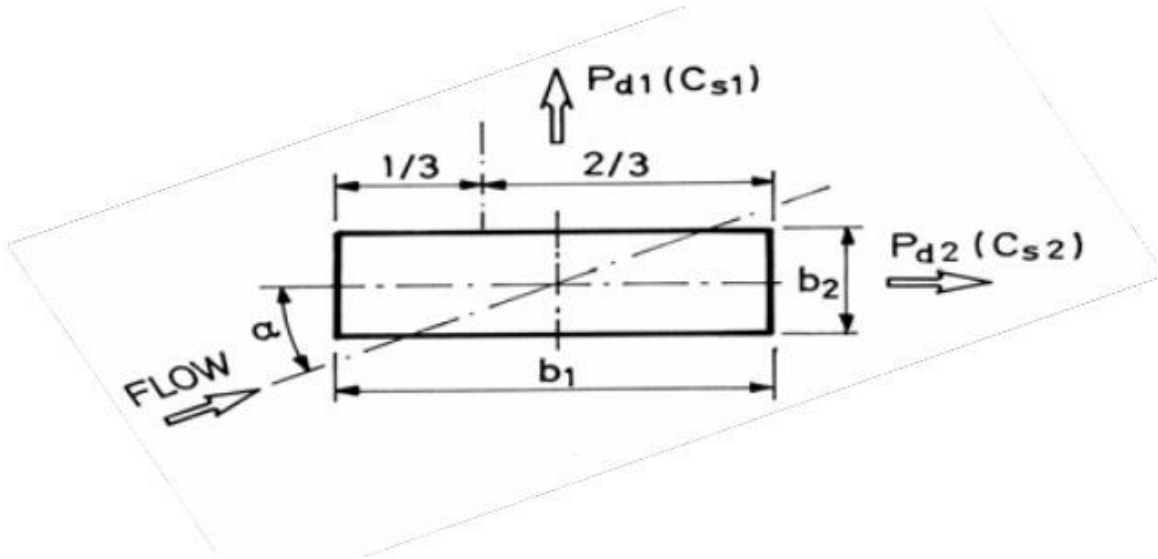


Figure C-10 Drag forces on a rectangular section (DNV, 2014b, sec. 5.4.2)

The shape coefficient C for individual members of finite length may be obtained as (DNV, 2014b, sec. 5.4.3):

$$C = \kappa C_{\infty} \quad (C-9)$$

Where κ is a reduction factor found in (DNV, 2014b) Table 6.2 based upon length and depth. Using the values in Table C-1; $l/d = 20[m]/7.5[m] = 2.67$ and as such a value of approximately 0.62 may be used.

Hence

$$C = \kappa C_{s1} = 0.62 * 2 = 1.24 \quad (C-10)$$

And therefore

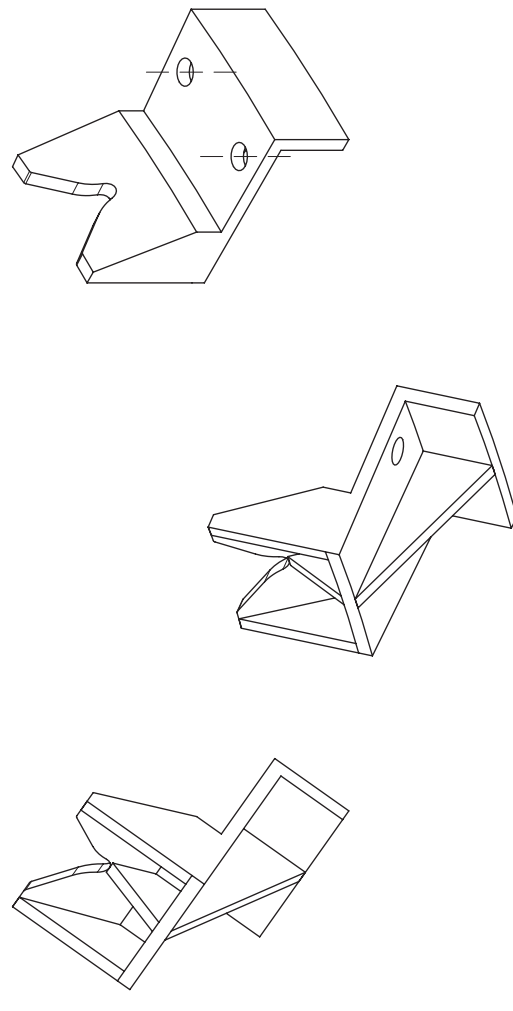
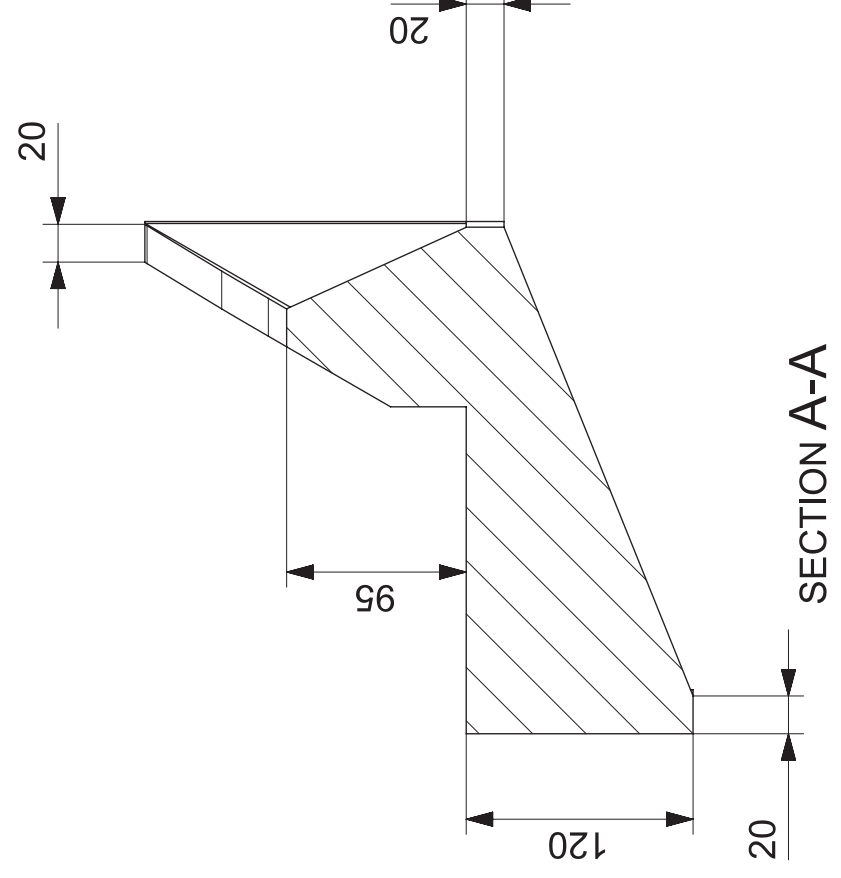
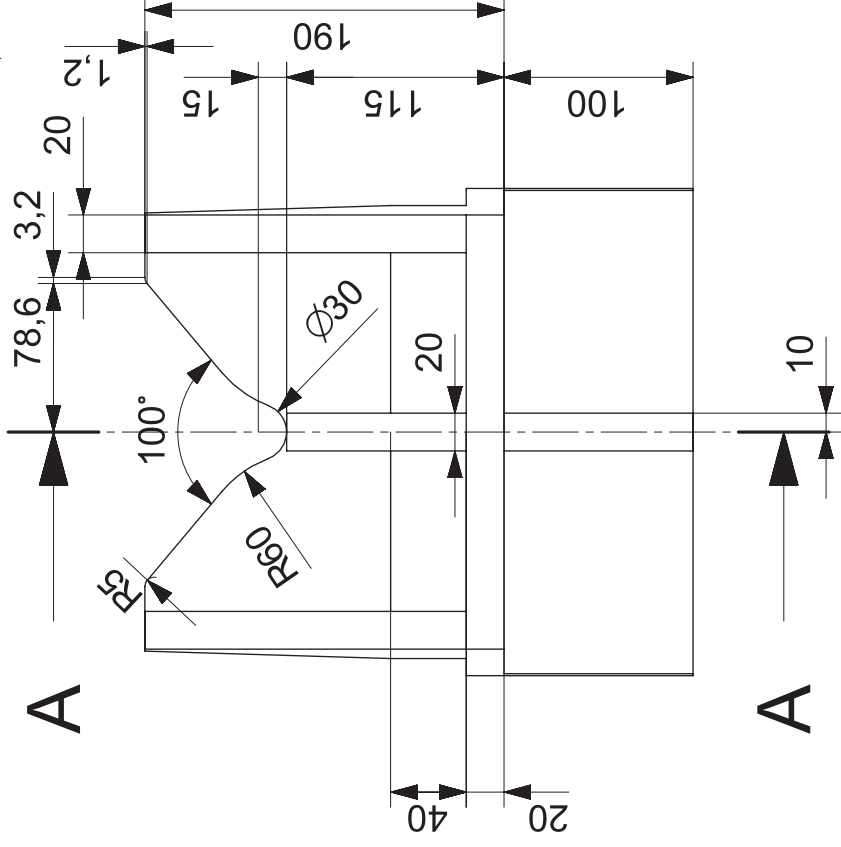
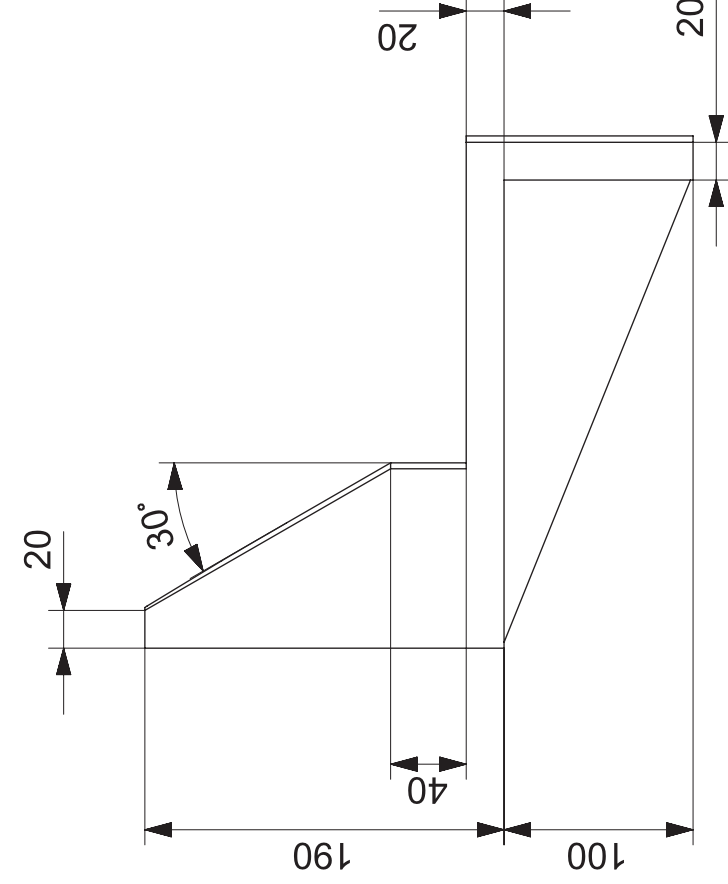
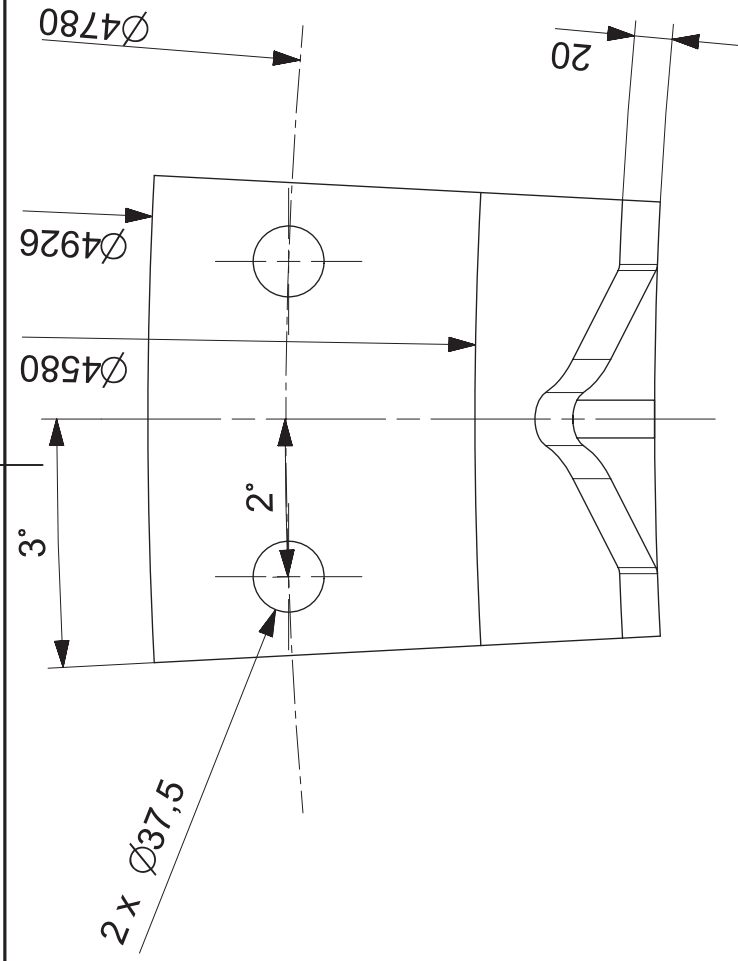
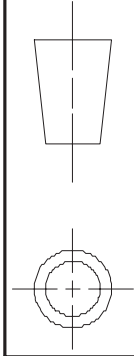
$$F_W = C q S \sin \alpha = 1.24 \quad * 88.3 \left[\frac{N}{m^2} \right] * 150 [m^2] * 1 = 16418 N \quad (C-11)$$

Thus in total

$$\begin{aligned}
 \text{Horizontal Load } (H) &= (0.05 * SHL) + F_W \\
 &= (0.05 * 2935643)[N] + 16418[N] = \mathbf{163201 [N]}
 \end{aligned}
 \tag{C-12}$$

$$\text{Vertical Load } (V) = (0.1 * SHL) = (0.1 * 2935643)[N] = \mathbf{293564 [N]}
 \tag{C-13}$$

C.4.2 CAD Drawing of Full-Scale Design



SIEMENS

FIRST ISSUED	31.03.2017
DRAWN BY	Mareike Leimeister
CHECKED BY	
APPROVED BY	

full scale - bottom guide

TITLE	bottomGuide_2holes_stiffeners		SHEET REV
SIZE	A3	A	
DRG NO.	SCALE 1:1		

ALL DIMENSIONS IN MM

SHEET 1 OF 2

1

2

3

4

5

6

A

B

C

D

A

B

C

D

1

2

3

4

5

6

C.4.3 FEA Analysis

The part was imported into Abaqus and an elastic plastic analysis was undertaken assuming standard S355 steel properties of $E = 210 \text{ GPa}$ and Poisson's Ratio=0.3 taken from (DNV, 2013, sec. 4) 'properties of S355 steel'.

Table 4-3 Proposed non-linear properties for S355 steels (Engineering stress-strain)			
	S355		
Thickness [mm]	$t \leq 16$	$16 < t \leq 40$	$40 < t \leq 63$
E [MPa]	210000		
$\sigma_{\text{prop}}/\sigma_{\text{yield}}$	0.9		
E_{p1}/E	0.001		
σ_{prop} [MPa]	319.5	310.5	301.5
σ_{yield} [MPa]	355	345	335
σ_{yield2} [MPa]	358.4	348.4	338.4
σ_{ult} [MPa]	470	470	450
ϵ_{p_y1}	0.004		
ϵ_{p_y2}	0.02		
ϵ_{p_ult}	0.15		
E_{p2}/E	0.0041	0.0045	0.0041

Figure C-11 Table 4-3 from (DNV, 2013), material properties to be used for S355 steel.

Support is assumed to come from the M36 screws, which would have a head diameter of 55 mm (Beardmore, 2008) across the underside of each hole. The screws will not be designed in this model and are therefore modelled as infinitely strong, immovable cylinders. The number of screws required can be back-calculated assuming sufficient tensile stress can be mobilised. (Hobson Technical, 2007) have M36 screws in grade 8.8 and 10.6 carbon-steel which are capable of 830 and 1040 MPa ultimate tensile stress respectively. M36s have a stress area of 817 mm² and are thus capable of ultimate tensile loads of 678 and 849 kN depending on class.

The load applied should be the worst-case combination of V and H (Equation A-12 & 13) as the upper section collides with the guide socket. (DNV GL, 2016a) calls for this to be applied to the extremities of the guide pin or socket. This collision will occur first as the upper flange hits the centralising conical surface. If correctly aligned this should be along the 30° conical surface. The worst case will be at the top conical surface, the flange will probably not collide across the full width

at first but rather a small section (Load case LC-30) with the horizontal force acting in the x direction, see Figure C-12)

After this point, the conical surface will guide the top section until the guide pin is to be employed in rotating the payload. Although circular in section this will apply force across the full thickness if the payload is approximately level. At this stage, the horizontal force may act in the y direction as shown in Figure C-12. The worst-case global loading would act at the top of this section (Load case LC-41).

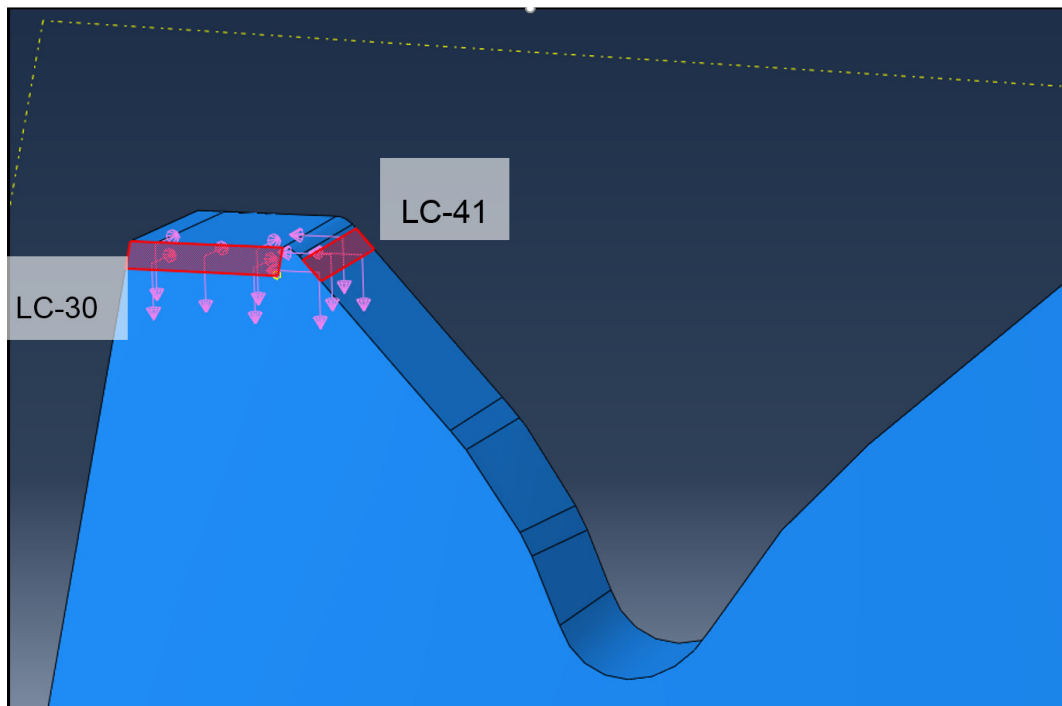


Figure C-12 ABAQUS Model Loads. Load case 30 and 41

Loads can be applied in either traction (over a surface) or as concentrated loads over a point. In order to attempt to avoid unrealistically large local stresses traction forces have been used, these are distributed forces in a given direction (in this case Vertical and Horizontal). A nominal sized face has been cut into the part at the locations shown in Figure C-12 ABAQUS Model Loads. Load case 30 and 41. These were cut to be approximately $20 * 5 \text{ mm}^2$ and $30 * 5 \text{ mm}^2$ respectively, but in order to ensure the correct loads are applied, the area of each was measured in the program by querying the distance between the central points. Hence, the areas can be found exactly and the Vertical / Horizontal forces changed to applied stress/traction as shown in Table C-2.

Table C-2 Loadcases to be analysed

	V	H	d1	d2	A	T _V	T _H
Load case	<i>kN</i>	<i>kN</i>	<i>mm</i>	<i>mm</i>	<i>mm²</i>	<i>N/mm²</i>	<i>N/mm²</i>
LC-30	293.6	163.2	30.003	5.025	150.78	1947	1082
LC-41	293.6	163.2	20.012	5.000	100.06	2934	1630

It is important to note two things here when considering the analysis:

- 1) The loads applied do not realistically represent the dynamic interaction, which is occurring as the load collides with the guide socket, however as described in Section C.4.1 these static loads can be used as a basis. Therefore, they can be applied as purely horizontal and vertical vectors.
- 2) Local plastic deformation is not necessarily an issue because these are guidance elements only. A dent due to a load colliding over a very small area would not cause any problems provided the integrity of the piece as a whole was sufficient to function during the lift. To mimic this in the analysis artificially large strains have been allowed.

Initial tests using steel showed that, using the original design, the 20 *mm* thickness element was yielding across the base and conical part in both load cases, Load case 41 is shown in Figure C-13. The highest stresses are found locally around the point of load and around the screw head. The area around the boltholes shows plastic failure throughout the thickness in both load cases; this would result in the guide socket breaking and therefore is not acceptable. This section currently weighs approximately 24 *kg* and is therefore already at the upper limit of the advised lifting weights see Figure C-14.

With dynamic analysis loads may be able to be reduced slightly and some material savings could be made by reducing the size of the vertical section, (which appears to be particularly underutilised) but the additional thickness required on the conical and horizontal parts would far

outweigh that material saving. Additional weight would certainly not be acceptable for a single person lift.

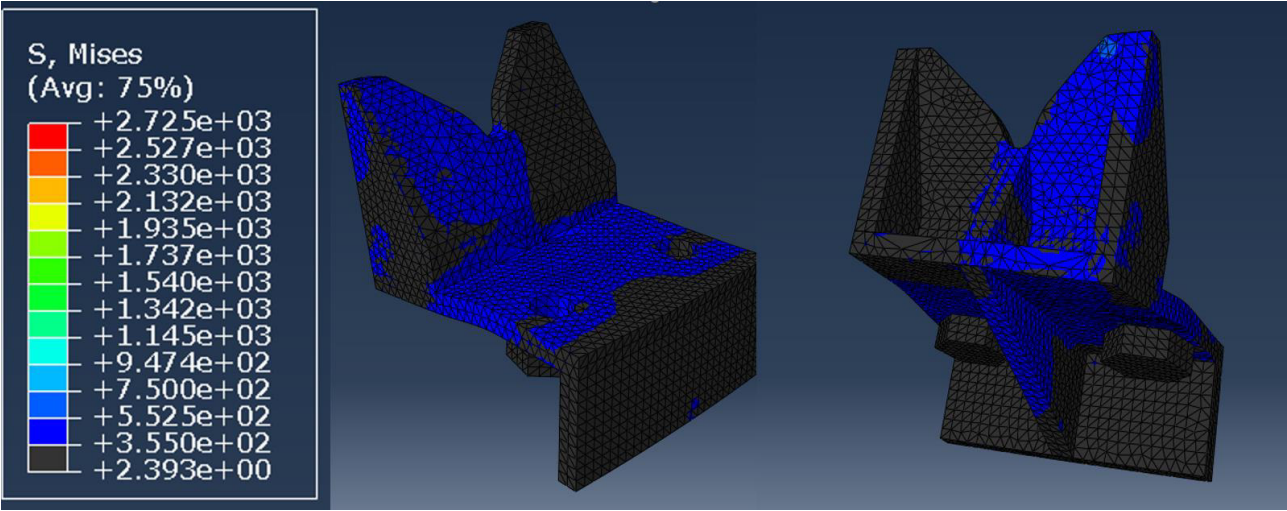


Figure C-13 Load case 41 in two views. Von misses stresses across the 20 mm thick section. Black indicates positions where stresses are below yield

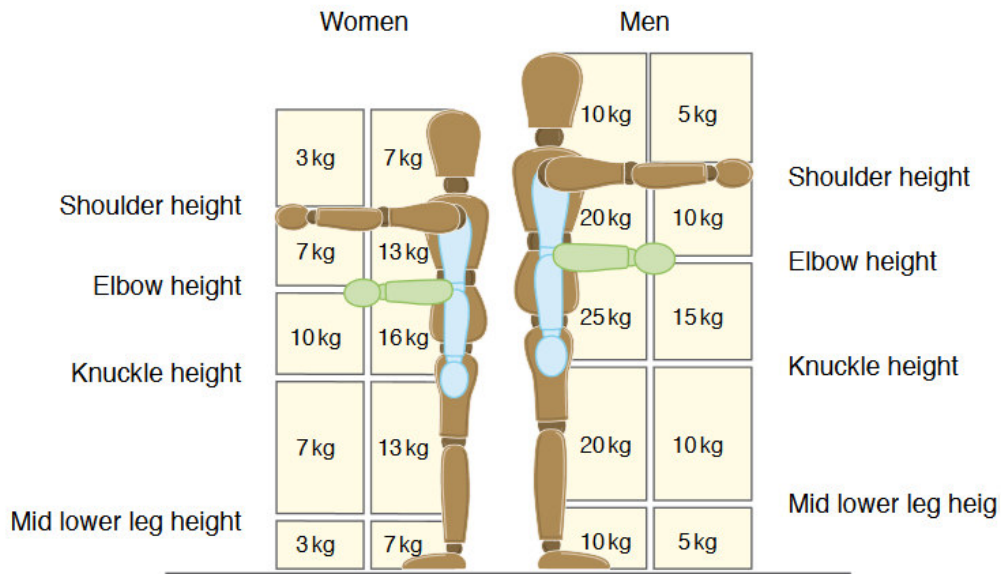


Figure 1 Lifting and lowering
Manual handling at work: A brief guide
Page 8 of 10

Figure C-14 Recommended weights for lifting (Health and Safety Executive, 2012)

Another option is producing the guiding element from a composite fibre-reinforced polymer (FRP). These are made from resin and reinforcement and benefit from a high strength and low weight,

good impact properties and have a good resistance to environmental effects. Mimicking reinforced concrete, fibres of high strength material (such as glass/carbon) are lain and bonded by a resin; these can be lain in a unidirectional, bi-directional or multidirectional orientation to give anisotropic to isotropic properties

A similar shape could be made from FRPs, having ribs (stiffeners) and a large thickness might limit this to spray/lay-up technique material properties are dependent on the choice of resin and reinforcement and the ratio of the two. For instance, a polyester-glass fibre woven lay-up might have properties as shown in Table C-3. This would give approximately 1/5 of the weight and only 1/2 of the strength and may therefore bring the section down to an allowable threshold whilst remaining structurally sound. FRPs are brittle so sufficient safety factors would be required. In order to bring this to reality further design and analysis is required.

Table C-3 Material properties of a lay-up FRP. Values edited from (“Technical Design Guide for FRP Composite Products And Parts,” 2017) **Imperial-metric. Poisson’s ratio from (Hussain, Reddy, & Reddy, 2008)**

Material	Density	Tensile Strength	Compressive Strength	Tensile Modulus	Poisson’s Ratio
	kg/m^3	N/mm^2	N/mm^2	N/mm^2	-
Polyester-Glass FRP	1633	255.1	186.2	15513	0.3

This section acts as an overview of what would be required when designing these connections and runs through a design of the socket section based on DNV guidelines. Further work would involve ensuring the guide pin is structurally robust and undertaking a dynamic analysis of both. With the time available it was chosen to check the guide socket section first (as this was heaviest), if required the pin can be heavily re-designed without affecting the possibility of handling greatly.

C.5 Mechanical Guiding Systems in Comparison

case	centralisation			rotational alignment					
	outer radius mm	distance to centr. edge mm	tolerance (+/-) %	angle (+/-) deg	arc @ bolt hole mm	bolt hole radius mm	radius @ bolts mm	approx. pin radius mm	tolerance (+/-) -
initial design	75	8.93	11.90	3.500	4.46	0.50	73		8.92
revised design	75	7.93	10.57	7.191	8.53	0.50	68		17.07
simplified revised design	657	78.70	11.98	5.386	56.40	8.75	600		6.45
full-scale design	2500	85.06	3.40	2.136	89.10	18.75	2390		4.75
current practice	2500	3.75	0.15	0.090	3.75	18.75	2390	15	0.20

Table C-4 Results of the tolerance margin computations

Appendix D Program Code for the Optimisation of the Assembly

D.1 Simple_GUI.m

```
function varargout = Simple_GUI(varargin)
% SIMPLE_GUI MATLAB code for Simple_GUI.fig
%     SIMPLE_GUI, by itself, creates a new SIMPLE_GUI or raises the existing
%     singleton*.
%
%     H = SIMPLE_GUI returns the handle to a new SIMPLE_GUI or the handle to
%     the existing singleton*.
%
%     SIMPLE_GUI('CALLBACK',hObject,eventData,handles,...) calls the local
%     function named CALLBACK in SIMPLE_GUI.M with the given input arguments.
%
%     SIMPLE_GUI('Property','Value',...) creates a new SIMPLE_GUI or raises the
%     existing singleton*. Starting from the left, property value pairs are
%     applied to the GUI before Simple_GUI_OpeningFcn gets called. An
%     unrecognized property name or invalid value makes property application
%     stop. All inputs are passed to Simple_GUI_OpeningFcn via varargin.
%
%     *See GUI Options on GUIDE's Tools menu. Choose "GUI allows only one
%     instance to run (singleton)".
%
% See also: GUIDE, GUIDATA, GUIHANDLES

% Edit the above text to modify the response to help Simple_GUI

% Last Modified by GUIDE v2.5 26-Mar-2017 19:34:39

% Begin initialization code - DO NOT EDIT
gui_Singleton = 1;
gui_State = struct('gui_Name',       mfilename, ...
                  'gui_Singleton',   gui_Singleton, ...
                  'gui_OpeningFcn', @Simple_GUI_OpeningFcn, ...
                  'gui_OutputFcn',  @Simple_GUI_OutputFcn, ...
                  'gui_LayoutFcn',  [], ...
                  'gui_Callback',    []);
if nargin && ischar(varargin{1})
    gui_State.gui_Callback = str2func(varargin{1});
end

if nargout
    [varargout{1:nargout}] = gui_mainfcn(gui_State, varargin{:});
else
    gui_mainfcn(gui_State, varargin{:});
end
% End initialization code - DO NOT EDIT

% --- Executes just before Simple_GUI is made visible.
function Simple_GUI_OpeningFcn(hObject, eventdata, handles, varargin)
handles.output = hObject;
guidata(hObject, handles);
% UIWAIT makes Simple_GUI wait for user response (see UIRESUME)
% uiwait(handles.figure1);

% -- OPENING PAGE
```

```

set(handles.axesopen,'visible','on'); %big picture on the right with turbine and
jack-up units explanation
axes(handles.axesopen);
image=imread('opening.png');
imshow(image);

% --Additional input data (time / tower transportation)
set(handles.uipaneltime,'visible','off');
set(handles.uibuttongrouptowmode,'visible','off');
% Simulation (methods) panels
set(handles.uipanelBE,'visible','off');
set(handles.uipanelROT,'visible','off');
set(handles.uipanelSP,'visible','off');

% -- TOWER SPLIT INITIAL/DEFAULT MODE--
H_tow=str2num(get(handles.inputHtow,'string'));
set(handles.inputHconn,'String',H_tow,'Enable','off');
set(handles.inputWconn,'String',0,'Enable','off')
set(handles.textHconn,'Enable','off');
set(handles.textWconn,'Enable','off');

% -- DEFAULT MODE BE METHOD
set(handles.inputTransvLongLimitBE,'Enable','on','String','');
set(handles.inputxyCoGpositionBE,'Enable','off','String',0);
set(handles.textxyCoGposition,'Enable','off');

function varargout = Simple_GUI_OutputFcn(hObject, eventdata, handles)
varargout{1} = handles.output;

function inputLcrane_Callback(hObject, eventdata, handles)
function inputLcrane_CreateFcn(hObject, eventdata, handles)
if ispc && isequal(get(hObject,'BackgroundColor'),
get(0,'defaultUicontrolBackgroundColor'))
    set(hObject,'BackgroundColor','white');
end

function inputMaxLoadcrane_Callback(hObject, eventdata, handles)
function inputMaxLoadcrane_CreateFcn(hObject, eventdata, handles)
if ispc && isequal(get(hObject,'BackgroundColor'),
get(0,'defaultUicontrolBackgroundColor'))
    set(hObject,'BackgroundColor','white');
end

function inputJspeed_Callback(hObject, eventdata, handles)
function inputJspeed_CreateFcn(hObject, eventdata, handles)
if ispc && isequal(get(hObject,'BackgroundColor'),
get(0,'defaultUicontrolBackgroundColor'))
    set(hObject,'BackgroundColor','white');
end

function inputJdepth_Callback(hObject, eventdata, handles)
function inputJdepth_CreateFcn(hObject, eventdata, handles)
if ispc && isequal(get(hObject,'BackgroundColor'),
get(0,'defaultUicontrolBackgroundColor'))
    set(hObject,'BackgroundColor','white');
end

function inputSpeed_Callback(hObject, eventdata, handles)
function inputSpeed_CreateFcn(hObject, eventdata, handles)

```

```

if ispc && isequal(get(hObject,'BackgroundColor'),
get(0,'defaultUicontrolBackgroundColor'))
    set(hObject,'BackgroundColor','white');
end

function inputMaxLoaddeck_Callback(hObject, eventdata, handles)
function inputMaxLoaddeck_CreateFcn(hObject, eventdata, handles)
if ispc && isequal(get(hObject,'BackgroundColor'),
get(0,'defaultUicontrolBackgroundColor'))
    set(hObject,'BackgroundColor','white');
end

function inputLoaddeck_Callback(hObject, eventdata, handles)
function inputLoaddeck_CreateFcn(hObject, eventdata, handles)
if ispc && isequal(get(hObject,'BackgroundColor'),
get(0,'defaultUicontrolBackgroundColor'))
    set(hObject,'BackgroundColor','white');
end

function inputAdeck_Callback(hObject, eventdata, handles)
function inputAdeck_CreateFcn(hObject, eventdata, handles)
if ispc && isequal(get(hObject,'BackgroundColor'),
get(0,'defaultUicontrolBackgroundColor'))
    set(hObject,'BackgroundColor','white');
end

function inputB_Callback(hObject, eventdata, handles)
function inputB_CreateFcn(hObject, eventdata, handles)
if ispc && isequal(get(hObject,'BackgroundColor'),
get(0,'defaultUicontrolBackgroundColor'))
    set(hObject,'BackgroundColor','white');
end

function inputL_Callback(hObject, eventdata, handles)
function inputL_CreateFcn(hObject, eventdata, handles)
if ispc && isequal(get(hObject,'BackgroundColor'),
get(0,'defaultUicontrolBackgroundColor'))
    set(hObject,'BackgroundColor','white');
end

function inputDepthFarm_Callback(hObject, eventdata, handles)
function inputDepthFarm_CreateFcn(hObject, eventdata, handles)
if ispc && isequal(get(hObject,'BackgroundColor'),
get(0,'defaultUicontrolBackgroundColor'))
    set(hObject,'BackgroundColor','white');
end

function inputDistanceTrb_Callback(hObject, eventdata, handles)
function inputDistanceTrb_CreateFcn(hObject, eventdata, handles)
if ispc && isequal(get(hObject,'BackgroundColor'),
get(0,'defaultUicontrolBackgroundColor'))
    set(hObject,'BackgroundColor','white');
end

function inputDistancePort_Callback(hObject, eventdata, handles)
function inputDistancePort_CreateFcn(hObject, eventdata, handles)
if ispc && isequal(get(hObject,'BackgroundColor'),
get(0,'defaultUicontrolBackgroundColor'))
    set(hObject,'BackgroundColor','white');
end

```



```

function inputNtrb_Callback(hObject, eventdata, handles)
function inputNtrb_CreateFcn(hObject, eventdata, handles)
if ispc && isequal(get(hObject,'BackgroundColor'),
get(0,'defaultUicontrolBackgroundColor'))
    set(hObject,'BackgroundColor','white');
end

function inputWbla_Callback(hObject, eventdata, handles)
function inputWbla_CreateFcn(hObject, eventdata, handles)
if ispc && isequal(get(hObject,'BackgroundColor'),
get(0,'defaultUicontrolBackgroundColor'))
    set(hObject,'BackgroundColor','white');
end

function inputDbra_Callback(hObject, eventdata, handles)
function inputDbra_CreateFcn(hObject, eventdata, handles)
if ispc && isequal(get(hObject,'BackgroundColor'),
get(0,'defaultUicontrolBackgroundColor'))
    set(hObject,'BackgroundColor','white');
end

function inputLbla_Callback(hObject, eventdata, handles)
function inputLbla_CreateFcn(hObject, eventdata, handles)
if ispc && isequal(get(hObject,'BackgroundColor'),
get(0,'defaultUicontrolBackgroundColor'))
    set(hObject,'BackgroundColor','white');
end

function inputNbla_Callback(hObject, eventdata, handles)
function inputNbla_CreateFcn(hObject, eventdata, handles)
if ispc && isequal(get(hObject,'BackgroundColor'),
get(0,'defaultUicontrolBackgroundColor'))
    set(hObject,'BackgroundColor','white');
end

function inputWhub_Callback(hObject, eventdata, handles)
function inputWhub_CreateFcn(hObject, eventdata, handles)
if ispc && isequal(get(hObject,'BackgroundColor'),
get(0,'defaultUicontrolBackgroundColor'))
    set(hObject,'BackgroundColor','white');
end

function inputDhub_Callback(hObject, eventdata, handles)
function inputDhub_CreateFcn(hObject, eventdata, handles)
if ispc && isequal(get(hObject,'BackgroundColor'),
get(0,'defaultUicontrolBackgroundColor'))
    set(hObject,'BackgroundColor','white');
end

function inputLhub_Callback(hObject, eventdata, handles)
function inputLhub_CreateFcn(hObject, eventdata, handles)
if ispc && isequal(get(hObject,'BackgroundColor'),
get(0,'defaultUicontrolBackgroundColor'))
    set(hObject,'BackgroundColor','white');
end

function inputWnac_Callback(hObject, eventdata, handles)
function inputWnac_CreateFcn(hObject, eventdata, handles)

```

```

if ispc && isequal(get(hObject,'BackgroundColor'),
get(0,'defaultUicontrolBackgroundColor'))
    set(hObject,'BackgroundColor','white');
end

function inputBnac_Callback(hObject, eventdata, handles)
function inputBnac_CreateFcn(hObject, eventdata, handles)
if ispc && isequal(get(hObject,'BackgroundColor'),
get(0,'defaultUicontrolBackgroundColor'))
    set(hObject,'BackgroundColor','white');
end

function inputInac_Callback(hObject, eventdata, handles)
function inputInac_CreateFcn(hObject, eventdata, handles)
if ispc && isequal(get(hObject,'BackgroundColor'),
get(0,'defaultUicontrolBackgroundColor'))
    set(hObject,'BackgroundColor','white');
end

function inputWtow_Callback(hObject, eventdata, handles)
function inputWtow_CreateFcn(hObject, eventdata, handles)
if ispc && isequal(get(hObject,'BackgroundColor'),
get(0,'defaultUicontrolBackgroundColor'))
    set(hObject,'BackgroundColor','white');
end

function inputThickTop_Callback(hObject, eventdata, handles)
function inputThickTop_CreateFcn(hObject, eventdata, handles)
if ispc && isequal(get(hObject,'BackgroundColor'),
get(0,'defaultUicontrolBackgroundColor'))
    set(hObject,'BackgroundColor','white');
end

function inputThickBase_Callback(hObject, eventdata, handles)
function inputThickBase_CreateFcn(hObject, eventdata, handles)
if ispc && isequal(get(hObject,'BackgroundColor'),
get(0,'defaultUicontrolBackgroundColor'))
    set(hObject,'BackgroundColor','white');
end

function inputDtowTop_Callback(hObject, eventdata, handles)
function inputDtowTop_CreateFcn(hObject, eventdata, handles)
if ispc && isequal(get(hObject,'BackgroundColor'),
get(0,'defaultUicontrolBackgroundColor'))
    set(hObject,'BackgroundColor','white');
end

function inputDtowBase_Callback(hObject, eventdata, handles)
function inputDtowBase_CreateFcn(hObject, eventdata, handles)
if ispc && isequal(get(hObject,'BackgroundColor'),
get(0,'defaultUicontrolBackgroundColor'))
    set(hObject,'BackgroundColor','white');
end

function inputHtow_Callback(hObject, eventdata, handles)
function inputHtow_CreateFcn(hObject, eventdata, handles)
if ispc && isequal(get(hObject,'BackgroundColor'),
get(0,'defaultUicontrolBackgroundColor'))
    set(hObject,'BackgroundColor','white');
end

```

```

function inputAng_Callback(hObject, eventdata, handles)
function inputAng_CreateFcn(hObject, eventdata, handles)
if ispc && isequal(get(hObject,'BackgroundColor'),
get(0,'defaultUicontrolBackgroundColor'))
    set(hObject,'BackgroundColor','white');
end

function inputDepthPort_Callback(hObject, eventdata, handles)
function inputDepthPort_CreateFcn(hObject, eventdata, handles)
if ispc && isequal(get(hObject,'BackgroundColor'),
get(0,'defaultUicontrolBackgroundColor'))
    set(hObject,'BackgroundColor','white');
end

function inputMaxLoadportcrane_Callback(hObject, eventdata, handles)
function inputMaxLoadportcrane_CreateFcn(hObject, eventdata, handles)
if ispc && isequal(get(hObject,'BackgroundColor'),
get(0,'defaultUicontrolBackgroundColor'))
    set(hObject,'BackgroundColor','white');
end

function inputHconn_Callback(hObject, eventdata, handles)
function inputHconn_CreateFcn(hObject, eventdata, handles)
if ispc && isequal(get(hObject,'BackgroundColor'),
get(0,'defaultUicontrolBackgroundColor'))
    set(hObject,'BackgroundColor','white');
end

function inputWconn_Callback(hObject, eventdata, handles)
function inputWconn_CreateFcn(hObject, eventdata, handles)
if ispc && isequal(get(hObject,'BackgroundColor'),
get(0,'defaultUicontrolBackgroundColor'))
    set(hObject,'BackgroundColor','white');
end

function inputTportBE_Callback(hObject, eventdata, handles)
function inputTportBE_CreateFcn(hObject, eventdata, handles)
if ispc && isequal(get(hObject,'BackgroundColor'),
get(0,'defaultUicontrolBackgroundColor'))
    set(hObject,'BackgroundColor','white');
end

function inputTportROT_Callback(hObject, eventdata, handles)
function inputTportROT_CreateFcn(hObject, eventdata, handles)
if ispc && isequal(get(hObject,'BackgroundColor'),
get(0,'defaultUicontrolBackgroundColor'))
    set(hObject,'BackgroundColor','white');
end

function inputTportSP_Callback(hObject, eventdata, handles)
function inputTportSP_CreateFcn(hObject, eventdata, handles)
if ispc && isequal(get(hObject,'BackgroundColor'),
get(0,'defaultUicontrolBackgroundColor'))
    set(hObject,'BackgroundColor','white');
end

function inputTbe_Callback(hObject, eventdata, handles)
function inputTbe_CreateFcn(hObject, eventdata, handles)

```

```

if ispc && isequal(get(hObject,'BackgroundColor'),
get(0,'defaultUicontrolBackgroundColor'))
    set(hObject,'BackgroundColor','white');
end

function inputTbla_Callback(hObject, eventdata, handles)
function inputTbla_CreateFcn(hObject, eventdata, handles)
if ispc && isequal(get(hObject,'BackgroundColor'),
get(0,'defaultUicontrolBackgroundColor'))
    set(hObject,'BackgroundColor','white');
end

function inputTnac_Callback(hObject, eventdata, handles)
function inputTnac_CreateFcn(hObject, eventdata, handles)
if ispc && isequal(get(hObject,'BackgroundColor'),
get(0,'defaultUicontrolBackgroundColor'))
    set(hObject,'BackgroundColor','white');
end

function inputTtow_Callback(hObject, eventdata, handles)
function inputTtow_CreateFcn(hObject, eventdata, handles)
if ispc && isequal(get(hObject,'BackgroundColor'),
get(0,'defaultUicontrolBackgroundColor'))
    set(hObject,'BackgroundColor','white');
end

function inputTrot_Callback(hObject, eventdata, handles)
function inputTrot_CreateFcn(hObject, eventdata, handles)
if ispc && isequal(get(hObject,'BackgroundColor'),
get(0,'defaultUicontrolBackgroundColor'))
    set(hObject,'BackgroundColor','white');
end

function inputTwork_Callback(hObject, eventdata, handles)
function inputTwork_CreateFcn(hObject, eventdata, handles)
if ispc && isequal(get(hObject,'BackgroundColor'),
get(0,'defaultUicontrolBackgroundColor'))
    set(hObject,'BackgroundColor','white');
end

function inputNbblastrBE_Callback(hObject, eventdata, handles)
function inputNbblastrBE_CreateFcn(hObject, eventdata, handles)
if ispc && isequal(get(hObject,'BackgroundColor'),
get(0,'defaultUicontrolBackgroundColor'))
    set(hObject,'BackgroundColor','white');
end

function inputTransvLongLimitBE_Callback(hObject, eventdata, handles)
function inputTransvLongLimitBE_CreateFcn(hObject, eventdata, handles)
if ispc && isequal(get(hObject,'BackgroundColor'),
get(0,'defaultUicontrolBackgroundColor'))
    set(hObject,'BackgroundColor','white');
end

function inputxyCoGpositionBE_Callback(hObject, eventdata, handles)
function inputxyCoGpositionBE_CreateFcn(hObject, eventdata, handles)
if ispc && isequal(get(hObject,'BackgroundColor'),
get(0,'defaultUicontrolBackgroundColor'))
    set(hObject,'BackgroundColor','white');
end

```

```

function inputLreinforcement_Callback(hObject, eventdata, handles)
function inputLreinforcement_CreateFcn(hObject, eventdata, handles)
if ispc && isequal(get(hObject,'BackgroundColor'),
get(0,'defaultUicontrolBackgroundColor'))
    set(hObject,'BackgroundColor','white');
end

```

```

function inputLongLimitROT_Callback(hObject, eventdata, handles)
function inputLongLimitROT_CreateFcn(hObject, eventdata, handles)
if ispc && isequal(get(hObject,'BackgroundColor'),
get(0,'defaultUicontrolBackgroundColor'))
    set(hObject,'BackgroundColor','white');
end

```

```

function inputTransvLimitROT_Callback(hObject, eventdata, handles)
function inputTransvLimitROT_CreateFcn(hObject, eventdata, handles)
if ispc && isequal(get(hObject,'BackgroundColor'),
get(0,'defaultUicontrolBackgroundColor'))
    set(hObject,'BackgroundColor','white');
end

```

```

function inputNmaxrotors_Callback(hObject, eventdata, handles)
function inputNmaxrotors_CreateFcn(hObject, eventdata, handles)
if ispc && isequal(get(hObject,'BackgroundColor'),
get(0,'defaultUicontrolBackgroundColor'))
    set(hObject,'BackgroundColor','white');
end

```

```

function inputNbblastrSP_Callback(hObject, eventdata, handles)
function inputNbblastrSP_CreateFcn(hObject, eventdata, handles)
if ispc && isequal(get(hObject,'BackgroundColor'),
get(0,'defaultUicontrolBackgroundColor'))
    set(hObject,'BackgroundColor','white');
end

```

```

%-----

```

```

% --- Executes on button press in SUBMIT_DATA_pushbtn.
function SUBMIT_DATA_pushbtn_Callback(hObject, eventdata, handles)

```

```

%-----

```

```

% Input data

```

```

%-----

```

```

% --Turbine--

```

```

H_tow=str2num(get(handles.inputHtow,'string'));
D_towBase=str2num(get(handles.inputDtowBase,'string'));
D_towTop=str2num(get(handles.inputDtowTop,'string'));
W_tow=str2num(get(handles.inputWtow,'string'));
L_nac=str2num(get(handles.inputLnac,'string'));
B_nac=str2num(get(handles.inputBnac,'string'));
W_nac=str2num(get(handles.inputWnac,'string'));
L_hub=str2num(get(handles.inputLhub,'string'));
D_hub=str2num(get(handles.inputDhub,'string'));
W_hub=str2num(get(handles.inputWhub,'string'));
N_bla=str2num(get(handles.inputNbla,'string'));
L_bla=str2num(get(handles.inputLbla,'string'));

```

```

D_bla=str2num(get(handles.inputDbla,'string'));
W_bla=str2num(get(handles.inputWbla,'string'));
% --Site (farm/port)--
Ntrb_farm=str2num(get(handles.inputNtrb,'string'));
DS_port=str2num(get(handles.inputDistancePort,'string'));      %(km or miles) to
decide
DS_trb=str2num(get(handles.inputDistanceTrb,'string'));
DP_farm=str2num(get(handles.inputDepthFarm,'string'));
DP_port=str2num(get(handles.inputDepthPort,'string'));
MaxLoad_port=str2num(get(handles.inputMaxLoadportcrane,'string'));
% --Vessel/barge--
L=str2num(get(handles.inputL,'string'));
B=str2num(get(handles.inputB,'string'));
A_deck=str2num(get(handles.inputAdeck,'string'));
ConLoad_deck=str2num(get(handles.inputLoaddeck,'string'));
MaxLoad_deck=str2num(get(handles.inputMaxLoaddeck,'string'));
speed=str2num(get(handles.inputSpeed,'string'));                %(kn)
Jdepth=str2num(get(handles.inputJdepth,'string'));
Jspeed=str2num(get(handles.inputJspeed,'string'));              %(m/min)
MaxLoad_crane=str2num(get(handles.inputMaxLoadcrane,'string'));
L_crane=str2num(get(handles.inputLcrane,'string'));
Ang_crane=str2num(get(handles.inputAng,'string'));

%-----
% Check input data
%-----

W_1trb=W_tow+W_nac+W_hub+N_bla*W_bla;
MaxAperture_crane=L_crane*sin(Ang_crane*pi/180);
if N_bla~=3 && N_bla~=2      % Blades (if 2 or 3 blades)
    errordlg('3 or 2 bladed wind turbines cases only')
    error('3 or 2 bladed wind turbines cases only');
elseif W_1trb>MaxLoad_deck    % Preliminary check tot weight on deck
    errordlg('The vessel cannot (even) load one turbine on the deck','Error');
    error('The vessel cannot (even) load one turbine on the deck');
elseif L_bla>H_tow           % Dimension checks
    errordlg('Error in the dimension of the blades (longer than the
tower)','Error');
    error('Error in the dimension of the blades (longer than the tower)');
elseif D_towBase<D_towTop    % Tower shape
    errordlg('Error in the dimension of the tower (lower diameter has to be
bigger than the upper)','Error');
    error('Error in the dimension of the tower (lower diameter has to be bigger
than the upper)');
elseif Jdepth<DP_farm        % Depth of the farm
    errordlg('The jack-up unit cannot reach the farm depth','Error');
    error('The jack-up unit cannot reach the farm depth');
elseif Jdepth<DP_port        % Depth of the port
    errordlg('The jack-up unit cannot reach the farm port','Error');
    error('The jack-up unit cannot reach the farm port');
else                          % IF EVERYTHING IS OK
    % Additional input data (time / tower transportation)
    set(handles.uipaneltime,'visible','on');
    set(handles.uibuttongrouptowmode,'visible','on');
    % Images
    cla(handles.axesopen);
    set(handles.axesopen,'visible','off');
    set(handles.axesturbine,'visible','on');
    axes(handles.axesturbine);
    image_turbine=imread('turbine.png');
    imshow(image_turbine);

```

```

set(handles.axesvessel, 'visible', 'on');
axes(handles.axesvessel);
image_vessel=imread('vessel.png');
imshow(image_vessel);
set(handles.axesbarge, 'visible', 'on');
axes(handles.axesbarge);
image_barge=imread('barge.png');
imshow(image_barge);
if W_tow>MaxLoad_crane
    msgbox('Attention! Jack-up crane cannot lift the weight of the whole
tower: split the tower in two elements','Warning')
    warning('Split the tower in two elements (due to jack-up crane)')
elseif W_tow>MaxLoad_port
    msgbox('Attention! Port crane cannot lift the weight of the whole tower:
split the tower in two elements','Warning')
    warning('Split the tower in two elements (due to port crane)')
elseif MaxAperture_crane<H_tow
    msgbox('Crane cannot lift the whole tower (height issue): split the
tower in two elements the select','Warning')
    warning('Split the tower in two elements (tower height)')
else
    msgbox('The whole tower trasportation is possible and
suggested','Message')
    warning('The whole tower trasportation is possible and suggested')
end
msgbox('Data insered are correct! Fill in now the time variables and the
tower transportation mode as suggested')
end

%-----
% --- Executes when selected object is changed in uibuttongrouptowmode (TOWER
SPLIT)
function uibuttongrouptowmode_SelectionChangedFcn(hObject, eventdata, handles)
%-----
%-----
H_tow=str2num(get(handles.inputHtow, 'string'));

selectiontowmode=get(handles.uibuttongrouptowmode, 'SelectedObject');
choicetowmode=get(selectiontowmode, 'string');
switch choicetowmode
    case 'one piece'
        set(handles.inputHconn, 'String', H_tow, 'Enable', 'off');
        set(handles.inputWconn, 'String', 0, 'Enable', 'off');
        set(handles.textHconn, 'Enable', 'off');
        set(handles.textWconn, 'Enable', 'off');
    case 'two pieces'
        set(handles.inputHconn, 'Enable', 'on', 'String', '');
        set(handles.inputWconn, 'Enable', 'on', 'String', '');
        set(handles.textHconn, 'Enable', 'on');
        set(handles.textWconn, 'Enable', 'on');
end

%-----
% --- Executes when selected object is changed in uibuttongroupBEMode (BE MODE)
function uibuttongroupBEMode_SelectionChangedFcn(hObject, eventdata, handles)
%-----
%-----
selectionBEMode=get(handles.uibuttongroupBEMode, 'SelectedObject');
choiceBEMode=get(selectionBEMode, 'string');

```

```

switch choiceBEmode
    case 'Transverse'
        set(handles.inputTransvLongLimitBE,'String','');
        set(handles.textTransvLongLimit,'String','Transv. overboard limit [m]');
        set(handles.inputxyCoGpositionBE,'Enable','off','String',0);
        set(handles.textxyCoGposition,'Enable','off','String','BE y-CoG on jack-
up unit [m]','Visible','on');
    case 'Longitudinal'
        set(handles.inputTransvLongLimitBE,'String','');
        set(handles.textTransvLongLimit,'String','Long. overboard limit [m]');
        set(handles.inputxyCoGpositionBE,'Enable','on','String','');
        set(handles.textxyCoGposition,'Enable','on','String','BE x-CoG on jack-
up unit [m] (set at L jack-up if unknown)');
end

%-----
% --- Executes when selected object is changed in uibuttongroupROTmode.
function uibuttongroupROTmode_SelectionChangedFcn(hObject, eventdata, handles)
%-----

N_bla=str2num(get(handles.inputNbla,'string'));
selectionROTmode=get(handles.uibuttongroupROTmode,'SelectedObject');
choiceROTmode=get(selectionROTmode,'string');
switch choiceROTmode
    case 'Mode 1'
        if N_bla==3
            set(handles.inputTransvLimitROT,'Enable','on','String','');
            set(handles.inputLongLimitROT,'Enable','on','String','');
        else
            set(handles.inputTransvLimitROT,'Enable','on','String','');
            set(handles.inputLongLimitROT,'Enable','off','String',0);
        end
    case 'Mode 2'
        if N_bla==3
            set(handles.inputTransvLimitROT,'Enable','on','String','');
            set(handles.inputLongLimitROT,'Enable','on','String','');
        else
            set(handles.inputTransvLimitROT,'Enable','off','String',0);
            set(handles.inputLongLimitROT,'Enable','on','String','');
        end
end

%-----

% --- Executes on button press in GO_TO_SIMULATION_pushbtn (go to simulation).
function GO_TO_SIMULATION_pushbtn_Callback(hObject, eventdata, handles)

%-----

% Checks (times - cranes/tower split)
%-----

H_tow=str2num(get(handles.inputHtow,'string'));
W_tow=str2num(get(handles.inputWtow,'string'));
H_conn=str2num(get(handles.inputHconn,'string'));
W_conn=str2num(get(handles.inputWconn,'string')); % for the check =
W_towConn in each method function
MaxLoad_port=str2num(get(handles.inputMaxLoadportcrane,'string'));
MaxLoad_crane=str2num(get(handles.inputMaxLoadcrane,'string'));

```



```

% --Tower --
if H_conn>H_tow
    errordlg('Tower second piece cannot be higher than the tower
    itself!','Error');
    error('Tower second piece cannot be higher than the tower itself!');
elseif H_conn==0
    errordlg('If tower is wanted in one piece set the "one piece" radio
    button','Error');
    error('If tower in one piece wanted, re-insert tower height (not 0)');
elseif W_conn>W_tow
    errordlg('Tower second piece is heavier than the tower itself','Error');
    error('Tower second piece is heavier than the tower itself');
elseif H_conn==H_tow && W_conn~=0 % reminder: set W_conn=0
    errordlg('Tower in one piece, so the weight of the second piece is not
    required. Change push button or value, consequently','Error');
    error('Tower in one piece, so the weight of the second piece is not
    required. Change push button or value, consequently');
end
% --Crane checks (splitting or not)--
L_crane=str2num(get(handles.inputLcrane,'string'));
Ang_crane=str2num(get(handles.inputAng,'string'));
MaxAperture_crane=L_crane*sin(Ang_crane*pi/180);
% Tower height checks
if MaxAperture_crane<H_tow
    errordlg('Jack-up crane cannot lift the whole tower (height issue): split
    the tower in two elements the select','Error');
    error('Split the tower in two elements (due to jack-up crane hook maximum
    height)');
elseif MaxAperture_crane<H_conn
    errordlg('Jack-up crane cannot lift the lower tower piece (height issue):
    reduce the element height','Error');
    error('Reduce the tower lower piece height');
elseif MaxAperture_crane<(H_tow-H_conn)
    errordlg('Jack-up crane cannot lift the upper tower piece (height issue):
    reduce the element height','Error');
    error('Reduce the tower upper piece height');
end
% Tower weight checks
if W_tow>MaxLoad_crane
    errordlg('Jack-up crane cannot lift the weight of the whole tower: split the
    tower in two elements','Error')
    error('Split the tower in two elements (due to jack-up crane)')
elseif W_tow>MaxLoad_port
    errordlg('Port crane cannot lift the weight of the whole tower: split the
    tower in two elements','Error')
    error('Split the tower in two elements (due to port crane)')
end
% Other cranes (jack-up/port) checks inside each method function

%-----
% Now show
%-----

% -- Simulations panels
set(handles.uipanelBE,'visible','on');
set(handles.uipanelROT,'visible','on');
set(handles.uipanelSP,'visible','on');

% -- Images methods off
set(handles.axesBE,'Visible','off');
set(handles.axesROT,'Visible','off');

```

```

set(handles.axesSP, 'Visible', 'off');
% Blades cage exemplification
set(handles.axes cage, 'Visible', 'on');
axes(handles.axes cage);
image=imread('cage.png');
imshow(image);

% Number of blades for layer for BE method
N_bla=str2num(get(handles.inputNbla, 'string'));
set(handles.inputNblastrBE, 'String', '', 'Enable', 'on');
if N_bla==2
    set(handles.inputNblastrBE, 'String', 0, 'Enable', 'off');
end
% Default method rotor
flag_model=get(handles.radiobtnROT1, 'Value');
if flag_model==1
    if N_bla==3
        set(handles.inputTransvLimitROT, 'Enable', 'on', 'String', '');
        set(handles.inputLongLimitROT, 'Enable', 'on', 'String', '');
    else
        set(handles.inputTransvLimitROT, 'Enable', 'on', 'String', '');
        set(handles.inputLongLimitROT, 'Enable', 'off', 'String', 0);
    end
else
    if N_bla==3
        set(handles.inputTransvLimitROT, 'Enable', 'on', 'String', '');
        set(handles.inputLongLimitROT, 'Enable', 'on', 'String', '');
    else
        set(handles.inputTransvLimitROT, 'Enable', 'off', 'String', 0);
        set(handles.inputLongLimitROT, 'Enable', 'on', 'String', '');
    end
end
end

%-----

% --- Executes on button press in SIMULATE_BE.
function SIMULATE_BE_Callback(hObject, eventdata, handles)

%-----

% BE Input data
%-----

% --Fitting--
H_tow=str2num(get(handles.inputHtow, 'string'));
D_towTop=str2num(get(handles.inputDtowTop, 'string'));
D_towBase=str2num(get(handles.inputDtowBase, 'string'));
t_towTop=str2num(get(handles.inputThickTop, 'string'));
t_towBase=str2num(get(handles.inputThickBase, 'string'));
W_tow=str2num(get(handles.inputWtow, 'string'));
H_conn=str2num(get(handles.inputHconn, 'string')); % Tower split flag
W_conn=str2num(get(handles.inputWconn, 'string')); % for the check =
W_towConn in BE function
L_nac=str2num(get(handles.inputLnac, 'string'));
B_nac=str2num(get(handles.inputBnac, 'string'));
W_nac=str2num(get(handles.inputWnac, 'string'));
L_hub=str2num(get(handles.inputLhub, 'string'));
D_hub=str2num(get(handles.inputDhub, 'string'));
W_hub=str2num(get(handles.inputWhub, 'string'));
N_bla=str2num(get(handles.inputNbla, 'string'));

```

```

if N_bla==3
    alfa=30*pi/180;
elseif N_bla==2
    alfa=0;
    N_blastr=0;
end
L_bla=str2num(get(handles.inputLbla,'string'));
D_bla=str2num(get(handles.inputDbbla,'string'));
W_bla=str2num(get(handles.inputWbla,'string'));
N_farm=str2num(get(handles.inputNtrb,'string'));
L=str2num(get(handles.inputL,'string'));
B=str2num(get(handles.inputB,'string'));
A_deck=str2num(get(handles.inputAdeck,'string'));
ConLoad_deck=str2num(get(handles.inputLoaddeck,'string'));
MaxLoad_deck=str2num(get(handles.inputMaxLoaddeck,'string'));
MaxLoad_crane=str2num(get(handles.inputMaxLoadcrane,'string'));
L_crane=str2num(get(handles.inputLcrane,'string'));
Ang_crane=str2num(get(handles.inputAng,'string'));
MaxLoad_port=str2num(get(handles.inputMaxLoadportcrane,'string'));

% --Time Calculations--
Ntrb_farm=str2num(get(handles.inputNtrb,'string'));
DS_port=str2num(get(handles.inputDistancePort,'string'));           %(naut. miles)
DS_trb=str2num(get(handles.inputDistanceTrb,'string'));
DP_farm=str2num(get(handles.inputDepthFarm,'string'));
DP_port=str2num(get(handles.inputDepthPort,'string'));
speed=str2num(get(handles.inputSpeed,'string'));                   %(kn)
Jdepth=str2num(get(handles.inputJdepth,'string'));
Jspeed=str2num(get(handles.inputJspeed,'string'));                 %(m/min)
T_portBE=str2num(get(handles.inputTportBE,'string'));              %(hrs/turbine)
T_tow=str2num(get(handles.inputTtow,'string'));                    %(hrs)
T_be=str2num(get(handles.inputTbe,'string'));
T_bla=str2num(get(handles.inputTbla,'string'));
T_workhrs=str2num(get(handles.inputTwork,'string'));

% --BE additional input data--
TransvLong_Limit=str2num(get(handles.inputTransvLongLimitBE,'string')); %
check/procedure inside the BE function
xCoG_position=str2num(get(handles.inputxyCoGpositionBE,'string')); %
check/procedure inside the BE function
N_blastr=str2num(get(handles.inputNblastrBE,'string')); %
assumed value for N_blastr

% Flags
flag_transv=get(handles.radiobtnTran,'Value');
flag_towsplit=get(handles.radiobtnltow,'Value'); % flag=1 => one piece

%-----
% BE images
%-----

if N_bla==3
    if flag_transv==1 && flag_towsplit==1 % model=on
        axes(handles.axesBE);
        image=imread('BE_3bla_transv_1tow.png');
        imshow(image);
    elseif flag_transv==1 && flag_towsplit==0
        axes(handles.axesBE);
        image=imread('BE_3bla_transv_2tow.png');
        imshow(image);
    end
end

```

```

elseif flag_transv==0 && flag_towsplit==1
    axes(handles.axesBE);
    image=imread('BE_3bla_long_1tow.png');
    imshow(image);
elseif flag_transv==0 && flag_towsplit==0
    axes(handles.axesBE);
    image=imread('BE_3bla_long_2tow.png');
    imshow(image);
end
else
    if flag_transv==1 && flag_towsplit==1 % model=on
        axes(handles.axesBE);
        image=imread('BE_2bla_transv_1tow.png');
        imshow(image);
    elseif flag_transv==1 && flag_towsplit==0
        axes(handles.axesBE);
        image=imread('BE_2bla_transv_2tow.png');
        imshow(image);
    elseif flag_transv==0 && flag_towsplit==1
        axes(handles.axesBE);
        image=imread('BE_2bla_long_1tow.png');
        imshow(image);
    elseif flag_transv==0 && flag_towsplit==0
        axes(handles.axesBE);
        image=imread('BE_2bla_long_2tow.png');
        imshow(image);
    end
end
end

%-----
% BE Checks
%-----

% Bunny ear COG position on the deck check inside the BE function
if TransvLong_Limit<0 || xCoG_position<0
    errordlg('Assign positive values to overboard limits and/or BE pre-assembly
CoG position from the aft','Attention!');
    error('Assign positive values to overboard limits and/or BE pre-assembly CoG
position from the aft');
end
% Blade cage layer (no. of blades)
if N_blastr~=fix(N_blastr)
    errordlg('The no. of blades per layer in the cage structure has to be an
integer positive (not 0) number','Attention!');
    error('The no. of blades has to be an integer positive (not 0) number');
end

%-----
% BE Conversions
%-----

t_towTop=t_towTop*10^(-3); % from (mm) to(m)
t_towBase=t_towBase*10^(-3);
speed=0.5144*speed*60; % from (kn) to (m/min)
DS_port=DS_port*1852; % from (naut. miles) to (m)
T_portBE=T_portBE*60; % from (hrs/turbine) to (min/turbine) %
T_portROT; % T_portSP;
T_be=T_be*60; % from (hrs) to (min)
T_bla=T_bla*60;
T_tow=T_tow*60; %T_rot=T_rot*60;%T_nac=T_nac*60;

```

```

%-----
%-----
% BE fitting code
%-----

[AreaEffOcc_BE,WeightOnDeck_BE,NtrbXvoy_BE,MaxLoadLift_BE,hF1,hF2]=...

fittingBE(H_conn,W_conn,TransvLong_Limit,xCoG_position,flag_transv,N_blastr,...

L,B,A_deck,MaxLoad_deck,ConLoad_deck,MaxLoad_crane,MaxLoad_port,H_tow,D_towBase,
D_towTop,t_towTop,t_towBase,W_tow,...
    L_nac,B_nac,W_nac,L_hub,D_hub,W_hub,N_bla,alfa,L_bla,D_bla,W_bla);

set(handles.outputAreaEffOcc_BE,'string',num2str(AreaEffOcc_BE,'%0.2f'));
set(handles.outputWeightOnDeck_BE,'string',num2str(WeightOnDeck_BE,'%0.1f'));
set(handles.outputMaxLoadLift_BE,'string',num2str(MaxLoadLift_BE,'%0.1f'));
set(handles.outputNtrbXvoy_BE,'string',NtrbXvoy_BE);
assignin('base','msg1_fittingBE',hF1)
assignin('base','msg2_fittingBE',hF2)
%-----
%-----
% BE Total no. of lifts
%-----

if N_bla==3
    if flag_towsplit==1
        Nlifts_lasmb1BE=3;      % (1) Bunny ear + (1)tow + (1) 3rd blade
    else      % tower splitted and survived to all the tower split checks
        Nlifts_lasmb1BE=4;      % (1) Bunny ear + (2)tow + (1) 3rd blade
    end
else
    if flag_towsplit==1
        Nlifts_lasmb1BE=2;      % (1) Bunny ear + (1)tow
    else
        Nlifts_lasmb1BE=3;      % (1) Bunny ear + (2)tow
    end
end
Nlift_totBE=Nlifts_lasmb1BE*Ntrb_farm;
set(handles.outputNtotLifts_BE,'string',Nlift_totBE);

%-----
%-----
% BE Time to install the farm
%-----

[T_totBE,T_reqdaysBE]=timeBE(Jspeed,speed,Ntrb_farm,DS_port,DS_trb,DP_port,DP_fa
rm,T_portBE,T_workhrs,T_be,T_bla,T_tow,NtrbXvoy_BE,N_bla,flag_towsplit);
set(handles.outputTotTime_BE,'string',num2str(T_totBE,'%0.1f'));
hT=msgbox(['Minimum number of days for installing the farm (continutive working
days) is ',num2str(T_reqdaysBE,'%0.2f')],'Message');
assignin('base','msg_timeBE',hT)

%-----
%-----
% --- Executes on button press in ClearBE.
function ClearBE_Callback(hObject, eventdata, handles)
%-----
%-----

cla(handles.axesBE);
set(handles.axesBE,'visible','off');

```

```

set(handles.outputAreaEffOcc_BE, 'string', '');
set(handles.outputWeightOnDeck_BE, 'string', '');
set(handles.outputMaxLoadLift_BE, 'string', '');
set(handles.outputNtrbXvoy_BE, 'string', '');
set(handles.outputNtotLifts_BE, 'string', '');
set(handles.outputTotTime_BE, 'string', '');
evalin('base', 'clear all variables')
% Number of blades for layer for BE method
N_bla=str2num(get(handles.inputNbla, 'string'));
set(handles.inputNblastrBE, 'String', '', 'Enable', 'on');
if N_bla==2
    set(handles.inputNblastrBE, 'String', 0, 'Enable', 'off');
end
% Default cleared conditions
flag_transv=get(handles.radiobtnTran, 'Value');
if flag_transv==1 % transv case
    set(handles.inputTransvLongLimitBE, 'String', '');
    set(handles.textTransvLongLimit, 'String', 'Transv. overboard limit [m]');
    set(handles.inputxyCoGpositionBE, 'Enable', 'off', 'String', 0);
    set(handles.textxyCoGposition, 'Enable', 'off', 'String', 'BE y-CoG on jack-up
unit [m]', 'Visible', 'on');
else % long case
    set(handles.inputTransvLongLimitBE, 'String', '');
    set(handles.textTransvLongLimit, 'String', 'Long. overboard limit [m]');
    set(handles.inputxyCoGpositionBE, 'Enable', 'on', 'String', '');
    set(handles.textxyCoGposition, 'Enable', 'on', 'String', 'BE x-CoG on jack-up
unit [m] (set at L jack-up if unknown)');
end

%-----

% --- Executes on button press in SIMULATE_ROT.
function SIMULATE_ROT_Callback(hObject, eventdata, handles)

%-----

% ROT Input data
%-----

% --Fitting--
H_tow=str2num(get(handles.inputHtow, 'string'));
D_towTop=str2num(get(handles.inputDtowTop, 'string'));
D_towBase=str2num(get(handles.inputDtowBase, 'string'));
t_towTop=str2num(get(handles.inputThickTop, 'string'));
t_towBase=str2num(get(handles.inputThickBase, 'string'));
W_tow=str2num(get(handles.inputWtow, 'string'));
H_conn=str2num(get(handles.inputHconn, 'string')); % Tower split
W_conn=str2num(get(handles.inputWconn, 'string')); % for the check =
W_towConn in BE function
L_nac=str2num(get(handles.inputLnac, 'string'));
B_nac=str2num(get(handles.inputBnac, 'string'));
W_nac=str2num(get(handles.inputWnac, 'string'));
L_hub=str2num(get(handles.inputLhub, 'string'));
D_hub=str2num(get(handles.inputDhub, 'string'));
W_hub=str2num(get(handles.inputWhub, 'string'));
N_bla=str2num(get(handles.inputNbla, 'string'));
if N_bla==3
    alfa=30*pi/180;
elseif N_bla==2
    alfa=0;

```

```

end
L_bla=str2num(get(handles.inputLbla,'string'));
D_bla=str2num(get(handles.inputDbbla,'string'));
W_bla=str2num(get(handles.inputWbla,'string'));
N_farm=str2num(get(handles.inputNtrb,'string'));
L=str2num(get(handles.inputL,'string'));
B=str2num(get(handles.inputB,'string'));
A_deck=str2num(get(handles.inputAdeck,'string'));
ConLoad_deck=str2num(get(handles.inputLoaddeck,'string'));
MaxLoad_deck=str2num(get(handles.inputMaxLoaddeck,'string'));
MaxLoad_crane=str2num(get(handles.inputMaxLoadcrane,'string'));
L_crane=str2num(get(handles.inputLcrane,'string'));
Ang_crane=str2num(get(handles.inputAng,'string'));
MaxLoad_port=str2num(get(handles.inputMaxLoadportcrane,'string'));

% --Time Calculations--
Ntrb_farm=str2num(get(handles.inputNtrb,'string'));
DS_port=str2num(get(handles.inputDistancePort,'string'));           %(naut. miles)
DS_trb=str2num(get(handles.inputDistanceTrb,'string'));
DP_farm=str2num(get(handles.inputDepthFarm,'string'));
DP_port=str2num(get(handles.inputDepthPort,'string'));
speed=str2num(get(handles.inputSpeed,'string'));                   %(kn)
Jdepth=str2num(get(handles.inputJdepth,'string'));
Jspeed=str2num(get(handles.inputJspeed,'string'));                 %(m/min)
T_portROT=str2num(get(handles.inputTportROT,'string'));            %(hrs/turbine)
T_tow=str2num(get(handles.inputTtow,'string'));                    %(hrs)
T_nac=str2num(get(handles.inputTnac,'string'));
T_rot=str2num(get(handles.inputTrot,'string'));
T_workhrs=str2num(get(handles.inputTwork,'string'));

% --ROT additional input data--
Transv_Limit=str2num(get(handles.inputTransvLimitROT,'string'));    %
check/procedure inside the ROT function
Long_Limit=str2num(get(handles.inputLongLimitROT,'string'));        %
check/procedure inside the ROT function
L_reinforce=str2num(get(handles.inputLreinforcement,'string'));      % assumed
value for L_reinforce
N_rotMax=str2num(get(handles.inputNmaxrotors,'string'));             % assumed value
for L_reinforce

% Flags
flag_model=get(handles.radiobtnROT1,'Value');
flag_towsplit=get(handles.radiobtn1tow,'Value'); % flag=1 => one piece

%-----
% ROT images
%-----

if N_bla==3
    if flag_model==1 && flag_towsplit==1 % model=on
        axes(handles.axesROT);
        image=imread('ROT_3bla_model_1tow.png');
        imshow(image);
    elseif flag_model==1 && flag_towsplit==0
        axes(handles.axesROT);
        image=imread('ROT_3bla_model_2tow.png');
        imshow(image);
    elseif flag_model==0 && flag_towsplit==1
        axes(handles.axesROT);
        image=imread('ROT_3bla_mode2_1tow.png');

```

```

        imshow(image);
elseif flag_model==0 && flag_towsplit==0
    axes(handles.axesROT);
    image=imread('ROT_3bla_mode2_2tow.png. ');
    imshow(image);
end
else
    if flag_model==1 && flag_towsplit==1 % model=on
        axes(handles.axesROT);
        image=imread('ROT_2bla_model_1tow.png. ');
        imshow(image);
    elseif flag_model==1 && flag_towsplit==0
        axes(handles.axesROT);
        image=imread('ROT_2bla_model_2tow.png. ');
        imshow(image);
    elseif flag_model==0 && flag_towsplit==1
        axes(handles.axesROT);
        image=imread('ROT_2bla_mode2_1tow.png. ');
        imshow(image);
    elseif flag_model==0 && flag_towsplit==0
        axes(handles.axesROT);
        image=imread('ROT_2bla_mode2_2tow.png. ');
        imshow(image);
    end
end
end

%-----
% ROT Checks
%-----

% Bunny ear CoG position on the deck check inside the BE function
if Transv_Limit<0 || Long_Limit<0
    errordlg('Assign positive values to overboard limits and/or BE pre-assembly
CoG position from the aft','Attention!');
    error('Assign positive values to overboard limits and/or BE pre-assembly CoG
position from the aft');
end
% Reinforcement for rotor loading
if L_reinforce<D_hub
    errordlg(['Insert the hub diameter (' ,num2str(D_hub), ') as minimum value for
the rotor loading reinforce structure'],'Attention')
    error('Dimension of the reinforce structure too small')
end

%-----
% ROT Conversions
%-----

t_towTop=t_towTop*10^(-3); % from (mm) to(m)
t_towBase=t_towBase*10^(-3);
speed=0.5144*speed*60; % from (kn) to (m/min)
DS_port=DS_port*1852; % from (naut. miles) to (m)
T_portROT=T_portROT*60; % from (hrs/turbine) to (min/turbine) %
T_portROT; % T_portSP;
T_nac=T_nac*60; % from (hrs) to (min)
T_rot=T_rot*60;
T_tow=T_tow*60;

```



```

%-----
% ROT fitting code
%-----

[AreaEffOcc_ROT,WeightOnDeck_ROT,NtrbXvoy_ROT,MaxLoadLift_ROT,hF0,hF1,hF2]=...

fittingROT(H_conn,W_conn,Transv_Limit,Long_Limit,L_reinforce,N_rotMax,flag_model
,...
    L,B,A_deck,MaxLoad_deck,ConLoad_deck,MaxLoad_crane,MaxLoad_port,...

H_tow,D_towBase,D_towTop,t_towTop,t_towBase,W_tow,L_nac,B_nac,W_nac,D_hub,W_hub,
N_bla,alfa,L_bla,D_bla,W_bla);

set(handles.outputAreaEffOcc_ROT,'string',num2str(AreaEffOcc_ROT,'%0.2f'));
set(handles.outputWeightOnDeck_ROT,'string',num2str(WeightOnDeck_ROT,'%0.1f'));
set(handles.outputMaxLoadLift_ROT,'string',num2str(MaxLoadLift_ROT,'%0.1f'));
set(handles.outputNtrbXvoy_ROT,'string',NtrbXvoy_ROT);
assignin('base','msg0_fittingROT',hF0)
assignin('base','msg1_fittingROT',hF1)
assignin('base','msg2_fittingROT',hF2)
%-----

% ROT Total no. of lifts
%-----

if flag_towsplit==1
    Nlifts_lasmb1ROT=3;      % (1) rotor + (1)tow + (1) nacelle
else % tower splitted and survived to all the tower split checks
    Nlifts_lasmb1ROT=4;      % (1) rotor + (2)tow + (1) nacelle
end
Nlift_totROT=Nlifts_lasmb1ROT*Ntrb_farm;
set(handles.outputNtotLifts_ROT,'string',Nlift_totROT);

%-----

% ROT Time to install the farm
%-----

[T_totROT,T_reqdaysROT]=timeROT(Jspeed,speed,Ntrb_farm,DS_port,DS_trb,DP_port,DP
_farm,T_portROT,T_workhrs,T_rot,T_nac,T_tow,NtrbXvoy_ROT,flag_towsplit);
set(handles.outputTotTime_ROT,'string',num2str(T_totROT,'%0.1f'));
hT=msgbox(['Minimum number of days for installing the farm (continulative working
days) is ',num2str(T_reqdaysROT,'%0.2f')],'Message');
assignin('base','msg_timeROT',hT)

%-----

% --- Executes on button press in ClearROT.
function ClearROT_Callback(hObject, eventdata, handles)
%-----

cla(handles.axesROT);
set(handles.axesROT,'visible','off');
set(handles.outputAreaEffOcc_ROT,'string','');
set(handles.outputWeightOnDeck_ROT,'string','');
set(handles.outputMaxLoadLift_ROT,'string','');
set(handles.outputNtrbXvoy_ROT,'string','');
set(handles.outputNtotLifts_ROT,'string','');
set(handles.outputTotTime_ROT,'string','');
evalin('base','clear all variables')

```

```

% Default method rotor
flag_model=get(handles.radiobtnROT1,'Value');
N_bla=str2num(get(handles.inputNbla,'string'));
if flag_model==1
    if N_bla==3
        set(handles.inputTransvLimitROT,'Enable','on','String','');
        set(handles.inputLongLimitROT,'Enable','on','String','');
    else
        set(handles.inputTransvLimitROT,'Enable','on','String','');
        set(handles.inputLongLimitROT,'Enable','off','String',0);
    end
else
    if N_bla==3
        set(handles.inputTransvLimitROT,'Enable','on','String','');
        set(handles.inputLongLimitROT,'Enable','on','String','');
    else
        set(handles.inputTransvLimitROT,'Enable','off','String',0);
        set(handles.inputLongLimitROT,'Enable','on','String','');
    end
end

%-----

% --- Executes on button press in SIMULATE_SP.
function SIMULATE_SP_Callback(hObject, eventdata, handles)

%-----

% SP Input data
%-----

% --Fitting--
H_tow=str2num(get(handles.inputHtow,'string'));
D_towTop=str2num(get(handles.inputDtowTop,'string'));
D_towBase=str2num(get(handles.inputDtowBase,'string'));
t_towTop=str2num(get(handles.inputThickTop,'string'));
t_towBase=str2num(get(handles.inputThickBase,'string'));
W_tow=str2num(get(handles.inputWtow,'string'));
H_conn=str2num(get(handles.inputHconn,'string'));           % Tower split flag
W_conn=str2num(get(handles.inputWconn,'string'));           % for the check =
W_towConn in BE function
L_nac=str2num(get(handles.inputLnac,'string'));
B_nac=str2num(get(handles.inputBnac,'string'));
W_nac=str2num(get(handles.inputWnac,'string'));
L_hub=str2num(get(handles.inputLhub,'string'));
D_hub=str2num(get(handles.inputDhub,'string'));
W_hub=str2num(get(handles.inputWhub,'string'));
N_bla=str2num(get(handles.inputNbla,'string'));
if N_bla==3
    alfa=30*pi/180;
elseif N_bla==2
    alfa=0;
end
L_bla=str2num(get(handles.inputLbla,'string'));
D_bla=str2num(get(handles.inputDbla,'string'));
W_bla=str2num(get(handles.inputWbla,'string'));
N_farm=str2num(get(handles.inputNtrb,'string'));
L=str2num(get(handles.inputL,'string'));
B=str2num(get(handles.inputB,'string'));
A_deck=str2num(get(handles.inputAdeck,'string'));

```

```

ConLoad_deck=str2num(get(handles.inputLoaddeck,'string'));
MaxLoad_deck=str2num(get(handles.inputMaxLoaddeck,'string'));
MaxLoad_crane=str2num(get(handles.inputMaxLoadcrane,'string'));
L_crane=str2num(get(handles.inputLcrane,'string'));
Ang_crane=str2num(get(handles.inputAng,'string'));
MaxLoad_port=str2num(get(handles.inputMaxLoadportcrane,'string'));

% --Time Calculations--
Ntrb_farm=str2num(get(handles.inputNtrb,'string'));
DS_port=str2num(get(handles.inputDistancePort,'string'));           %(naut. miles)
DS_trb=str2num(get(handles.inputDistanceTrb,'string'));
DP_farm=str2num(get(handles.inputDepthFarm,'string'));
DP_port=str2num(get(handles.inputDepthPort,'string'));
speed=str2num(get(handles.inputSpeed,'string'));                   %(kn)
Jdepth=str2num(get(handles.inputJdepth,'string'));
Jspeed=str2num(get(handles.inputJspeed,'string'));                 %(m/min)
T_portSP=str2num(get(handles.inputTportSP,'string'));              %(hrs/turbine)
T_tow=str2num(get(handles.inputTtow,'string'));                    %(hrs)
T_bla=str2num(get(handles.inputTbla,'string'));
T_nac=str2num(get(handles.inputTnac,'string'));
T_workhrs=str2num(get(handles.inputTwork,'string'));

% --SP additional input data--
N_blastr=str2num(get(handles.inputNblastrSP,'string'));            % assumed value
for N_blastr

% Flags
flag_towsplit=get(handles.radiobtnltow,'Value'); % flag=1 => one piece

%-----
% SP images
%-----

if N_bla==3
    if flag_towsplit==1
        axes(handles.axesSP);
        image=imread('SP_3bla_1tow.png');
        imshow(image);
    elseif flag_towsplit==0
        axes(handles.axesSP);
        image=imread('SP_3bla_2tow.png');
        imshow(image);
    end
else
    if flag_towsplit==1 % model=on
        axes(handles.axesSP);
        image=imread('SP_2bla_1tow.png');
        imshow(image);
    elseif flag_towsplit==0
        axes(handles.axesSP);
        image=imread('SP_2bla_2tow.png');
        imshow(image);
    end
end

%-----
% SP Checks
%-----

```

```

% Blade cage layer (no. of blades)
if N_blastr~=fix(N_blastr) && N_blastr<N_bla
    error('The no. of blades per layer in the cage structure has to be an
positive integer, bigger than the number of blades of one turbine','Attention');
    error('The no. of blades has to be an integer positive (not 0) number');
end

%-----
% SP Conversions
%-----

t_towTop=t_towTop*10^(-3);      % from (mm) to(m)
t_towBase=t_towBase*10^(-3);
speed=0.5144*speed*60;         % from (kn) to (m/min)
DS_port=DS_port*1852;          % from (naut. miles) to (m)
T_portSP=T_portSP*60;          % from (hrs/turbine) to (min/turbine)      %
T_portROT; % T_portSP;
T_nac=T_nac*60;                % from (hrs) to (min)
T_bla=T_bla*60;
T_tow=T_tow*60;                %T_rot=T_rot*60;%T_nac=T_nac*60;

%-----
% SP fitting code
%-----

[AreaEffOcc_SP,WeightOnDeck_SP,NtrbXvoy_SP,MaxLoadLift_SP,hF]=...

fittingSP(H_conn,W_conn,N_blastr,A_deck,MaxLoad_deck,ConLoad_deck,MaxLoad_crane,
MaxLoad_port,...

H_tow,D_towBase,D_towTop,t_towTop,t_towBase,W_tow,L_nac,B_nac,W_nac,L_hub,W_hub,
N_bla,L_bla,D_bla,W_bla);

set(handles.outputAreaEffOcc_SP,'string',num2str(AreaEffOcc_SP,'%0.2f'));
set(handles.outputWeightOnDeck_SP,'string',num2str(WeightOnDeck_SP,'%0.1f'));
set(handles.outputMaxLoadLift_SP,'string',num2str(MaxLoadLift_SP,'%0.1f'));
set(handles.outputNtrbXvoy_SP,'string',NtrbXvoy_SP);
assignin('base','msg_fittingSP',hF)

%-----
% SP Total no. of lifts
%-----

flag_towsplit=get(handles.radiobtnltow,'Value'); % flag=1 => one piece
if N_bla==3
    if flag_towsplit==1
        Nlifts_lasmb1SP=5;      % (1) tow + (3) blades + (1) nacelle+hub
    else % tower splitted and survived to all the tower split checks
        Nlifts_lasmb1SP=6;      % (2) tow + (3) blades + (1) nacelle+hub
    end
else
    if flag_towsplit==1
        Nlifts_lasmb1SP=4;      % (1) tow + (2) blades + (1) nacelle+hub
    else
        Nlifts_lasmb1SP=5;      % (2) tow + (2) blades + (1) nacelle+hub
    end
end
end

```

```

Nlift_totSP=Nlifts_lasmbSP*Ntrb_farm;
set(handles.outputNtotLifts_SP,'string',Nlift_totSP);

%-----
% SP Time to install the farm
%-----

[T_totSP,T_reqdaysSP]=timeSP(Jspeed,speed,Ntrb_farm,DS_port,DS_trb,DP_port,DP_fa
rm,T_portSP,T_workhrs,T_nac,T_bla,T_tow,NtrbXvoy_SP,N_bla,flag_towsplit);
set(handles.outputTotTime_SP,'string',num2str(T_totSP,'%0.1f'));
hT=msgbox(['Minimum number of days for installing the farm (continuative working
days) is ',num2str(T_reqdaysSP,'%0.2f')],'Message');
assignin('base','msg_timeSP',hT);

%-----
% --- Executes on button press in ClearSP.
function ClearSP_Callback(hObject, eventdata, handles)
%-----

cla(handles.axesSP);
set(handles.axesSP,'visible','off');
set(handles.outputAreaEffOcc_SP,'string','');
set(handles.outputWeightOnDeck_SP,'string','');
set(handles.outputMaxLoadLift_SP,'string','');
set(handles.outputNtrbXvoy_SP,'string','');
set(handles.outputNtotLifts_SP,'string','');
set(handles.outputTotTime_SP,'string','');
set(handles.inputNblastrSP,'string','');
evalin('base','clear all variables')

% --- Executes on button press in pushbtnCLEAR_ALL_DATA.
function pushbtnCLEAR_ALL_DATA_Callback(hObject, eventdata, handles)
axes(handles.axesopen);
image=imread('opening.png');
imshow(image);
set(handles.inputHtow,'string','');
set(handles.inputDtowBase,'string','');
set(handles.inputDtowTop,'string','');
set(handles.inputThickTop,'string','');
set(handles.inputThickBase,'string','');
set(handles.inputWtow,'string','');
set(handles.inputLnac,'string','');
set(handles.inputBnac,'string','');
set(handles.inputWnac,'string','');
set(handles.inputLhub,'string','');
set(handles.inputDhub,'string','');
set(handles.inputWhub,'string','');
set(handles.inputNbla,'string','');
set(handles.inputLbla,'string','');
set(handles.inputDbbla,'string','');
set(handles.inputWbla,'string','');
% --Site (farm/port)--
set(handles.inputNtrb,'string','');
set(handles.inputDistancePort,'string','');           %(km or miles) to decide
set(handles.inputDistanceTrb,'string','');
set(handles.inputDepthFarm,'string','');
set(handles.inputDepthPort,'string','');
set(handles.inputMaxLoadportcrane,'string','');

```

```

% --Vessel/barge--
set(handles.inputL,'string','');
set(handles.inputB,'string','');
set(handles.inputAdeck,'string','');
set(handles.inputLoaddeck,'string','');
set(handles.inputMaxLoaddeck,'string','');
set(handles.inputSpeed,'string',''); % (kn)
set(handles.inputJdepth,'string','');
set(handles.inputJspeed,'string',''); % (m/min)
set(handles.inputMaxLoadcrane,'string','');
set(handles.inputLcrane,'string','');
set(handles.inputAng,'string','');

% --Additional input data (time / tower transportation)
set(handles.uipaneltime,'visible','off');
set(handles.uibuttongrouptowmode,'visible','off');
% Simulation (methods) panels
set(handles.uipanelBE,'visible','off');
set(handles.uipanelROT,'visible','off');
set(handles.uipanelSP,'visible','off');

% -- TOWER SPLIT INITIAL/DEFAULT MODE--
H_tow=str2num(get(handles.inputHtow,'string'));
set(handles.inputHconn,'String',H_tow,'Enable','off');
set(handles.inputWconn,'String',0,'Enable','off');
set(handles.textHconn,'Enable','off');
set(handles.textWconn,'Enable','off');

% -- DEFAULT MODE BE METHOD
set(handles.inputTransvLongLimitBE,'Enable','on','String','');
set(handles.inputxyCoGpositionBE,'Enable','off','String',0);
set(handles.textxyCoGposition,'Enable','off');

% set(handles.inputTportSP,'string'); % (hrs/turbine)
% set(handles.inputTtow,'string'); % (hrs)
% set(handles.inputTbla,'string');
% set(handles.inputTnac,'string');
% set(handles.inputTwork,'string');

```

D.2 fittingBE.m

```
function [AreaEffOcc_BE,WeightOnDeck_BE,NtrbXvoy_BE,MaxLoadLift_BE,hF1,hF2]=...

fittingBE(H_conn,W_conn,TransvLong_Limit,xCoG_position,flag_transv,N_blastr,L,B,
A_deck,MaxLoad_deck,ConLoad_deck,MaxLoad_crane,MaxLoad_port,...

H_tow,D_towBase,D_towTop,t_towTop,t_towBase,W_tow,L_nac,B_nac,W_nac,L_hub,D_hub,
W_hub,N_bla,alfa,L_bla,D_bla,W_bla)
disp('BUNNY EAR (BE) PRE-ASSEMBLY METHOD LAUNCHED')
%% TOWER SPLITTING SETUP
%-----

Dint_towTop=D_towTop-2*t_towTop;
Dint_towBase=D_towBase-2*t_towBase;
D_towConn=D_towTop+2*((D_towBase-D_towTop)/2*(H_tow-H_conn))/H_tow;
Dint_towConn=Dint_towTop+2*((Dint_towBase-Dint_towTop)/2*(H_tow-H_conn))/H_tow;
% UN-SPLITTED CASE
if H_conn==H_tow && W_conn==0
    W_towConn=W_conn;
    W_towBase=W_tow;
end
% SPLITTED CASE
if H_conn~=H_tow && W_conn~=0 % known weight of the
transitional piece
    W_towConn=W_conn;
    W_towBase=W_tow-W_conn;
elseif H_conn~=H_tow && W_conn==0 % volume proportionality
to subdivide the weight in 2 pieces
    Vext_towBase=1/12*H_conn*(D_towBase^2+(D_towBase*D_towConn)+D_towConn^2);
    Vext_towConn=1/12*(H_tow-
H_conn)*(D_towConn^2+(D_towTop*D_towConn)+D_towTop^2);
    Vext_towTot=Vext_towBase+Vext_towConn;

Vint_towBase=1/12*H_conn*(Dint_towBase^2+(Dint_towBase*Dint_towConn)+Dint_towCon
n^2);
    Vint_towConn=1/12*(H_tow-
H_conn)*(Dint_towConn^2+(Dint_towTop*Dint_towConn)+Dint_towTop^2);
    Vint_towTot=Vint_towBase+Vint_towConn;
    V_towBase=Vext_towBase-Vint_towBase;
    V_towConn=Vext_towConn-Vint_towConn;
    V_towTot=Vext_towTot-Vint_towTot;
    W_towConn=(W_tow*V_towConn)/V_towTot;
    W_towBase=(W_tow*V_towBase)/V_towTot;
end

%% BE 1TURBINE (trb) FITTING
%-----

% FITTING CONDITIONS
% Tower with/without connection
% Tower with/without connection
% A_towBase=pi*(D_towBase/2)^2;
% A_towConn=pi*(D_towConn/2)^2;
A_towBase=D_towBase^2;
A_towConn=D_towConn^2;
if D_towConn~=D_towTop
    A_tow=A_towConn+A_towBase;
else
    A_tow=A_towBase;
```

```

end
% Bunny ear layout
A_nac=L_nac*B_nac;
OpenEncumb_be=D_hub+2*(L_bla*cos(alfa)); % BE opening
encumbrance (direct or proiection) - hub+2blades (BE "length")
Width_be=max(L_hub,D_bla); % BE encumbrance along the
rotation-axis direction (BE "width")
% -- Transverse transportation--
if flag_transv==1
    if B<OpenEncumb_be && (B/2)+TransvLong_Limit>=(OpenEncumb_be/2)
        %msgbox('BE pre-assembly extension bigger than the jack-up unit
beam','Message')
        hF1=msgbox('Transverse (overboard) transportation of BE pre-
assembly','Message');
        warning('BE overboard transverse transportation')
        A_be=B*(L_nac+Width_be); % deck strip
occupied by the bunny ear (nothing more loaded next to it)
    elseif B>OpenEncumb_be
        %msgbox('BE pre-assembly extension smaller than the jack-up unit
beam','Message')
        hF1=msgbox('Transverse (inboard) transportation of BE pre-
assembly','Message');
        warning('BE inboard transverse transportation')
        A_be=OpenEncumb_be*(L_nac+Width_be);
    else
        errordlg('Transverse trasportation of BE pre-assembly not possible,
either increase transverse overboar limit or change transportation
mode','Error')
        error('BE transverse transportation not possible (either increase
overboard limit or change transportation mode)')
    end
else
% --Longitudinal transportation--
    CoG_be=OpenEncumb_be/2; % longitudinal position of the BE CoG, with
reference to its extension
    xCoG_deck=L-CoG_be; % default position of the BE CoG with respect to the
vessel/barge aft (depending on the encumbrance)
    if L<OpenEncumb_be
        %msgbox('BE pre-assembly extension bigger than the jack-up unit
length','Message')
        if xCoG_deck>0 && L+TransvLong_Limit>=OpenEncumb_be
            if xCoG_position==L
                hF1=msgbox('Longitudinal (overboard-default) transportation of
BE pre-assembly','Message');
                warning('BE overboard (default) longitudinal transportation')
                A_be=L*(L_nac+Width_be);
            elseif xCoG_position>=0 && xCoG_position<=xCoG_deck
                hF1=msgbox('Longitudinal (overboard) transportation of BE pre-
assembly, CoG position assigned','Message');
                warning('BE overboard (CoG postion assigned) longitudinal
transportation')
                A_be=(xCoG_position+OpenEncumb_be/2)*(L_nac+Width_be);
            else
                errordlg('BE CoG position (from aft) not acceptable because of
encumbrance on the bow, either reduce it or choose default mode','Error')
                error('BE CoG position not acceptable (for encumbrance on the
bow)')
            end
        elseif xCoG_deck<0
            errordlg('Longitudinal transportation of BE pre-assembly not
possible (CoG of BE structure out of the deck), either change transportation
mode or jack-up unit','Error')

```



```

        error('BE CoG position not acceptable (out of the deck loading)')
    else
        errordlg('Longitudinal trasportation of BE pre-assembly not
possible, either increase longitudinal overboard limit or change transportation
mode','Error')
        error('BE longitudinal transportation not possible (either increase
overboard limit or change transportation mode)')
    end
    elseif L>OpenEncumb_be
        %msgbox('BE pre-assembly extension smaller than the jack-up unit
length','Message')
        if TransvLong_Limit==0 %no limite long => caricazione BE a bordo (per
ogni baricentro entrino, io lo ignoro)
            hF1=msgbox('Longitudinal (inboard) transportation of BE pre-
assembly: BE CoG position free, depending on stability','Message');
            warning('BE inboard longitudinal transportation')
            A_be=OpenEncumb_be*(L_nac+Width_be);
        elseif TransvLong_Limit>0 && TransvLong_Limit<=CoG_be %limite overboard
long tale da avere baricentro BE ancora a bordo
            if xCoG_position==L %non assegno posizione
                hF1=msgbox('Longitudinal (overboard-default) transportation of
BE pre-assembly: BE CoG position set depending on max overboard
limit','Message');
                warning('BE inboard longitudinal transportation')
                A_be=(OpenEncumb_be-TransvLong_Limit)*(L_nac+Width_be);
            elseif xCoG_position>=0 && xCoG_position+CoG_be<=L %se assegno
posizione e questa >=0, in piu' va bene per ingombro a prua
                if xCoG_position<CoG_be %Se posizione assegnata e' minore di
meta' estensione rotore, ho ancora un overboard...
                    hF1=msgbox(['Longitudinal (overboard) transportation of BE
pre-assembly: CoG postion assigned and longitudinal overboard equal to
',num2str(OpenEncumb_be/2-xCoG_position,'%0.2f')'],'Message');
                    warning('BE inboard longitudinal transportation')
                    A_be=(xCoG_position+OpenEncumb_be/2)*(L_nac+Width_be);
                elseif xCoG_position>=CoG_be %Altrimenti diventa un inboard, e
non ho piu' il beneficio dell'overboard (se era fattibile)
                    hF1=msgbox('Longitudinal (inboard) transportation of BE pre-
assembly with CoG postion assigned: reduce BE CoG position from aft if
overboard transportation in wanted','Message');
                    warning('BE inboard longitudinal transportation')
                    A_be=OpenEncumb_be*(L_nac+Width_be);
                end
            else % problemi ingombro a prua
                errordlg('BE CoG position (from aft) not acceptable because of
encumbrance on the bow, either reduce it or choose default mode','Error')
                error('BE CoG position not acceptable (for encumbrance on the
bow)')
            end
        else %se LongLimit e' troppo grande mi puo' far finire il baricentro di
BE (nel caso =L) fuori dal ponte!
            errordlg(['Reduce longitudinal overboard limit (not to have BE CoG
overboard the aft side): suggested maximum value
',num2str(CoG_be,'%0.2f')'],'Error')
            error('Reduce longitudinal overboard limit')
        end
    end
end
end
% 3rd blade
A_3bla=L_bla*D_bla;
if N_bla==2
    A_3bla=0;
end

```

```

%-----
%
-
% AREA (EFFECTIVELY) OCCUPIED (even if without direct contact) - WEIGHT
A_EffOcc1=A_tow+A_3bla+A_be; % deck area occupied/not anymore
available for loading after 1 turbine loaded
W_1trb=W_tow+W_nac+W_hub+N_bla*W_bla; % weight 1trb
W_be=W_nac+W_hub+2*W_bla; % weight bunny ear structure
%-----
%
-
% DECK LOADS CHECK: Total/concentrated load on deck (except for blade structure)
if W_1trb>MaxLoad_deck
    errordlg('Deck cannot (even) support the weight of one turbine','Error');
    error('Deck cannot (even) support the weight of one turbine');
end
ConcLoad_towConn=W_towConn/A_towConn;
if ConcLoad_towConn>ConLoad_deck
    errordlg('Deck cannot support the concentrate weight of the upper tower
piece','Error');
    error('Deck cannot support the concentrate weight of the upper tower
piece');
end
ConcLoad_towBase=W_towBase/A_towBase;
if ConcLoad_towBase>ConLoad_deck
    if ConcLoad_towConn==0
        errordlg('Deck cannot support the concentrate weight of the whole
tower','Error');
        error('Deck cannot support the concentrate weight of the whole tower');
    else
        errordlg('Deck cannot support the concentrate weight of the lower tower
piece','Error');
        error('Deck cannot support the concentrate weight of the lower tower
piece');
    end
end
ConcLoad_be=W_be/A_nac;
if ConcLoad_be>ConLoad_deck
    errordlg('Deck cannot support the concentrate weight of the "bunny ear"
structure','Error');
    error('Deck cannot support the concentrate weight of the "bunny ear"
structure');
end
% NB: 3rd blade automatically verified if bunny ear case is verified (=less
weight, more area)
% if N_bla==3
%     ConcLoad_3bla=W_bla/A_3bla;
%     if ConcLoad_3bla>Load_deck
%         errordlg('Deck cannot even support one blade weight','Error');
%         error('Deck cannot even support one blade weight');
%     end
% end

%-----
%
-
% CRANE LOADS CHECK: loads lifted
% Offshore crane
if W_towConn>MaxLoad_crane
    errordlg('Jack-up crane cannot lift the weight of the upper tower
piece','Error');

```

```

        error('Jack-up crane cannot lift the weight of the upper tower piece');
    end
    if W_towBase>MaxLoad_crane
        if W_towConn==0
            errordlg('Jack-up crane cannot lift the weight of the whole
turbine','Error');
            error('Jack-up crane cannot lift the weight of the whole turbine');
        else
            errordlg('Jack-up crane cannot lift the weight of the lower tower
piece','Error');
            error('Jack-up crane cannot lift the weight of the lower tower piece');
        end
    end
    if W_be>MaxLoad_crane
        errordlg('Jack-up crane cannot lift the weight of the "bunny ear"
structure','Error');
        error('Jack-up crane cannot lift the weight of the "bunny ear" structure');
    end
    % Port crane(s)
    if W_towConn>MaxLoad_port
        errordlg('Port crane cannot lift the weight of the upper tower
piece','Error');
        error('Port crane cannot lift the weight of the upper tower piece');
    end
    if W_towBase>MaxLoad_port
        if W_towConn==0
            errordlg('Port crane cannot lift the weight of the whole
turbine','Error');
            error('Crane cannot lift the weight of the whole turbine');
        else
            errordlg('Port crane cannot lift the weight of the lower tower
piece','Error');
            error('Port crane cannot lift the weight of the lower tower piece');
        end
    end
    if W_be>MaxLoad_port
        errordlg('Port crane cannot lift the weight of the "bunny ear"
structure','Error');
        error('Port crane cannot lift the weight of the "bunny ear" structure');
    end
    % NB: 3rd blade lifted weight check automatically verified if bunny ear case is
    verified (=less weight)
    % if N_bla==3
    %     if W_bla>MaxLoad_crane
    %         errordlg('Crane cannot lift one blade weight','Error');
    %         error('Crane cannot lift one blade weight');
    %     end
    % end

%% ---BE FITTING ALGORITHM---
%-----
%
% AREA AND WEIGHT FITTING ALGORITHM
kN=1;
A_EffOcc=A_EffOcc1;           % deck area available after 1st trb loaded
A_box=N_blastr*A_3bla;        % for N==3, 3rd blade can be loaded one over
the other, deciding the no. of blades at the base
while A_EffOcc<A_deck
    W_kNtrb=W_1trb*kN;        % weigth initialisation**
    if W_kNtrb>MaxLoad_deck
        kN=kN-1;
    end
end

```

```

W_kNtrb=W_1trb*kN;
if N_bla==3 && kN>N_blastr
    A_EffOcc=A_box+(A_tow+A_be)*kN;
else
    A_EffOcc=A_EffOcc1*kN;
end
disp('Fitting algorithm arrested for net weight on deck')
break
else
    A_Avail=A_deck-A_EffOcc;
    W_kNtrb=W_1trb*kN;
    if N_bla==3 && kN<N_blastr
        if A_Avail<A_EffOcc1
            disp('Fitting algorithm arrested for area available')
            break
        else
            kN=kN+1;
            if kN>N_blastr
                A_EffOcc=A_box+(A_tow+A_be)*kN;
            else
                A_EffOcc=A_EffOcc1*kN;
            end
        end
    elseif N_bla==3 && kN>=N_blastr
        if A_Avail<A_EffOcc1-A_3bla
            disp('Fitting algorithm arrested for area available')
            break
        else
            kN=kN+1;
            if kN>N_blastr
                A_EffOcc=A_box+(A_tow+A_be)*kN;
            else
                A_EffOcc=A_EffOcc1*kN;
            end
        end
    elseif N_bla==2
        if A_Avail<A_EffOcc1
            disp('Fitting algorithm arrested for area available')
            break
        else
            kN=kN+1;
            A_EffOcc=A_EffOcc1*kN;
        end
    end
end
end
end
%-----
%-----
-
% DECK LOAD CHECK: Concentrated weight of the 3rd blades structure
if N_bla==3
    if kN>N_blastr
        ConcLoad_3blastr=(kN*W_bla)/A_box;
        if ConcLoad_3blastr>ConLoad_deck
            errordlg('Deck cannot support blade-gathering structure weight,
change blades structure size (No. of blade on the base)','Error');
            error('Deck cannot support blade-gathering structure weight,change
blades structure size (No. of blade on the base)');
        end
    else
        ConcLoad_3blastr=W_bla/A_3bla;
    end
end

```

```

else
    ConcLoad_3blastr=0;          % in case of 2-bladed trb, we don't have the 3rd
end

%% RESULTS
%-----
%
-
% AREA OCCUPIED (effectively or encumbrance) & NO. TURBINES ON DECK
AreaEffOcc_BE=A_EffOcc;          % ~= AreaOcc_BE1=A_Occ*wN;
NtrbXvoy_BE=kN;

% TOTAL ON DECK & MAXIMUM LIFTED LOADS
WeightOnDeck_BE=W_kNtrb;
MaxLoadLift_BE=max([W_towConn,W_towBase,W_be]);
if MaxLoadLift_BE==W_towConn;
    nameMaxLoadLift='tower upper piece';
elseif MaxLoadLift_BE==W_towBase;
    nameMaxLoadLift='tower (lower) piece';
elseif MaxLoadLift_BE==W_be;
    nameMaxLoadLift='bunny ear pre-assembly';
end
MaxConcLoad_BE=max([ConcLoad_towConn,ConcLoad_towBase,ConcLoad_be,ConcLoad_3blas
tr]);
if MaxConcLoad_BE==ConcLoad_towConn;
    nameConcLoadLift='tower upper piece';
elseif MaxConcLoad_BE==ConcLoad_towBase;
    nameConcLoadLift='tower (lower) piece';
elseif MaxConcLoad_BE==ConcLoad_be;
    nameConcLoadLift='bunny ear pre-assembly';
elseif MaxConcLoad_BE==ConcLoad_3blastr;
    nameConcLoadLift='blade structure';
end
hF2=msgbox(['The heaviest element lifted is the ',nameMaxLoadLift,'
(' ,num2str(MaxLoadLift_BE,'%0.1f'),' tons), and the maximum concentrated load on
the deck caused by the ',nameConcLoadLift,' (' ,num2str(MaxConcLoad_BE,'%0.2f'),'
t/m^2)'], 'Message');

```

D.3 timeBE.m

```

function
[T_totBE,T_reqdaysBE]=timeBE(Jspeed,speed,Ntrb_farm,DS_port,DS_trb,DP_port,DP_fa
rm,T_portBE,T_workhrs,T_be,T_bla,T_tow,NtrbXvoy_BE,N_bla,flag_towsplit)
%% TIME REQUIRED ALGORITHM
% General
T_1jport=DP_port/Jspeed;      % jacking at port (up/down)
T_1voy=DS_port/speed;         % voyage time (from port to farm)
T_1jfarm=DP_farm/Jspeed;      % jacking at farm (up/down)
T_1betwtrb=DS_trb/speed;      % between turbines time
% No. of voyages -----BE
N_voy=Ntrb_farm/NtrbXvoy_BE;
N_fix=fix(N_voy);
N_ceil=ceil(N_voy);
Ntrb_resid=(N_voy-N_fix)*NtrbXvoy_BE;

% Total time estimation
T_jfarm=(2*T_1jfarm*(Ntrb_farm-1))+T_1jfarm; % until last turbine is assembled
(no last jack down)
if flag_towsplit==0
    T_tow=2*T_tow; % tower 2 pieces
end
if N_bla==3
    T_lassembly=T_tow+T_be+T_bla; % time offshore lift/installation 1 trb with
BE methods
else
    T_lassembly=T_tow+T_be;
end
T_assembly=T_lassembly*Ntrb_farm;

if N_voy==N_fix %---ROUND NO. OF voyAGES---
    % Time at port (total)
    T_port=N_fix*((T_portBE*NtrbXvoy_BE)+(2*T_1jport)); %-----BE
    % Time to voyage (farm and back / between turbines) and jack up/down
    T_voys=(2*T_1voy*(N_fix-1))+T_1voy; % there&back, until the last
one
    T_betwtrb=(T_1betwtrb*(NtrbXvoy_BE-1))*N_fix;
else
T_port=N_fix*(T_portBE*NtrbXvoy_BE)+(T_portBE*Ntrb_resid)+N_ceil*(2*T_1jport);
%-----BE
    % Time to voyage (farm and back / between turbines) and jack up/down
    T_voys=(2*T_1voy*(N_ceil-1))+T_1voy; % there&back, until the last
one
    T_betwtrb=(T_1betwtrb*(NtrbXvoy_BE-1))*N_fix+(T_1betwtrb*(Ntrb_resid-1));
end
T_reqmin=T_port+T_voys+T_betwtrb+T_jfarm+T_assembly; % (min)
T_reqhrs=T_reqmin/60; % (hrs)
T_stophrs=fix(T_reqhrs/T_workhrs)*(24-T_workhrs); % tot no working
hours in the total period (consecutive installation time)
T_tothrs=T_reqhrs+T_stophrs;
T_totdays=T_tothrs/24;

%% RESULT % (days)
%-----
-
T_reqdaysBE=T_reqhrs/24; % required consecutive days of work

```

```
T_totBE=T_totdays;           % tot number of days considering the avarage working  
sloth hours per day
```

D.4 fittingROT.m

```
function
[AreaEffOcc_ROT,WeightOnDeck_ROT,NtrbXvoy_ROT,MaxLoadLift_ROT,hF0,hF1,hF2]=...

fittingROT(H_conn,W_conn,Transv_Limit,Long_Limit,L_reinforce,N_rotMax,flag_model
,L,B,A_deck,MaxLoad_deck,ConLoad_deck,MaxLoad_crane,MaxLoad_port,...

H_tow,D_towBase,D_towTop,t_towTop,t_towBase,W_tow,L_nac,B_nac,W_nac,D_hub,W_hub,
N_bla,alfa,L_bla,D_bla,W_bla)
disp('ROTOR (ROT) PRE-ASSEMBLY METHOD LAUNCHED')
%% TOWER WITH/WITHOUT CONNECTION SETUP
%-----
%-----

Dint_towTop=D_towTop-2*t_towTop;
Dint_towBase=D_towBase-2*t_towBase;
D_towConn=D_towTop+2*((D_towBase-D_towTop)/2*(H_tow-H_conn))/H_tow;
Dint_towConn=Dint_towTop+2*((Dint_towBase-Dint_towTop)/2*(H_tow-H_conn))/H_tow;
% WITHOUT CONNECTION CASE
if H_conn==H_tow && W_conn==0
    W_towConn=W_conn;
    W_towBase=W_tow;
end
% WITH CONNECTION CASE
if H_conn~=H_tow && W_conn~=0 % known weight of the
transitional piece
    W_towConn=W_conn;
    W_towBase=W_tow-W_conn;
elseif H_conn~=H_tow && W_conn==0 % volume proportionality
to subdivide the weight in 2 pieces
    Vext_towBase=1/12*H_conn*(D_towBase^2+(D_towBase*D_towConn)+D_towConn^2);
    Vext_towConn=1/12*(H_tow-
H_conn)*(D_towConn^2+(D_towTop*D_towConn)+D_towTop^2);
    Vext_towTot=Vext_towBase+Vext_towConn;

Vint_towBase=1/12*H_conn*(Dint_towBase^2+(Dint_towBase*Dint_towConn)+Dint_towCon
n^2);
    Vint_towConn=1/12*(H_tow-
H_conn)*(Dint_towConn^2+(Dint_towTop*Dint_towConn)+Dint_towTop^2);
    Vint_towTot=Vint_towBase+Vint_towConn;
    V_towBase=Vext_towBase-Vint_towBase;
    V_towConn=Vext_towConn-Vint_towConn;
    V_towTot=Vext_towTot-Vint_towTot;
    W_towConn=(W_tow*V_towConn)/V_towTot;
    W_towBase=(W_tow*V_towBase)/V_towTot;
end

%% BE 1TURBINE (trb) FITTING
%-----
%-----

% FITTING CONDITIONS
% Tower with/without connection
% Tower with/without connection
% A_towBase=pi*(D_towBase/2)^2;
% A_towConn=pi*(D_towConn/2)^2;
A_towBase=D_towBase^2;
A_towConn=D_towConn^2;
if D_towConn~=D_towTop
    A_tow=A_towConn+A_towBase;
else
```



```

    A_tow=A_towBase;
end
A_nac=L_nac*B_nac;

% Rotor layout
OpenEncumb_rot=D_hub+2*(L_bla*cos(alfa));
Width_1bla=max(D_bla,D_hub);
% -- Opening encumbrance of the rotor --
if N_bla==3
    if B<OpenEncumb_rot && (B/2)+Transv_Limit>=(OpenEncumb_rot/2)
        hF0=msgbox('Transverse overboard trasportation of ROT pre-
assembly','Message');
        warning('ROT overboard transportation (within the limit)')
        B_ref=B;
    elseif B>OpenEncumb_rot
        hF0=msgbox('Transverse inboard transportation of ROT pre-
assembly','Message');
        warning('ROT inboard transverse transportation')
        B_ref=OpenEncumb_rot;
    else
        errordlg('Transversal extension of ROT pre-assembly over the
transportation limit, either increase the overboard limit or change pre-assembly
transportation mode/method','Error')
        error('Mode 1 not possible (either increase transversal overboard limit
or change pre-assemble method)')
    end
elseif flag_model==1 && N_bla==2
    if B<OpenEncumb_rot && (B/2)+Transv_Limit>=(OpenEncumb_rot/2)
        hF0=msgbox('Transverse overboard trasportation of ROT pre-
assembly','Message');
        warning('ROT overboard transportation (within the limit)')
        B_ref=B;
    elseif B>OpenEncumb_rot
        hF0=msgbox('Transverse inboard transportation of ROT pre-
assembly','Message');
        warning('ROT inboard transverse transportation')
        B_ref=OpenEncumb_rot;
    else
        errordlg('Transversal extension of ROT pre-assembly over the
transportation limit, either increase the overboard limit or change pre-assembly
transportation mode/method','Error')
        error('Mode 1 not possible (either increase transversal overboard limit
or change pre-assemble method)')
    end
end
% -- Mode 1 --
if flag_model==1
    if N_bla==3
        L_ref=(B_ref/2)*sin(alfa)/cos(alfa);
        L_1bla=D_hub/2+L_bla;
        L_rot=L_ref+L_1bla;
        A_2bla=B_ref*((B_ref/2)*sin(alfa)/cos(alfa));
        %xCoG_ref=L-L_ref;
        if Long_Limit==0 && L_rot<=L
            hF1=msgbox('Longitudinal inboard transportation of ROT pre-
assembly','Message');
            warning('ROT inboard longitudinal transportation')
            A_1bla=L_1bla*Width_1bla;
        elseif Long_Limit==0 && L_rot>L
            errordlg('ROT pre-assembly longitudinal inboard trasportation not
possible (long. encumbrance bigger than jack-up unit length), increase the
overboard limit','Error')

```

```

        errordlg('ROT pre-assembly longitudinal inboard trasportation not
possible')
    elseif Long_Limit>0 && Long_Limit<=L_1bla
        hF1=msgbox('Longitudinal overboard transportation of ROT pre-
assembly','Message');
        warning('ROT overboard longitudinal transportation')
        A_1bla=(L_1bla-Long_Limit)*Width_1bla;
    else
        errordlg(['Reduce longitudinal overboard limit, not to have ROT CoG
overboard (from aft side): suggested maximum value
',num2str(L_1bla,'%0.2f')],'Error')
        error('Reduce longitudinal ROT pre-assembly overboard limit')
    end
    else % N_bla==2 (as BE transverse transportation)
        A_2bla=B_ref*Width_1bla;
        A_1bla=0; % whatever they insert in the xCoG and Long_Limit
condition = I DON'T CARE
    end
    A_rot=A_2bla+A_1bla;
else
    % -- Mode 2 --
    if N_bla==3
        L_ref=(B_ref/2)*sin(alfa)/cos(alfa);
        L_1bla=D_hub/2+L_bla;
        L_rot=L_ref+L_1bla;
        A_1bla=L_1bla*Width_1bla;
        %xCoG_ref=L-L_1bla;
        if Long_Limit==0 && L_rot<=L
            hF1=msgbox('Longitudinal inboard transportation of ROT pre-
assembly','Message');
            warning('ROT inboard longitudinal transportation')
            A_2bla=B_ref*L_ref;
        elseif Long_Limit==0 && L_rot>L
            errordlg('ROT pre-assembly longitudinal inboard trasportation not
possible (long. encumbrance bigger than jack-up unit length), increase the
overboard limit','Error')
            errordlg('ROT pre-assembly longitudinal inboard trasportation not
possible')
        elseif Long_Limit>0 && Long_Limit<=L_ref
            hF1=msgbox('Longitudinal overboard transportation of ROT pre-
assembly','Message');
            warning('ROT overboard longitudinal transportation')
            A_2bla=(L_ref-Long_Limit)*B_ref;
        else
            errordlg(['Reduce longitudinal overboard limit, not to have ROT CoG
overboard (from aft side): suggested maximum value
',num2str(L_ref,'%0.2f')],'Error')
            error('Reduce longitudinal ROT pre-assembly overboard limit')
        end
    else % N_bla==2 (as BE transverse transportation)
        L_1bla=D_hub/2+L_bla;
        L_ref=L_1bla;
        L_rot=L_ref+L_1bla;
        A_1bla=L_1bla*Width_1bla;
        if Long_Limit==0 && L_rot<=L
            hF1=msgbox('Longitudinal inboard) transportation of ROT pre-
assembly','Message');
            warning('ROT inboard longitudinal transportation')
            A_2bla=Width_1bla*L_ref;
        elseif Long_Limit==0 && L_rot>L

```

```

        errordlg('ROT pre-assembly longitudinal inboard transportation not
possible (long. encumbrance bigger than jack-up unit length), increase the
overboard limit','Error')
        errordlg('ROT pre-assembly longitudinal inboard transportation not
possible')
        elseif Long_Limit>0 && Long_Limit<=L_ref
            hF1=msgbox('Longitudinal overboard transportation of ROT pre-
assembly','Message');
            warning('ROT overboard longitudinal transportation')
            A_2bla=(L_ref-Long_Limit)*Width_1bla;
        else
            errordlg(['Reduce longitudinal overboard limit, not to have ROT CoG
overboard (from aft side): suggested maximum value
',num2str(L_ref,'%0.2f')], 'Error')
            error('Reduce longitudinal ROT pre-assembly overboard limit')
        end
    end
    A_rot=A_2bla+A_1bla;
end

%-----
%-----
-
% AREA (EFFECTIVELY) OCCUPIED - WEIGHT
%A_Occ=A_tow+A_nac+A_3bla; % deck area occupied by (in contact
with) 1 turbine pieces
A_EffOccl=A_tow+A_nac+A_rot; % deck area occupied/not anymore
available for loading after 1 turbine loaded
W_1trb=W_tow+W_nac+W_hub+N_bla*W_bla; % weight 1trb
W_rot=W_hub+N_bla*W_bla; % weight rot ear structure
%-----
%-----
-
% DECK LOADS CHECK (1st): Total/concentrated load on deck (except for rotor
structure)
if W_1trb>MaxLoad_deck
    errordlg('Deck cannot (even) support the weight of one turbine','Error');
    error('Deck cannot (even) support the weight of one turbine');
end
ConcLoad_towConn=W_towConn/A_towConn;
if ConcLoad_towConn>ConLoad_deck
    errordlg('Deck cannot support the concentrate weight of the upper tower
piece','Error');
    error('Deck cannot support the concentrate weight of the upper tower
piece');
end
ConcLoad_towBase=W_towBase/A_towBase;
if ConcLoad_towBase>ConLoad_deck
    if ConcLoad_towConn==0
        errordlg('Deck cannot support the concentrate weight of the whole
tower','Error');
        error('Deck cannot support the concentrate weight of the whole tower');
    else
        errordlg('Deck cannot support the concentrate weight of the lower tower
piece','Error');
        error('Deck cannot support the concentrate weight of the lower tower
piece');
    end
end
ConcLoad_nac=W_nac/A_nac;
if ConcLoad_nac>ConLoad_deck

```

```

        errordlg('Deck cannot support the concentrate weight of the
nacelle','Error');
        error('Deck cannot support the concentrate weight of the nacelle
structure');
    end

%-----
%
% CRANE LOADS CHECK: loads lifted
% Offshore crane
if W_towConn>MaxLoad_crane
    errordlg('Crane cannot lift the weight of the upper tower piece','Error');
    error('Crane cannot lift the weight of the upper tower piece');
end
if W_towBase>MaxLoad_crane
    if W_towConn==0
        errordlg('Jack-up crane cannot lift the weight of the whole
turbine','Error');
        error('Jack-up crane cannot lift the weight of the whole turbine');
    else
        errordlg('Jack-up crane cannot lift the weight of the lower tower
piece','Error');
        error('Jack-up crane cannot lift the weight of the lower tower piece');
    end
end
if W_nac>MaxLoad_crane
    errordlg('Jack-up crane cannot lift the weight of the nacelle','Error');
    error('Jack-up crane cannot lift the weight of the nacelle');
end
if W_rot>MaxLoad_crane
    errordlg('Jack-up crane cannot lift the weight of the rotor
structure','Error');
    error('Jack-up crane cannot lift the weight of the rotor structure');
end
% Port crane(s)
if W_towConn>MaxLoad_port
    errordlg('Port crane cannot lift the weight of the upper tower
piece','Error');
    error('Port crane cannot lift the weight of the upper tower piece');
end
if W_towBase>MaxLoad_port
    if W_towConn==0
        errordlg('Port crane cannot lift the weight of the whole
turbine','Error');
        error('Crane cannot lift the weight of the whole turbine');
    else
        errordlg('Port crane cannot lift the weight of the lower tower
piece','Error');
        error('Port crane cannot lift the weight of the lower tower piece');
    end
end
if W_nac>MaxLoad_port
    errordlg('Port crane cannot lift the weight of the nacelle','Error');
    error('Port crane cannot lift the weight of the nacelle');
end
if W_rot>MaxLoad_port
    errordlg('Port crane cannot lift the weight of the rotor
structure','Error');
    error('Port crane cannot lift the weight of the rotor structure');
end

```

```

%% ---BE FITTING ALGORITHM---
%-----
-
% AREA AND WEIGHT FITTING ALGORITHM
kN=1;
A_EffOcc=A_EffOcc1; % deck area occupied after 1st trb loaded
A_reinforce=L_reinforce^2;
while A_EffOcc<A_deck
    W_kNtrb=W_1trb*kN; % weigth initialisation**
    A_EffOcc=A_rot+(A_tow+A_nac)*kN;
    if W_kNtrb>MaxLoad_deck
        kN=kN-1;
        W_kNtrb=W_1trb*kN;
        A_EffOcc=A_rot+(A_tow+A_nac)*kN;
        disp('Fitting algorithm stopped because net weight on the deck exceeded
threshold')
        break
    elseif (kN*W_rot)/A_reinforce>=ConLoad_deck
        kN=kN-1;
        W_kNtrb=W_1trb*kN;
        A_EffOcc=A_rot+(A_tow+A_nac)*kN;
        disp('Fitting algorithm stopped because concentrated load on the deck
(of rotor pre-assembly) exceeded threshold')
        ConcLoad_rotMax=(kN*W_rot)/A_reinforce;
        break
    elseif kN>N_rotMax
        kN=kN-1;
        W_kNtrb=W_1trb*kN;
        A_EffOcc=A_rot+(A_tow+A_nac)*kN;
        disp('Fitting algorithm stopped because no. of overlying rotors exceeded
imposed threshold')
        ConcLoad_rotMax=(kN*W_rot)/A_reinforce;
        break
    end
    A_Avail=A_deck-A_EffOcc;
    if A_Avail<(A_EffOcc1-A_rot)
        break
    else
        kN=kN+1;
    end
end

%% RESULTS
%-----
-
% AREA OCCUPIED (effectively or encumbrance) & NO. TURBINES ON DECK
AreaEffOcc_ROT=A_EffOcc;
NtrbXvoy_ROT=kN;

% TOTAL ON DECK & MAXIMUM LIFTED LOADS
WeightOnDeck_ROT=W_kNtrb;
MaxLoadLift_ROT=max([W_towConn,W_towBase,W_rot,W_nac]);
if MaxLoadLift_ROT==W_towConn;
    nameMaxLoadLift='tower upper piece';
elseif MaxLoadLift_ROT==W_towBase;
    nameMaxLoadLift='tower (lower) piece';
elseif MaxLoadLift_ROT==W_rot;
    nameMaxLoadLift='rotor pre-assembly';
elseif MaxLoadLift_ROT==W_nac
    nameMaxLoadLift='nacelle';

```

```

end
MaxConcLoad_ROT=max([ConcLoad_towConn,ConcLoad_towBase,ConcLoad_rotMax,ConcLoad_
nac]);
if MaxConcLoad_ROT==ConcLoad_towConn;
    nameConcLoadLift='tower upper piece';
elseif MaxConcLoad_ROT==ConcLoad_towBase;
    nameConcLoadLift='tower (lower) piece';
elseif MaxConcLoad_ROT==ConcLoad_rotMax;
    nameConcLoadLift='rotor pre-assembly';
elseif MaxConcLoad_ROT==ConcLoad_nac;
    nameConcLoadLift='nacelle';
end
hF2=msgbox(['The heaviest element lifted is the ',nameMaxLoadLift,'
(',num2str(MaxLoadLift_ROT,'%0.1f'),' tons), and the maximum concentrated load
on the deck caused by the ',nameConcLoadLift,'
(',num2str(MaxConcLoad_ROT,'%0.2f'),' t/m^2)'], 'Message');

```

D.5 timeROT.m

```

function
[T_totROT,T_reqdaysROT]=timeROT(Jspeed,speed,Ntrb_farm,DS_port,DS_trb,DP_port,DP
_farm,T_portROT,T_workhrs,T_rot,T_nac,T_tow,NtrbXvoy_ROT,flag_towsplit)
%% TIME REQUIRED ALGORITHM
% General
T_1jport=DP_port/Jspeed;      % jacking at port (up/down)
T_1voy=DS_port/speed;         % voyage time (from port to farm)
T_1jfarm=DP_farm/Jspeed;      % jacking at farm (up/down)
T_1betwtrb=DS_trb/speed;      % between turbines time
% No. of voyages -----ROT
N_voy=Ntrb_farm/NtrbXvoy_ROT;
N_fix=fix(N_voy);
N_ceil=ceil(N_voy);
Ntrb_resid=(N_voy-N_fix)*NtrbXvoy_ROT;

% Total time estimation
T_jfarm=(2*T_1jfarm*(Ntrb_farm-1))+T_1jfarm; % until last turbine is assembled
(no last jack down)
if flag_towsplit==0
    T_tow=2*T_tow; % tower 2 pieces
end
T_lassembly=T_tow+T_rot+T_nac; % time offshore lift/installation 1 trb with BE
methods
T_assembly=T_lassembly*Ntrb_farm;

%---ROUND NUMBER OF voyAGES---
if N_voy==N_fix
    % Time at port (total)
    T_port=N_fix*((T_portROT*NtrbXvoy_ROT)+(2*T_1jport)); %-----ROT
    % Time to voyage (farm and back / between turbines) and jack up/down
    T_voys=(2*T_1voy*(N_fix-1))+T_1voy; % there&back, until the last
one
    T_betwtrb=(T_1betwtrb*(NtrbXvoy_ROT-1))*N_fix;
else
    %---ODD NUMBER OF voyAGES---

T_port=N_fix*(T_portROT*NtrbXvoy_ROT)+(T_portROT*Ntrb_resid)+N_ceil*(2*T_1jport)
; %-----ROT
    % Time to voyage (farm and back / between turbines) and jack up/down
    T_voys=(2*T_1voy*(N_ceil-1))+T_1voy; % there&back, until the last
one
    T_betwtrb=(T_1betwtrb*(NtrbXvoy_ROT-1))*N_fix+(T_1betwtrb*(Ntrb_resid-1));
end
T_reqmin=T_port+T_voys+T_betwtrb+T_jfarm+T_assembly; % (min)
T_reqhrs=T_reqmin/60; % (hrs)
T_stophrs=fix(T_reqhrs/T_workhrs)*(24-T_workhrs); % tot no working
hours in the total period (consecutive installation time)
T_tothrs=T_reqhrs+T_stophrs;
T_totdays=T_tothrs/24;

%% RESULT %(days)
%
%
%
T_reqdaysROT=T_reqhrs/24; % required consecutive days of work
T_totROT=T_totdays; % tot number of days considering the avarage
working sloth hours per day

```

D.6 fittingSP.m

```
function [AreaEffOcc_SP,WeightOnDeck_SP,NtrbXvoy_SP,MaxLoadLift_SP,hF]=...

fittingSP(H_conn,W_conn,N_blastr,A_deck,MaxLoad_deck,ConLoad_deck,MaxLoad_crane,
MaxLoad_port,...

H_tow,D_towBase,D_towTop,t_towTop,t_towBase,W_tow,L_nac,B_nac,W_nac,L_hub,W_hub,
N_bla,L_bla,D_bla,W_bla)
disp('SINGLE PIECES (SP) ASSEMBLY METHOD LAUNCHED')
%% TOWER WITH/WITHOUT CONNECTION SETUP
%-----

Dint_towTop=D_towTop-2*t_towTop;
Dint_towBase=D_towBase-2*t_towBase;
D_towConn=D_towTop+2*((D_towBase-D_towTop)/2*(H_tow-H_conn))/H_tow;
Dint_towConn=Dint_towTop+2*((Dint_towBase-Dint_towTop)/2*(H_tow-H_conn))/H_tow;
% WITHOUT CONNECTION CASE
if H_conn==H_tow && W_conn==0
    W_towConn=W_conn;
    W_towBase=W_tow;
end
% WITH CONNECTION CASE
if H_conn~=H_tow && W_conn~=0 % known weight of the
transitional piece
    W_towConn=W_conn;
    W_towBase=W_tow-W_conn;
elseif H_conn~=H_tow && W_conn==0 % volume proportionality
to subdivide the weight in 2 pieces
    Vext_towBase=1/12*H_conn*(D_towBase^2+(D_towBase*D_towConn)+D_towConn^2);
    Vext_towConn=1/12*(H_tow-
H_conn)*(D_towConn^2+(D_towTop*D_towConn)+D_towTop^2);
    Vext_towTot=Vext_towBase+Vext_towConn;

Vint_towBase=1/12*H_conn*(Dint_towBase^2+(Dint_towBase*Dint_towConn)+Dint_towCon
n^2);
    Vint_towConn=1/12*(H_tow-
H_conn)*(Dint_towConn^2+(Dint_towTop*Dint_towConn)+Dint_towTop^2);
    Vint_towTot=Vint_towBase+Vint_towConn;
    V_towBase=Vext_towBase-Vint_towBase;
    V_towConn=Vext_towConn-Vint_towConn;
    V_towTot=Vext_towTot-Vint_towTot;
    W_towConn=(W_tow*V_towConn)/V_towTot;
    W_towBase=(W_tow*V_towBase)/V_towTot;
end

%% BE 1TURBINE (trb) FITTING
%-----

% FITTING CONDITIONS
% Tower with/without connection
% A_towBase=pi*(D_towBase/2)^2;
% A_towConn=pi*(D_towConn/2)^2;
A_towBase=D_towBase^2;
A_towConn=D_towConn^2;
if D_towConn~=D_towTop
    A_tow=A_towConn+A_towBase;
else
    A_tow=A_towBase;
end
```



```

% Nacelle - Blade
A_nachub=(L_nac+L_hub)*B_nac;
A_nac=L_nac*B_nac;
A_bla=L_bla*D_bla;

%-----
%
% AREA (EFFECTIVELY) OCCUPIED (even if without direct contact) - WEIGHT
A_EffOccl=A_tow+A_nachub+N_bla*A_bla;      % deck area occupied/not anymore
available for loading after 1 turbine loaded
W_ltrb=W_tow+W_nac+W_hub+N_bla*W_bla;    % weight ltrb
W_nachub=W_nac+W_hub;
%-----
%
% DECK LOADS CHECK: Total/concentrated load on deck (except for blade structure)
if W_ltrb>MaxLoad_deck
    errordlg('Deck cannot (even) support the weight of one turbine','Error');
    error('Deck cannot (even) support the weight of one turbine');
end
ConcLoad_towConn=W_towConn/A_towConn;
if ConcLoad_towConn>ConLoad_deck
    errordlg('Deck cannot support the concentrate weight of the upper tower
piece','Error');
    error('Deck cannot support the concentrate weight of the upper tower
piece');
end
ConcLoad_towBase=W_towBase/A_towBase;
if ConcLoad_towBase>ConLoad_deck
    if ConcLoad_towConn==0
        errordlg('Deck cannot support the concentrate weight of the whole
tower','Error');
        error('Deck cannot support the concentrate weight of the whole tower');
    else
        errordlg('Deck cannot support the concentrate weight of the lower tower
piece','Error');
        error('Deck cannot support the concentrate weight of the lower tower
piece');
    end
end
ConcLoad_nachub=W_nachub/A_nac;
if ConcLoad_nachub>ConLoad_deck
    errordlg('Deck cannot support the concentrate weight of the nacelle (with
pre-assembled hub)','Error');
    error('Deck cannot support the concentrate weight of the nacelle (with pre-
assembled hub)');
end
ConcLoad_bla=W_bla/A_bla;
if ConcLoad_bla>ConLoad_deck
    errordlg('Deck cannot support the concentrate weight of a blade','Error');
    error('Deck cannot support the concentrate weight of a blade');
end

%-----
%
% CRANE LOADS CHECK: loads lifted
% Offshore crane
if W_towConn>MaxLoad_crane
    errordlg('Crane cannot lift the weight of the upper tower piece','Error');
    error('Crane cannot lift the weight of the upper tower piece');
end

```

```

end
if W_towBase>MaxLoad_crane
    if W_towConn==0
        errordlg('Jack-up crane cannot lift the weight of the whole
turbine','Error');
        error('Jack-up crane cannot lift the weight of the whole turbine');
    else
        errordlg('Jack-up crane cannot lift the weight of the lower tower
piece','Error');
        error('Jack-up crane cannot lift the weight of the lower tower piece');
    end
end
if W_nachub>MaxLoad_crane
    errordlg('Jack-up crane cannot lift the weight of the nacelle (with pre-
assembled hub)','Error');
    error('Jack-up crane cannot lift the weight of the nacelle (with pre-
assembled hub)');
end
if W_bla>MaxLoad_crane
    errordlg('Jack-up crane cannot lift the weight of a blade','Error');
    error('Jack-up crane cannot lift the weight of a blade');
end
% Port crane(s)
if W_towConn>MaxLoad_port
    errordlg('Port crane cannot lift the weight of the upper tower
piece','Error');
    error('Port crane cannot lift the weight of the upper tower piece');
end
if W_towBase>MaxLoad_port
    if W_towConn==0
        errordlg('Port crane cannot lift the weight of the whole
turbine','Error');
        error('Crane cannot lift the weight of the whole turbine');
    else
        errordlg('Port crane cannot lift the weight of the lower tower
piece','Error');
        error('Port crane cannot lift the weight of the lower tower piece');
    end
end
if W_nachub>MaxLoad_port
    errordlg('Port crane cannot lift the weight of the nacelle (with pre-
assembled hub)','Error');
    error('Port crane cannot lift the weight of the nacelle (with pre-assembled
hub)');
end
if W_bla>MaxLoad_port
    errordlg('Port crane cannot lift the weight of a blade','Error');
    error('Port crane cannot lift the weight of a blade');
end

%% ---BE FITTING ALGORITHM---
%-----
-----
-
% AREA AND WEIGHT FITTING ALGORITHM
kN=1;
A_box=N_blastr*A_bla;
A_EffOcc=A_EffOcc1;

while A_EffOcc<A_deck
    W_kNtrb=W_ltrb*kN;
    if W_kNtrb>MaxLoad_deck
        % weigth initialisation**

```

```

kN=kN-1;
W_kNtrb=W_ltrb*kN;
if kN*N_bla>N_blastr
    A_EffOcc=A_box+(A_tow+A_nachub)*kN;
else
    A_EffOcc=A_EffOcc1*kN;
end
disp('Fitting algorithm arrested for net weight on deck')
break
else
    A_Avail=A_deck-A_EffOcc;
    if kN*N_bla>N_blastr
        if A_Avail<(A_tow+A_nachub)
            disp('Fitting algorithm arrested for area available (another
tower/nacelle do not fit anymore)')
            break
        elseif (kN*N_bla*W_bla)/A_box>ConLoad_deck
            disp('Fitting algorithm arrested for concentrated load of blades
cage structure')
            break
        else
            kN=kN+1;
            if kN*N_bla>N_blastr
                A_EffOcc=A_box+(A_tow+A_nachub)*kN;
            else
                A_EffOcc=A_EffOcc1*kN;
            end
        end
    else
        if A_Avail<A_tow+A_nachub+A_bla*((N_bla*kN)-N_blastr)
            disp('Fitting algorithm arrested for area available (just one
layer of blade in the blades cage)')
            break
        else
            kN=kN+1;
            if kN*N_bla>N_blastr
                A_EffOcc=A_box+(A_tow+A_nachub)*kN;
            else
                A_EffOcc=A_EffOcc1*kN;
            end
        end
    end
end
end
end

%-----
%-----
-
% DECK LOAD CHECK: Concentrated weight of the blades structure
if kN*N_bla>N_blastr
    ConcLoad_blastr=(kN*N_bla*W_bla)/A_box;
    if ConcLoad_blastr>ConLoad_deck
        errordlg('Deck cannot support blade-gathering structure weight, change
blades structure size (No. of blade on the base)','Error');
        error('Deck cannot support blade-gathering structure weight,change
blades structure size (No. of blade on the base)');
    end
end

%% RESULTS

```

```

%-----
%
% AREA OCCUPIED (effectively or encumbrance) & NO. TURBINES ON DECK
AreaEffOcc_SP=A_EffOcc;
NtrbXvoy_SP=kN;

% TOTAL ON DECK & MAXIMUM LIFTED LOADS
WeightOnDeck_SP=W_kNtrb;
MaxLoadLift_SP=max([W_towConn,W_towBase,W_nachub,W_bla]);
if MaxLoadLift_SP==W_towConn;
    nameMaxLoadLift='tower upper piece';
elseif MaxLoadLift_SP==W_towBase;
    nameMaxLoadLift='tower (lower) piece';
elseif MaxLoadLift_SP==W_nachub;
    nameMaxLoadLift='nacelle (with pre-assembled hub)';
elseif MaxLoadLift_SP==W_bla;
    nameMaxLoadLift='blade';
end

if kN*N_bla>N_blastr

MaxConcLoad_SP=max([ConcLoad_towConn,ConcLoad_towBase,ConcLoad_nachub,ConcLoad_b
lastr]);
else

MaxConcLoad_SP=max([ConcLoad_towConn,ConcLoad_towBase,ConcLoad_nachub,ConcLoad_b
la]);
end

if MaxConcLoad_SP==ConcLoad_towConn;
    nameConcLoadLift='tower upper piece';
elseif MaxConcLoad_SP==ConcLoad_towBase;
    nameConcLoadLift='tower (lower) piece';
elseif MaxConcLoad_SP==ConcLoad_nachub;
    nameConcLoadLift='nacelle (with pre-assembled hub)';
elseif MaxConcLoad_SP==ConcLoad_blastr;
    nameConcLoadLift='blade structure';
elseif MaxConcLoad_SP==ConcLoad_bla;
    nameConcLoadLift='blade';
end
hF=msgbox(['The heaviest element lifted is the ',nameMaxLoadLift,'
(',num2str(MaxLoadLift_SP,'%0.1f'),' tons), and the maximum concentrated load on
the deck caused by the ',nameConcLoadLift,' (',num2str(MaxConcLoad_SP,'%0.2f'),'
t/m^2)'], 'Message');

```

D.7 timeSP.m

```
function
[T_totSP,T_reqdaysSP]=timeSP(Jspeed,speed,Ntrb_farm,DS_port,DS_trb,DP_port,DP_fa
rm,T_portSP,T_workhrs,T_nac,T_bla,T_tow,NtrbXvoy_SP,N_bla,flag_towsplit)
%% TIME REQUIRED ALGORITHM
% General
T_1jport=DP_port/Jspeed;      % jacking at port (up/down)
T_1voy=DS_port/speed;         % voyage time (from port to farm)
T_1jfarm=DP_farm/Jspeed;      % jacking at farm (up/down)
T_1betwtrb=DS_trb/speed;      % between turbines time
% No. of voyages -----SP
N_voy=Ntrb_farm/NtrbXvoy_SP;
N_fix=fix(N_voy);
N_ceil=ceil(N_voy);
Ntrb_resid=(N_voy-N_fix)*NtrbXvoy_SP;

% Total time estimation
T_jfarm=(2*T_1jfarm*(Ntrb_farm-1))+T_1jfarm; % until last turbine is assembled
(no last jack down)
if flag_towsplit==0
    T_tow=2*T_tow; % tower 2 pieces
end
T_lassembly=T_tow+T_nac+N_bla*T_bla; % time offshore lift/installation 1 trb
with SP methods
T_assembly=T_lassembly*Ntrb_farm;

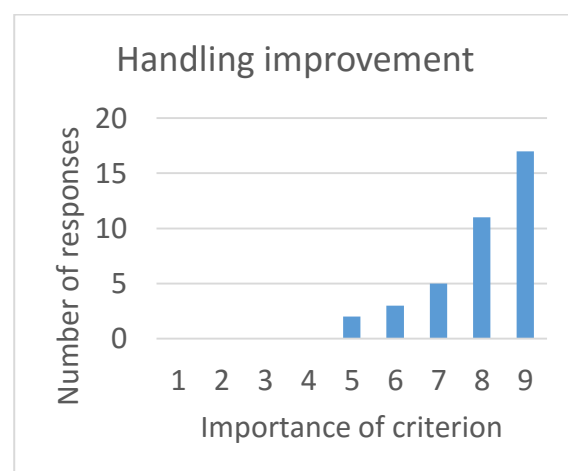
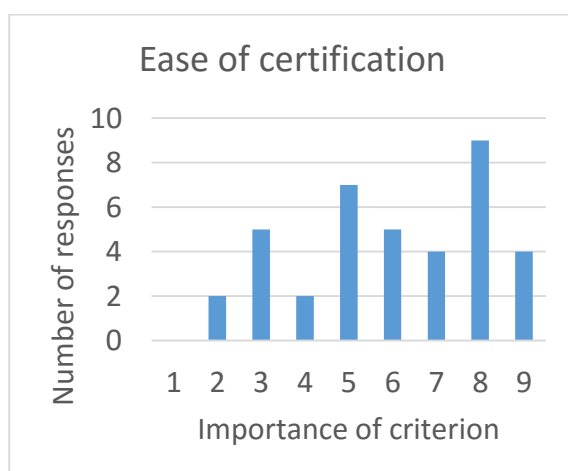
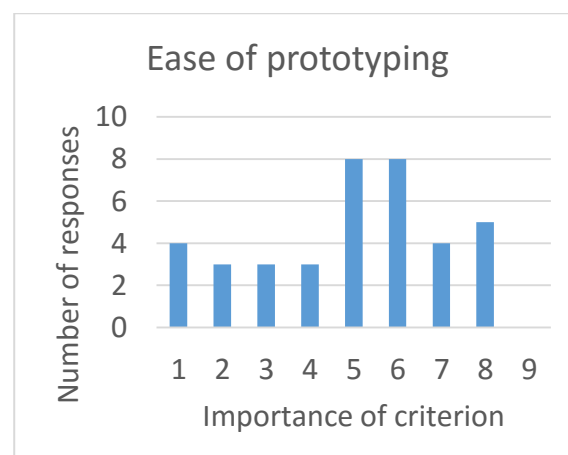
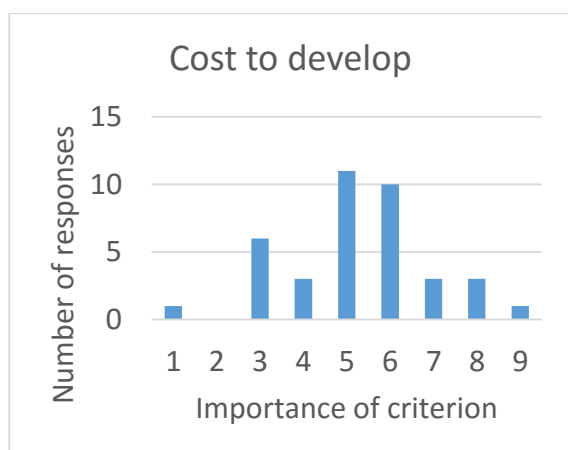
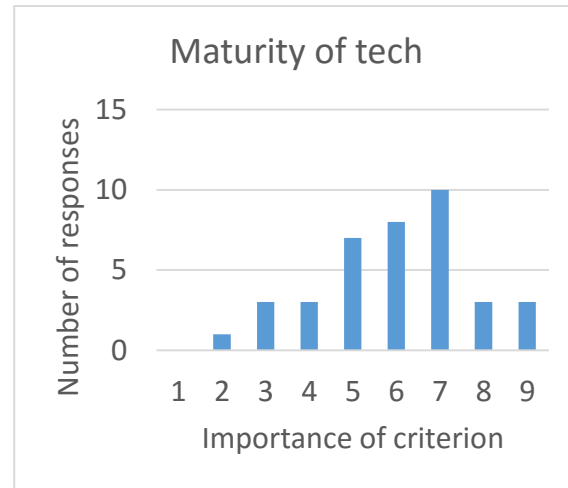
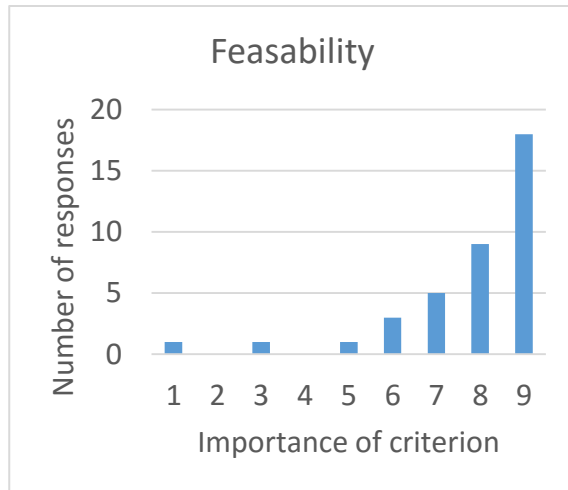
%---ROUND NO. OF voyAGES---
if N_voy==N_fix
    % Time at port (total)
    T_port=N_fix*((T_portSP*NtrbXvoy_SP)+(2*T_1jport)); %-----SP
    % Time to voyage (farm and back / between turbines) and jack up/down
    T_voys=(2*T_1voy*(N_fix-1))+T_1voy; % there&back, until the last
one
    T_betwtrb=(T_1betwtrb*(NtrbXvoy_SP-1))*N_fix;
else
T_port=N_fix*(T_portSP*NtrbXvoy_SP)+(T_portSP*Ntrb_resid)+N_ceil*(2*T_1jport);
%-----SP
    % Time to voyage (farm and back / between turbines) and jack up/down
    T_voys=(2*T_1voy*(N_ceil-1))+T_1voy; % there&back, until the last
one
    T_betwtrb=(T_1betwtrb*(NtrbXvoy_SP-1))*N_fix+(T_1betwtrb*(Ntrb_resid-1));
end
T_reqmin=T_port+T_voys+T_betwtrb+T_jfarm+T_assembly; % (min)
T_reqhrs=T_reqmin/60; % (hrs)
T_stophrs=fix(T_reqhrs/T_workhrs)*(24-T_workhrs); % tot no working
hours in the total period (consecutive installation time)
T_tothrs=T_reqhrs+T_stophrs;
T_totdays=T_tothrs/24;

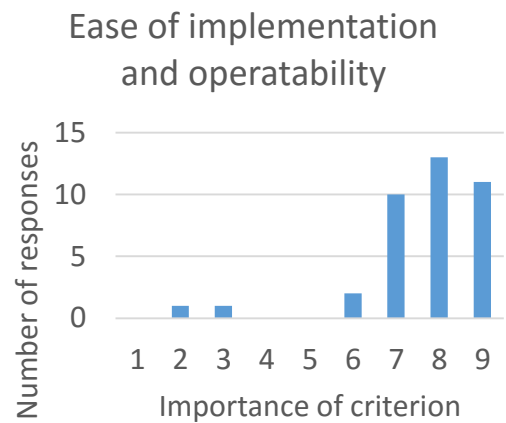
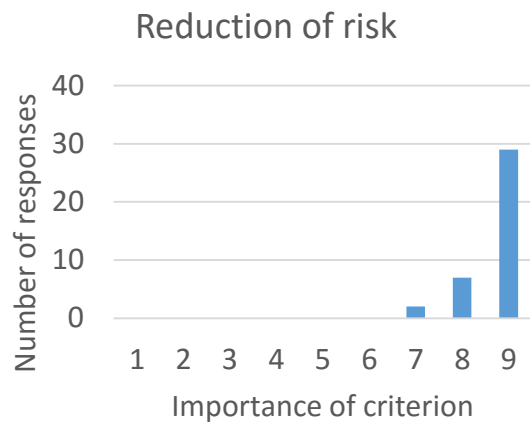
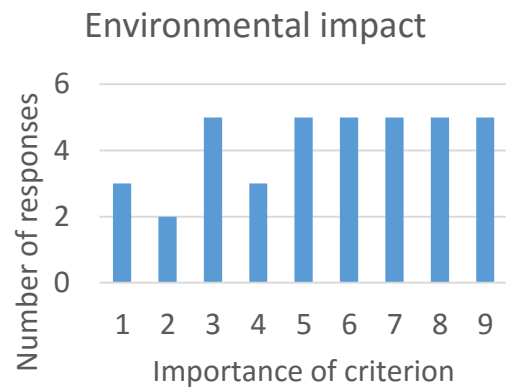
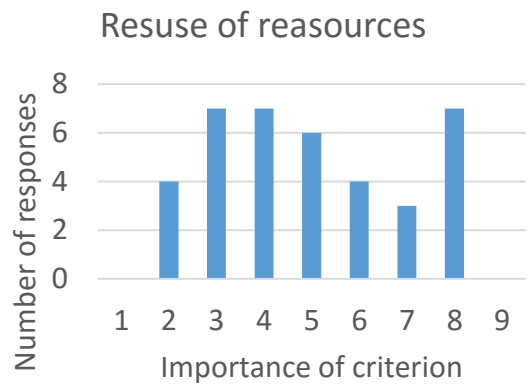
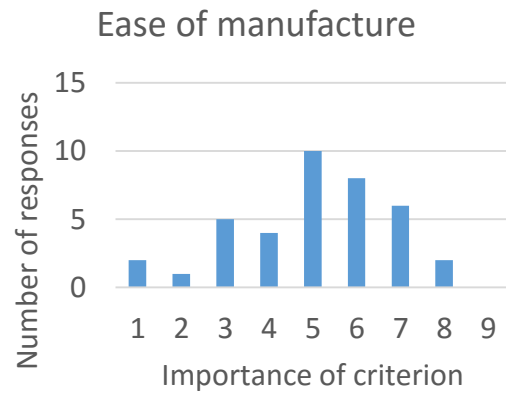
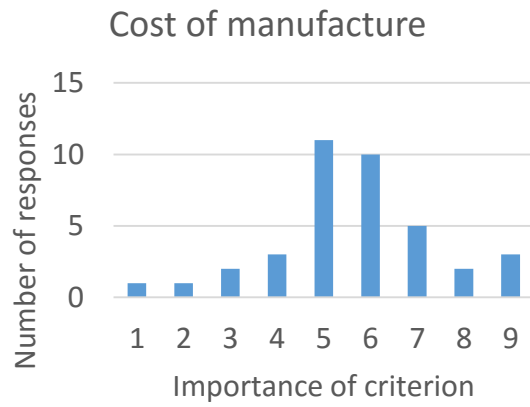
%% RESULT %(days)
%-----
-
T_reqdaysSP=T_reqhrs/24; % required consecutive days of work
T_totSP=T_totdays; % tot number of days considering the avarage working
sloth hours per day
```

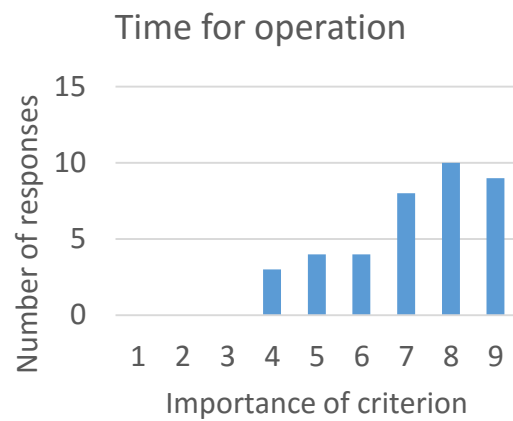
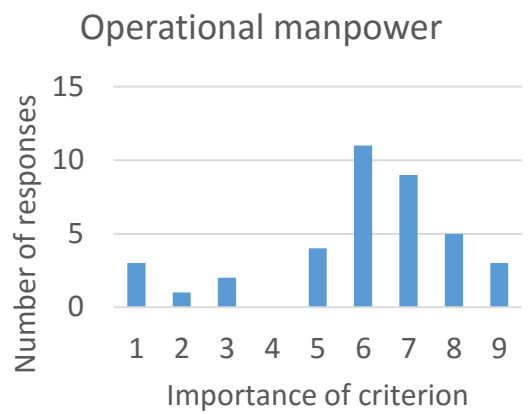
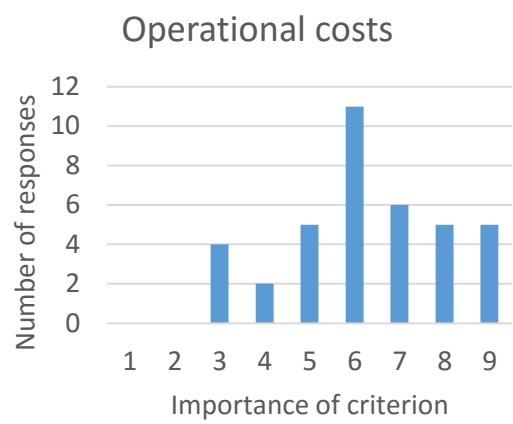
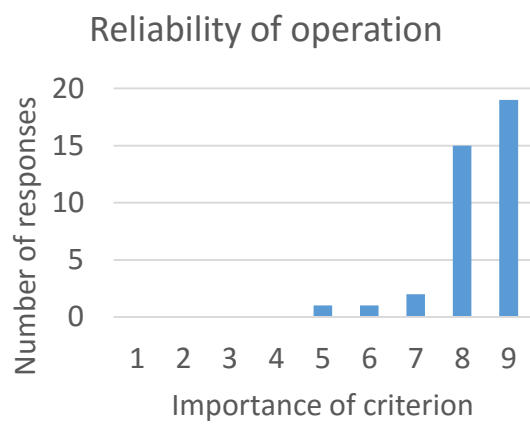
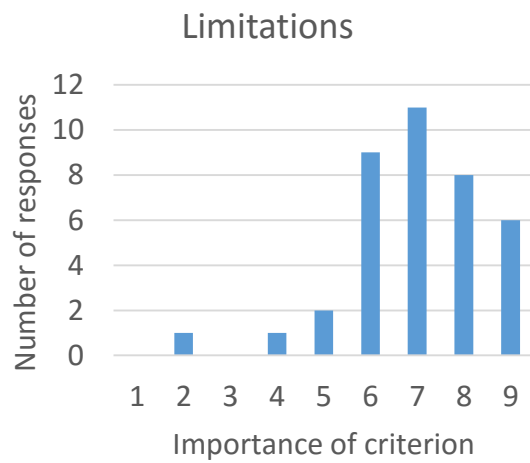
Appendix E MCDA Appendix

E.1 Detailed Survey Responses

E.1.1 Response Histograms







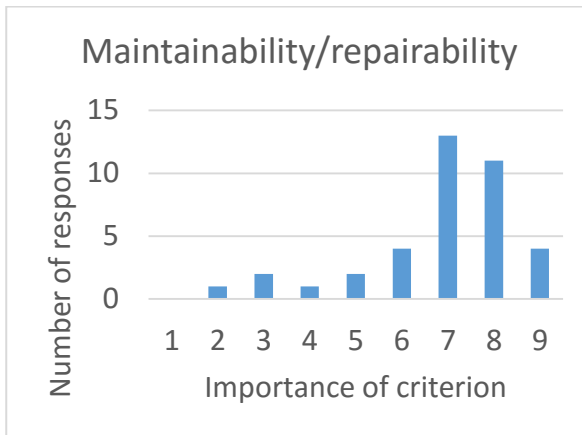
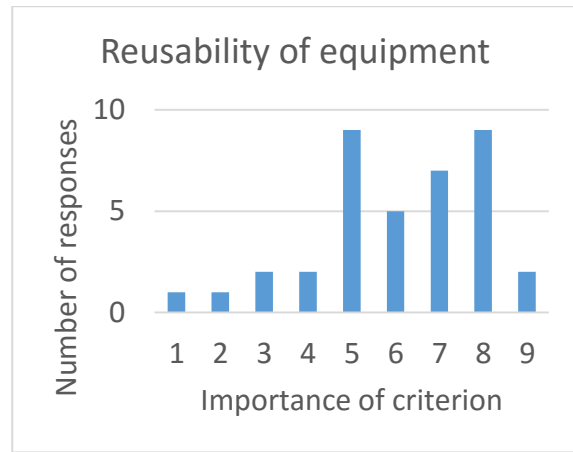
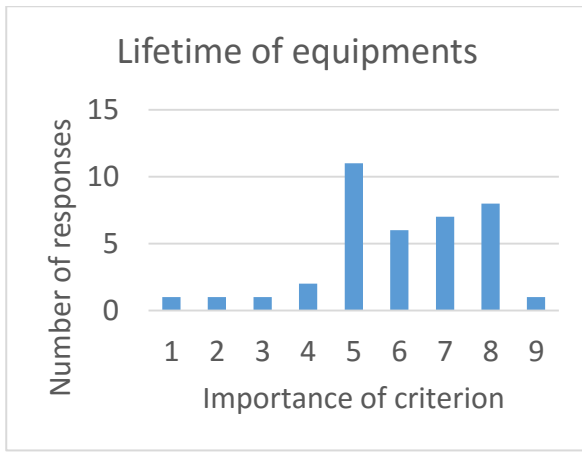


Figure E-1 Response histograms

E.1.2 Criteria Weight Values

Table E-1 Criteria weighting

	standard deviation	Average	Experience weighted	Years weighted
Years exp	6.69	9.89		
level exp	0.95	3.13		
Feasibility	1.75	7.79	7.84	8.05
Maturity of tech	1.71	5.97	6.10	5.97
Cost to develop	1.67	5.26	5.22	5.15
Ease of prototyping	2.14	4.92	5.07	5.04
Ease of certification	2.10	6.00	5.91	5.89
handling improvement	1.17	8.00	8.01	7.94
cost of manufacture	1.75	5.63	5.55	5.49
ease of manufacture	1.74	5.03	5.10	5.05
reuse of resources	1.99	4.95	5.01	5.08
environmental impact	2.46	5.50	5.59	5.64
Reduction of risk	0.56	8.71	8.72	8.76
ease of implementation and operability	1.49	7.63	7.68	7.43
limitations	1.48	6.97	6.97	7.07
required training	2.02	5.58	5.67	5.18
reliability of operation	0.89	8.32	8.29	8.27
operational costs	1.76	6.26	6.19	6.26
operational manpower	2.11	5.97	5.98	5.97
time for operation	1.55	7.18	7.27	7.40
lifetime of equipment	1.75	5.97	6.03	5.90
reusability of equipment	1.90	6.08	6.19	6.20
maintainability/ reparability	1.66	6.87	6.95	6.75

E.2 TOPSIS Code

```

clc
clear
MCDA_method='TOPSIS'
%clf
%Input alternative
AltData = 'Alternativedata.xlsx';
A=xlsread(AltData);
%Which columns are negative values?
neg=[3,7,10,13,14,16,17,18];
[k,l]=size(neg);
for i=1:l
    A(:,neg(i))=A(:,neg(i))*(-1);
end
%Input Weight
WeightData = 'Weightdata.xlsx';
B=xlsread(WeightData);
%Normalise Alternative array
[m,n]=size(A);
Normfact=zeros(n,1);
for i=1:n
    for j=1:m
        Normfact(i)=Normfact(i)+A(j,i)^2;
    end
end
Normfact=Normfact.^(1/2);
for i=1:n
    Anorm(:,i)=A(:,i)./Normfact(i);
end

%Weighting
Aweight=zeros(size(A));
for i=1:n
    Aweight(:,i)=B(i).*Anorm(:,i);
end

%Positive Ideal and Negative Ideal solutions
PIS=zeros(n,1); NIS=zeros(n,1);
for j=1:n
    PIS(j)=max(Aweight(:,j));
end
for j=1:n
    NIS(j)=min(Aweight(:,j));
end

%Distance of each alternative from PIS and NIS
sip=zeros(m,1);
sin=zeros(m,1);
for i=1:m
    for j=1:n
        sip(i)=sip(i)+(Aweight(i,j)-PIS(j))^2;
        sin(i)=sin(i)+(Aweight(i,j)-NIS(j))^2;
    end
end
sip=sip.^(1/2);
sin=sin.^(1/2);
%Closeness
C=zeros(m,1);
for i=1:m
    C(i)=sin(i)/(sip(i)+sin(i));
end
C

```